

THE GEOCHEMISTRY OF SUSPENDED PARTICLES IN THE TAMAR ESTUARY

BY

John Smith Findlay B.Sc., M.Sc.

A thesis submitted to the Council for National
Academic Awards in partial fulfilment of the
requirements for admittance to the degree of:

DOCTOR OF PHILOSOPHY

UNDERTAKEN AT:

University of Cambridge
Department of Earth Sciences
Bullard Laboratories
Madingley Road
Cambridge, U.K.

IN COLLABORATION WITH:

Plymouth Marine Laboratory
Prospect Place
West Hoe
Plymouth
Devon, U.K.

SPONSORING ESTABLISHMENT:

Institute of Marine Studies
Polytechnic South West (Plymouth)
Drake Circus
Plymouth
Devon, U.K.

Submitted June 1990

REFERENCE ONLY

LIBRARY STORE

REFERENCE ONLY

STORE

- 8 OCT 2002

- 9 MAR 2004

STORE

29 JAN 2004

UNIVERSITY OF PLYMOUTH

PLYMOUTH LIBRARY

**POLYTECHNIC SOUTH WEST
LIBRARY SERVICES**

Item
No.

9000 34613-1

Class
No.

T 551.4609 FIN

Contl
No.

X 70 234 9843

90 0034613 1

TELEPEN

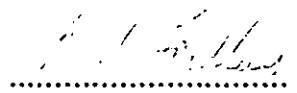


REFERENCE ONLY

COPYRIGHT

Attention is drawn to the fact that the copyright of this thesis rests with the author, and that no quotation from the thesis nor information derived from it may be published without the prior written consent of the author.

This thesis will be made available for consultation within the Polytechnic South West (Plymouth) library, and may be photocopied or lent to other libraries for the purposes of consultation.

Signed: 

DECLARATIONS

At no time during the registration for the degree of Doctor of Philosophy has the candidate been registered for any other C.N.A.A. or University award without the Council's specific permission. No material in this thesis has been used in any other submission for an academic award. This study was financed by a research assistantship under grant GST/02/63 from the Natural Environment Research Council.

Meetings Attended:

EUG III, Strasbourg, April 1985.

NERC Estuarine Processes Workshop, University of Liverpool, April 1986. Oral presentation of part of progress report (see below).

NERC Geocolloids Meeting, Polytechnic South West, Plymouth, April 1990. Oral presentation: 'Rare earth element geochemistry of suspended particles in the Tamar Estuary.'

Publications:

Elderfield, H, Morris, A.W., Whitfield, M., Upstill-Goddard, R.C. & Findlay, J.S., 1986: Variations in the chemical composition of suspended particles in estuaries: the role of benthic fluxes and processes at the turbidity maximum in chemical scavenging. *N.E.R.C. Progress Report on Special Topic Grant GST/02/63*.

Upstill-Goddard, R.C., Findlay, J.S., Elderfield, H. & Sholkovitz, E.R., 1986: Rare earth elements in rivers and estuaries. *EOS*, **67** (44), p 1065.

ACKNOWLEDGEMENTS

It is impossible to name all the people whose talents and effort have contributed to this work, however, I would like to thank a few personally.

Firstly, my supervisors: Harry Elderfield, for his hiring me to work on the project in the first place, and his tireless efforts to inject rigour into my efforts once I'd started. Alan Morris, his co-conspirator, most of all for his encyclopaedic knowledge of the chemistry of the Tamar and enthusiasm for yet more particulate trace metal data. Geoff Millward for his unstinting encouragement, critical reviews, and timely stick waving.

There would have been no lab without the patience of the Bullard labs workshop staff, whose five-minute courses in how to use a milling machine and do three-phase electrics were vital.

The clean lab at Cambridge would have ground to a halt without the efforts of countless geochemists, but in particular Mervyn Greaves. Also Brenda Elderfield and Linda Godfrey must be thanked for their tolerance of my rather uncompromising view of how the 'yellow lab' should be run, and their assistance in keeping that most ersatz of facilities functioning.

Field work on the Tamar would have been far less fun without the good cheer and technical skills of Steve Boswell and Rob Goddard. Things were never the same once 'Fiddler' Jennings showed us to the Swan. Thanks also to Robin Howland, Tony Bale and Peter Watson at the Plymouth Marine Laboratory for their assistance with the work, fruitful discussions, and the analyses they provided.

This work was funded by NERC grant GST/02/63. Its completion would not have been possible without the indulgence of my parents, and Jenny's patience.

THE GEOCHEMISTRY OF SUSPENDED PARTICLES IN THE TAMAR ESTUARY

John Smith Findlay

ABSTRACT

ICP analyses of total rare earth element (REE) abundances in intertidal sediments and suspended particles from the Tamar Estuary show little variation in REE concentrations along the estuary and only minor fractionation relative to standard shale. Fe, Mn, Cu, Zn, Ni & Co abundances in the estuarine suspended particles show significant variations in the turbid upper estuary. Acid leachable REE display different shale normalised patterns with slight enrichment of the mid to heavy REE. Sediment porewater analyses confirm the diagenetic mobility of the REE and show significant heavy REE enrichment consistent with their derivation from a non-detrital source. Detailed studies of suspended particles in the turbidity maximum zone reveal the importance of physical processes in the immediate local control of the bulk chemical composition of the suspended particles. Settling experiments performed on particle samples from the turbidity maximum show clear distinctions between populations of particles which are tidally resuspended versus those which remain permanently in suspension. Trace metal-Al ratios and shale normalised REE patterns in the two fractions are consistent with greater non-detrital content in the permanently suspended particles. Modelling of mixing between detrital REE and the riverine REE removed from solution in the low salinity zone indicates that a significant proportion of the leachable particulate REE may be derived from a non-detrital source. Budget calculations using annual fluxes of dissolved REE, Fe, Cu, Ni & Zn and riverine sediment supply confirm that significant modification of particle composition due to uptake of non-detrital metals is likely, but indicate that not all the sediment supplied to the estuary may participate in the chemical scavenging processes.

Contents

1	Introduction	1
1.1	Estuarine Processes	1
1.1.1	The Geochemical Significance of Estuaries	1
1.1.2	Freshwater - Seawater Mixing and Particle Interactions	2
1.1.3	Sedimentation and Diagenesis	5
1.2	The Chemistry of the Rare Earth Elements	7
1.3	The Tamar Estuary	10
1.3.1	Location, Drainage & Hydrodynamics	10
1.3.2	Previous Chemical Studies of the Tamar	13
1.4	Outline of the Project	15
1.4.1	NERC Special Topics Programme	15
1.4.2	Objectives and Structure of this Study	15
1.4.3	Outline of the Thesis	16
2	Sampling and Analytical Methods	18
2.1	General Considerations	18
2.1.1	Laboratory Usage	18
2.1.2	Reagents	18
2.1.3	Sample containers	19
2.1.4	Blanks	20
2.2	Sampling Methods	21
2.2.1	Collection of Sediment Cores and Separation of Pore Waters	21
2.2.2	Collection and Filtration of Estuarine Waters	23
2.2.3	Back-up Data	26
2.3	I.C.P. Spectrometry	28
2.3.1	Sample Digestion	29
2.3.2	Leaching Procedures	34
2.3.3	Column Chemistry	36
2.3.4	Data Quality	42
2.4	Mass Spectrometry	47
2.4.1	Details of Method	48
2.4.2	Data Quality	49
3	Results I: Major Elements, Trace Elements & Background Data	51
3.1	Sediments	51
3.1.1	Major Elements	51
3.1.2	Trace Elements	52
3.2	Pore Waters	56
3.3	Axial Surveys	59
3.3.1	Background	59
3.3.2	Major Elements	60
3.3.3	Trace Elements	60
3.4	Turbidity Maximum, Surface Samples	70
3.4.1	Major Elements	70
3.4.2	Trace Elements	71

3.5	Turbidity Maximum Profiles	76
3.5.1	Major Elements	76
3.5.2	Trace Elements	76
3.6	Settling Procedure	81
3.6.1	Major Elements	81
3.6.2	Trace Elements	82
4	Results II: Rare Earth Elements	88
4.1	Sediments	88
4.2	Pore Waters	92
4.3	Spring Tide Axial Survey	100
4.4	Turbidity Maximum, Surface Samples	104
4.5	Turbidity Maximum Profiles	108
4.6	Settling Procedure	113
5	Discussion & Conclusions	119
5.1	Analytical Artifacts	119
5.1.1	Leaching	119
5.1.2	Settling Procedure	123
5.2	Particle Populations	126
5.3	Sources of Metals in Suspended Particles	132
5.4	Fluxes of Metals in the Tamar	137
5.4.1	REE	137
5.4.2	Other Metals	139
5.5	Conclusions	141
	References	145
	Data Appendices	158
A:	Sediments	158
B:	Pore Waters	161
C:	Axial Surveys	164
D:	Turbidity Maximum, Surface Samples	170
E:	Turbidity Maximum Profiles	174
F:	Settling Procedure	178

List of Tables

1.1	Example Nd concentrations in environmental samples	9
2.1	List of sampling exercises.	21
2.2	Subdivision of porewater samples	22
2.3	Major element oxide and trace element analyses provided by the ICP.	29
2.4	Elution procedure for separation of REE from major elements prior to ICP analysis.	42
2.5	Precision of ICP analyses	45
2.6	Scheme for separation of REE for mass spectrometry.	49
3.1	Comparison of major element levels in core 1 sediment samples of high and low REE content.	53
3.2	River Tamar discharge data	59
3.3	Comparison of correlation coefficients between Fe and trace metals in separated particle populations.	83
4.1	Comparison of molar REE ratios in estuarine waters, sediments, and pore waters.	94
4.2	Comparison of light REE enrichments in estuarine samples.	94
4.3	Total heavy REE concentrations in springs survey SPM.	100
4.4	Comparison of REE concentrations in permanently suspended and resuspending particles.	114
4.5	Comparison of REE leach/total ratios in different sample sets.	114
4.6	Comparison of correlation coefficients between Fe and REE in separated particle populations.	116
5.1	Mean Fe/Al and Co/Al ratios in Tamar sediments and Springs Survey SPM.	124
5.2	Mean element-Al ratios in PSP and RSS.	124
5.3	Summary of principal geochemical characteristics of sample sets analysed.	127
5.4	Trace element removal and calculated sediment enhancements.	140

List of Figures

1.1	Idealised estuarine salinity - concentration profiles.	3
1.2	Schematic diagram showing principal estuarine removal and input processes.	4
1.3	Example of shale normalised REE abundance plots.	9
1.4	Map of S.W. England showing the location of the Tamar Estuary.	11
1.5	Map of the Tamar Estuary.	12
2.1	Radiochemical calibration of 12.6 <i>cm</i> column	39
2.2	ICP calibration of 12.6 <i>cm</i> column	39
2.3	Radiochemical calibration of 7 <i>cm</i> column	41
2.4	Radiochemical REE recovery check	41
3.1	Sediment core 1: Al ₂ O ₃ & Fe ₂ O ₃ vs. Depth.	54
3.2	Sediment core 1: MnO vs. Depth.	54
3.3	Sediment core 1: Co & Ni vs. Depth.	55
3.4	Sediment core 1: Cu & Zn vs. Depth.	55
3.5	Sediment pore waters: NH ₃ & SO ₄ ²⁻ vs. Depth.	57
3.6	Sediment pore waters: PO ₄ ³⁻ & Si vs. Depth.	57
3.7	Sediment pore waters: Fe & Mn vs. Depth.	58
3.8	Neaps survey: turbidity and salinity vs. distance down estuary.	64
3.9	Springs survey: turbidity and salinity vs. distance down estuary.	65
3.10	Axial surveys: dissolved Si vs. salinity.	65
3.11	Axial surveys: particulate Fe ₂ O ₃ vs. distance down estuary.	65
3.12	Neaps survey: total particulate MnO vs. distance down estuary.	66
3.13	Springs survey: total particulate MnO vs. distance down estuary.	66
3.14	Axial surveys: total particulate Li vs. distance down estuary.	66
3.15	Axial surveys: particulate Ni vs. distance down estuary.	67
3.16	Neaps survey: Cu & Ni leach/total ratios vs. distance down estuary.	67
3.17	Springs survey: Cu & Ni leach/total ratios vs. distance down estuary.	67
3.18	Axial surveys: particulate Cu vs. distance down estuary.	68
3.19	Springs survey: particulate Zn vs. distance down estuary.	68
3.20	Neaps survey: particulate Zn vs. distance down estuary.	68
3.21	Neaps survey: particulate Co vs. distance down estuary.	69
3.22	Springs survey: particulate Co vs. distance down estuary.	69
3.23	Turbidity maximum, surface samples: Neaps; salinity and turbidity vs. time.	72
3.24	Turbidity maximum, surface samples: Springs; salinity and turbidity vs. time.	72
3.25	Turbidity maximum, surface samples: particulate Fe ₂ O ₃ vs. turbidity.	72
3.26	Turbidity maximum, surface samples: particulate Al ₂ O ₃ vs. turbidity.	73
3.27	Turbidity maximum, surface samples: particulate P ₂ O ₅ vs. turbidity.	73

3.28	Turbidity maximum, surface samples: total particulate MnO vs. turbidity.	73
3.29	Turbidity maximum, surface samples: dissolved Fe vs. turbidity.	74
3.30	Turbidity maximum, surface samples: particulate Co vs. turbidity.	74
3.31	Turbidity maximum, surface samples: particulate Ni vs. turbidity.	74
3.32	Turbidity maximum, surface samples: particulate Cu vs. turbidity.	75
3.33	Turbidity maximum, surface samples: particulate Zn vs. turbidity.	75
3.34	Turbidity maximum profiles: total particulate Na ₂ O vs. turbidity.	78
3.35	Turbidity maximum profiles: total particulate Na ₂ O vs. particle size.	78
3.36	Turbidity maximum profiles: total particulate Na ₂ O vs. time.	78
3.37	Turbidity maximum profiles: Total particulate TiO ₂ vs. turbidity.	79
3.38	Turbidity maximum profiles: particulate Co vs. turbidity.	79
3.39	Turbidity maximum profiles: particulate Co vs. time.	79
3.40	Turbidity maximum profiles: total particulate Cu vs. turbidity.	80
3.41	Turbidity maximum profiles: particulate Zn vs. turbidity.	80
3.42	Turbidity maximum profiles: distribution of total Cu concentrations in SPM with respect to depth and time of sampling.	80
3.43	Settling procedure: Sample depths and water depth with respect to time.	84
3.44	Settling procedure: particulate Fe ₂ O ₃ vs. turbidity.	84
3.45	Settling procedure: particulate P ₂ O ₅ vs. turbidity.	84
3.46	Settling procedure: particulate Fe ₂ O ₃ vs. time.	85
3.47	Settling procedure: Fe ₂ O ₃ leach/total ratios vs. turbidity.	85
3.48	Settling procedure: particulate Fe ₂ O ₃ vs. turbidity.	85
3.49	Settling procedure: total particulate TiO ₂ vs. turbidity.	86
3.50	Settling procedure: total particulate MnO vs. turbidity.	86
3.51	Settling procedure: total particulate Cu vs. turbidity.	86
3.52	Settling procedure: total particulate Zn vs. turbidity.	87
3.53	Settling procedure: particulate Ni vs. turbidity.	87
3.54	Settling procedure: particulate Co vs. turbidity.	87
4.1	Sediment core 1: La & Gd vs. depth.	90
4.2	Sediment core 1: REE leach/total ratios vs. depth	90
4.3	Sediment core 1: shale normalised REE patterns for the 8–9 cm interval.	91
4.4	Sediment core 1: shale normalised REE patterns for the 4–5 cm and 8–9 cm interval.	91
4.5	Pore water Nd vs. depth, cores 2 & 3.	95
4.6	Pore water Ce vs. depth, cores 2 & 3.	95
4.7	Pore water Sm vs. depth, cores 2 & 3.	96
4.8	Pore water Dy vs. depth, cores 2 & 3.	96
4.9	Core 3: pore water Er & Eu vs. depth.	97
4.10	Core 1: pore water Nd vs depth.	97
4.11	Core 3: shale normalised REE patterns for porewater REE.	98
4.12	Shale normalised REE patterns from dissolved estuarine REE collected during neaps survey.	99
4.13	Springs survey: particulate Nd vs. distance down estuary	102
4.14	Springs survey: particulate Yb vs. distance down estuary	102
4.15	Springs survey: particulate Gd vs. distance down estuary	102
4.16	Springs Survey: example shale patterns for total REE.	103
4.17	Springs Survey: REE leach/total ratios in suspended particles.	103
4.18	Springs Survey: comparison of shale normalised REE patterns from leach and total analyses.	103
4.19	Turbidity maximum, surface samples: particulate Nd vs. turbidity.	105
4.20	Turbidity maximum, surface samples: particulate Dy vs. turbidity.	105
4.21	Turbidity maximum, surface samples: particulate Gd vs. turbidity.	105

4.22	Turbidity maximum, surface samples: shale normalised REE patterns for neap tide.	106
4.23	Turbidity maximum, surface samples: REE shale normalised REE patterns for spring tide.	106
4.24	Turbidity maximum, surface samples: leach/total ratios in suspended particles.	107
4.25	Turbidity maximum surface samples, plus spring tide axial survey: Ho leach/total ratios vs. turbidity.	107
4.26	Turbidity maximum profiles: particulate Nd vs. time.	110
4.27	Turbidity maximum profiles: particulate Gd vs. time.	110
4.28	Turbidity maximum profiles: particulate Eu vs. median particle size.	110
4.29	Turbidity maximum profiles: particulate Eu vs. turbidity.	111
4.30	Turbidity maximum profiles: shale normalised REE in the 1600 h, 0.1 m sample.	111
4.31	Turbidity maximum profiles: shale normalised REE in the 1830 h, 2.5 m sample.	111
4.32	Comparison of chondrite normalised REE patterns in turbidity maximum sample and granite.	112
4.33	Settling procedure: total particulate Gd vs. turbidity.	117
4.34	Settling procedure: leachable particulate Gd vs. turbidity.	117
4.35	Settling procedure: shale normalised REE for the 10:30 h, 1m sample.	117
4.36	Settling procedure: shale normalised REE for the 19:00 h, 4.5 m sample.	118
4.37	Settling procedure: leachable Gd in PSP and RSS vs. time.	118
4.38	Settling procedure: total Gd in PSP and RSS vs. time.	118
5.1	Comparison of leach/total ratios obtained from other estuarine and marine sediments with Tamar sediments.	121
5.2	Comparison of mean leachable shale normalised REE patterns from Tamar sediments and PSP.	122
5.3	Settling procedure: Particulate Fe ₂ O ₃ vs. Al ₂ O ₃	129
5.4	Settling procedure: Particulate P ₂ O ₅ vs. Al ₂ O ₃	129
5.5	Shale normalised REE patterns generated by mixing of removed riverine REE with residual sediment REE.	135
5.6	Comparison of theoretical and actual leachable REE patterns.	135
5.7	Schematic diagram of processes and fluxes controlling estuarine particle compositions.	142

Chapter 1

Introduction

1.1 Estuarine Processes

1.1.1 The Geochemical Significance of Estuaries

Estuaries are complex and dynamic environments, forming the principal link between the terrestrial and marine aquatic environments. They are also often the site of intense human and industrial activity, and, with the exception of such activities as the deliberate offshore dumping of sewage sludges, are the main route of our wastes into the sea. Hence, estuaries have a very important role in aqueous geochemical cycling.

The delivery of the riverine dissolved and suspended loads into the marine environment is not a simple case of dilution of the riverine material and subsequent dispersion. The chemical forms, and hence biological and chemical availability, of trace metals undergo significant changes within estuaries. It is important therefore, given the fact we can and do modify the chemical balance of estuaries, that we have an adequate understanding of the processes operating in these environments. This is true both at a local level, where we need information on the likely effect of human activities on individual estuaries, as well as on a larger scale, where there is a need to understand the implications of estuarine processes on global geochemical cycles. Our understanding of estuarine processes can be applied to the interpretation of fossil records of marine geochemical conditions as well as to prognoses for the future.

The River Tamar is hardly globally significant in terms of its discharge, (annual mean discharge: Tamar – $18 \text{ m}^3 \text{ s}^{-1}$, Amazon – $1.75 \times 10^5 \text{ m}^3 \text{ s}^{-1}$, taken from

Lerman, 1980 and Uncles *et al.*, 1983) but the processes operating within the confines of this estuary are not unique, and results from studies of its characteristics can be applied to other larger and perhaps more significant systems. There is the advantage that a considerable body of research on the basic physical and chemical features of the Tamar has already been conducted, allowing more specialist work to be done there and set within an established framework, without the labour of investigating the basic characteristics of the estuary (*e.g.* Morris *et al.*, 1982a).

1.1.2 Freshwater - Seawater Mixing and Particle Interactions

As mentioned above, the mixing of sea and river waters in estuarine environments is not simply a case of dispersal and dilution for all the constituents. Using the salinity as a measure of dilution of the river water it is possible to assess whether or not the concentrations of any dissolved component are conserved during estuarine mixing. Those species which show linear relationships of concentration against salinity in an estuary are said to show conservative behaviour, conversely, those which do not, display non-conservative behaviour (Boyle *et al.*, 1974; Liss, 1976). The latter can take the form of either an excess or deficit (relative to the concentration predicted by conservative mixing of the end members) of the component at a particular point in the estuary. This would imply that local addition or removal of the component had been taking place. Some chemical species may show both removal and addition in different parts of the same estuary (fig. 1.1).

There are a number of factors operating to generate non-conservative behaviour in estuaries. The increase in salt concentration and hence ionic strength of the solution as the river water becomes saline acts to destabilise and flocculate the organic and hydrous metal oxide colloidal matter present in the river water (Eckert & Sholkovitz, 1976; Sholkovitz, 1976 & 1978, Boyle *et al.*, 1977; Sholkovitz *et al.*, 1978). This results in a significant removal of dissolved (*i.e.* 0.45 μm filterable) metallic elements from the low salinity part of an estuary (Sholkovitz, 1978). The material removed then either forms small particles (Eisma *et al.*, 1980) or can be taken up by pre-existing detrital particulate matter (Duinker &

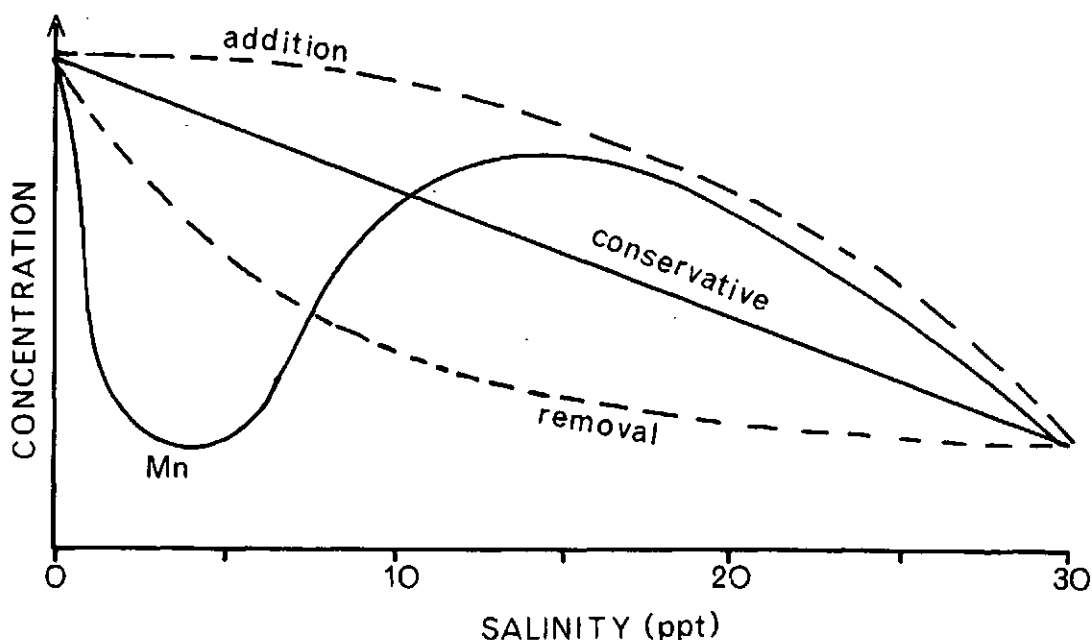


Figure 1.1: Estuarine salinity - concentration plots showing conservative mixing, removal, addition, and schematised Mn behaviour.

Nolting, 1978; Duinker *et al.*, 1979).

A feature of partially mixed estuaries is the development of a turbidity maximum zone (Officer 1976). This hydrodynamically controlled zone of enhanced turbidity is located in the low salinity upper estuary, and has much greater suspended loads than either the inflowing river water or more saline lower estuary. For some fractions of the sediment load the suspension will be semi-permanent as particles become trapped in the turbidity maximum (Festa & Hansen, 1978). It is within this zone that considerable chemical and biological activity takes place (Morris *et al.*, 1978) as the pH, ionic strength and dissolved O₂ concentrations change rapidly.

Removal of trace metals from the water column in this zone can occur by scavenging (Goldberg, 1954) as well as by flocculation, and is accelerated by the elevated turbidities (Aston & Chester, 1973). Oxyhydroxides of Fe and Mn generated by non-conservative removal add to the solid material derived from the riverine suspension and tidally resuspended estuarine sediments. These fresh materials have considerable scavenging capacity and contribute further to the

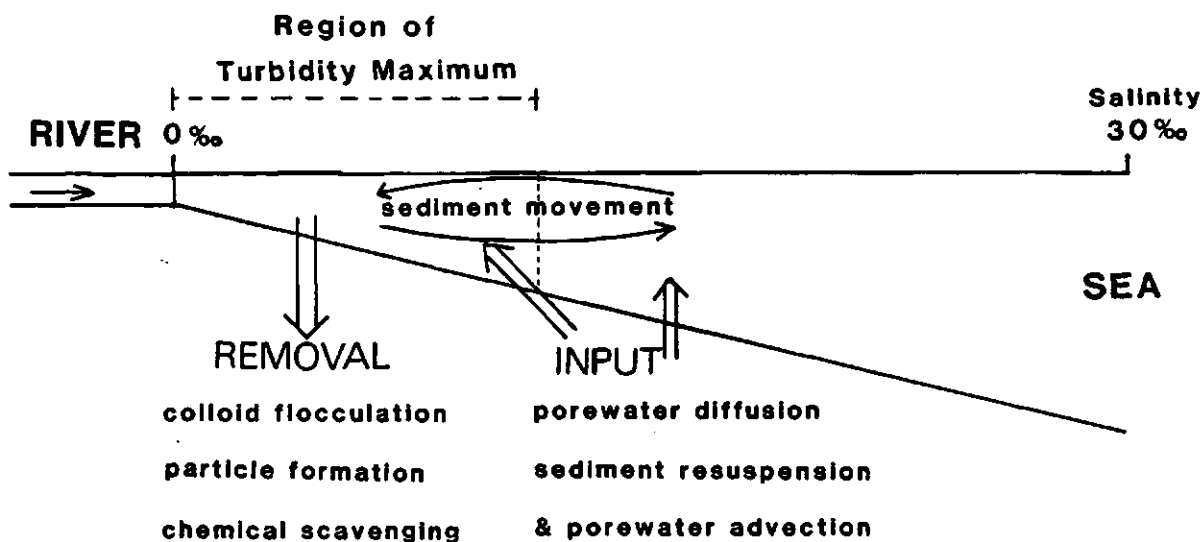


Figure 1.2: Schematic diagram showing principal estuarine removal and input processes.

removal of other metals from solution (Lion *et al.*, 1982).

Input of dissolved constituents to the estuarine waters can also occur here, and result from either desorption of metals from particle surfaces during mixing (Van der Weijden *et al.*, 1977; Li *et al.*, 1984) or advective fluxes from sediment interstitial waters as bed sediment is resuspended (Morris *et al.*, 1982b). A schematic diagram showing the principal input and removal processes operating in an estuary is given in figure 1.2.

The relative importance of the various processes is of course dependent on the natural variability of the weather and tides which impose significant effects on the discharge of rivers, suspended load and energy of tidal mixing. It is almost impossible to calculate the net effect of removal of, say, dissolved Fe in the low salinity zone on the concentrations of Fe in the suspended particles in that zone. Comparisons of dissolved and particulate Fe abundances in estuarine turbidity maxima reveal 4-5 orders of magnitude difference between the two phases which suggest that no significant modification of particle compositions could take place. However, such comparisons may not reflect the net fluxes of either phase through

the reactive zone, and given the highly seasonal nature of the variations in the discharge and sediment movement of estuaries such as the Tamar annual fluxes would be more appropriate. We are also as yet unable to determine whether all the particulate material passing through the reactive zone actually participates in the reactions or if some of it is essentially inert.

1.1.3 Sedimentation and Diagenesis

Estuaries are often sites of significant sediment accumulation, either underwater or on intertidal mudflats. If the sediments contain a significant quantity of organic material its microbial degradation rapidly results in consumption of the available oxygen, particularly when the sediments are fine grained and diffusion of interstitial fluids is restricted. Reducing conditions are thus established, often within a few *mm* of the sediment surface, and can lead to elevated porewater concentrations of nutrients and metabolic products released by the decomposition of the organic matter (Goldhaber *et al.*, 1977). The difference in concentration of species between the interstitial fluids and the (perhaps intermittently) overlying water results in their diffusion out of the sediments and the development of porewater nutrient and metal concentration gradients with depth which are regarded as characteristic of diagenesis in organic rich sediments. Fe and Mn are solubilised during organic diagenesis due to the reduction of oxyhydroxides attached to the detrital sediments (Elderfield *et al.*, 1981). This has implications for elements whose cycling may be driven, to an extent, by Fe and Mn as adsorbed metals are released when the oxides dissolve (Gendron *et al.*, 1986). For some elements the diffusional fluxes from sediments contribute significantly to the overall estuarine flux and produce non-conservative behaviour (Knox *et al.*, 1981). In Chesapeake Bay, for example, the annual diffusive Mn flux from the anoxic sediments is estimated to be $2 \times 10^{10} \text{ g y}^{-1}$, four times greater than the annual total of dissolved and particulate Mn fluxes ($5 \times 10^9 \text{ g y}^{-1}$) from the Susquehanna River (Eaton, 1979).

Fe can also become fixed in the sediment by the formation of insoluble sulfides (Balzer, 1982), or trapped at the surface of the sediment by re-oxidation to insoluble Fe^{3+} . The fate of any given element depends on a combination of

kinetic as well as thermodynamic factors. In oxygenated water, for example, the stable form of Mn is insoluble Mn^{4+} , but Mn^{2+} can persist in the water column of the outer (15–30 ppt salinity) estuary because the low turbidities present result in a slow enough oxidation rate ($t_{\frac{1}{2}} = 3\text{--}5\text{ d}$ at $60\text{--}30\text{ mg l}^{-1}$ turbidity; from Morris & Bale, 1979) for the Mn^{2+} released from the sediments to persist. Fluxes of dissolved species from the sediments can be suppressed by the bioturbation and oxygenation of the interstitial fluids by burrowing organisms (Aller & Yingst, 1978) or can be enhanced by their pumping of fluids through the sediments (Aller, 1978). Diagenesis also results in changes in the composition and surface properties of the sediments as the organic matter is consumed and metal hydroxides are solubilised.

1.2 The Chemistry of the Rare Earth Elements

The rare earth elements (REE), La to Lu, are unique amongst the chemical elements in that they form a large and very coherent group. Their electronic structure is such that inner $4f$ shells are filled as the atomic number increases, resulting in no major variations in chemical reactivity across the series (Cotton & Wilkinson, 1980). The inefficient shielding of the outer electrons from the increasing nuclear charge by these additional $4f$ electrons results in a steady decrease in ionic radius from La to Lu (the lanthanide contraction). The resultant systematic variations in bonding, complexation and surface adsorption properties of the REE produces fractionation of the elements relative to each other when involved in chemical reactions in geologic or hydrologic environments (Henderson, 1984; Fleet, 1984).

The REE generally exist in the $3+$ oxidation state, but there are additional oxidation states possible in the case of Ce and Eu. Eu^{2+} is encountered in magmatic systems and this can affect the mobility of Eu in hydrothermal (Michard *et al.*, 1983) as well as 'dry' magmatic environments. In oxic waters Ce^{3+} can be oxidised to Ce^{4+} and then removed from solution (Elderfield, 1988). In estuarine environments the REE behave in a similar manner to Fe, showing a marked non-conservative behaviour during freshwater - seawater mixing (Hoyle *et al.*, 1984) and remobilisation during organic diagenesis (Elderfield & Sholkovitz, 1987), although, with the possible exception of Ce, this does not involve any redox reactions.

Interpretation of the abundances of the REE is facilitated by normalisation of the individual REE concentrations to an appropriate standard, usually a sample which is a part of the system under investigation, or an arbitrary standard of similar REE composition. For geologic samples abundances of REE in chondritic meteorites are used as the standard, whereas studies of aquatic sediments or waters have used REE abundances in composite or standard shales. In this study the standard shale used is from Piper (1974). Depiction of these normalised abundances as plots of sample/standard ratio versus atomic number produces patterns which only deviate moderately from a straight line. This allows easy identification

of any fractionation between samples compared, and use of a logarithmic scale for the ordinate preserves the geometry of the pattern of sample/shale ratios in samples of similar inter-REE abundance ratios but different absolute abundances. This technique allows the identification of similarity between the relative REE abundances in a given sample with those of the reference or putative source materials, as well as investigation of any fractionation or redox processes operating within an environment of interest.

An example is shown in figure 1.3. Patterns A & B have identical shapes, with heavy REE enrichment, so we would conclude that, despite the displacement of the patterns, the two samples they represent contain REE of the same origin. Pattern C on the other hand is light REE enriched, and the REE in this sample could not be derived from the same source as A & B without considerable fractionation. The application of this to the study of estuarine processes is that given the removal of mid to heavy enriched dissolved REE during estuarine mixing (Hoyle *et al.* 1984) it may be possible to trace their fate on the estuarine suspended particulate matter (SPM), if the SPM have shale-like patterns (significantly different from the removed material) and the removed material makes an analytically significant addition to the detrital REE.

The additional oxidation states possible for Eu and Ce produce patterns where their normalised abundances fall away from the trend defined by the other REE. This is referred to as a Eu or Ce anomaly, and can be quantified, for example, as Eu/Eu^* where Eu^* is the normalised Eu abundance interpolated from the neighbouring REE.

Examples of Nd concentrations in environmental samples are given in table 1.1. Note that there are 5–6 orders of magnitude difference between the dissolved and particulate REE concentrations. This means that any modification of particulate REE composition due to uptake of dissolved REE will be highly dependent on the balance between the water and sediment masses involved.

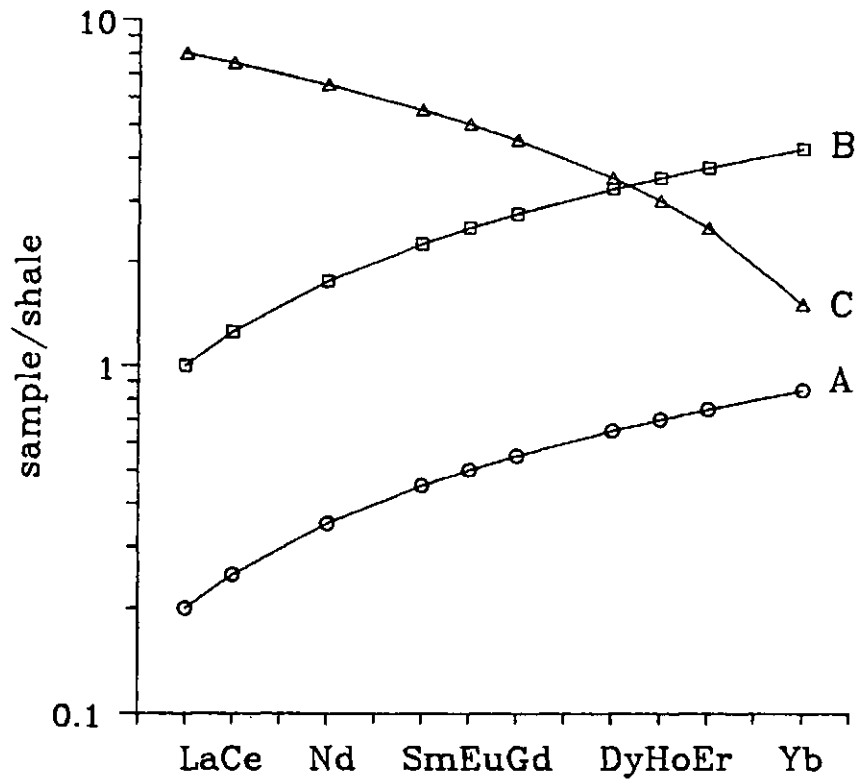


Figure 1.3: Example of shale normalised REE abundance plots.

Sample Type	Nd concentration	Reference
River Water	10-450 $ng\ kg^{-1}$	Goldstein & Jacobsen, 1988
Ocean Water	0.7-4 $ng\ kg^{-1}$	Elderfield, 1988
Nearshore Sediment Porewater	9.4-115 $ng\ kg^{-1}$	Elderfield & Sholkovitz, 1987
Nearshore Sediments	35 $mg\ kg^{-1}$	Elderfield & Sholkovitz, 1987
Riverine Suspended Particles	12-52 $mg\ kg^{-1}$	Goldstein & Jacobsen, 1988
Average Shale	38 $mg\ kg^{-1}$	Piper, 1974

Table 1.1: Example Nd concentrations in environmental samples

1.3 The Tamar Estuary

1.3.1 Location, Drainage & Hydrodynamics

The River Tamar drains a substantial area of agricultural land in Cornwall and Devon, running between the granite masses of Bodmin Moor and Dartmoor (fig. 1.4), and including areas underlain by Carboniferous and Devonian sediments. The emplacement of the granites, and subsequent hydrothermal activity, was responsible for substantial mineralisation of both the granites themselves and the surrounding sediments (Perkins, 1972), with economically important deposits of Fe, Pb/Zn, Sn, Cu, Ag, W and As as well as the huge china clay (kaolinite) workings. There have in the past been mine workings (Booker, 1971; Hamilton-Jenkin, 1974) as far down as the tidal upper estuary, although most, if not all, of the metal mining activity in the Tamar Valley has now ceased.

The tidal estuary extends from a weir at Gunnislake to Plymouth Sound, a total of 31 km (fig. 1.5). All uses of the term 'distance down estuary' are based on measurements from the weir. Maximum water depths in the main channel vary between 20–25 m at the mouth to 3–4 m in the mid to upper estuary. There are extensive intertidal mudflats in the lower estuary, between 20 and 30 km below the weir, with steeper mudbanks characteristic of the upper estuary. The deposition and erosion of the sediments varies depending on the location and season. Areas such as St. John's lake have relatively stable sediments (Clifton & Hamilton, 1979), whereas the sediments around Cargreen (20 km) and further up estuary undergo significant remobilisation on seasonal and tidal bases (Bale *et al.*, 1985).

The estuary is classified as being partially mixed (Officer, 1976), with significant vertical salinity gradients in the the water column. This changes towards well-mixed characteristics when the river discharge is low (Uncles *et al.*, 1983). A particularly important feature is the development and maintenance of a turbidity maximum in the upper estuary. As mentioned above, this is a zone of enhanced turbidity, the maintenance of which is dependent on the magnitude of the riverine and marine sediment inputs, sediment particle size and energy of estuarine circulation (Festa & Hansen, 1978).

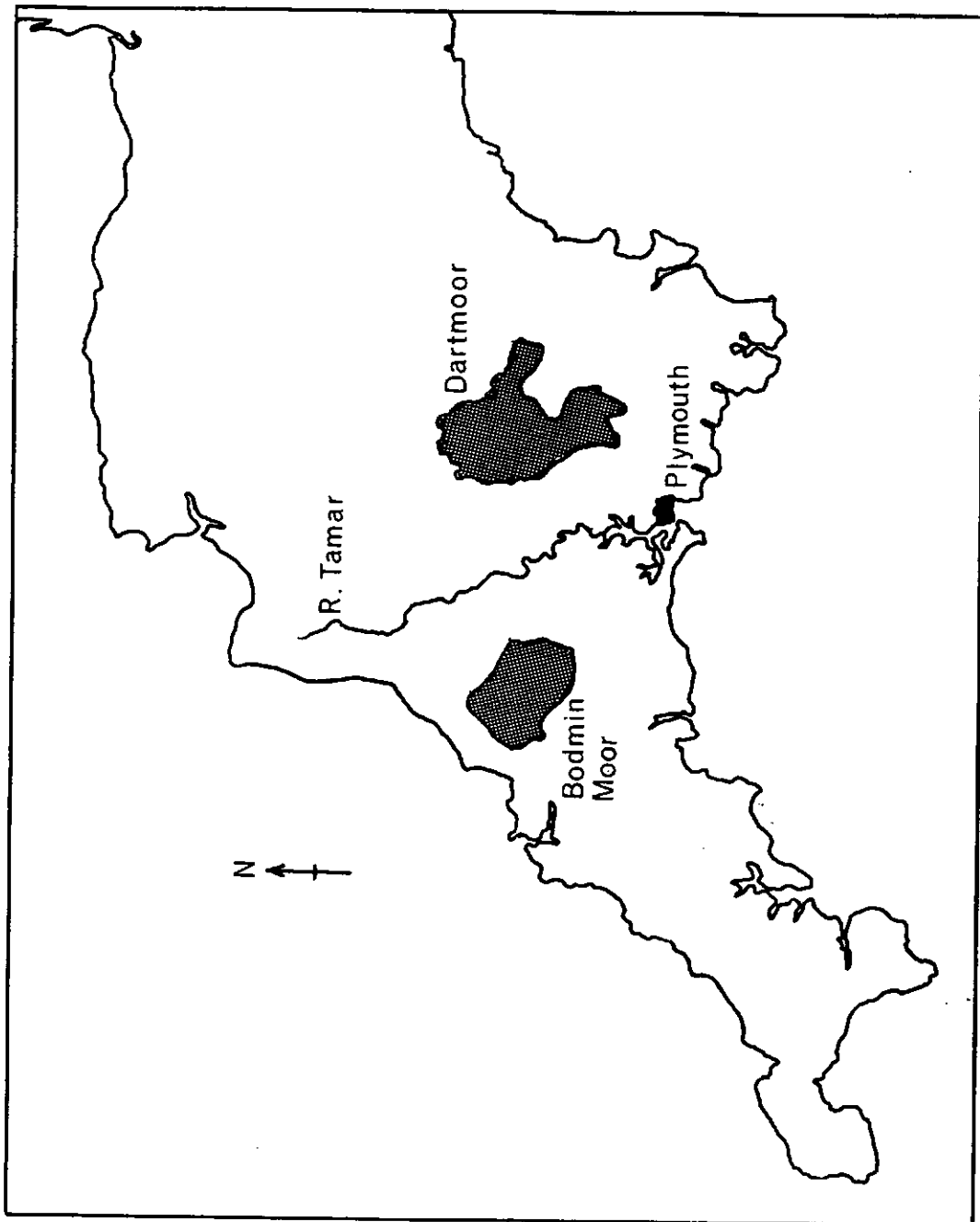


Figure 1.4: Map of S.W. England showing the location of the Tamar Estuary.

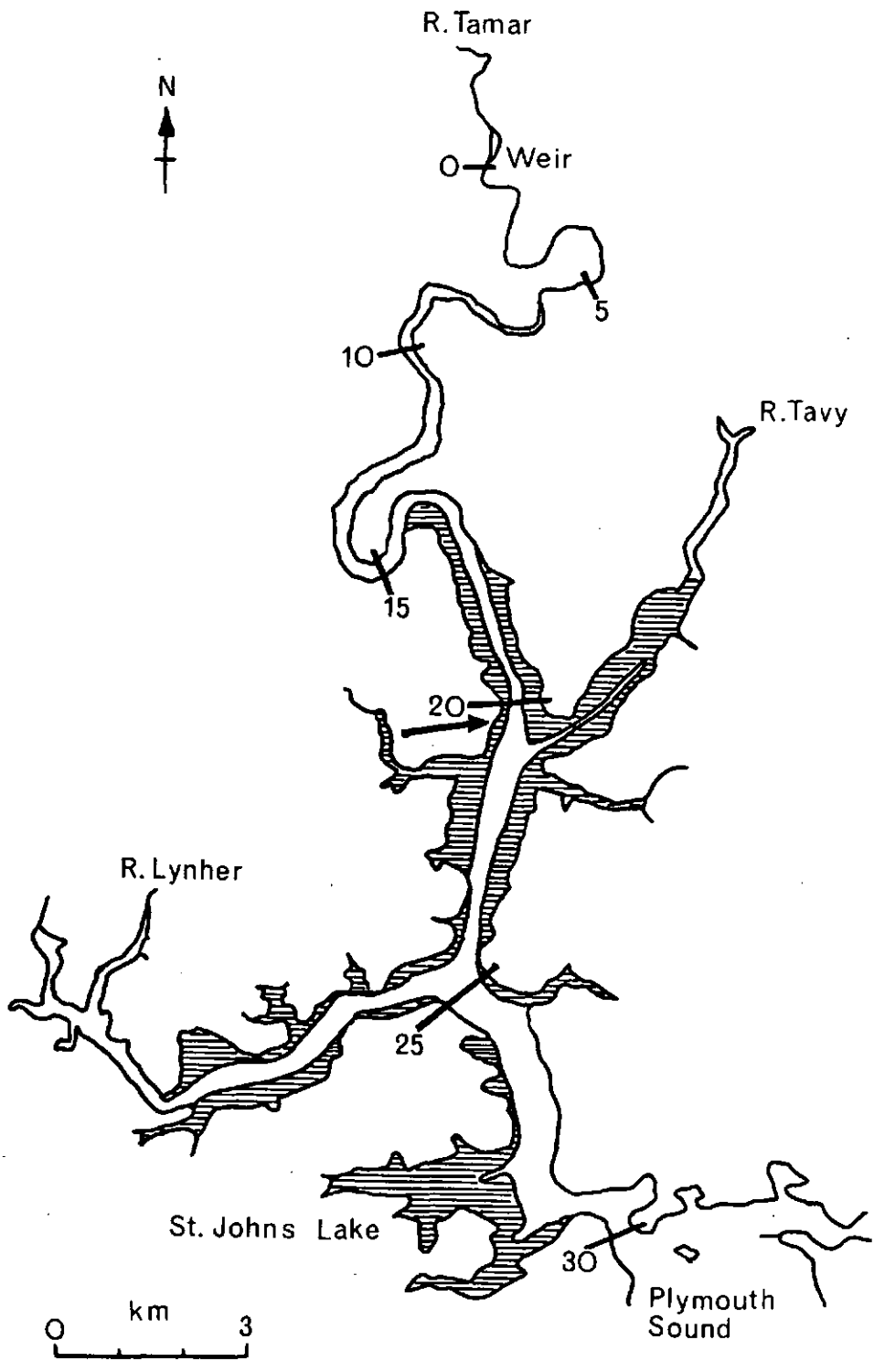


Figure 1.5: Map of the Tamar Estuary showing the extent of the intertidal sediments (shaded area) and the distance markers used to define sampling locations. Arrow indicates Neal Point sediment coring Site.

1.3.2 Previous Chemical Studies of the Tamar

Morris *et al.* (1978) presented the first comprehensive data set to identify the low salinity zone of the Tamar estuary as one where significant biological and chemical reactions were taking place. There then followed more specific research attempting to identify processes operating in the low salinity zone. Phosphate removal was investigated in field studies as well as laboratory experiments (Morris *et al.*, 1981; Bale & Morris, 1981), although the precise mechanisms responsible were not elucidated. Manganese cycling received attention via field and laboratory measurements (Morris & Bale, 1979; Morris *et al.*, 1982b) and numerical modelling of estuarine profiles (Knox *et al.*, 1981), revealing the importance of suspended particles in the removal of manganese from the water column, and both the advective and diffusive addition of Mn to the water column. Subsequent detailed study of diagenesis by Upstill-Goddard *et al.* (1989) has shown the importance of advective rather than diffusive benthic exchange in the overall estuarine budgets of phosphate, ammonia and manganese. The relative importance of porewater infusions compared to desorption from suspended particles in controlling the estuarine distribution of dissolved metals has been shown for Cu and Zn (Ackroyd *et al.*, 1986) and Al (Morris *et al.*, 1986b). Properties of the suspended particles in terms of surface areas and the trace metal adsorption properties of iron oxyhydroxides are reported in Titley *et al.* (1987) and Millward & Moore (1982) respectively.

Seasonal variations in the composition of the estuarine sediments were identified by Ackroyd *et al.* (1987), but studies of the suspended particles in the turbidity maximum could discern little effect of the removal of dissolved Fe removal on their composition (Morris *et al.*, 1986a). However, this study considered the effect of the daily fluxes of Fe on the mass of resuspending sediment and therefore presents only a snapshot of the processes rather than considering the net annual effect. Morris (1986) modelled the removal of Mn in the turbidity maximum in terms of sorptive equilibrium of Mn on the estuarine suspended particles and concluded that the depletion of labile metals on the particles in the turbidity maximum was due to internal cycling of resuspendable sediment. The variability of the composition of the SPM in the turbidity maximum zone (Morris *et al.*,

1982c; Loring *et al.*, 1983; Morris *et al.*, 1987) suggested that the bulk composition was controlled by the mixing of a permanently suspended population of particles, trapped within the turbidity maximum zone, and a tidally resuspended fraction. This inferred distinction was not tested, however, and is the subject of part of this work. Variations in the association of bacteria with the two particle populations identified here (analyses carried out on the same samples as collected for this study) are reported in Plummer *et al.* (1987).

1.4 Outline of the Project

1.4.1 NERC Special Topics Programme

The Special Topics Programme on estuarine processes was conceived in order to enable researchers to co-operate more effectively in research into estuarine processes and to effect coordination of the fieldwork so that, where possible, different workers were actually analysing the same samples. This allows direct rather than general correlation of results. Fieldwork programmes were coordinated through staff at the Plymouth Marine Laboratory (PML), and in some cases field sampling exercises and laboratory experiments were planned co-operatively. The programme also included reports and meetings in which the results obtained from the various studies were circulated and discussed.

In this work the 1985 sampling of estuarine waters provided filtered samples for determination of dissolved REE (Elderfield *et al.*, 1990). Aliquots of the large volume samples collected in 1986 for the settling experiment were used for the bacterial activity determinations reported in Plummer *et al.* (1987).

1.4.2 Objectives and Structure of this Study

The aim of this project was to investigate the processes affecting the chemical composition of the suspended particles in the Tamar Estuary by means of a comprehensive set of multi-element geochemical data. Of special interest was a study of the REE as little or no information was available on their behaviour in coastal or estuarine sediments at the time of inception of this project. In particular, it was intended to examine the physical and chemical processes occurring in the turbidity maximum, and to use the inherent tracer properties of the REE to develop a model of trace metal transport in the estuary.

The first season's fieldwork fell into two distinct operations. The primary objective was to obtain a comprehensive set of data on the variability of the trace metal composition of the suspended particles in the estuary, as well as making a more detailed study of the suspended particles in the turbidity maximum. This required systematic surveys along the length of the estuary from the seawater end to the freshwater/seawater interface, and time series sampling at the turbidity

maximum. This work was done in July 1985 at the same time as a number of other projects were being carried out under the N.E.R.C. Special Topics Programme on Estuarine Processes.

In order to be better able to interpret these data, and to be able to investigate the fluxes of dissolved and solid material across the sediment-water interface, analysis of estuarine sediments and associated porewaters was required. Sampling of these took place in April 1985, prior to the axial surveys.

Examination of the results from the samples taken in 1985 indicated that a more detailed study of processes at the turbidity maximum should be undertaken during the second field season in 1986. The objective here was to examine in greater detail the impact of the physical process of sediment resuspension on the bulk chemistry of the estuarine particles, and to determine whether or not there exists in the turbidity maximum a geochemically distinct population of permanently suspended particles, as had been implicated in previous studies on the Tamar (Morris *et al.*, 1987) and other estuaries (Duinker *et al.*, 1982b, 1985). This entailed two separate sampling exercises. The first utilised onsite measurements of particle size, turbidity and salinity simultaneous with multi-level sampling of waters and entrained SPM. The second involved large volume sampling of the estuarine waters for a laboratory fractionation of the SPM by means of a settling procedure.

In addition to determining the total amounts of the various trace metals present in the samples it was also intended to look at the mobile or labile fraction of these elements in the particles. Some way had to be found to chemically differentiate this non-detrital material from the detrital silicates. This entailed development of a leaching method.

1.4.3 Outline of the Thesis

Chapter 2 describes the analytical and sampling techniques employed for this work. This includes consideration of the overriding constraints on methods, followed by descriptions of the techniques used, and, in the case of the two main instrumental methods, the developments required and assessments of analytical performance. The extent of discussion reflects the effort involved in establishing

the method. Where analyses were carried out by other workers at Cambridge or PML this is mentioned in the text.

The bulk of the results from each of the sampling exercises are reported sequentially in chapter 3. The REE data are reported separately in chapter 4 as these data are novel and the group behaviour of the REE and methods employed for its interpretation require a slightly different approach. The database created by this work is very large, particularly as regards the analyses of major and trace elements, and so brevity is needed in its description. Where an element is not mentioned during the discussion of any particular sample set, this is because no significant features were found in its behaviour. Where appropriate, correspondences with previous work on the Tamar or other related environments are noted, and interrelationships of the various datasets obtained here are indicated. Forward references have been avoided where possible. These chapters necessarily include some discussion of the results where significant features arise, but this has been restricted to points of immediate relevance to the dataset under consideration.

Discussion of the results as a whole centres on certain key issues, and these are explored in detail in the sections of chapter 5, followed by the concluding remarks and an assessment of the implications of the results for estuarine processes as a whole.

Chapter 2

Sampling and Analytical Methods

2.1 General Considerations

2.1.1 Laboratory Usage

All porewater REE analyses were carried out in the marine chemistry clean laboratory in the Department of Earth Sciences at Cambridge University. Analyses of particulate samples were performed in a separate laboratory established for this work. Glass and metal surfaces were eliminated from the facilities where possible, and all sample handling was done with polythene, polypropylene, PTFE or silicone rubber apparatus. Manipulations of porewater solutions were performed under class 100 laminar flow hoods. All sample evaporations were performed photolytically using infrared lamps and PTFE hoods which were purged with filtered air in order to prevent airborne particulate contamination of the samples.

2.1.2 Reagents

Water. Various grades of water were used in this work. The purification system consisted of, in sequence, a commercial water softener, a Millipore reverse osmosis system (RO) backed up with an Elga de-ionising cartridge, a Millipore Milli-Q system, and a sub-boiling still fitted with a pure quartz cold finger and collector. The Milli-Q and quartz distilled (QD) water were collected and stored in 10 l polythene aspirators. The performance of the water purification system was monitored by regular analysis of the output of the reverse osmosis system for Na and Ca, measurement of the resistivity of the Milli-Q water, and periodic testing

of the quartz distilled (QD) water for REE by mass spectrometry (see section 2.1.4 for details of blanks). The softener replaces the Ca with Na, but does not remove ions from the water. The RO/Elga system then removes 100% of the Ca, 97% of all metal cations from solution. The Resistivity of the water is by this stage $0.5 \text{ M}\Omega\text{cm}^{-1}$, and the Milli-Q process increases this to $18 \text{ M}\Omega\text{cm}^{-1}$. The final distillation makes a further slight improvement on this.

Reagent Acids. Stock conc. HNO_3 and 6M HCl were made in batches by distillation in an all Quartz sub-boiling still (Kuehner *et al.*, 1972) using B.D.H. AnalaR grade acids as feed (prior dilution of the conc. HCl to 6M with Milli-Q water). Both were stored in 1 l Nalgene FEP bottles. Dilute acids (2M HNO_3 and 1.75M HCl) were made from these two stocks by dilution with QD water, and stored in 10 l polythene aspirators. Any solutions used in the sediment laboratory were never returned for use in the clean lab in case of any particulate contamination.

The HF used in the digestion of the solid samples was Aristar grade B.D.H. 40% HF. Due to the small quantities used in each preparation, and its hazardous nature, the HF was not redistilled.

Cleaning Acids. All acids used for cleaning procedures were made up from B.D.H. AnalaR grade stock mixed with R.O grade water.

2.1.3 Sample containers

In order to avoid significant contamination of samples during prolonged storage as liquids, care had to be taken to avoid any contamination due to contact with container surfaces. In view of the work by Marchant & Klopper (1978), Moody & Lindstrom (1977) and Roberston (1968a,b) and in line with practice in the marine geochemistry group at Cambridge University, all vessels and devices with which the samples came into contact were made of polyethene, polypropylene or silicone. Since the samples were not to be analysed for organic compounds, any potential organic contamination from the walls of the containers would not be significant.

All containers, tubes, etc. used during the sampling and storage were cleaned as follows:-

1. 24 hour soak in 50% HCl.
2. 24 hour soak in 10% HNO₃.
3. Triple rinse with RO, Milli-Q, then QD water.

2.1.4 Blanks

Mass spectrometric analysis of the acid reagents for REE (M. Greaves, *pers. comm.*) showed the concentration of Nd to be $\approx 0.05 \text{ pg ml}^{-1}$ for all reagents. Assuming a requirement of 40 ml of the various acids this would lead to a total of 2 pg of Nd being added to the sample. This is not the only contribution to the blank, however, and blank analyses for the whole process (Greaves *et al.*, 1989), showed the total to be less than 4 pg for Nd. The porewater samples analysed contained 30–90 pg ml^{-1} of Nd and ranged from 7–40 ml in size. As a minimum, therefore, the sample Nd would comprise approximately 200 pg. Blank contributions to results were thus less than 2%, which would be significant given the 1 % precision of the method for seawater samples (Greaves *et al.*, 1989), but is well within the precision of the results actually obtained in this work, typically 5–10%.

The particulate samples studied contained at least 30 ppm Nd, so using a small (70 mg) sample of sediment there would be at least 2 μg of Nd present. Processing typically required 160 ml of solutions, which would only contribute 8 pg, insignificant for these samples. A possible source of measurable contamination was the undistilled Aristar HF. The impurity data provided did not include REE values, but did quote Ni and Cu at less than 0.002 ppm. Taking this as a worst possible figure for Nd, the 10 ml of HF used in the digestion would contribute 0.02 μg Nd, i.e. at most 1% of sample Nd. This is also insignificant when compared to the quoted precision of the method (3.5% RSD for Nd Walsh *et al.*, 1981) or the values obtained here (table 2.5). Blanks were determined for the entire process by conducting complete preparations with no sample present. These gave results below detection limits for all analytes.

2.2 Sampling Methods

All the fieldwork done for this project was governed by two factors; firstly, trace metal contamination had to be avoided where possible, and second, it would be desirable to collect at least 300 *mg* of sediment or suspended particles from each sample for ICP analysis. Additionally, sediment pore waters were required, and estuarine waters from the axial surveys and turbidity maximum surface samples. Table 2.1 shows the timing of the three field exercises.

2.2.1 Collection of Sediment Cores and Separation of Pore Waters

Access to the intertidal sediments at Neal Point (20.5 *km* down estuary) was gained from 'Tamaris' (a Rotork sea-truck operated by PML) via a small inflatable craft. Three 30 *cm* long cores, spaced 5 *m* apart, were taken by slowly pushing 15 *cm* diameter cylindrical perspex corers into the sediment a short distance below the waterline, enabling the sediment to be removed along with a sample of the overlying water. A base was then forced down through the sediment adjacent to the corer and fitted before the core was removed from the sediment in order to minimise entry of air. Subsampling began immediately on return to PML, within 3 *h* of coring.

Subsampling of the cores was done in a N₂ filled glove-box as any contact by the reduced chemical species in the lower parts of the core with oxygen in the

Sampling Exercise	Date
Sediment Coring	17/4/85
Axial Surveys	
1. Neap Tide	12/8/85
2. Spring Tide	19/8/85
Turbidity Maximum Sampling	
1. Surface Samples	14/8/85 & 21/8/85
2. Vertical Profiles	8/7/86
3. Large volume sampling for settling procedure	8/7/86

Table 2.1: List of sampling exercises.

Fraction	Purpose	Container	Acidified?
1	Nutrients	20 ml P.P. vial	no
2	Fe&Mn	20 ml P.P. vial	yes
3	REE	20 ml P.P. vial	yes
4	Alkalinity	5 ml Glass Vacutainer	no

Table 2.2: Subdivision of porewater samples. Note:- P.P.= polypropylene.

atmosphere was to be avoided. The glove box itself had been specially designed for the purpose of handling anoxic sediment cores and was fitted with air locks for entry of materials without disrupting the N₂ blanket. The corers were adapted to seal against the base of the glovebox, and a jacking arrangement enabled the core to be pushed up into the body of the box for subsampling. Full details of the design of the glove-box and corers can be found in Upstill-Goddard (1985). The glove-box was continually flushed with oxygen-free N₂ and maintained at a positive internal pressure to prevent entry of air. The integrity of the N₂ blanket was monitored with a Beckman Model 0260 O₂ analyser mounted inside the glove-box.

Measured 1 cm slices of core were extruded, scraped off and placed in air-tight centrifuge bottles. These provided at least 200 g of wet sediment per slice. The centrifuge bottles were then removed from the glove-box via the air lock before the next core was processed. Centrifugation (for 15 minutes at 5000 rpm) began immediately. Whilst awaiting centrifugation, and during subsequent storage prior to filtration, the bottles were stored in a N₂ flooded box at 4°C. Volumes of porewaters obtained varied between 70 ml in the top portion to less than 30 ml per section at 17–18 cm depth.

Filtration of the pore-waters obtained was done in the glove-box using 20 ml polythene syringes and acid-cleaned 25 mm diameter Nuclepore 0.45 µm polycarbonate membrane filters. The filtrates from cores 1 and 2 were subdivided as shown in table 2.1. Porewaters from core 3 were divided into two subsamples; one for nutrient analyses and the other much larger volume for REE analysis.

Acidification was carried out by adding QD 6M HCl in quantities calculated to ensure that pH ≈ 1.5. Eppendorf adjustable micro-pipettes with disposable

polypropylene tips were used for all such operations. Nutrient analyses were carried out immediately after filtration and splitting; all other samples were refrigerated. The pH of the aliquots for REE analysis was checked again before prolonged storage, and re-adjusted where necessary.

The residual sediments from each sample were dried in air at 60°C and then ground to a fine powder in an agate lined 'Fritsch' mechanical mortar and pestle. Subsequent storage was in sealed polystyrene vials. It is possible that the drying at 60°C will have led to the volatilisation and loss of elements such as As, Cd and Hg, but as these are not being analysed for, and the elements determined in this work are of a more refractory behaviour, this is not significant.

2.2.2 Collection and Filtration of Estuarine Waters

Axial Survey & Turbidity Maximum Surface Sampling

Collection. The axial surveys of the Tamar Estuary were done from the vessel 'Tamaris' on the 12th August (neap tides), and on the 19th August (spring tides). Sampling began at the breakwater in Plymouth Sound and continued up-estuary on the rising tide.

Due to the fact that the waters from these samples were to be analysed for dissolved REE and dissolved Zr and Hf for other work, no compromises were possible in the sampling methods used, as contamination had to be kept to an absolute minimum. It would have been desirable to have distributed aliquots of the same sample to the various research groups operating from the vessel, but each had their own requirements as regards methods used, and this proved impossible to organise.

Samples were taken of the estuarine waters (20 on each survey) using a Watson-Marlow Model 601 peristaltic pump which operated at 15 l min⁻¹. The tubing used was polypropylene in the rigid parts of the assembly, and silicone in the flexible parts. The end of the sampling tube was held away from the side of the vessel by attaching it to a 5 m long rigid PVC pole. Samples were pumped into 60 l polypropylene carboys where low turbidities were anticipated, otherwise 10 l Nalgene high density polythene jerricans were employed. All containers were rinsed with a small amount of the sample before being finally filled.

Samples could more easily and rapidly have been taken using the on-board pump fitted to 'Tamaris', but this was ruled out on the grounds that it has a stainless steel rotor which could have contaminated the samples. On-board equipment enabled the PML staff to measure continually for salinity, temperature, dissolved oxygen, turbidity and pH (see section 2.2.3 for details), which enabled sampling sites to be identified. Individual measurements of salinity and turbidity of the actual samples obtained were carried out on return to PML.

Note that the surveys do not provide 'snapshots' of the estuarine conditions as the samples were taken consecutively, beginning shortly after low water in Plymouth Sound, and ending in the upper estuary $5\frac{1}{2}$ h later.

Two days after each of the surveys, time series of six samples of surface waters were collected on the rising tide from the turbidity maximum. Turbidities were anticipated to be in excess of 100 mg l^{-1} which meant that only a 2 l sample was required to provide enough solid material for the ICP analyses. Sampling was done from Tamaris by simply dipping a 2 l polypropylene bottle into the surface waters, after identifying the site of maximum turbidity with the sensors on board 'Tamaris'.

Filtration. Filtration of the samples began immediately on return to the laboratory at PML. Samples were agitated with a magnetic stirrer and pumped through 142 mm diameter $0.45 \mu\text{m}$ Nuclepore polycarbonate membrane filters which were mounted in a rigid polypropylene/PTFE rig. Filtration was slow, sometimes requiring 2 days per sample, and took 5 weeks to complete. 250 ml subsamples of filtrate were taken for determination of salinity, dissolved silicate, and dissolved Fe and Mn. After filtration the water samples were acidified to pH 2. The suspended particles were dried in a laminar flow cabinet at room temperature before being scraped off the filters with PTFE spatulas and further oven-dried at 60°C to maintain moisture content consistency with the sediments. They were then hand ground with an agate mortar and pestle. Both filtrates and removed particles were weighed to determine the turbidity of the samples.

The prolonged contact between the particles and the water in the samples caused concern because of the possibility of ongoing reactions distorting the re-

sults. However, the analyses of dissolved REE from the same samples showed no evidence of any effect due to the long storage, and as the REE in the particles are 10^5 – 10^6 times more abundant than in the waters there was not likely to be any discernible effect on the particulate REE abundances.

Turbidity Maximum Profiles & Settling Procedure

Collection. For both these sampling exercises, compromises were possible in the methods used to collect and treat the samples due to the less exacting requirements as regards trace metal contamination. Since no work was to be done on the trace metals in the dissolved phase from these samples it was possible to take samples from the river using the pumps on board the two vessels in use. This speeded up operations considerably and was vital as the intention was to take samples from various depths more or less simultaneously.

Depth profiles of estuarine waters in the turbidity maximum were obtained from a raft operated by Dr. J. West of the University of Birmingham at a site 10.5 km down estuary. The apparatus allowed simultaneous in-situ measurements of current velocity, particle size, turbidity and salinity (see Bale *et al.*, 1990 for details) to be made at a number of depths. Data for the latter three parameters were provided by J. West. Samples were taken from near-surface, mid water, and near bottom at six different times on the rising tide. The pumps were of PVC construction and were connected to the surface with silicone tubing. Samples were collected in 2 l polypropylene bottles.

The samples for the settling procedure were pumped into 60 l carboys using the pump on board 'Tamaris' (anchored at 10.2 km down estuary), returned to the laboratory at PML, stirred and allowed to settle for 12 hours. After settling, the liquid containing the remaining suspended particles was carefully siphoned off prior to filtration of the two separate fractions. Sub-samples of each fraction taken at this stage enabled measurements of turbidity and salinity to be made. Workers from PML used aliquots from the same initial large volume samples for determination of bacterial abundances (Plummer *et al.* 1987). Turbidity and salinity data quoted for these samples were provided by D. Plummer.

Filtration. Filtration of both sets of samples was done on a N₂ pressure filtration apparatus provided at PML. Its use had been precluded in the earlier work as the stainless steel support for the filters might have contaminated the waters passing through. The nature of the support and the pressures employed meant that a stronger filter than those used previously had to be selected, and a Sartorius 142 mm diameter 0.4 μm cellulose acetate membrane was used. These filters were not acid-cleaned.

Removal of the solids from the air-dried filters proved more difficult with the cellulose acetate membranes used in this work. Whereas previously the solid material only needed gentle encouragement with a spatula, this was inadequate in this case. Furthermore, the filters themselves became brittle when dry, and could not withstand even moderate manipulation without breaking up. The solution found involved wetting the filter with QD water, washing the solids off into a 100 ml PTFE beaker (acid cleaned) with as little QD water as possible, and evaporating off the water. The deposit from this was then hand ground and transferred to a polystyrene storage vial.

2.2.3 Back-up Data

The data from the ICP and mass spectrometric analyses is supported by information on nutrients, salinity and other trace metals in the estuarine and sediment porewater samples studied.

Pore Waters. Nutrient and NH₃ analyses were carried out by R.C. Upstill-Goddard immediately after retrieval of the samples from the glove-box. Fe & Mn and alkalinity were analysed subsequently at PML by P. Watson, and the sulphate on return to Cambridge. Methods used are listed below:-

- NH₃: Chemlab autoanalyser method CW2-008-11.
- Si : Chemlab autoanalyser method CW2-083-04.
- PO₄³⁻: Chemlab autoanalyser method CW2-075-20.

- Fe & Mn: Atomic absorption spectrophotometry, PYE-Unicam SP9 in flame mode.
- SO_4^{2-} : Radiochemical BaSO_4 precipitation (Rosenbauer *et al.*, 1979).
- HCO_3^- : Computer controlled titration (Wilson, 1983).

Estuarine Waters. During the axial surveys, continuous monitoring of the parameters salinity, temperature, dissolved oxygen, pH and turbidity was carried with equipment installed onboard 'Tamaris'. This enabled samples to be taken at optimum sites as well as providing position data for the interpretation of the results. The techniques used are described fully in Morris *et al.* (1982a). Due to the high variability of the estuarine waters, especially at low salinity and high turbidity, and the fact that the samples analysed for REE *etc.* were not taken using the vessel's pumping system which fed the continuous monitors, individual measurements of salinity and turbidity were made on return to the laboratory. Turbidity was determined gravimetrically as mentioned in 2.2.2. Accurate salinities were determined by R. Howland at PML from aliquots of the water samples. Techniques used were a chloride electrode where salinity was less than 2 ppt, and an Autolab bench salinometer at higher salinities.

2.3 I.C.P. Spectrometry

All the solid samples obtained in this project were analysed by Inductively Coupled Plasma Emission Spectrometry (ICP). The method involves obtaining a solution of the sample by an appropriate means, and then introducing it into an Argon plasma 'flame'. In this environment the solution dissociates completely, and the excited atoms emit their characteristic spectra. These spectra are then resolved and measured by an optical spectrometer, and the concentrations of the various elements can be calculated by reference to appropriate standards (Thomson & Walsh, 1983).

As an analytical technique I.C.P. analysis has a number of advantages over the more traditional methods such as X.R.F. or A.A.S. for multiple trace element analyses, particularly for REE. Atomic absorption spectrophotometers (Price, 1979) have adequate detection limits, but can only deal with one element at a time, and with the number of samples generated by this work the task would have been enormous. X-Ray Fluorescence would have been more useful in view of its simultaneous analysis capability (Norrish & Chappell, 1977), but the quantities of solid material required by the pressed powder pellet method were unattainable from any of the fieldwork carried out in this project other than the sediment sampling. Neutron activation (Henderson & Pankhurst, 1984) is difficult and time consuming. The rapidity of the actual analysis, the relative (compared to XRF) freedom from matrix effects and inter-element spectral interferences, and the much greater linearity of the machine response to elemental concentrations (Thomson & Walsh, 1983), make ICP analysis a very powerful technique for trace metal work.

The facility used for all the ICP analyses presented here is run for N.E.R.C. by Dr. J.N. Walsh, and was located at Kings College, London, before moving to Royal Holloway and Bedford New College, Egham, in 1986. The facility was used routinely, involving separate runs for the determination of the REE versus the major, minor and other trace metals. The details of the analytical conditions and performance are described in Walsh (1980), Walsh & Howie (1980), Walsh *et al.* (1981) and Thomson & Walsh (1983). The 'Traces' and REE programs provide

TRACES		REE
weight %	ppm	ppm
Al ₂ O ₃	Ba Ce	La Ce Pr
Fe ₂ O ₃	Cu Cr	Nd Sm Eu
MgO	Co La	Gd Dy Ho
CaO	Li Mo	Er Yb Lu
Na ₂ O	Nb Ni	Ba Sr Cu
K ₂ O	Sc Sr	Cr Ca Fe
TiO ₂	V Y	
P ₂ O ₅	Zn Zr	
MnO		

Table 2.3: Major element oxide and trace element analyses provided by the ICP.

the analyses shown in table 2.2. The preparative chemistry used differs from that mentioned in these papers, however, and is discussed in detail in sections 2.3.1 to 2.3.3. For this reason, and also because of the precision of the analysis for some elements (see section 2.3.4), not all the data from both analyses were finally used.

Sample digestion for the 'Traces' analysis could have been avoided by the use of a slurry atomisation technique (Ebdon & Cave, 1982). However, there was simply not enough material from most of the estuarine particle samples, given the need for carefully graded samples with particle sizes $< 10 \mu\text{m}$, and 4–5 ml of a 10% suspension. Also, samples would still have to be digested for the separation of the REE.

Due to the distance between Cambridge and London, the samples were simply processed and stored until a large enough batch was built up to make a trip to the analytical facility worthwhile. It proved possible to run 100 samples plus appropriate standards per day. Usually one day was devoted to REE work, and the following day to the 'Traces' program.

2.3.1 Sample Digestion

Obtaining complete solution of silicate samples can present problems as the decomposition of the mineral lattices necessitates the use of HF. Some methods also specify HClO₄, which cannot be used in plastic lined fume cupboards. An alternative to the sand-bath decomposition using HF and HClO₄ described in Walsh

(1980) had been developed in Cambridge (Kennedy & Elderfield, 1985). These were adopted as the starting point for the techniques used in this work.

The procedure was as follows:-

1. Weigh 0.1 g of dry sample into a clean 30 ml PTFE beaker.
2. Add 8 ml Aristar 40% HF, stand cold for 2-6 hours.
3. Add 2 ml QD conc. HNO₃, evaporate to dryness overnight.
4. Add 2 ml QD conc. HNO₃, evaporate.
5. Repeat above step if necessary to oxidise white fluorides.
6. Add 8 ml 6M QD HCl, evaporate.
7. Add 10 ml 1.75M QD HCl and transfer sample to screw-top plastic vial for ICP analysis.

It is not clear exactly what temperature the samples reach whilst evaporating, however the bulk of the process proceeds photolytically with the solution at about 70–80°C. As the sample approaches dryness and forms a paste the temperature rises to over 100°C.

This technique was adequate for the deep-sea sediments being analysed at the time (Kennedy & Elderfield, 1985), and had a number of advantages over the methods in use at Kings College. Firstly, the whole process could be carried out in a particle free environment (see section 2.1.1), avoiding any potential airborne contamination. The small quantities of clean reagents used reduced the risk of significant analytical blanks. These reagents demand a rather labour-intensive preparation, so keeping the quantities used to a minimum is essential. Also, the use of platinum vessels is avoided, which helps to reduce the exposure of the sample to any potential trace metal contamination, as well as keeping the laboratory costs down.

When this procedure was tried out on the estuarine sediments obtained in the April 1985 fieldwork, problems soon became evident. A scum of small black particles would appear on the surface of the solution in the final stages of preparation, and a small quantity of fine particles were deposited on the bottom of the beaker.

Organic Matter. Digestion of the sediment after ashing in a LFE Corporation LTA-302 low temperature asher did not produce the black scum previously observed, indicating that it had been due to the presence of organic material. Weight loss of the sediment during this procedure showed the combustible organic content to be $\approx 1.5\%$.

The routine use of the asher was rejected as the labour involved was considerable. Only a few samples could be processed at a time, the ashing had to be carried out more than once in a shallow glass dish, with risk of disturbing and losing some of the finely powdered sediment as it was stirred between runs. Weighing the samples after the ashing proved difficult because the weight changed continually as the sample absorbed moisture from the atmosphere. An attempt was made to carry out the ashing in the PTFE beaker used for the digestion, but the ashing was always incomplete as the oxygen could not efficiently reach the sample at the bottom of the tall narrow beaker. It was also found that the process was measurably eroding the beakers at a rate of up to 50 mg h^{-1} , which was considered to be undesirable. It was subsequently found that the organic matter could be degraded by simply repeating stage 4 of the digestion process until the scum disappeared.

Resistant Minerals. The fine sediment deposited in the beaker was thought to consist of some resistant mineral phase or phases, but might have included some partially digested aluminosilicate. Ultrasonic agitation during the HF soak was adopted to alleviate the evident aggregation, which was suspected as a possible cause of incomplete attack by the HF on the solids. This did reduce the amount of sediment left at the end of the digestion, but did not eliminate it entirely. It is likely that the grinding process did not reduce the grain size of the resistant phases sufficiently to allow complete digestion.

Subsequently, attempts were made to dissolve this resistate by carrying out the digestion in sealed PTFE bombs held in stainless steel pressure cases at 200°C . This still proved insufficient, and would have substantially decreased the rate at which the samples could have been processed had it been adopted as standard practice.

In order to determine the significance of these phases, 3 g of sediment were digested, yielding less than 2 mg of minerals. These were then analysed on a Laser Induced Mass Analyser (LIMA) in order to identify the elements present and the likely phases. The LIMA (operated by the Metallurgy department at Cambridge University) provides a mass spectrum from almost any type of solid sample, but was not at that time capable of producing quantitative concentration data from materials more complex than simple alloys. A laser beam is focussed on the desired part of the sample. This causes volatilisation and ionisation of a 1 μm wide spot of the material, which is then resolved on a time-of-flight mass spectrometer. The advantage of this device over other micro-analysis methods is its sensitivity, and the fact that no preparation of the sample is required other than mounting it on some sticky tape. Spectra obtained indicated the presence of organic matter (C,H,O), Zircons (Zr,U,Hf,Si), Rutile (Ti,O), Tourmaline (Li,B,F), Ilmenite (Fe,Ti), and an unidentified Sn mineral in the resistate. Given the tiny quantities left by the digestion, and the levels of Ti, Fe and Li in the samples (Zr,Hf,U and Sn were not analysed for), the loss of this material is insignificant. Centrifugation in acid-cleaned polypropylene tubes was used to separate the residue. Although referred to as a 'total' analysis, this method is therefore only measuring open-beaker HF/HNO₃ soluble concentrations of the elements concerned.

Final Procedure. The final method was therefore as follows:-

1. Weigh 0.1 g of dry sample into a clean 30 ml teflon beaker.
2. Add 8 ml Aristar 40% HF, agitate in ultrasonic bath for 5 minutes, stand cold for 2-6 hours.
3. Add 2 ml QD conc. HNO₃, evaporate overnight.
4. Add 2 ml QD conc. HNO₃, evaporate.
5. Repeat above step if necessary to oxidise white fluorides and decompose organic matter.
6. Add 8 ml 6M QD HCl, evaporate.
7. A) Add 10 ml 10% QD HNO₃, agitate sample in ultrasonic bath for 5 minutes, leave to stand overnight. Transfer sample to centrifuge tube,

centrifuge at 5000 rpm for 10 minutes. Pour off most of supernatant liquid into screw-topped plastic vial for ICP analysis.

OR

B) Add 5 ml 1.75M QD HCl, agitate sample in ultrasonic bath for 5 minutes, leave to stand overnight. Transfer sample to centrifuge tube, centrifuge at 5000 rpm for 10 minutes. Load 4 ml of the solution onto column for separation of the REE.

During the waiting stages the samples were covered with parafilm, and with the exception of the HF soak, were stored in a laminar flow clean hood. Quantities of acid in 7A above were dispensed using Eppendorf 5 ml adjustable pipettes with disposable polypropylene tips, and measured by weighing. For 7B quantities were measured with Eppendorf 1ml pipettes and disposable tips. Volumetric precision for the dispensing was 0.1% R.S.D. or better in both cases.

Container Cleaning. All PTFE beakers were cleaned as follows:-

- 1 hour clean with Decon 90 in ultrasonic bath.
- 48 hour soak in 50% HCl.
- 48 hour soak in 50% HNO₃ at 60°C.
- Storage in RO water.

Sample vials were cleaned as follows:-

- 48 hour soak in 50% HCl.
- 48 hour soak in 10% HNO₃.
- Storage in RO water.

Centrifuge tubes were simply soaked in 50% HCl for 24 hours, and then rinsed and dried before use. Vessels were stored in water in sealed tubs, then rinsed with QD water and dried in a laminar flow clean hood as required. Samples awaiting analysis were stored in a fridge at 4°C.

In a few cases where turbidities had been less than anticipated there was less than 200 mg of sample available . As this was not enough for a separate leach and digestion, the digestion was carried out on the residue from the leach process. The total could then be calculated from the two results. Replicate analyses of the Tamar composite sediment described in 2.3.4 showed no significant difference between the results obtained in this way and those from the simple digestion.

2.3.2 Leaching Procedures

In theory, pH balanced leaching procedures (Aplin & Cronan, 1985; Boust, 1982; Chester & Hughes, 1967; Tessier *et al.*, 1979) selectively dissolve the individual Fe and Mn oxides adhering to the detrital silicates. Such procedures are often complex and are not completely specific as regards trace metal speciation in the various oxide phases dissolved (Robinson, 1984). Comparisons of the results of selective leaching procedures with the trace metal distributions obtained by electron microprobe analyses (Lee & Kittrick, 1984a,b; Tipping *et al.*, 1985) have indicated that selective leaching routines can create artifacts in terms of the mineralogical phase residence of certain elements. In view of this, and with the simplicity of analytical procedures in mind, it was decided to use a single stage leach which would remove all the phases likely to harbour the labile fractions of the trace and other metals with minimal attack on the detrital silicate minerals. Agemian & Chau (1976, 1977) reported that 0.5M HCl successfully extracted all the labile metal content from aquatic sediments as long as there was sufficient H⁺ present to neutralise all the carbonate present, and with minimal attack on the silicates. Also Malo (1977) has shown with serial 0.3M HCl leaches that the limiting factor for metal extraction is the ultimate digestion of the oxides rather extraction from the silicates. A test leach using HCl on the Tamar Composite sediment was therefore carried out.

Four separate 120 mg aliquots of the Tamar composite sediment were leached in 5 ml each of 0.5, 1, 2, 3 & 4M QD HCl. Leaching was carried out over one hour with continuous agitation in an ultrasonic bath, and complete resuspension of the sample every 15 minutes. The samples were then centrifuged at 5000 rpm for 10 minutes, and 4 ml of the supernatant solution transferred to a PTFE beaker

for evaporation. Finally the solids were taken up in 5 ml 10% HNO₃ for ICP analysis.

Results obtained from the ICP raw intensity program showed that levels of Fe and Mn were lowest in the 0.5M, higher and steady in the 1, 2, and 3M solutions, and significantly higher in the 4M. However, the levels of Al and B rose substantially in the 4M sample, indicating that the silicates were suffering more severe attack. Taking account of the fact that there was a plateau in the levels of Fe & Mn in the solutions from the 1, 2 & 3M leaches, that 1.75M HCl was already available in the laboratory and was also used as the loading solution for the cation exchange columns, it was decided to adopt the 1.75M acid as the standard leach reagent.

The leaching procedure was as therefore as follows:-

1. Weigh out 120–150 mg of sample into centrifuge tube.
2. Add 5 ml 1.75M QD HCl.
3. Agitate for 1 hour in ultrasonic bath with complete resuspension every 15 minutes.
4. Centrifuge for 10 minutes at 5000 rpm.
5. A) Transfer 4 ml of the supernatant to a 30 ml PTFE beaker, evaporate down and take up in 5 ml 10% QD HNO₃ for ICP analysis.

OR

- B) Transfer 4 ml of the supernatant directly to a column for REE separation.

All solutions were measured using Eppendorf 1 ml pipettes with disposable tips. Larger devices would have been more convenient, but could neither reach the bottom of the centrifuge tube, nor load samples onto the columns without touching the sides. This conveniently eliminated the need for any inter-device calibrations.

Publications subsequent to the adoption of this method (Kersten & Förstner, 1987; Martin *et al.*, 1987; Rapin *et al.*, 1986) have examined the problems associated with 'selective' leaching procedures in great detail. In particular, anoxic

sediments are extremely sensitive to exposure to air prior to extraction, and the air drying used for the sediment samples here would have rendered any selective leach data invalid.

2.3.3 Column Chemistry

Cation exchange chromatography is the preferred method for the separation of the REE from the major elements in a sample prior to ICP analysis (Brenner *et al.*, 1984; Crock *et al.*, 1984). The reason for separating the REE from the other elements is to minimise the spectral interferences that elements such as Fe, Ca, and Ba cause, hence improving the precision of the analyses (Thomson & Walsh, 1983; Walsh *et al.*, 1981). The differing binding characteristics of the various elements or groups of elements with the cation exchange resin (Strelow, 1960; Strelow *et al.*, 1965) enable them to be separated from each other when loaded onto a column of the resin and then eluted with specific acids (Strelow, 1966 & 1980). The methods previously established at Cambridge (Kennedy & Elderfield, 1985) used a bed of 200–400 mesh Bio-Rad AG 50W-X8 resin supported in pure quartz columns, and had been used for the separation of Sr for mass spectrometric analysis. As a result, the separation of the REE from major elements was not optimized.

The methods in use were adequate, but the desire to improve this coincided with the need to develop an integrated method for the determination of the REE and other elements. The existing routines involved separate digestions of the solid sample for the REE and 'Traces' determinations, and the major elements eluted from the column before the REE were simply discarded. This seemed wasteful, and with the number of samples to be processed in this work, would lead to substantial duplication of the dissolution and leaching processes. If the major elements could be quantitatively recovered from the columns in a convenient volume, then one dissolution of the sample would suffice for both analytical programs.

In order to be sure of the separation of the REE group from the other elements the column chemistry had to be changed. The controlling factor in this procedure is the distribution (measured as K_d) of any given element between the resin and

and the acid solution. These have been documented for Bio-Rad AG 50W-X8 for HCl, H₂SO₄, and HNO₃ solutions of various molarities (Strelow, 1960; Strelow *et al.*, 1965). From the data in these papers it can be seen that in order to best separate Fe from the REE, 1.75M HCl had to be used for some part of the elution (Strelow, 1966), and to optimize the separation of Ba from the REE (Strelow, 1980) 2M HNO₃ would also have to be used (the existing methods lacked a HNO₃ stage). Another important consideration is the total amount of cations being loaded on to the column versus the exchange capacity of the resin. Knowing the approximate major element composition of the samples, the H⁺ equivalent charge (in terms of *mmol*) can be determined from the ionic charge of each species, and is expressed in *meq*. To optimize the shape of the elution curves and avoid excessive tailing, the ratio of the amount of charge in the sample divided by the capacity of the column (Q), should be maintained in the range 0.1–0.4. If Q is too low, the retention of the cations on the column is increased and large volumes of high molarity acid are needed to retrieve them. If Q is too large the various elements run through the column very quickly and the separations are poor (Strelow *et al.*, 1965).

Taking all these factors into account, a batch of 1 *cm* internal diameter quartz columns were set up with a resin bed of 12.6 *cm* (as used previously). The capacity of the resin is 1.7 *meq ml*⁻¹ of resin bed, so an anticipated load of 2 *meq* (calculated for 150 *mg* sediment) would yield Q≈0.12. The resin was cleaned in 6M HCl after floating off any fines, then measured into the columns in 1.75M HCl. In order to test the separation achieved the columns were calibrated by both ICP analysis and radiochemical means. The procedure used was as follows:-

- Load sample onto column in 1 *ml* 1.75M HCl.
- Wash in with 4 *ml* 1.75M HCl.
- Elute with 50 *ml* 1.75M HCl.
- Elute with 2M HNO₃ until all REE recovered.

The radiochemical calibration was achieved by adding 100 μCi ¹³³Ba, 300 μCi ¹⁵³Gd and 700 μCi ¹³⁹Ce to the sample, evaporating it to dryness and re-

dissolving to ensure equilibration, and then counting the radioactivity in each of the 3 ml (50 drops) fractions collected from the column as the sample was eluted. The separation between Ba and the REE was acceptable, at least 50 ml (fig 2.1), so another calibration to check the relative positions of the other elements was done by analysing the fractions obtained by ICP. A selection of the elution curves obtained are presented in figure 2.2 Note that none of the elements of interest were eluted in the interval between Ba and the REE.

Once satisfied that all the major and minor elements of interest could be recovered by collecting all the material coming off the columns until the end of the barium peak, the removal of the REE could be achieved by stripping them off the resin with 50 ml of 6M QD HCl (Kennedy & Elderfield, 1985).

Ideal as this procedure was in terms of the good separations, it soon became obvious when attempting to use it routinely that it would have to be modified. The major elements to Ba required over 150 ml of acid to elute. This required two beakers to collect, as the maximum size of PTFE beaker that could be accommodated in the evaporators was 100 ml (see section 2.1.1.). The number of transfers, rinses, and hours of evaporation that were needed to re-unite the samples made management difficult and throughput slow. The obvious solution was to shorten the columns to reduce the volumes required, but the danger in this was that the increased value of Q would possibly reduce the separation to an impractical point. Halving the column length would raise Q to 0.24, still reasonable, so a column length of 7 cm was adopted. In order to maintain the relative element separations of the previous longer columns, the proportions of the first two eluants would have to be held roughly consistent.

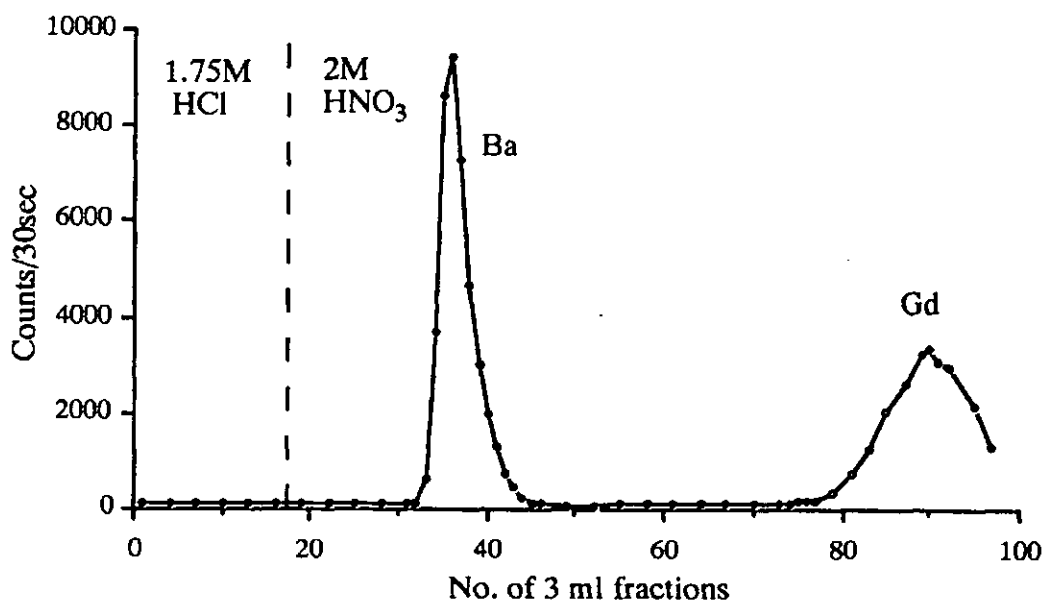


Figure 2.1: Elution curves for 12.6 cm column showing separation between Ba and the REE.

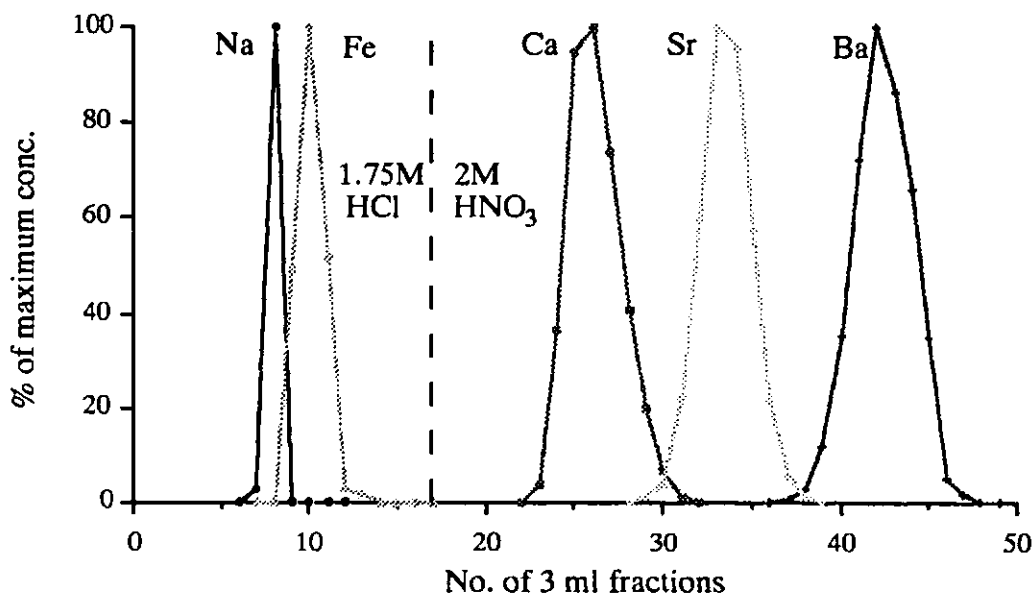


Figure 2.2: ICP calibration of 12.6 cm column to show relative positions of major and minor elements. Not all elements analysed are shown.

Coincident with these developments, the dissolution methods for the samples were being adapted and the leach developed. The new routines meant that the load volume was now 4 ml, so the calibration carried out was as follows:-

- Load sample onto column in 4 ml 1.75M HCl.
- Wash in with 2 × 1 ml 1.75M HCl.
- Elute with 25 ml 1.75M HCl.
- Elute with 2M HNO₃ until end of Ce tracer.

As before all the 3 ml fractions collected were checked for radioactivity. The elution curves obtained are shown in figure 2.3. Note the 12 fraction separation between the Ba and Gd peaks.

On this basis, a set of columns were made up with 7 cm resin beds. Two were selected at random and calibrated again, only the HNO₃ was stopped at 60 ml, and the REE were stripped off with 6M HCl. The results showed the two columns to be identical as regards which fractions contained any tracer, and all the ¹³⁹Ce was recovered by 45 ml of 6M HCl. (See fig. 2.4.)

In order to be sure that all the elements to Ba were being recovered quantitatively from the columns, a set of six identical samples were analysed on the ICP both after separation of the REE, and by simple dissolution of the sample. The results from the two sets of samples were indistinguishable within the limits of precision reported in section 2.3.4. The method finally adopted as routine is shown in table 2.4.

The solutions containing the major and trace elements were collected in a 100 ml PTFE beaker, evaporated, taken up in 10 ml 10% HNO₃, and transferred to a plastic vial for ICP analysis. The eluant containing the REE was collected in a 50 ml PTFE beaker, evaporated, taken up in 5 ml 10% HNO₃, and stored in a plastic vial until analysis. All acids used were QD, except for the column washing where a cleaning grade made up from AnalaR stock and Milli-Q water was used.

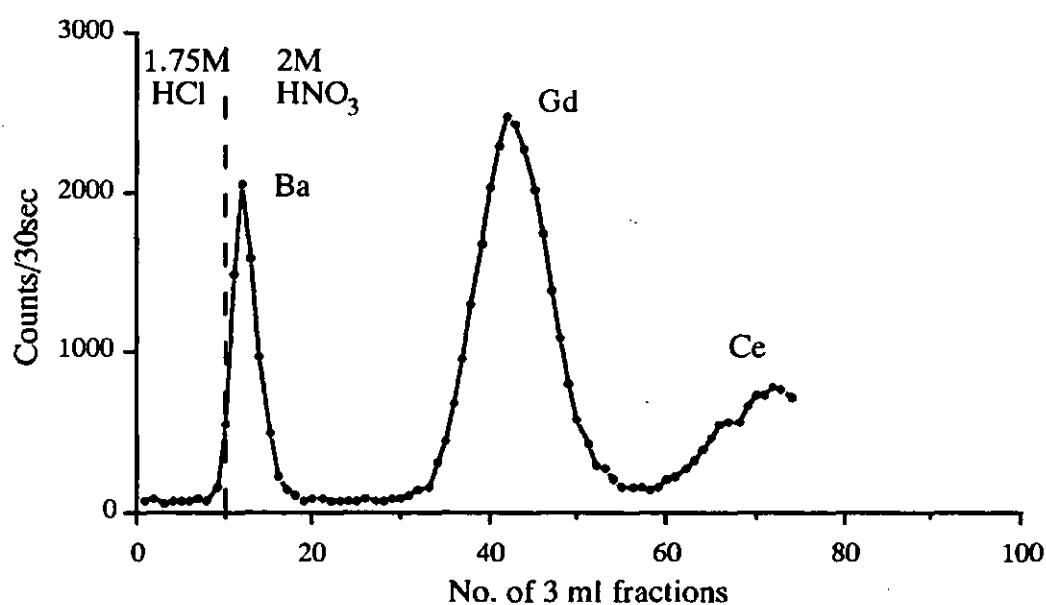


Figure 2.3: Elution curves for the shortened (7 cm) column showing the persistent separation of the REE from Ba.

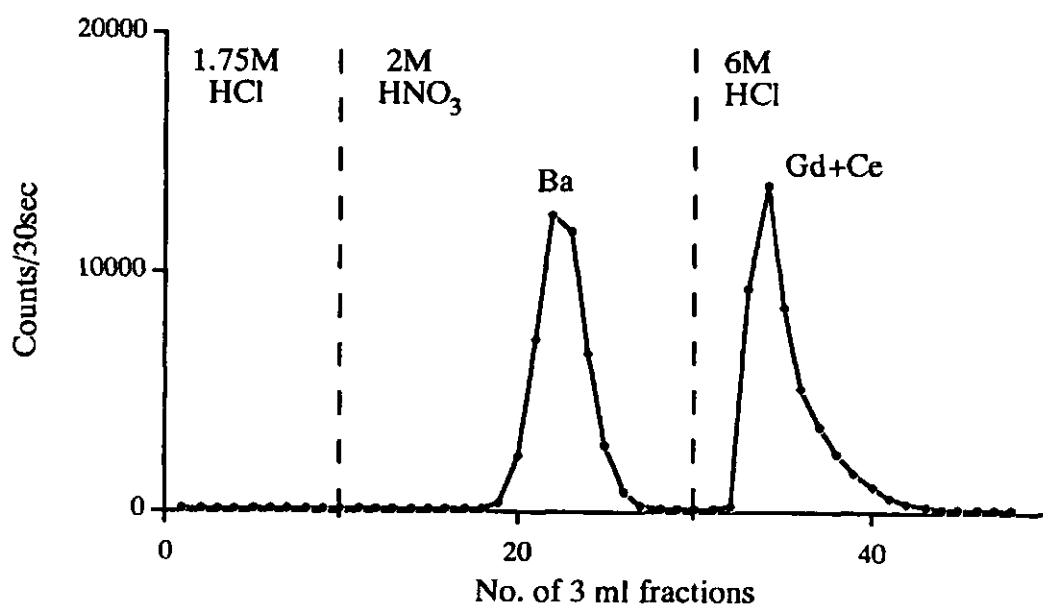


Figure 2.4: Elution curves for the 7 cm column showing the complete recovery of the ¹³⁹Ce tracer by 45 ml 6M HCl after elution with 30 ml 1.75M HCl and 60 ml 2M HNO₃.

Precondition column	10 ml 1.75M HCl	Discard
Load sample	4 ml 1.75M HCl	Collect for major and trace elements
Wash in sample	2 × 1 ml 1.75M HCl	
Elute	25 ml 1.75M HCl	
Elute	60 ml 2M HNO ₃	
Elute	50 ml 6M HCl	Collect for REE
Wash column	full bowl 6M HCl	Discard
Displace acid	10 ml water	

Table 2.4: Elution procedure for separation of REE from major elements prior to ICP analysis.

The three types of beakers used for the digestion, major element collection, and the REE collection were kept separate at all times to avoid any potential contamination, and the cleaning acids were replaced at regular intervals. The resin in the columns was replaced after every 7–8 runs as its exposure to 6M HCl eventually causes degradation, and any change in the elution characteristics was to be avoided.

2.3.4 Data Quality

The data provided by the analyses assume that standard weights of sample and volumes of final solution (100 mg in 10 ml for 'Traces' and 500 mg in 5 ml for REE) have been used. The results have thus to be corrected for the quantities actually used. These adjusted data then have to be corrected for machine drift. During a session the calibration of the instrument varies, but this can be accounted for by analysing a sample of known composition after every six or so samples, and then calculating (as a factor) the deviation of each analyte from the expected value. These factors are then applied to the samples analysed between the standards, using corrections derived from the nearest standard in time. The

correction factors were not interpolated between the standards as the machine drift is not necessarily linear. The standard used for the 'Traces' analyses in this study (KC11, an in-house rock standard from King's College) was chosen because of the proximity of the concentrations of a number of the analytes to the levels expected in the estuarine samples.

The data presented in the appendices do not contain all the information provided by the ICP analyses (see table 2.2). The 'Traces' analysis provides data for La, Ce, Nd, Sc, Y and Zr which are retained by the REE fraction, so these data were discarded. The Y data shown were in fact transferred from the REE analyses for each sample. Of the remaining results, a further three were rejected for the following reasons:-

- Mo: The data given for the standard KC11 do not show a value for Mo, despite its presence. Examination of the results from the estuarine samples showed numerous zero results as well as an inconsistent relationship between the values for Mo in the two batches of KC11 solution being used. (One batch was provided at the facility, and the other made up at Cambridge.) This indicated poor precision at the levels of Mo present.
- Nb: The leached samples provided zero results, and the values of ≈ 20 ppm from the digested samples were very close to the detection limit of 10 ppm (Thomson & Walsh, 1983). As with Mo, the relationship between the results for Nb in the two standards was erratic.
- Cr: Poor precision was indicated as the values obtained for Cr in successive analyses of KC11 varied by up to 25% whilst other elements (Co & Cu) varied by less than 3%.

The REE results provide information on the levels of elements which interfere spectrally with the REE, such as Ba, Ca and Fe, for samples where the separation of these is inadequate. The much improved separation of these elements (see section 2.3.3) ensured that all (with the exception of Y, mentioned above) gave near zero results, and produced insignificant interference.

To monitor the overall precision of the methods used, multiple analyses of a standard sediment were conducted. In addition, analyses of international rock standards were done to assess the accuracy. The standard used for the replicate analyses was created by mixing aliquots from each of the sediment samples from the cores. Use of a known rock standard would have given a false impression of the precision as such materials were found to be easier to prepare for analysis than the estuarine samples. The rock standards have usually been carefully sieved and graded, making the refractory minerals easier to digest, and the standards available did not contain significant quantities of organic matter. Use of an estuarine material prepared by the same methods as the actual samples studied gives a more realistic assessment of the overall precision of the method. The estuarine samples studied in this work were analysed over just two machine runs. Aliquots of the Tamar composite sediment were analysed during both.

Inspection of the data showed clearly that the results for most elements of both the REE and Traces analyses were higher in the second run. What this was due to is not clear, as the in-house rock standards provided should have been consistent, however, the machine's move from King's to Royal Holloway and Bedford New College may have been significant. Fortunately the differences were generally small, *e.g.* the mean Nd values obtained for the composite sediment were 30.3 and 32.4 *ppm* for the two machine runs respectively, a difference of less than 6.5%.

Analyses of the international standards G-2 and SY-3 (done only in the second run) gave values for the REE and major elements that accorded well with those in the literature (Abbey, 1979; Brenner *et al.*, 1984; Crocké & Lichte, 1982; Flanagan, 1973; Walsh *et al.*, 1981). To test whether the first run would have given a better correspondence, mean values for each analyte in the four types of analysis were calculated from the many analyses of the composite sediment in both runs. The relationship between these means was calculated as a factor, and applied to the analyses of the international standards to generate values that would have been obtained if they had been analysed in the first run. The correspondence was less satisfactory, so the analyses obtained in run 2 were taken to be more accurate. To take account of difference between the runs, all the data from run 1 were

Precision of ICP Analyses (% RSD)					
	TRACES			REE	
	Digestion	Leach		Digestion	Leach
Al ₂ O ₃	1.2	7.5	La	2.5	3.1
Fe ₂ O ₃	1.1	3.8	Ce	2.4	3.2
MgO	1.0	3.7	Pr		
CaO	1.8	2.2	Nd	2.4	2.5
Na ₂ O	0.8	1.4	Sm	2.1	3.7
K ₂ O	0.9	4.4	Eu	2.0	5.0
TiO ₂	3.0		Gd	3.8	5.0
P ₂ O ₅	3.4	2.3	Dy	2.3	1.9
MnO			Ho	3.3	4.9
Ba	4.0	9.5	Er	2.4	5.0
Co	4.6	5.6	Yb	2.9	5.5
Cu	2.4	2.0	Lu		
Li	2.4				
Ni	1.8	6.1			
Sr	1.5	1.4			
V	1.2	3.4			
Zn	3.1	6.1			
Y	1.1	4.9			

Table 2.5: Table showing precision of ICP analyses for all four analytical routines.

corrected to 'run 2' values by application of the relevant factor.

Of the REE, Pr and Lu required factors of 1.7 and 1.4 respectively, which cast doubt on their accuracy. The 278 ppm Pr measured in the international standard SY-3 is substantially different from the 100 ppm obtained by Brenner *et al.*, (1984), but is closer to the 239 ppm derived by Crocke & Lichte (1982). However, the large difference between the runs was considered unsatisfactory and neither Pr nor Lu data have been included in the interpretation.

The precisions calculated from the adjusted data are presented in table 2.5. The blank entries and instances of poor precision are explained below:-

- TiO₂ & Li: The leachates contained virtually none of these two analytes as they are concentrated in the resistant minerals. Hence the precision was ≈ 30% and the results meaningless. No data for these elements are quoted in the leach results.

- MnO: The Tamar composite sediment contains only 0.06% MnO, which creates artifacts in the statistics as the results are only quoted to 2 decimal places. The levels in the estuarine particles are higher at 0.2–0.8%, and the concentrations measured in the international standards accorded well with published values. From the information in Thomson & Walsh (1983) and the performance of the procedures overall, estimates have been made of < 3% precision for the digestion, and < 5% for the leach.
- Ba: Thomson & Walsh (1983) suggest that poor precision for Ba can be caused by BaSO₄ insolubility when sulphides are present in the sample. The Tamar composite sediment certainly contains sulphides, and any insoluble phases would have been centrifuged off after the leaching process. However, accuracy is good, the 428 ppm Ba measured in SY-3 being very close to the 430 ppm reported by Abbey (1979).
- Co: This element suffers statistically in the same way as MnO, with only 16 ppm in the sediment. Levels of up to 60 ppm in the estuarine particles would certainly improve the apparent precision. Accuracy is good with 12 ppm Co in SY-3 corresponding exactly with Abbey (1979).
- Cu: Although precision is good, the 33 ppm Cu measured in SY-3 is double the figure of 16 ppm reported in Abbey (1979). Comparison of the estuarine Cu values with the previous Tamar data in Morris *et al.* (1986a) does not reveal a discrepancy of this magnitude, so the data were retained.

Overall, the precision of the analyses is satisfactory considering the unpredictable properties of the partially digested resistant phases, and the small size of the samples for the REE (120–150 mg rather than the 500 mg recommended for the procedure in Thomson and Walsh, 1983).

2.4 Mass Spectrometry

The porewater samples collected in this work were analysed for REE by Isotope Dilution Mass Spectrometry (IDMS) on a V.G. Isomass 54E mass spectrometer at Cambridge University. The technique depends on the fact that most of the rare earth elements have more than one isotope. By adding a known amount of a spike with artificially modified isotope ratios to a natural sample with an unknown concentration of the element concerned, it is possible to calculate the concentration of the element from the new ratios between the various isotopes as measured on a mass spectrometer (Faure, 1986). The technique has the virtue that because isotope ratios are being measured, once the sample has been spiked and equilibrated, quantitative recovery of the element of interest is no longer necessary. As long as the isotope ratios are preserved the analysis is valid. The chemical processes used here cannot cause any significant mass fractionation.

The method used consists of co-precipitation of the REE from a mixed sample and spike solution with $\text{Fe}(\text{OH})_3$, followed by separation of the Fe and other sea-salt cations from the REE by cation exchange chromatography. The REE are then loaded onto a Re/Ta filament for the mass spectrometry. A full description of the method can be found in Greaves *et al.* (1989), and this itself is based on the work done by Elderfield & Greaves (1983) and Thirlwall (1982). (Note that IDMS can only analyse for the poly-isotopic rare earths, which means that Pr, Pm, Tb, Ho and Tm cannot be measured. ICP analysis does, however provide data for Pr and Ho.) The method was used routinely according to the standard methods set up in the clean laboratory at Cambridge, and all the details of the procedures, particularly the machine conditions and isobaric interferences between the various rare earths and Ba will not be discussed here. However, as the column chemistry was developed in part from some of the calibrations done for the ICP work reported here, details of the sample treatment prior to machine analysis are described below.

2.4.1 Details of Method

One week before spiking, samples were checked to ensure that the pH was 2, and adjusted if necessary. Using values for enrichments of REE in estuarine sediment porewaters from Elderfield & Sholkovitz (1987) of 20–30 times seawater concentrations to estimate the amount of Nd present, samples were spiked on the basis of 0.2 g of the Cambridge mixed REE spike per litre of seawater equivalent. The first samples analysed bore out this estimate, and enabled more accurate spiking in the subsequent runs. Fe for the co-precipitation was then added in the form of 100 μ l of 1000 ppm Fe (as FeCl₃).

After spiking, the samples were left to equilibrate with the spike at room temperature for at least two days, after which the pH was adjusted to within the range 7.0–8.0 by addition of QD ammonia solution. When this was achieved the samples were left for at least three days for the Fe(OH)₃ precipitate to form.

Once the waiting stage was completed the samples were filtered through acid cleaned 0.4 μ m Nuclepore polycarbonate membrane filters in a Millipore glass buchner filtration assembly. The glass components were cleaned between samples in a vat of 6M HCl, and well rinsed with QD water before use.

Samples were removed from the filters in 10 ml 5% HCl, evaporated to dryness, and then refluxed for 12 hours in 5 ml conc. HNO₃ to destroy any organic material present. (This stage is not normally carried out on the sea-water samples as there is not enough organic material present to be troublesome.) After a further evaporation they were rendered to chloride by evaporation with 3 ml 6M HCl. The column chemistry used to separate the REE from the other cations present, in particular Fe and Ba, is based on the same principles as that used for the ICP samples (section 2.3.3), uses the same resin and differs mainly in scale. Polypropylene funnels with a stem i.d. of 3 mm, and a bed volume of \approx 0.25 ml were used with the procedure shown in table 2.6.

The two REE fractions were collected separately, then evaporated to dryness before loading onto combined Re/Ta filament assemblies prior to mass spectrometric analysis. All containers used for sample collection or evaporation were 'Savilex' PFA teflon screw-topped vials in 30, 10, and 7 ml sizes. All acids were

Precondition Column	3 ml 1.75M HCl	Discard
Load sample	50 μ l 1.75M HCl	
Clean vial & load	50 μ l 1.75M HCl	
Rinse sample onto resin bed	2 \times 50 μ l 1.75M HCl	
Elute Fe	1.5 ml 1.75M HCl	
Elute Ba	3.0 ml 2M HNO ₃	
Elute heavy REE	7.0 ml 2M HNO ₃	Collect
Elute Ce & La	7.0 ml 2M HNO ₃	Collect

Table 2.6: Scheme for separation of REE for mass spectrometry.

QD, and all operations involving open sample containers (except evaporation) were conducted in laminar flow clean hoods. Due to the unpredictable properties of any residual organic material, the resin was replaced after each sample run through the columns.

2.4.2 Data Quality

Inevitably, when trying to analyse small samples with properties not as predictable as the normal open ocean waters usually analysed by this method, the machine runs were not always as successful as would have been desired. The beam sizes were often well below the values expected for the amount of Nd eventually calculated to be present. Exactly what was responsible for this was not determined as there was not enough material for samples to be run twice. The presence of dissolved organic material which had passed through the 0.4 μ m filter was suspected to be responsible as the estuarine waters analysed at about the same time (R.C. Upstill Goddard, *pers. comm.*) behaved similarly, and when the HNO₃ reflux stage was extended the overall run quality improved. Whether the presence of this organic matter could also have inhibited the recovery of the REE from the co-precipitation stage is not known.

Inspection of the data (Appendix B) reveals a number of blank entries. These are often due to the machine completely failing to find a beam for that element, but are also due to the data being rejected because of poor quality. Where the precision of the analyses is worse than $\pm 10\%$ RSD the error is quoted alongside the result. In other cases the machine provided results which were clearly artifacts (very large or negative numbers), and these were also discarded. Unfortunately, a number of different elements have isotopes of the same mass, which means that the value obtained for one ratio has to be corrected for the value of another e.g. the determination of Lu from the mass ratio 176/175 is dependent on a correction for the Yb 176/171 ratio.. This means that a poor run for one element can preclude the determination of another, despite that second element running comparatively well. Consequently substantial gaps do appear in these data.

Chapter 3

Results I: Major Elements, Trace Elements & Background Data

3.1 Sediments

All three sediment cores obtained consisted of a brown oxidised surface layer approximately 1cm thick below which the sediment was black. Sampling at Neal Point in April ensured that the cores were taken at a site which had been undergoing a period of sediment deposition prior to coring (Bale *et al.*, 1985). The existence of burrows, and the disturbed nature of the nutrient profiles (section 3.2) in core 1 (the number has no significance, the three cores were labelled at random when processed) indicate that the reducing conditions had been recently disturbed in this core.

3.1.1 Major Elements

The sediments from core 1 (cores 2 & 3 were not analysed) show little systematic variation in major element concentration with depth, see figure 3.1 for profiles of the constituents Fe and Al (expressed as oxides). Only Mn shows a distinct increase at the sediment water interface, nearly doubling in concentration (fig. 3.2). This is due to the diagenetic remobilisation of Mn under the reducing conditions at depth and its oxidative fixation in the uppermost oxic sediment. All elements analysed give values which correspond with data reported in Alexander (1985) for sediments collected at Cargreen Dock, approximately 1 km up-estuary from the site of this sampling.

3.1.2 Trace Elements

The elements Co and Ni show no systematic concentration decreases with depth (fig. 3.3) and much less overall variation than Cu and Zn (fig. 3.4), which also show no systematic trend with depth. The leachable and total Co profiles in these Tamar sediments were compared with data from lower St. Lawrence Estuary sediment core data (Gendron *et al.*, 1986). The Canadian data show a distinct decrease in leachable Co with depth, and over the range 4–2.5 ppm rather than the 9–5 ppm range observed in these Tamar sediments. In both cases the concentration of detrital or non-leachable Co is constant with respect to depth, producing a systematic decrease in leach/total ratios down the core. The difference in the amount of leachable Co between the two estuaries can in part be attributed to the more vigorous nature of the 1.75M HCl leach used on the Tamar samples (Gendron *et al.* used a hydroxylamine/acetic acid extraction). The HCl leach also produces higher leach/total ratios for other elements (Fe - 0.28, Cu - 0.72, Zn - 0.8) than those derived by the acetic acid leaches of Tamar sediments (Fe - 0.1, Cu - 0.2, Zn - 0.6) reported in Ackroyd *et al.* (1987). The similarity of the Co and Ni profiles in the Tamar sediments indicates that Ni, like Co, is liable to mobilization under reducing conditions.

Peaks in concentration for Cu & Zn, and to a lesser extent Co & Ni, occur in the 8–9 cm interval. Despite the lack of Si data, we can infer this to be due to an increase in the detrital aluminosilicate content at the expense of quartz in the sediment, by noting the increased Al, Fe, and other major constituents in this sample (table 3.1). This is consistent with the behaviour of Cu, Zn, Ni, and Co in sediments of the St. Lawrence Estuary (Loring, 1978 & 1979) where concentrations of these elements proved to be highly correlated with the mud content of the sediments, and the findings of Ackroyd *et al.* (1987) where the Cu and Zn contents of surface sediments from the Tamar were found to be highly correlated with Fe.

Note that the leachable proportions (expressed as leachable concentrations divided by the total concentrations) of Cu and Zn (0.6–0.9) are much higher than in the case of Co and Ni (0.3–0.5). The relationship between the leachable and total concentrations of elements analysed is expressed in this fashion to reflect

the fact that it is an operationally defined value, rather than a representation of any specific properties of the samples analysed, such as would be implied by the use of the term ‘% labile’. The values of leach/total ratio obtained for Cu and Zn suggest that they are not resident in the same sites within minerals, or possibly even the same phases in the sediment, as Co and Ni. Further data in sections 3.3 to 3.6 confirm this. The presence of a number of Cu ore bodies and mineworkings around the upper estuary (Ackroyd *et al.*, 1987) could provide a source of non-silicate minerals. Levels of ≈ 270 ppm Cu and ≈ 200 ppm Zn reported in the same paper correspond well with the data shown in figure 3.4.

sample depth	weight %		
	Al ₂ O ₃	MgO	K ₂ O
4–5 cm	13.3	1.39	2.22
8–9 cm	15.8	1.61	2.70

Table 3.1: Comparison of major element levels in sediment samples of high (8–9 cm) and low (4–5 cm) trace metal content.

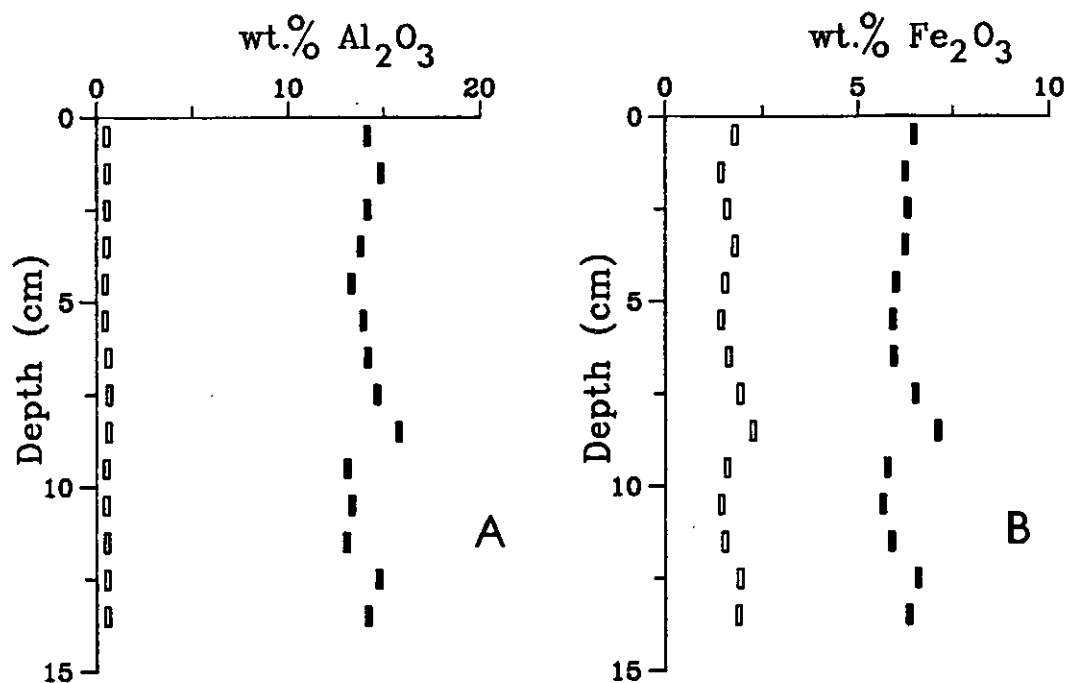


Figure 3.1: Core 1: A- Al₂O₃ vs. depth, B- Fe₂O₃ vs. depth. Filled symbols - total, open symbols - leachable.

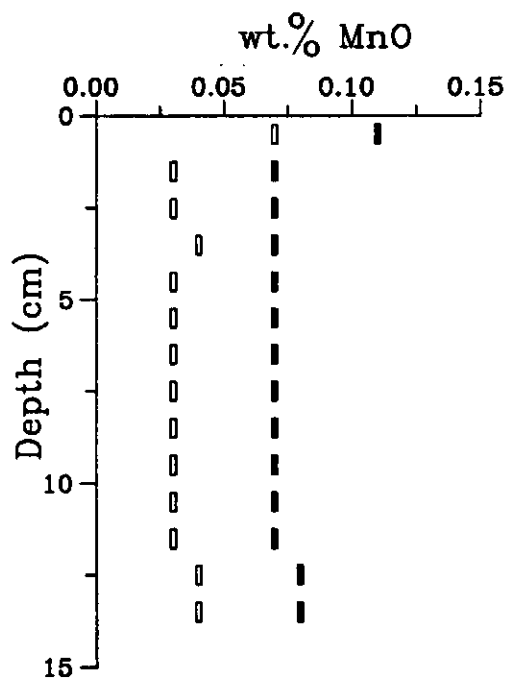


Figure 3.2: Core 1: MnO vs depth. Filled symbols - total, open symbols - leachable.

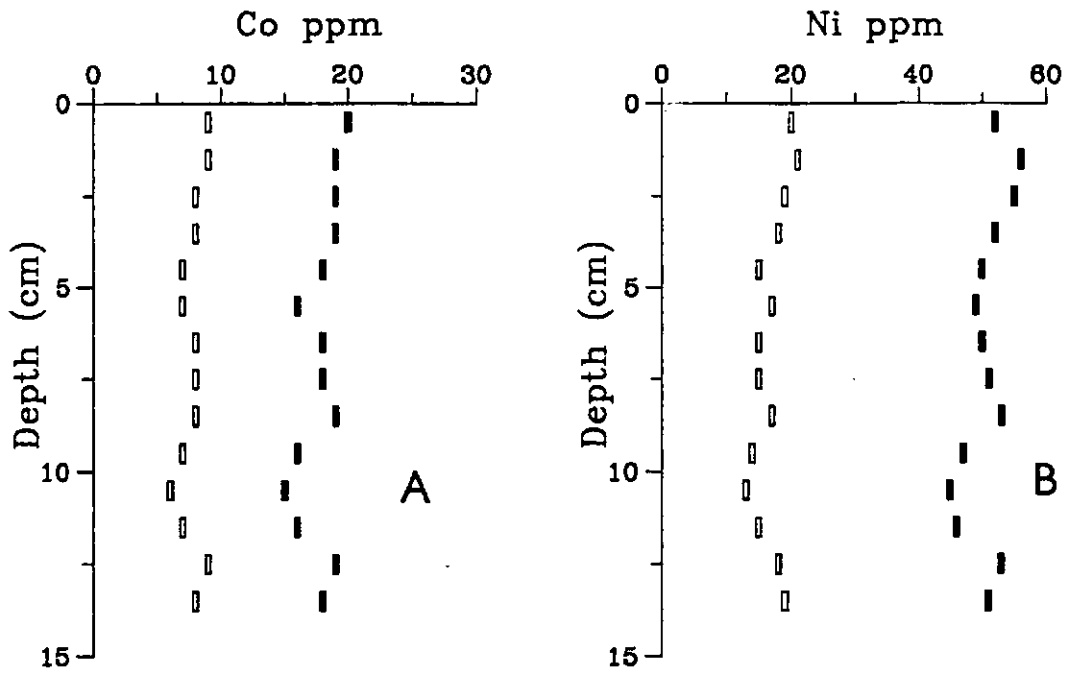


Figure 3.3: Core 1: A- Co vs. depth, B- Ni vs. depth. Filled symbols - total, open symbols - leachable.

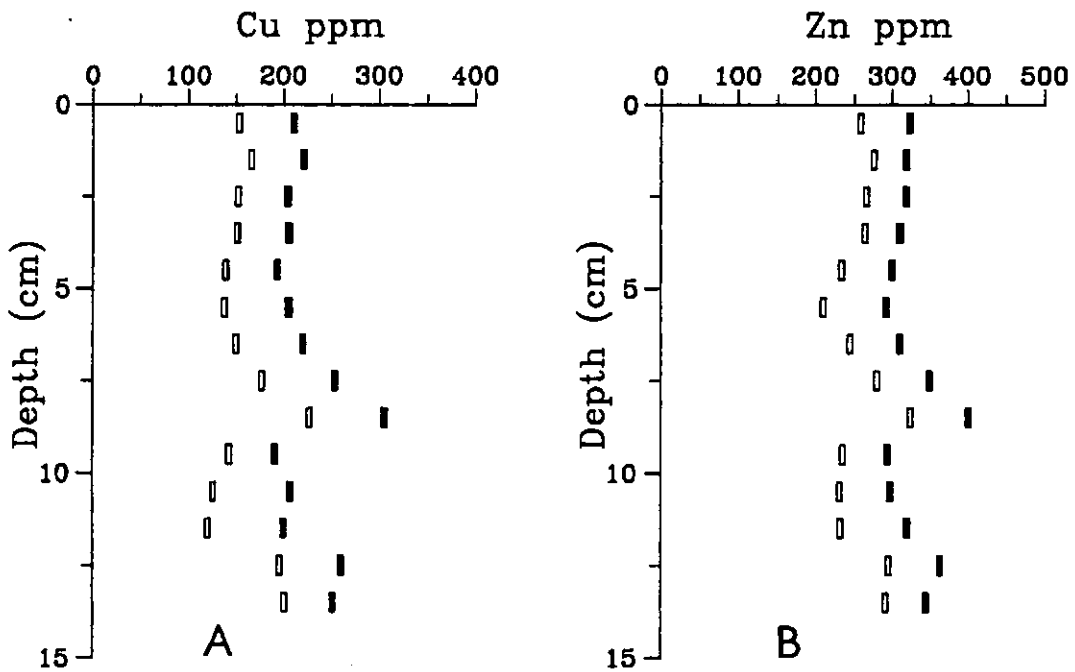


Figure 3.4: Core 1: A- Cu vs. depth, B- Zn vs. depth. Filled symbols - total, open symbols - leachable.

3.2 Pore Waters

Profiles of NH_3 , SO_4^{2-} , phosphate and silicate for cores 1 & 2 are shown in figs. 3.5 & 3.6. Nutrient profiles for core 3 are closely similar to those found in core 2 and are not shown here. Levels of all the above species are comparable with data reported in Watson *et al.* (1985). The profiles for SO_4^{2-} in core 2 indicate the onset of reducing conditions within 1–2 *cm* of the surface. Note the increase in the SO_4^{2-} concentrations in the upper 4 *cm* of the sediment before concentrations begin to decrease. This is most likely due to the oxidation of sulphide diffusing upwards through the sediment (Upstill-Goddard *et al.*, 1989). The other three nutrients all show increasing concentrations with depth from the surface downwards in core 2, but core 1 has disturbed profiles with concentrations beginning to increase only below 12 *cm*. This, and the burrows noted in section 3.1, suggest that core 1 has been subjected to bioturbation which has disrupted the normal reducing conditions.

Fe and Mn data are shown in fig. 3.7. Profiles for Fe are well developed and show distinct subsurface maxima in both cores at the 2–3 *cm* level. This is consistent with the redox cycling of dissolved Fe in anoxic pore waters. Hydrated Fe oxides dissolve in reducing conditions, and dissolved Fe^{2+} diffuses upwards, but the solubility of Fe is controlled by the precipitation of amorphous Fe sulphides which progressively remove Fe from solution. Note that the Fe profiles in core 1 are very similar to those in core 2 despite the nutrient profiles showing distinct differences. The effect of bioturbation is limited to a depression of the maximum Fe concentration observed in the 2–3 *cm* interval. Profiles for Mn show considerable scatter.

The nutrient and metal profiles clearly show the establishment of reducing conditions typical of shallow burial diagenesis in organic rich sediments in the Tamar (Watson *et al.*, 1985; Upstill-Goddard *et al.*, 1989) and elsewhere Elderfield *et al.*, 1981). The distinct differences between cores 1 and 2 have implications for the interpretation of the REE pore water data in section 4.2.

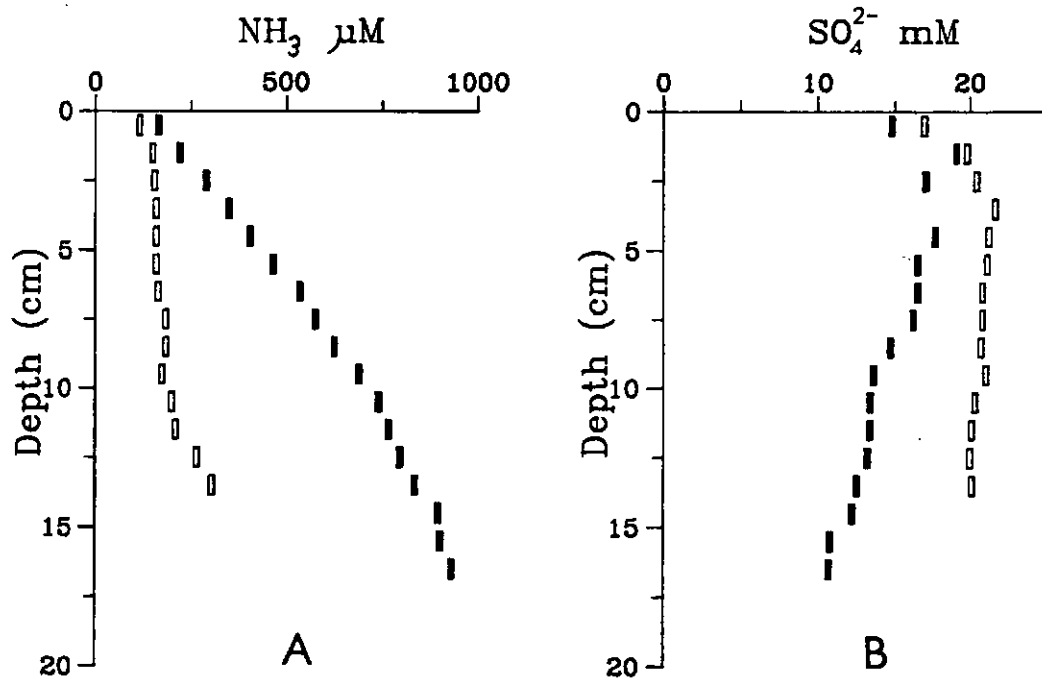


Figure 3.5: Sediment pore waters: A- NH₃ vs. depth, B- SO₄²⁻ vs. depth. Open symbols - core 1, filled symbols - core 2.

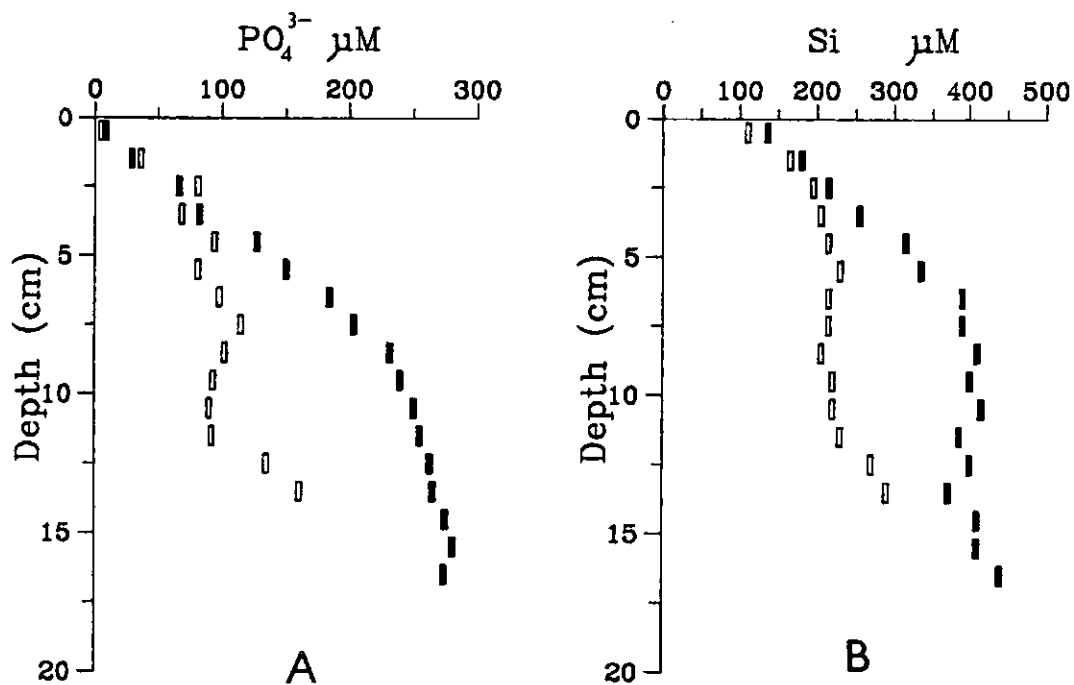


Figure 3.6: Sediment pore waters: A- PO₄³⁻ vs. depth, B- Si vs. depth. Open symbols - core 1, filled symbols - core 2.

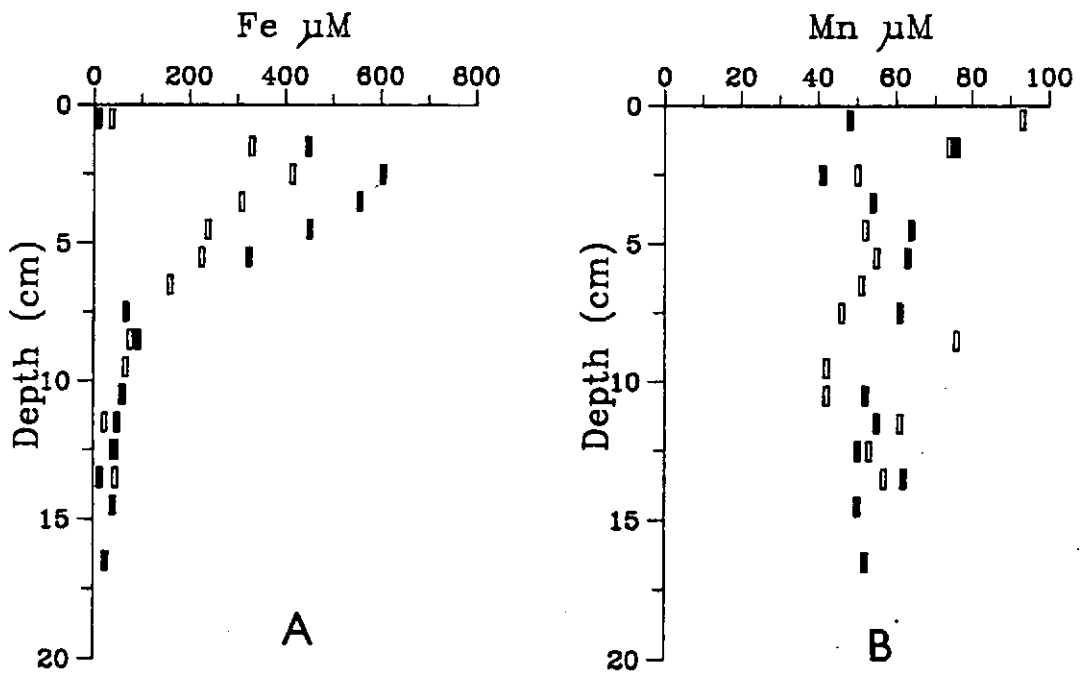


Figure 3.7: Sediment pore waters: A- Fe vs. depth, B- Mn vs. depth. Open symbols - core 1, filled symbols - core 2.

3.3 Axial Surveys

3.3.1 Background

The axial surveys were carried out at a time of unseasonably high rainfall and hence run-off. Table 3.2 shows data for the actual and typical river discharges at the time. The spring tide survey (19/8/85) was less seriously affected than the neap tide survey (12/8/85) as the run-off had abated. Salinity and turbidity profiles for the surveys are shown in figures 3.8 & 3.9. Note that in the neaps survey the zone of high turbidity was less clearly developed, and the 10 ppt salinity level was displaced at least 5 km further down estuary. Plots of dissolved silicate against salinity (fig. 3.10) show typical conservative mixing for this component. Inspection of this diagram reveals a high density of the data points at 0–1 ppt salinity. As this is an important zone in terms of estuarine processes, the analyses of particulate trace metals presented here are shown with distance down estuary as the X-axis, enabling much greater resolution of the changes occurring in the low salinity zone. Since the chemical composition of the suspended particles is not simply controlled by dilution of riverine material with marine, 'conservative mixing' as normally applied to dissolved constituents is of less significance, and presentation of the results as component concentration against distance down estuary does not hinder interpretation. Where dissolved constituents are discussed, conventional mixing diagrams are used. Both surveys are depicted on a single diagram in cases where the data sets are distinct.

River Tamar discharge data ($m^3 s^{-1}$)	
Daily Mean 12/8/85	28.8
Daily Mean 19/8/85	16.9
August 1985 Mean	20.7
Typical January Mean	38
Typical June Mean	5

Table 3.2: River Tamar discharge: 1985 data courtesy of South West Water Authority, typical data from Uncles *et al.* (1983).

3.3.2 Major Elements

Profiles of particulate Fe_2O_3 are shown in figure 3.11. The two surveys give similar results with the most notable differences in the lower estuary where the levels of Fe are significantly higher in the neaps survey. The 7–10% Fe_2O_3 recorded here is consistent with the 4–7% Fe (5.7–10% Fe_2O_3) reported in Morris *et al.*, (1986). These levels are higher than the 6–7% Fe_2O_3 found in the estuarine sediments (section 3.1), and are due to differences in the amounts of leachable Fe, the residual (total minus leachable) remaining relatively constant at 3.6–3.8% Fe_2O_3 . Leach/total ratios in the suspended particles reflect this, falling in the range 0.35–0.5 compared with 0.23–0.30 in the sediments. As noted in the case of the sediments (section 3.1) these values are higher, due to the use of a more aggressive leach, than the leach/total ratios of 0.18 (Loring *et al.*, 1983) and ≈ 0.1 (Morris *et al.*, 1986a) reported previously for Fe in suspended particles from the Tamar Estuary.

In contrast, Mn (measured as wt.% MnO) shows substantial differences between the two surveys. The neaps survey (fig. 3.12) shows simply a broad minimum in the upper–mid estuary, with elevated levels in the lower estuary and one exceptional data point. The springs survey (fig. 3.13) is quite different, with a pronounced minimum in the upper estuary, coincident with the zone of maximum turbidity, and a sharp maximum to seaward of this. The leach data are not shown as virtually 100% of the Mn content of the suspended particles was found to be leachable with the technique used. Comparison of these results with the salinity and turbidity profiles in figs. 3.8 & 3.9 shows how the Mn content of the particles is sensitive to changes in the estuarine conditions caused by variations in run-off and tidal stresses (this agrees with the findings of Loring *et al.*, 1983) and in fact is inversely related to the turbidity.

3.3.3 Trace Elements

Of the trace metals measured, some appear to be sensitive to the run-off variations and others do not. Of those relatively insensitive, Li (fig. 3.14) is of particular interest. The Li concentrations are generally consistent between surveys, but in the springs high turbidity zone from 10–15 km down estuary the Li concentra-

tions are persistently elevated. In the granites which drain into the Tamar, Li is concentrated in tourmalines which resist weathering and can accumulate in the estuarine sediments rather than being uniformly dispersed in the suspended particulate matter (section 2.3.1). Resuspension of estuarine sediments within the turbidity maximum could therefore easily generate the enhanced levels of particulate Li. Note that the elevated Li concentrations are restricted to the saline part of the turbidity maximum. Up-estuary from 10 km where the salinity was ≤ 0.1 ppt, the turbidity is still high (fig. 3.9) but the Li concentrations in the suspended particles are not elevated.

Nickel, although relatively consistent between surveys shows subtle variations in the leachable fraction (fig. 3.15). At very low salinity (3–7 km down estuary) the leachable Ni drops rapidly, and then declines more slowly with only a slight dip in the springs data in the 12–15 km zone. These data are easier to interpret if the leach/total ratios are calculated (figs. 3.16 & 3.17). The neaps data are erratic, but show an overall decline in the leach/total ratio from the upper to lower estuary. The springs data are clearer and show a distinct decline in the leach/total ratios with a pronounced dip within the 10–15 km zone. As for Li (above) this is consistent with the resuspension of bed sediment with its lower (0.29–0.38) Ni leach/total ratio, but is restricted to the saline part of the turbidity maximum (salinity ≥ 0.24 ppt) despite the persistence of high turbidity at lower salinities.

A similar down-estuary decline in the leachable proportion of the total Co content is reported by Loring (1978) for sediments of the St. Lawrence Estuary. Although an acetic acid leach was used (releasing only moderately reducible elements), their overall results are similar, and show that the proportion of leachable Co is significantly higher in the uppermost part of the estuary. Titley *et al.* (1987) report higher surface areas and porosities for suspended particles in the low salinity part of the Tamar Estuary. Given that the leach process acts upon particle surfaces it is likely that these two results are related. The effect of variations of particle surface area on the results of the leaching procedure is discussed in section 5.1.1.

The leach/total data for Cu (presented in the same diagrams) show virtually

identical behaviour to Ni, despite the levels of Cu in the riverine end-member particles showing large differences between the surveys (fig. 3.18). These two elements, Cu & Ni, which appear to have substantially different behaviour in terms of their susceptibility to variations in river discharge, in fact show very similar behaviour when their relative leachable proportions are considered.

Although consideration of the sediment data for Li, Ni & Cu would lead to the conclusion that resuspension of sediment could provide the material for the turbidity over the 10–15 km zone, the change in the trace metal composition up-estuary from 10 km requires explanation. With respect to these three elements, the composition of the SPM in these most turbid samples does not correspond with that of the sediments. The Li, Cu & Ni data suggest that resuspended sediment is not the primary source of the particles suspended in this zone, unless abrupt variations in the composition of the sediments are likely. Ackroyd *et al.* (1987) studied the variation of the composition of estuarine sediments axially and temporally. Their data for July 1981 do show steep changes in the Fe, Mn, Cu & Zn contents of the sediments, but in the zone 0–3 km down estuary, rather than at 10 km where the changes are observed in this study. It seems less likely therefore that changes in the composition of the material being resuspended can account for the rapid changes in the composition of the SPM over the upper estuary.

If, on the other hand, we assume that resuspension of laterally homogeneous bed sediment is the primary source for the bulk of the material suspended in the turbidity maximum we must be able to attribute the variations in the composition to some process which physically fractionates the resuspending material. Given that the sediments do contain heavy minerals (Fe & Ti oxides, tourmalines, zircons, Cu ore minerals, etc.), we can consider the behaviour of a mixture of minor amounts of these with a bulk of aluminosilicates.

For example, the material suspended in the uppermost estuary might not (in this case) have been resuspended locally, but been derived from a zone down-estuary where active suspension of sediment was actually taking place. Up-estuary from this zone (characterised by the steepest salinity gradients) the turbulence of the water column was insufficient to maintain the heavy minerals in

suspension and they settle out. Such a process would be consistent with the net up-estuary transport of the sediment which occurs at this time of year (Bale *et al.*, 1985) and would effectively fractionate its trace metal composition. This situation need not necessarily persist throughout the entire flood.

Alternatively, if we assume no net up-estuarine transport and a laterally homogeneous sediment, variations in the energy of the resuspension, and hence selection of particles, could account for lateral variations in the composition of the SPM. Data from the time series surface samples collected in the turbidity maximum on 21st July (fig. 3.32) show that when the turbidity exceeds 200 mg l^{-1} there is resuspension of sediment taking place of sufficient intensity to bring the implicated heavy minerals into suspension in the uppermost (0–10 km) part of the estuary. The importance of mineral density in controlling the composition of estuarine SPM has been suggested before by Duinker *et al.* (1985) and Morris *et al.* (1987).

Substantial differences in concentration between the neaps and springs riverine particulate concentrations are observed for Zn as for Cu. Total and leachable Zn concentrations in the springs survey SPM (fig. 3.19) vary in a similar manner to those of Cu with enhanced residual concentrations in the 10–15 km zone. The neaps data (fig. 3.20) show a simple inverse correlation between turbidity and Zn concentration, with no heavy mineral input. Note that, as for the sediments (section 3.1.2), leach/total ratios obtained for Zn are higher (mean 0.88) than for previous analyses of Tamar SPM (0.67: Loring *et al.*, 1983; \approx 0.7: Morris *et al.*, 1986) due to the more vigorous leach employed.

Co distributions in the estuarine SPM are shown in figures 3.21 & 3.22. Comparison of these profiles with the sample turbidities (figs. 3.8 & 3.9) indicate that Co concentrations are independent of any heavy mineral control and simply reflect the mixing of a population of high Co content SPM with tidally resuspended sediments with lower Co concentrations.

In summary, the trace metal concentrations in the SPM can be explained by the mixing of 'normal' estuarine particles having high levels of Co and Zn with tidally resuspending sediment which has lower concentrations of these elements.

The relationship is subject to disruption, however, when the energy of resus-

pension is sufficient to bring heavy minerals, with much higher concentrations (and different phase residences) of Zn, Cu & Ni, into the water column. Only one element, Gd - fig. 4.15, shows concentration variations which correlate positively with the turbidity profile in the estuary. Its behaviour, along with the other REE is discussed in section 4.3.

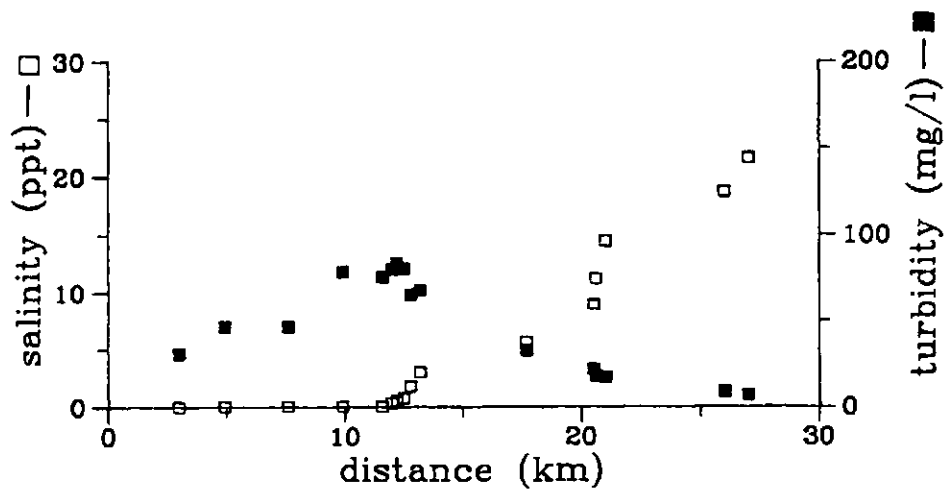


Figure 3.8: Neaps survey: turbidity and salinity vs. distance down estuary.

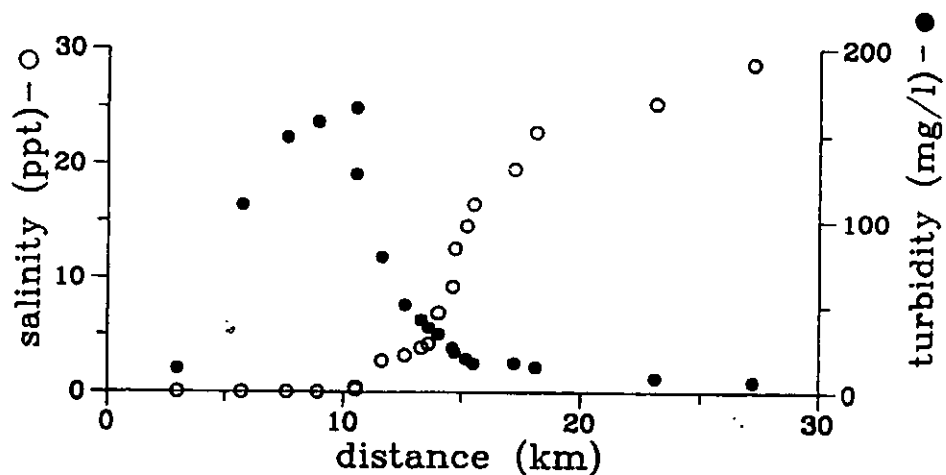


Figure 3.9: Springs survey: turbidity and salinity vs. distance down estuary.

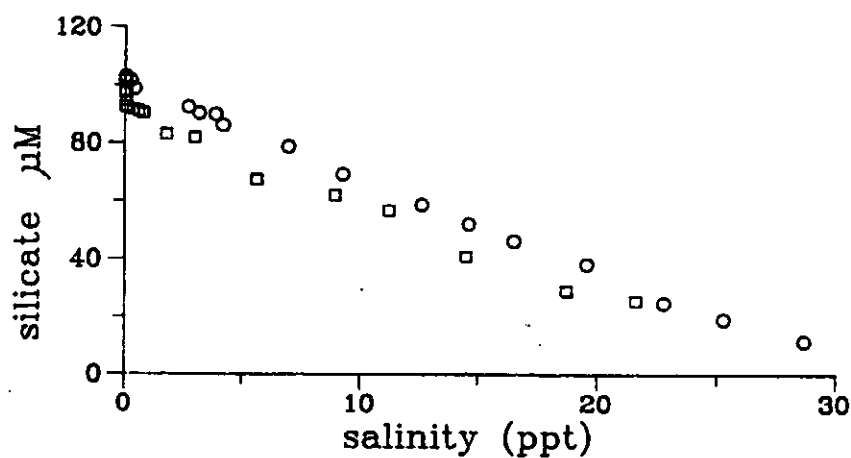


Figure 3.10: Axial surveys: dissolved Si vs. salinity. Squares - neaps, circles - springs.

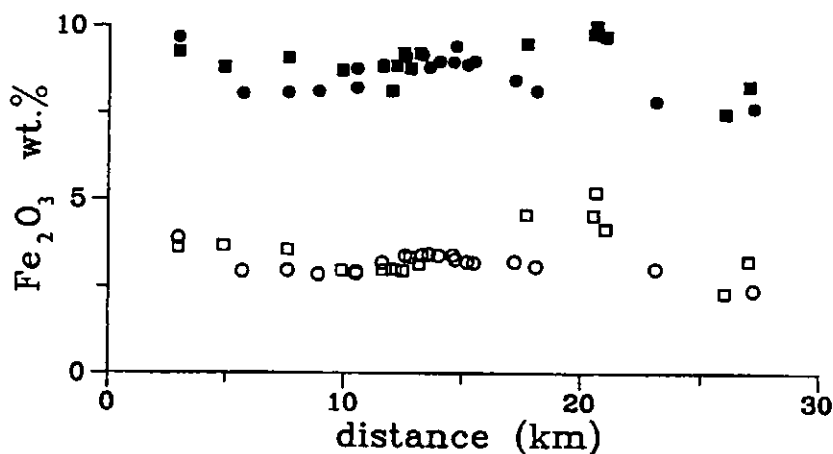


Figure 3.11: Axial surveys: particulate Fe_2O_3 vs. distance down estuary. Squares - neaps, circles - springs. Filled symbols - total, open symbols - leachable.

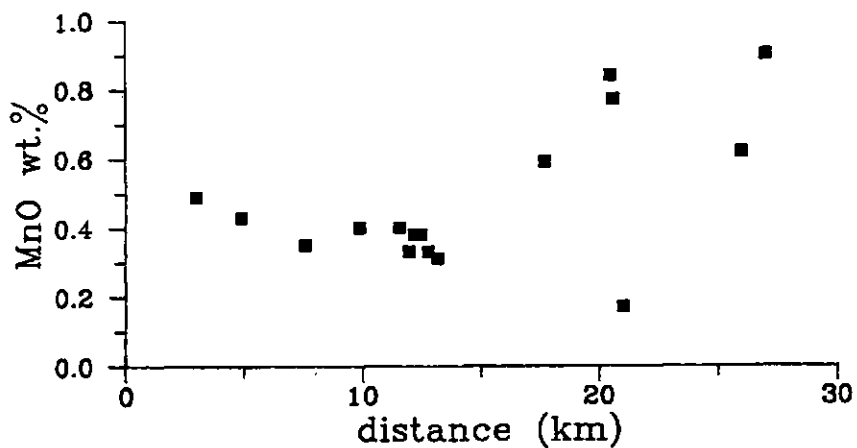


Figure 3.12: Neaps survey: total particulate MnO vs. distance down estuary.

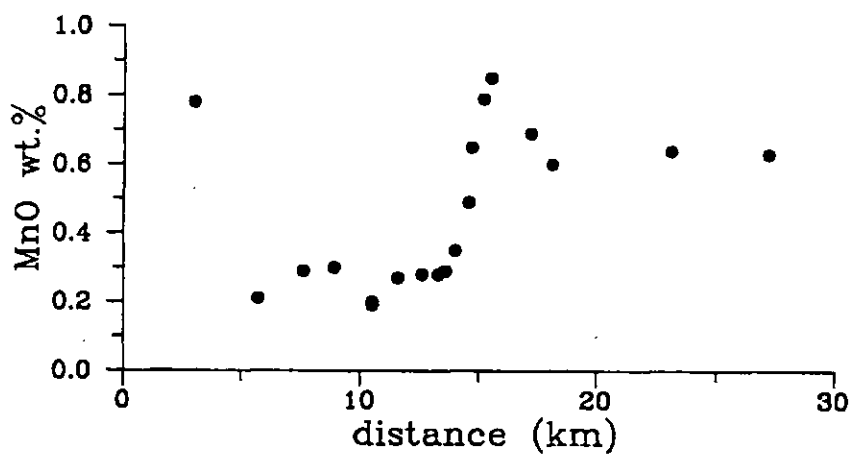


Figure 3.13: Springs survey: total particulate MnO vs. distance down estuary.

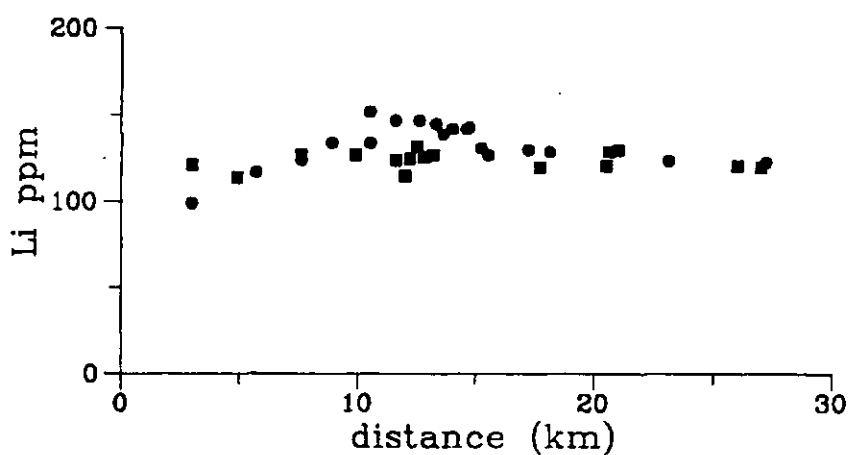


Figure 3.14: Axial surveys: total particulate Li vs distance down estuary. Squares - neaps, circles - springs.

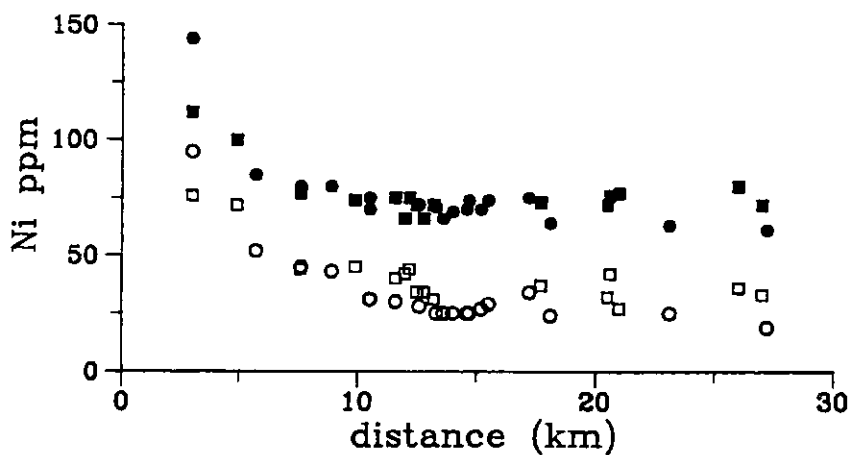


Figure 3.15: Axial surveys: particulate Ni vs. distance down estuary. Squares - neaps, circles - springs. Filled symbols - total, open symbols - leachable.

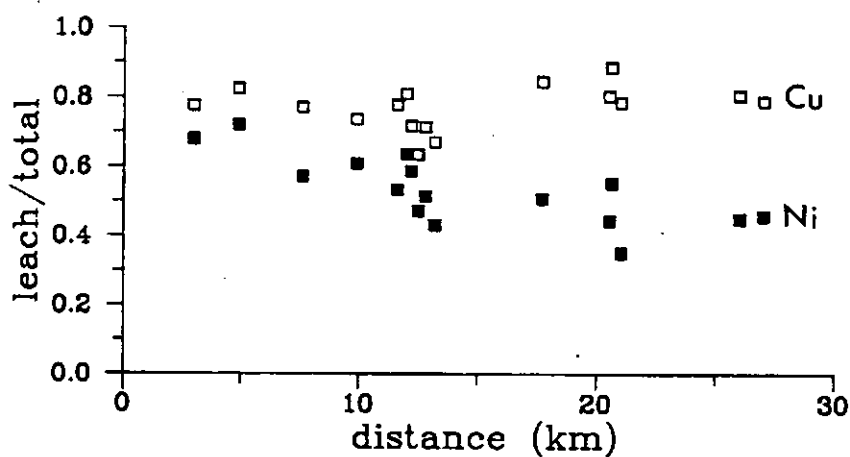


Figure 3.16: Neaps survey: Cu & Ni leach/total ratios vs. distance down estuary.

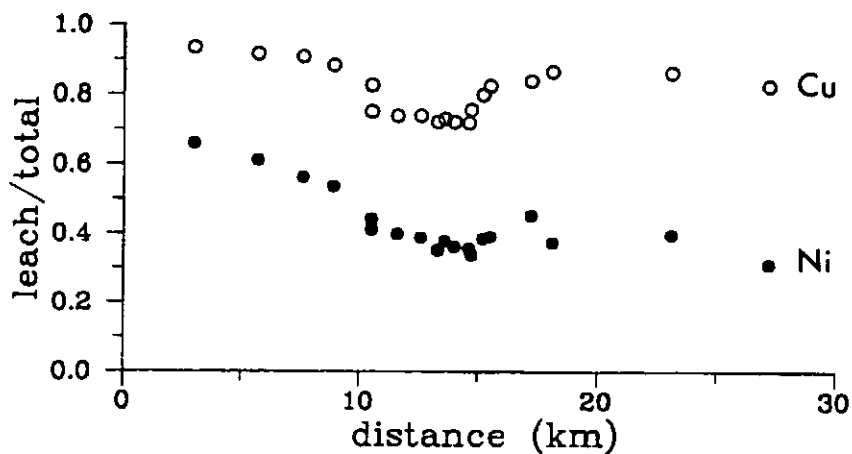


Figure 3.17: Springs survey: Cu & Ni leach/total ratios vs. distance down estuary.

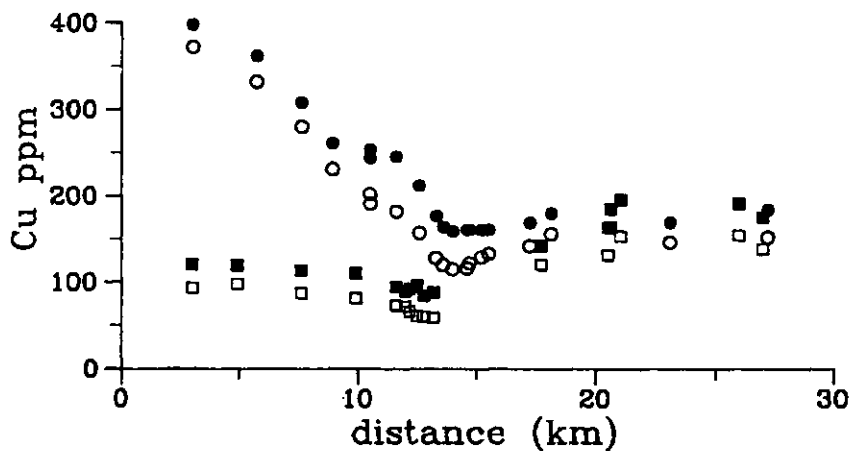


Figure 3.18: Axial surveys: particulate Cu vs. distance down estuary. Squares - neaps, circles - springs. Filled symbols - total, open symbols - leachable.

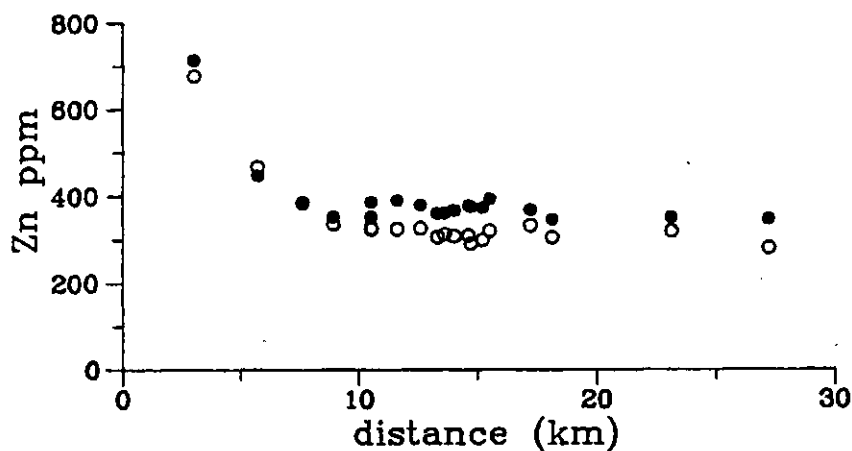


Figure 3.19: Springs survey: particulate Zn vs. distance down estuary. Filled symbols - total, open symbols - leachable.

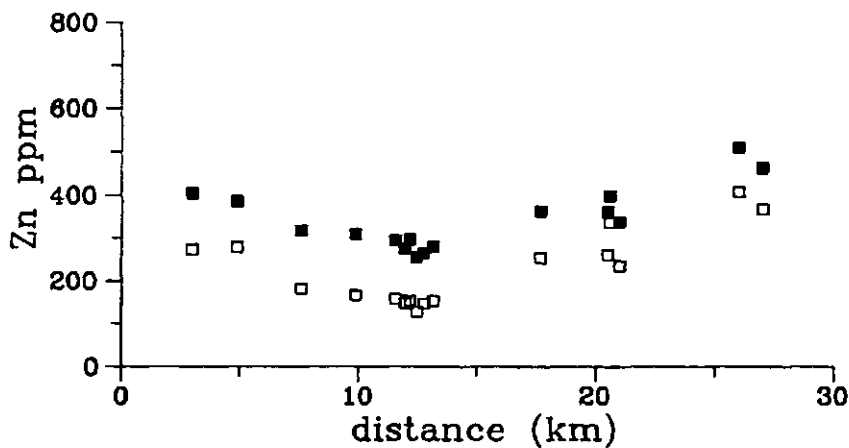


Figure 3.20: Neaps survey: particulate Zn vs. distance down estuary. Filled symbols - total, open symbols - leachable.

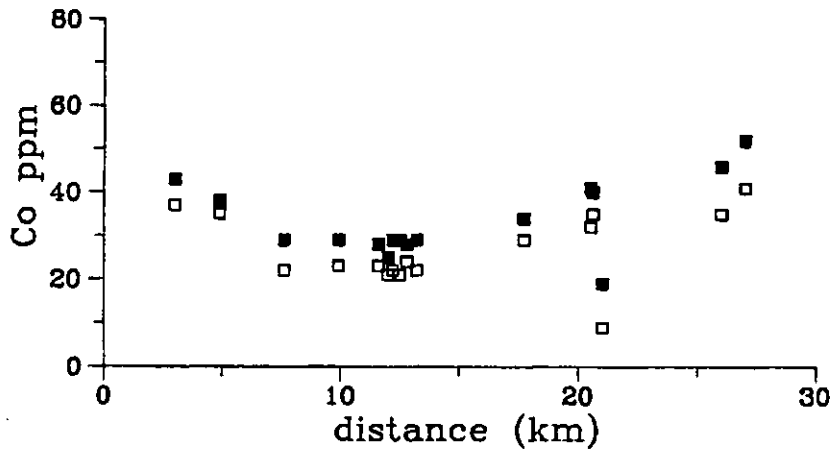


Figure 3.21: Neaps survey: particulate Co vs. distance down estuary. Filled symbols - total, open symbols - leachable.

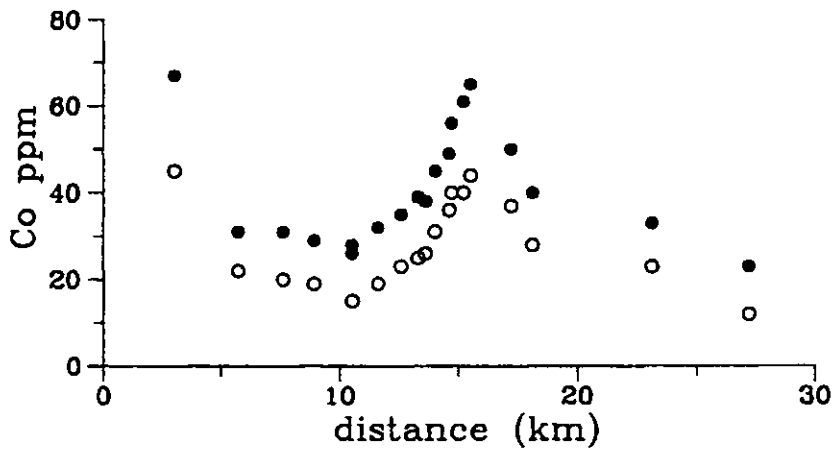


Figure 3.22: Springs survey: particulate Co vs. distance down estuary. Filled symbols - total, open symbols - leachable.

3.4 Turbidity Maximum, Surface Samples

Turbidities and salinities for the surface water samples collected in the two 1985 turbidity maximum sampling exercises are presented in figures 3.23 & 3.24. As mentioned in section 2.2.3 the turbidity meter on-board Tamaris was used to maintain the vessel over the site of greatest turbidity. In order to combine the data from the two sets, the results are shown as components against turbidity.

3.4.1 Major Elements

Most of the major elements show little systematic variation with turbidity. Al and Fe (figs. 3.25 & 3.26) appear to show a decrease in their residual concentrations with increasing turbidity, and then a step up to higher levels in the samples with turbidities greater than 150 mg l^{-1} . However that lack of consistency of this pattern in the other major constituents suggests that these differences are as likely to be caused by random variations in the composition of the SPM as they are by a significant relationship.

Only P and Mn (figs. 3.27 & 3.28) show obvious relationships between concentration and turbidity. Residual P concentrations decline steadily with rising turbidity, and, although the data show a discontinuity, the Mn levels are persistently lower in the high turbidity samples. Both these observations are consistent with the hypothesis that resuspension of estuarine sediment, with its low levels of P and Mn (section 3.1.1), provides the bulk of the suspended material present in the turbidity maximum.

The evidence for resuspension of bed sediment in the turbidity maximum is strengthened by the fact that the levels of dissolved Fe (fig. 3.29) and dissolved REE (R.C.Upstill-Goddard, *pers.comm.*) are higher in samples with high turbidity. Both Fe and the REE are present in the porewaters of reducing estuarine sediments at greatly enhanced concentrations compared to the overlying estuarine waters (see section 4.2), and would be released into the water column during resuspension of bed sediment. Evidence for the advection of porewater Mn into the water column under these conditions is reported in Morris *et al.* (1982b).

3.4.2 Trace Elements

Some of the trace metal data from these samples support the notion that resuspension of bed sediment provides the bulk of the suspended matter in the turbidity maximum. Leachable Co (fig. 3.30) shows a clear overall drop with rising turbidity between 80 and 200 $mg\ l^{-1}$, beyond which the levels steady. Ni (fig. 3.31) also shows this behaviour, although the changes are less marked. In contrast, Cu and Zn (figs. 3.32 & 3.33) behave in the opposite manner. The data for Cu are the clearer, but both elements show a distinct rise in leachable concentrations with rising turbidity. From comparison of the the Zn concentrations in these samples with the sediment (3.1.2) and axial survey (3.3.3) data one would expect that resuspension of sediment would produce a negative correlation between Zn concentrations in the SPM and turbidity. Ackroyd *et al.* (1987) show the locations of a number of old Cu mine workings in the upper estuary. It is likely that the enhanced Cu concentrations observed at high turbidity are due to resuspension of heavy Cu ore minerals present in the estuarine sediments, and that the Zn abundances are controlled in the same manner. This positive correlation between suspended load and Cu content has been reported previously for Tamar SPM by Morris *et al.* (1986a) who also found such behaviour for Pb. The absence of high levels (430 *ppm*) of Zn in the sediments collected at Neal point does not contradict the argument as we have already deduced from the axial survey data that the resuspension of sediment is capable of fractionating the bulk composition of the SPM, and hence the sediment itself is not necessarily uniform along the estuary.

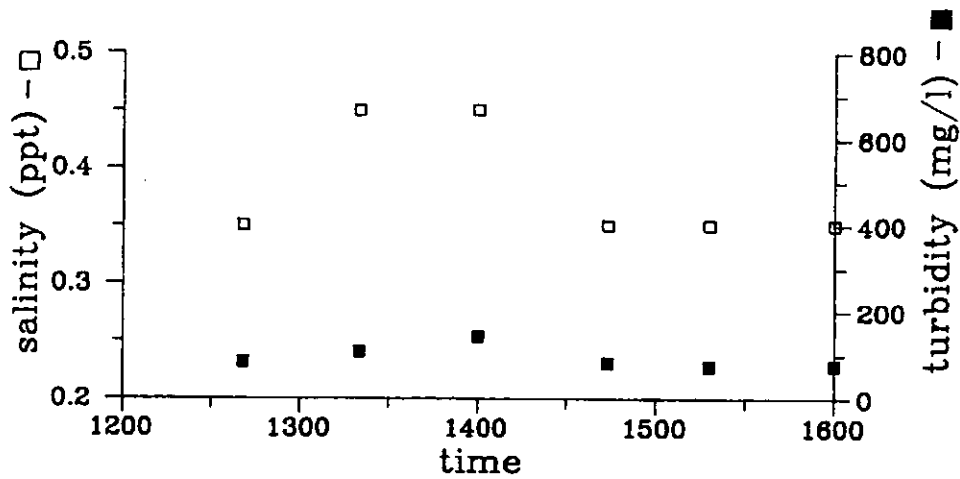


Figure 3.23: Turbidity maximum, surface samples: Neaps; salinity and turbidity vs. time.

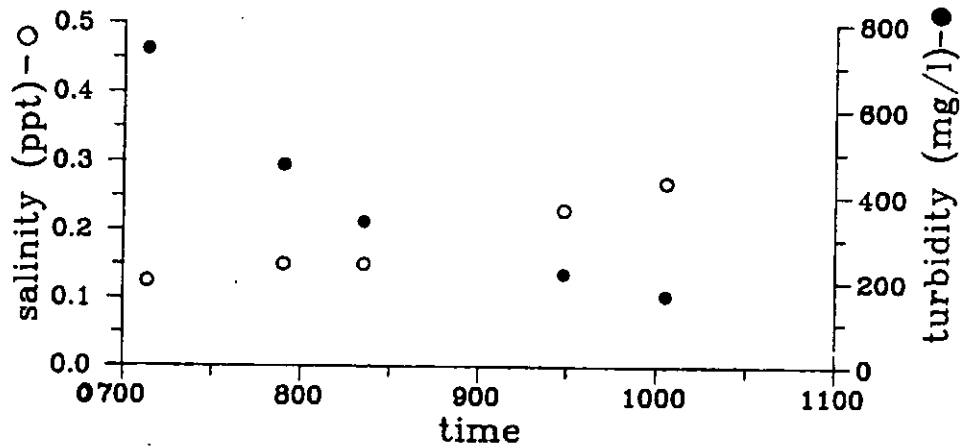


Figure 3.24: Turbidity maximum, surface samples: Springs; salinity and turbidity vs. time.

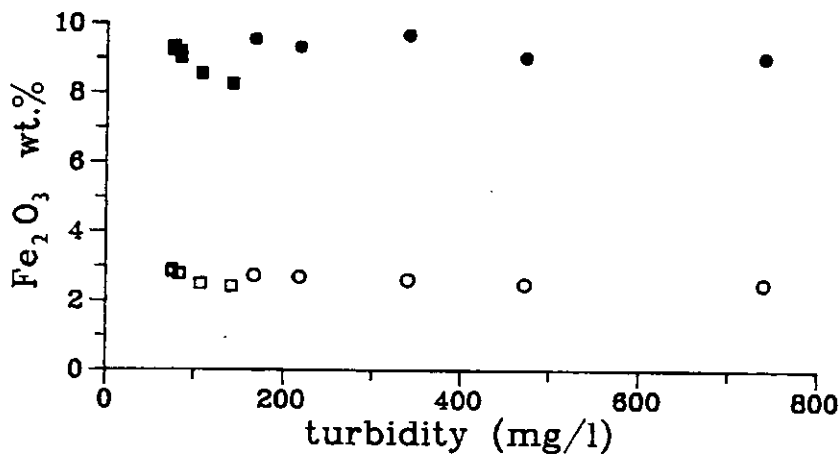


Figure 3.25: Turbidity maximum, surface samples: particulate Fe₂O₃ vs. turbidity. Squares - neaps, circles - springs. Filled symbols - total, open symbols - leachable.

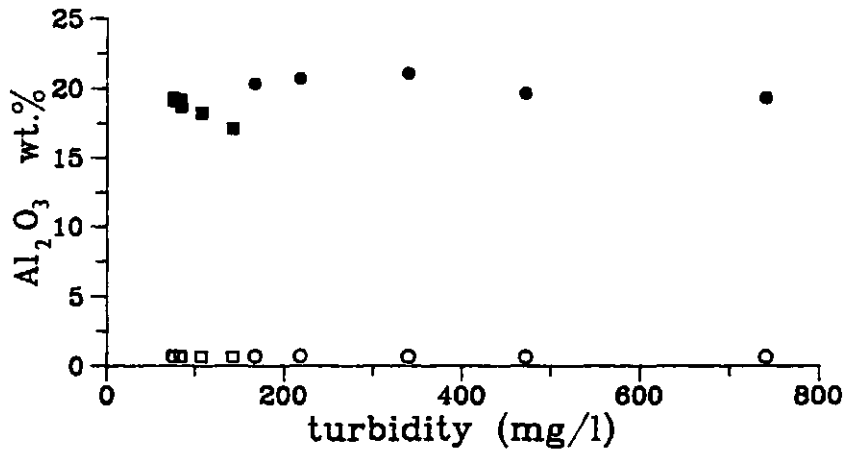


Figure 3.26: Turbidity maximum, surface samples: particulate Al₂O₃ vs. turbidity. Squares - neaps, circles - springs. Filled symbols - total, open symbols - leachable.

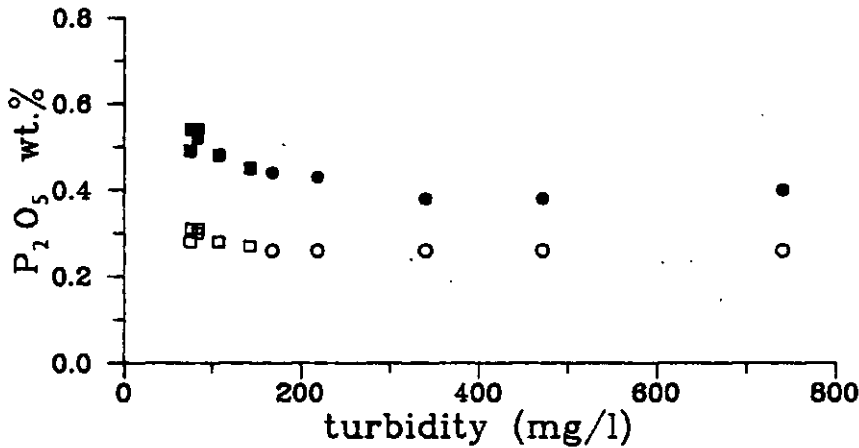


Figure 3.27: Turbidity maximum, surface samples: particulate P₂O₅ vs. turbidity. Squares - neaps, circles - springs. Filled symbols - total, open symbols - leachable.

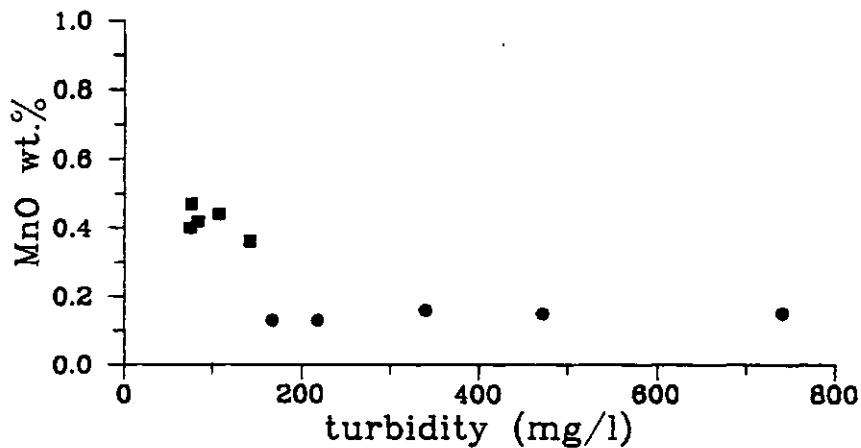


Figure 3.28: Turbidity maximum, surface samples: total particulate MnO vs. turbidity. Squares - neaps, circles - springs.

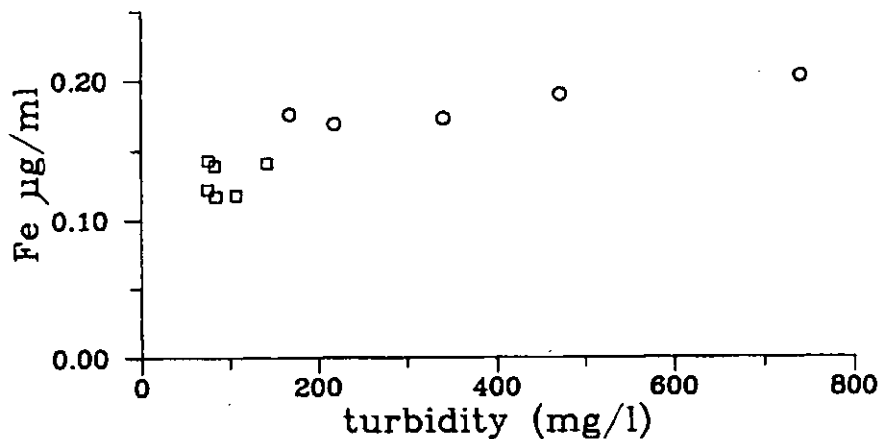


Figure 3.29: Turbidity maximum, surface samples: dissolved Fe vs. turbidity. Squares - neaps, circles - springs.

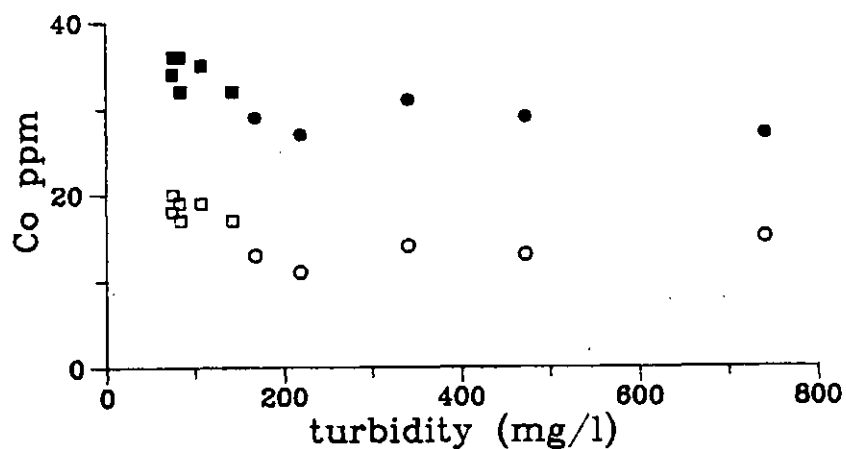


Figure 3.30: Turbidity maximum, surface samples: particulate Co vs. turbidity. Squares - neaps, circles - springs. Filled symbols - total, open symbols - leachable.

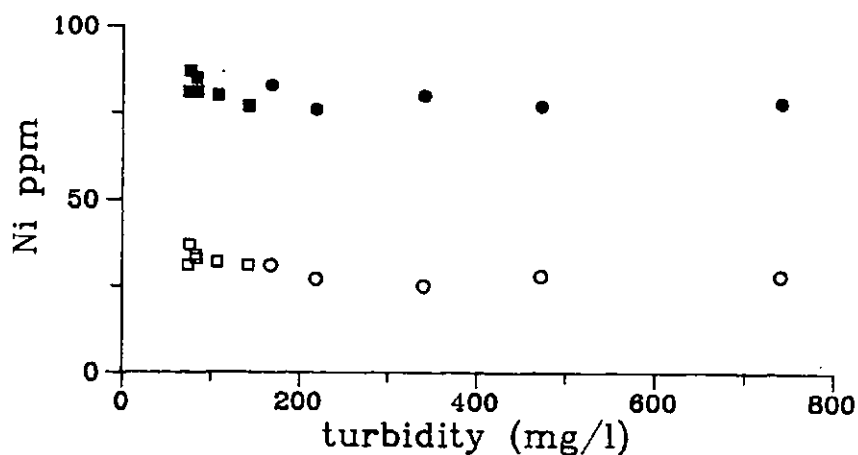


Figure 3.31: Turbidity maximum, surface samples: particulate Ni vs. turbidity. Squares - neaps, circles - springs. Filled symbols - total, open symbols - leachable.

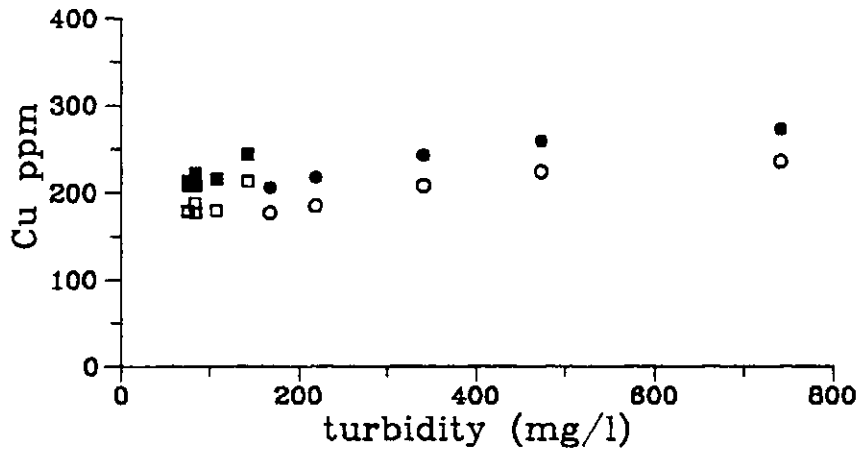


Figure 3.32: Turbidity maximum, surface samples: particulate Cu vs. turbidity. Squares - neaps, circles - springs. Filled symbols - total, open symbols - leachable.

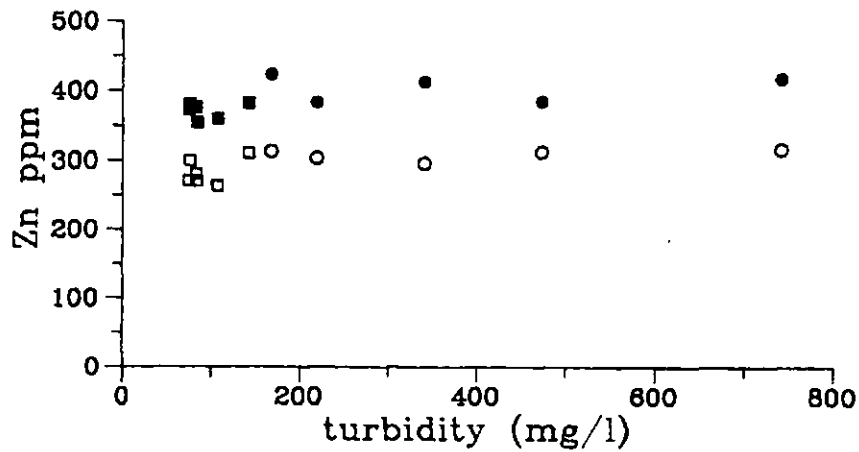


Figure 3.33: Turbidity maximum, surface samples: particulate Zn vs. turbidity. Squares - neaps, circles - springs. Filled symbols - total, open symbols - leachable.

3.5 Turbidity Maximum Profiles

This sampling exercise constituted a more detailed examination of the variability of the composition of the SPM in the turbidity maximum. An extra degree of resolution of the results is provided by the addition of depth and particle size data to the elemental concentrations. Initial presentation of the results is by means of component/turbidity plots as for the surface samples in section 3.3. Particle size and depth relationships are additionally portrayed where significant features become apparent.

3.5.1 Major Elements

In contrast with the surface samples, the major element composition of the SPM in this study varies substantially. The variability with respect to turbidity is greatest for Na (see figure 3.34). The high levels of Na are associated with low turbidity, and a large mean particle size (fig. 3.35). The influx of SPM with this particular composition is dependent on the tidal state (fig. 3.36). Most other major constituents show this feature, but to a lesser degree. The source of this material is difficult to determine when only considering the major and trace elements, but the REE data (section 4.6) show features consistent with derivation of the material directly from assemblages of granite alteration products. This is despite an up-estuary tidal flow over the sampling period. The influx of such unique material makes comparison of the data with results from the other turbidity maximum studies difficult as changes in the mineralogy implicit in the major element variations will also affect the abundances of other elements.

TiO₂ concentrations remain unaffected by this change in major element composition, and show a slight rise with increasing turbidity (fig. 3.37), reflecting the presence in the resuspending sediments of dense Fe-Ti oxides.

3.5.2 Trace Elements

Some trace metals behave similarly to Na, such as Co (fig. 3.38), but the association between low turbidity and high metal content is less marked. Although the axial survey data for Co also show this relationship (figs. 3.21 & 3.22), care must

be exercised in interpretation of this feature for the reasons mentioned above. Use of time for the x-axis (fig. 3.39) reveals the changing Co concentrations in the SPM much more clearly.

Characteristically, the turbidity relationships of Cu & Zn concentrations (figs. 3.40 & 3.41) are dominated by the presence of high metal concentrations in the highest turbidity samples, reflecting the heavy mineral associations revealed in the axial survey data. Additionally, the Cu content of the SPM is stratified in the water column, with highest levels of Cu found in those samples nearest the bottom (fig. 3.42). Note that the increase in Cu concentrations is greatest in the lower part of the water column. There is no significant stratification of any other trace metal concentrations in the SPM. These results contrast with the studies of SPM in the Weser and Elbe estuaries (Duinker *et al.*, 1982a & 1982b), where higher levels of Cu, Zn and other metals were found in the surface water SPM than in the bottom water SPM.

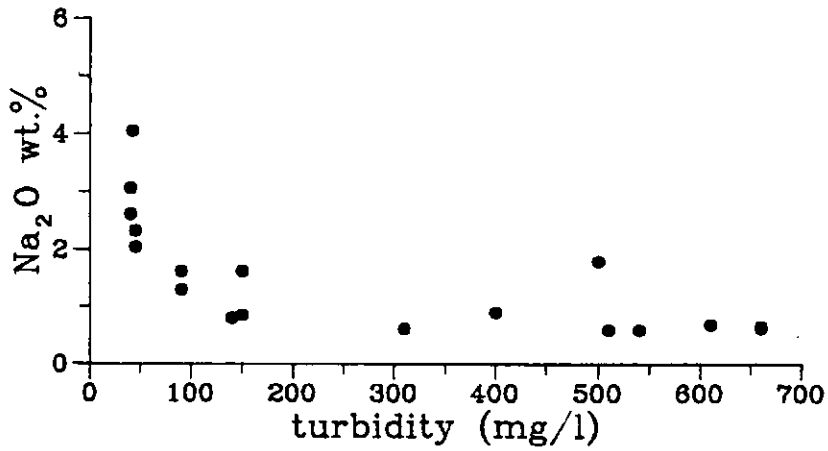


Figure 3.34: Turbidity maximum profiles: total particulate Na₂O vs. turbidity.

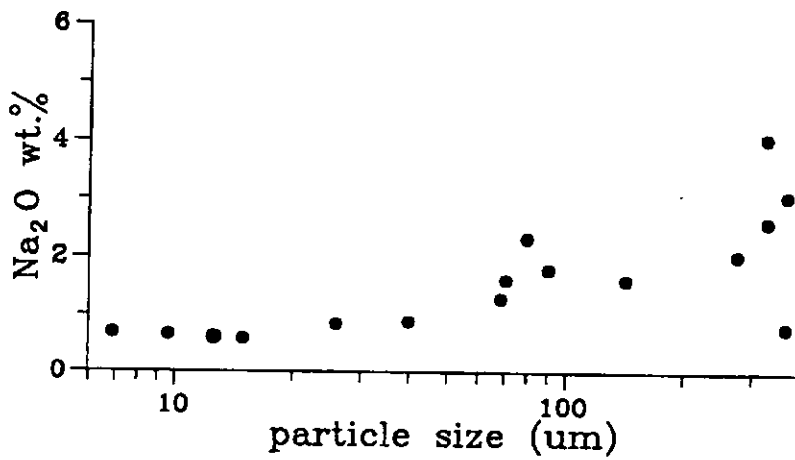


Figure 3.35: Turbidity maximum profiles: total particulate Na₂O vs. particle size.

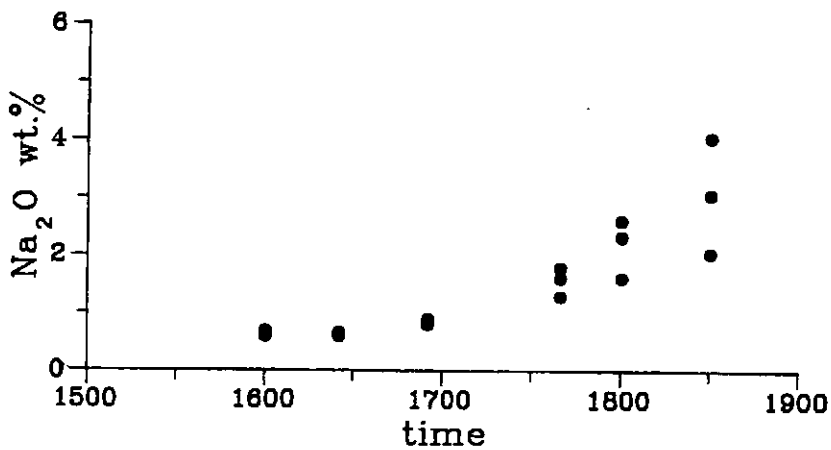


Figure 3.36: Turbidity maximum profiles: total particulate Na₂O vs. time.

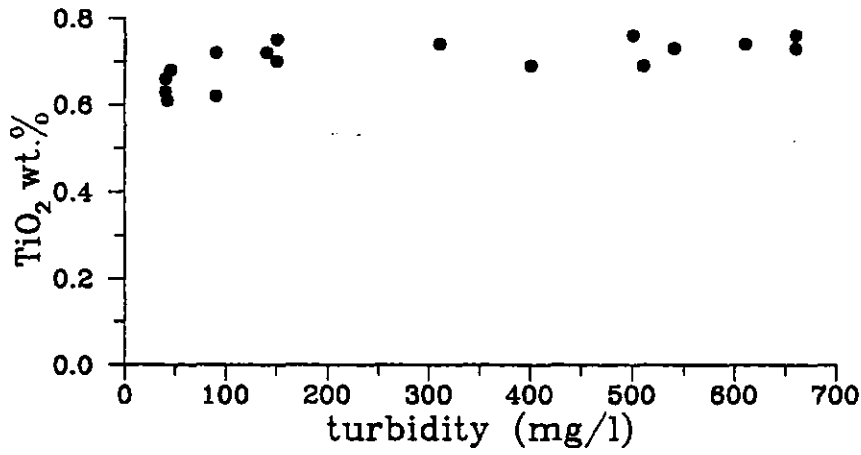


Figure 3.37: Turbidity maximum profiles: Total particulate TiO_2 vs. turbidity.

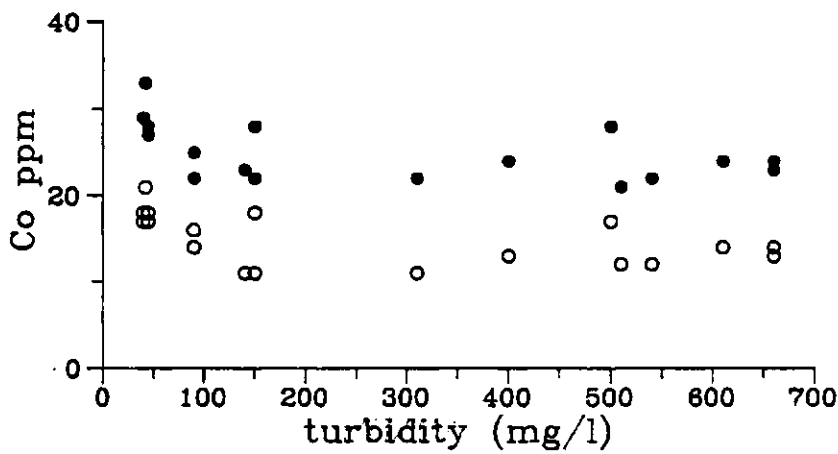


Figure 3.38: Turbidity maximum profiles: particulate Co vs. turbidity. Filled symbols - total, open symbols - leachable.

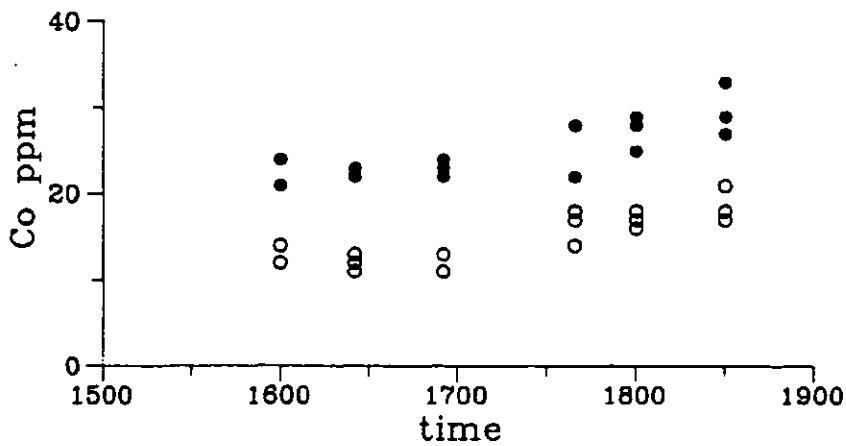


Figure 3.39: Turbidity maximum profiles: particulate Co vs. time. Filled symbols - total, open symbols - leachable.

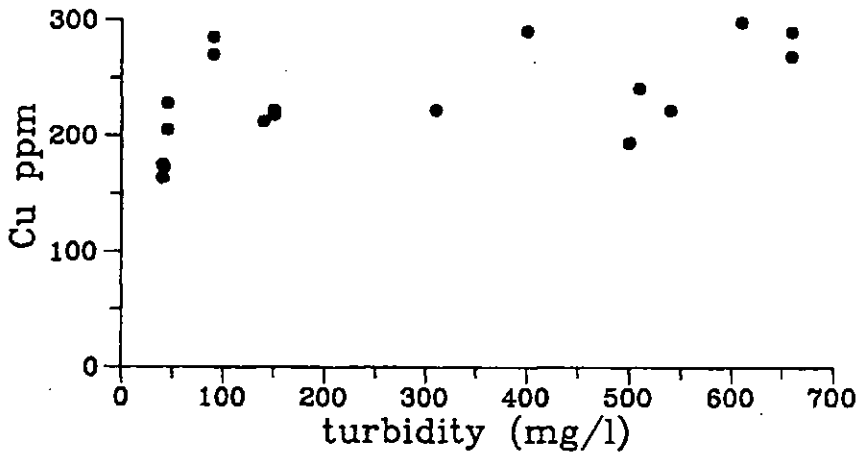


Figure 3.40: Turbidity maximum profiles: total particulate Cu vs. turbidity.

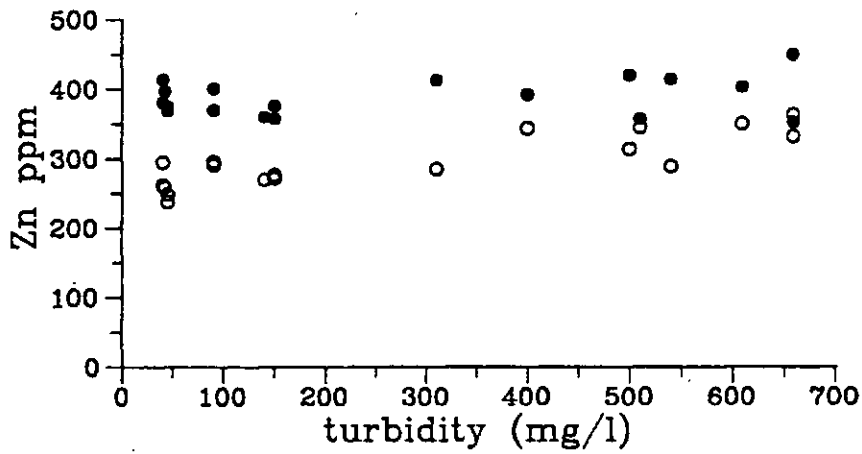


Figure 3.41: Turbidity maximum profiles: particulate Zn vs. turbidity. Filled symbols - total, open symbols - leachable.

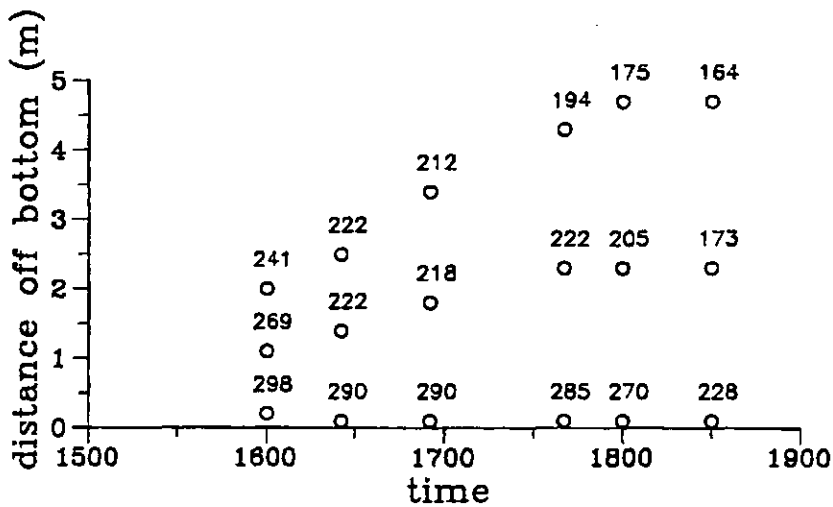


Figure 3.42: Turbidity maximum profiles: distribution of total Cu concentrations in SPM (ppm) with respect to depth and time of sampling.

3.6 Settling Procedure

The previous sampling exercises in the turbidity maximum have examined the variability of the SPM and its relationship to the suspended load. This settling procedure attempts to distinguish any permanently suspended particles (PSP) from those undergoing tidally induced resuspension (RSS). The validity of the procedure as a means of chemically distinguishing particle populations is discussed in 5.1.2.

The relationship between the compositions of these two particle populations, and its dependence on the turbidity of the samples, is examined by using plots of component concentration against turbidity. Since there is a high density of samples at low turbidities a logarithmic axis has been used to allow resolution of the individual data points. Most of the elements studied show little temporal variation, but in cases where significant features are seen plots of concentration against time are shown. Initial use of a concentration/time diagram for Fe is for illustrative purposes only. In all diagrams the PSP and RSS are distinguished by the use of different symbols. The disposition of the samples with respect to time and water depth is shown in figure 3.43.

3.6.1 Major Elements

A number of the major components show significant differences in concentration between the PSP and RSS. Figures 3.44 & 3.45 show quite clearly that the levels of total and leachable Fe_2O_3 and P_2O_5 are higher in the PSP than in the RSS. The constancy of this relationship over the sampling period is shown in figure 3.46. Leach/total ratios for Fe are shown in figure 3.47, and, with the exception of one data point, are consistently higher in the PSP. This indicates that the differences between the particle populations are not simply related to the abundance of the Fe bearing phase(s) in the sample.

Accepting that the procedure has accomplished a significant (in terms of chemical composition) differentiation of particle populations, we must consider how the compositions of the two types of particle are controlled or produced. It is helpful here to depict the Fe-turbidity relationship using a linear x-axis (fig. 3.48). This

shows how the composition of the RSS is largely independent of the suspended load, but that the PSP shows a modest variability in Fe_2O_3 content over a very restricted turbidity range. If the RSS is derived by resuspension of a sediment of relatively consistent major element composition we would expect such behaviour, but the composition of the PSP is by definition independent of the physical resuspension process. As the major chemical process occurring in the turbidity maximum is the removal from solution of significant quantities of Fe and other metals it seems likely that this process plays a part in controlling the composition of the PSP whose physical properties (bouyancy, due to low net density and large surface area) are advantageous for chemical scavenging. The derivation of the enhanced Fe and other metals (following section) from the removal process or otherwise is discussed fully in section 5.3.

There is further major element evidence for mineralogical differences between the two populations in the TiO_2 concentrations, which reach higher levels in the most turbid RSS samples than in the PSP (fig. 3.49). This is consistent with the behaviour of Ti which concentrates in ilmenite and rutile, both dense minerals and likely to settle out in the procedures used here.

Mn behaves similarly to Fe and P, but the elevation of Mn concentrations in the PSP over those found in the RSS is not as consistent (fig. 3.50).

3.6.2 Trace Elements

In keeping with the behaviour observed in the surface samples collected in the previous exercises Cu (fig. 3.51) shows increasing concentrations with turbidity in the RSS, the RSS attaining higher maximum Cu concentrations than the PSP, suggesting that Cu is concentrated in some heavy minerals as well as being present in the more bouyant clay minerals. Unusually, Zn behaves more like Fe (fig. 3.52), showing higher levels in the PSP and little variation in the RSS, with no evidence of heavy Zn-rich minerals in the RSS. Ni (fig. 3.53) shows features of both these types of behaviour, the low turbidity RSS samples yielding lower Ni concentrations than the PSP, but with Ni levels in the RSS rising at turbidities greater than 200 mg l^{-1} . As seen before, Co (fig. 3.54) behaves similarly to Ni, but note that this is the only case in which the highest turbidity samples show

rising levels of Co. Previous sampling exercises (fig. 3.38) have shown a simple inverse correlation between Co concentrations and turbidity.

Leach/total ratios for these metals clearly reflect the incorporation into the RSS of trace metal rich phases, and do not provide a simple means of distinguishing the two particle populations. The REE data (section 4.6) on the other hand, do show distinct differences between the two particle populations in terms of concentration and leach/total ratios.

Inter-element correlation matrices were derived for leachable and total concentrations of all major and trace elements analysed in both populations of particles. Care must be taken in interpretation of these results as there are only 14 samples per matrix, but it is clear that there is only a significant correlation between Fe and trace elements such as Cu etc. in the leachable fraction of the PSP (table 3.3), suggesting that high leachable concentrations of both Fe and other trace metals may be linked.

Briefly, the levels of some major elements (Fe, Mn, P) are significantly higher in the fraction of the samples which remained in suspension after 12 hours. The leachable proportions of many elements are also higher in this permanently suspended fraction. The trace element data are ambiguous due to the presence of heavy minerals with high concentrations of Cu, Ni & Zn in the resuspending sediment. These results agree with the work of van der Sloot & Dunker (1982) and Wellershaus (1981) where estuarine SPM samples were separated into fractions by a continuous centrifugation process. The authors found higher concentrations of Fe, Cu, Zn, La & organic carbon in the permanently suspended fraction.

Fraction	Fe - trace element correlation			
	Co	Cu	Ni	Zn
PSP Total	0.36	0.22	-0.04	0.55
PSP Leach	0.91	0.71	0.79	0.97
RSS Total	0.23	0.06	0.47	-0.15
RSS Leach	0.14	-0.12	-0.37	0.20

Table 3.3: Comparison of correlation coefficients between Fe and trace metals in separated particle populations. Significance level 0.46 at 90% confidence, 0.66 at 99% confidence.

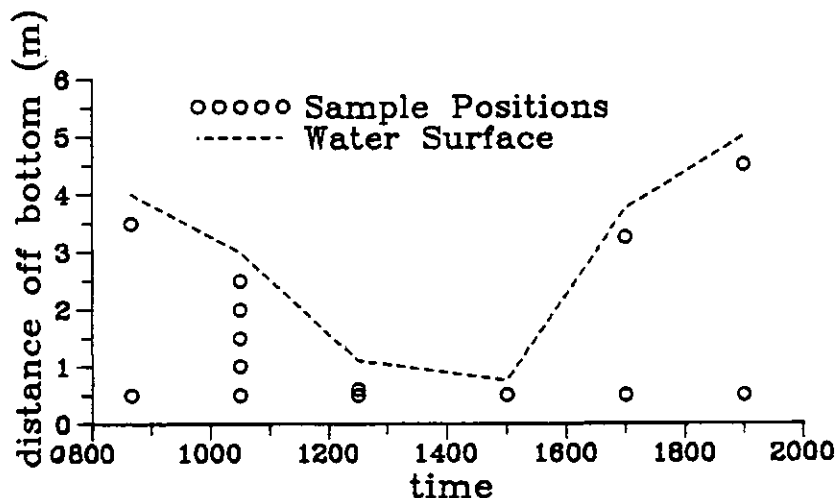


Figure 3.43: Settling procedure: Sample depths and water depth with respect to time.

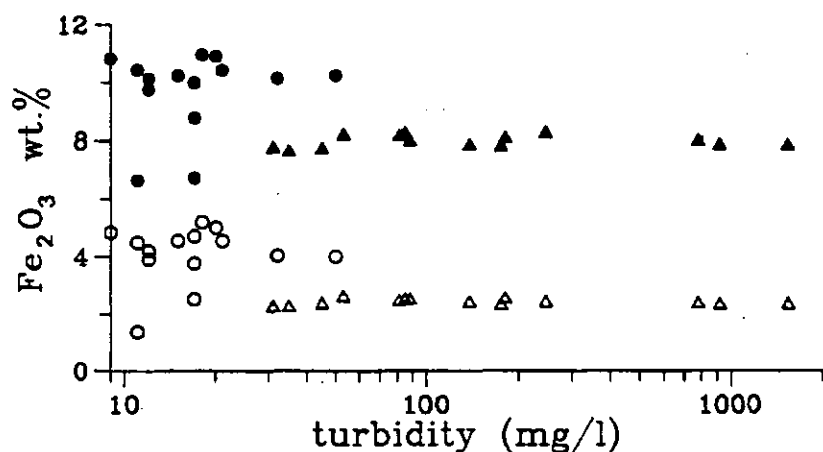


Figure 3.44: Settling procedure: particulate Fe_2O_3 vs. turbidity. Circles - PSP, triangles - RSS. Filled symbols - total, open symbols - leachable.

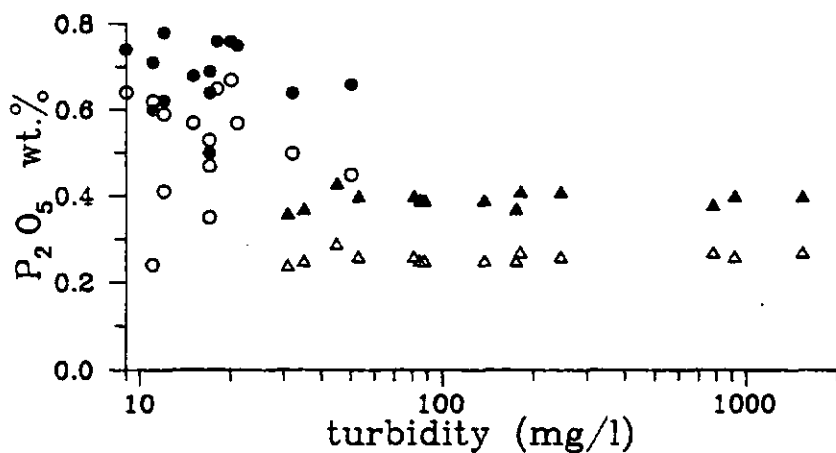


Figure 3.45: Settling procedure: particulate P_2O_5 vs. turbidity. Circles - PSP, triangles - RSS. Filled symbols - total, open symbols - leachable.

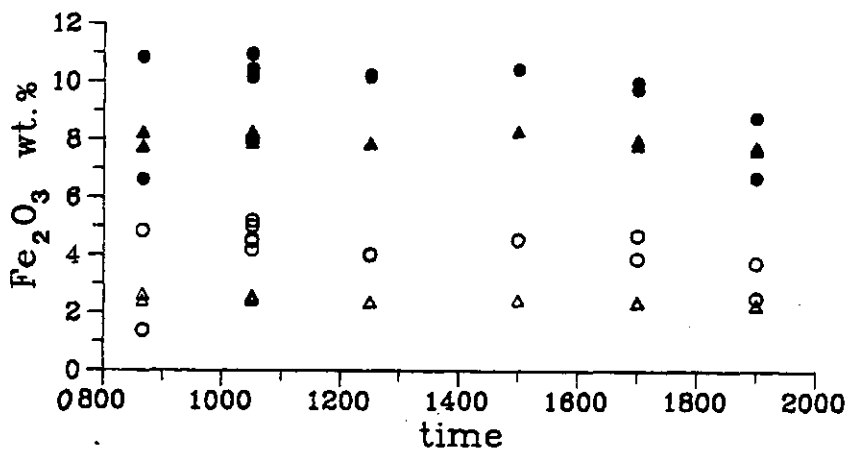


Figure 3.46: Settling procedure: particulate Fe₂O₃ vs. time. Circles - PSP, triangles - RSS. Filled symbols - total, open symbols - leachable.

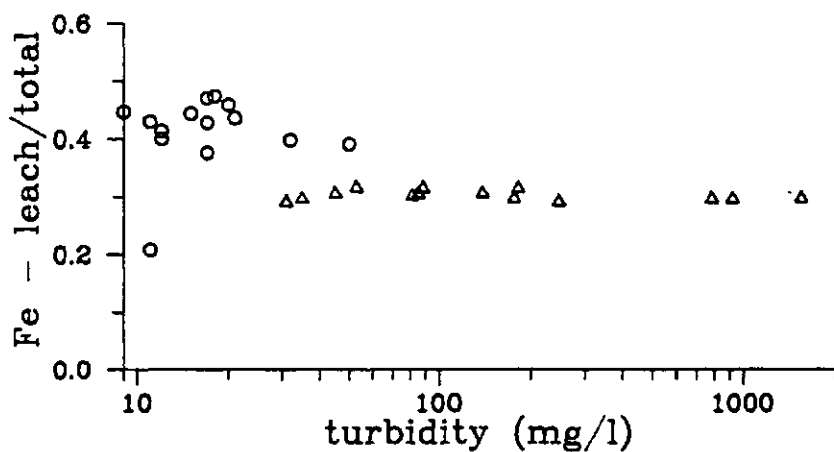


Figure 3.47: Settling procedure: Fe₂O₃ leach/total ratios vs. turbidity. Circles - PSP, triangles - RSS.

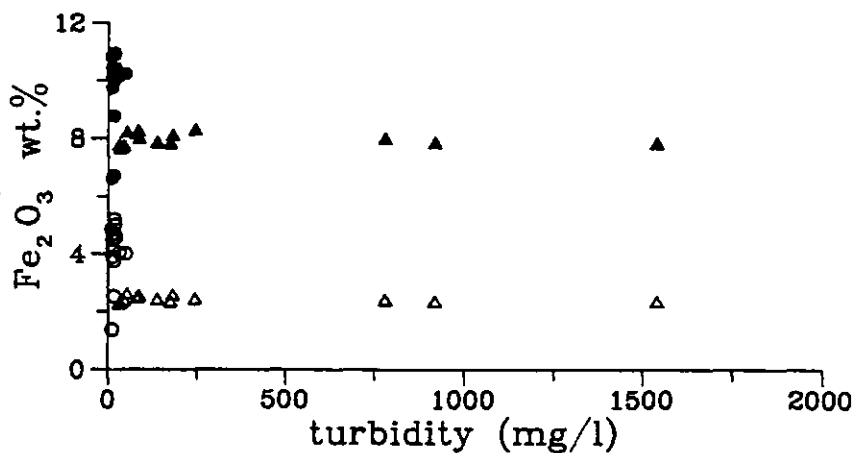


Figure 3.48: Settling procedure: particulate Fe₂O₃ vs. turbidity. N.B. Linear x-axis. Circles - PSP, triangles - RSS. Filled symbols - total, open symbols - leachable.

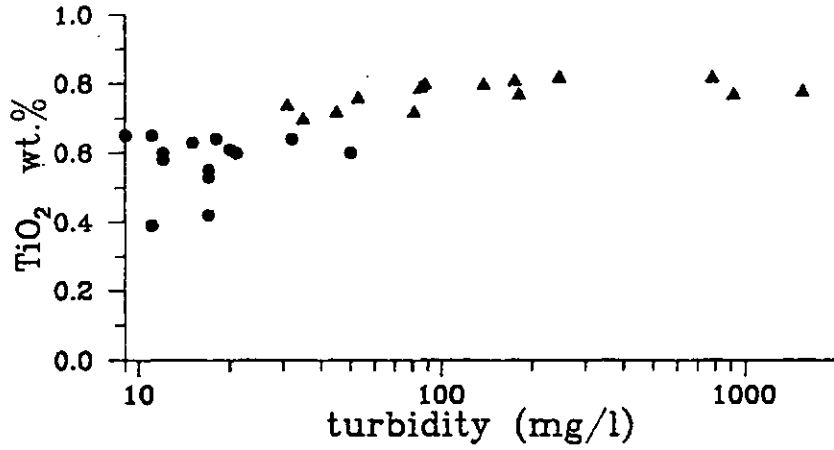


Figure 3.49: Settling procedure: total particulate TiO₂ vs. turbidity. Circles - PSP, triangles - RSS.

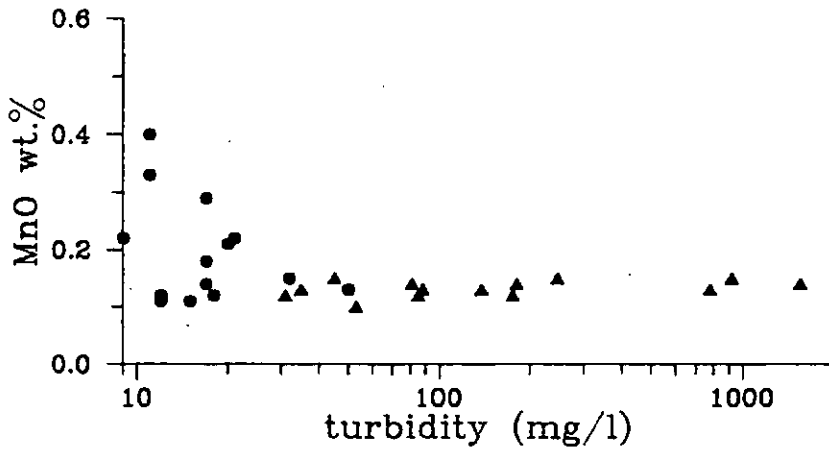


Figure 3.50: Settling procedure: total particulate MnO vs. turbidity. Circles - PSP, triangles - RSS.

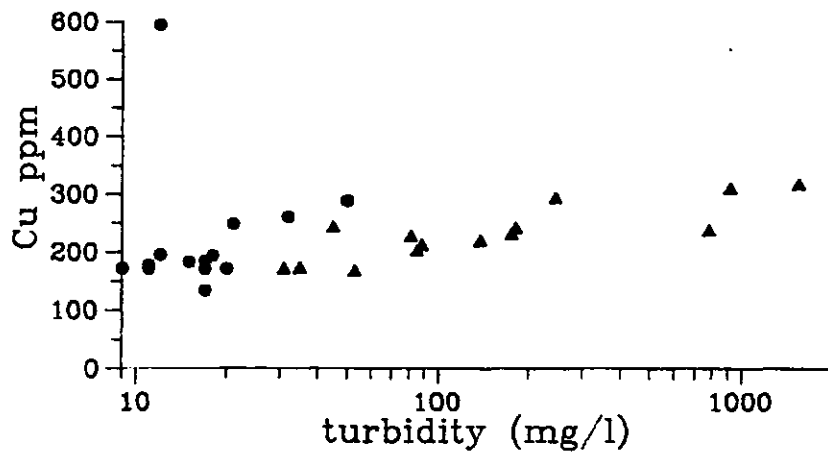


Figure 3.51: Settling procedure: total particulate Cu vs. turbidity. Circles - PSP, triangles - RSS.

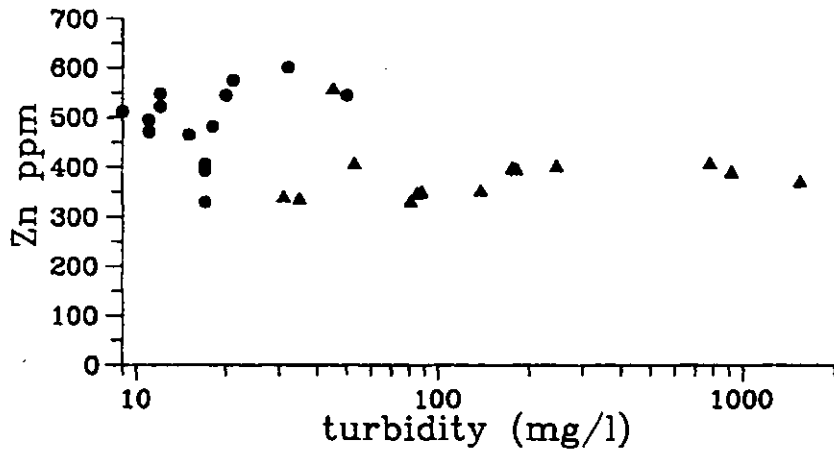


Figure 3.52: Settling procedure: total particulate Zn vs. turbidity. Circles - PSP, triangles - RSS.

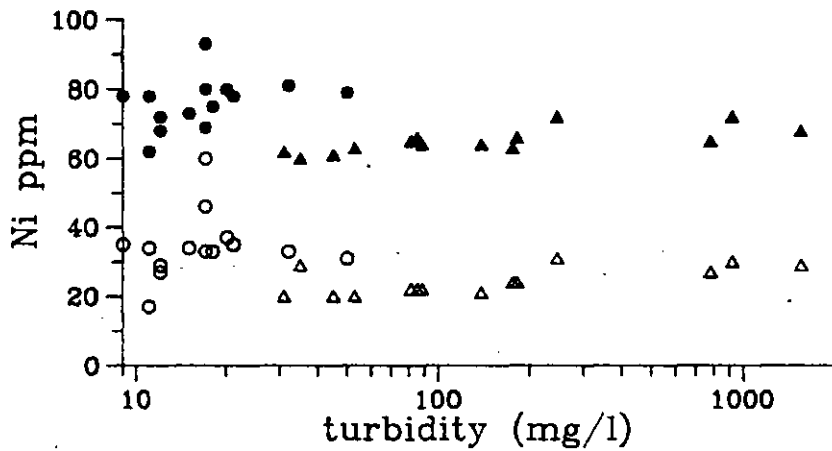


Figure 3.53: Settling procedure: particulate Ni vs. turbidity. Circles - PSP, triangles - RSS. Filled symbols - total, open symbols - leachable.

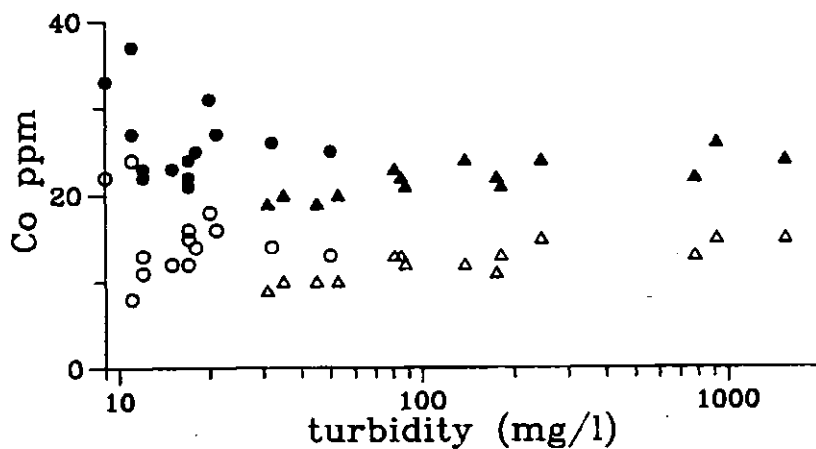


Figure 3.54: Settling procedure: particulate Co vs. turbidity. Circles - PSP, triangles - RSS. Filled symbols - total, open symbols - leachable.

Chapter 4

Results II: Rare Earth Elements

4.1 Sediments

Profiles of REE concentrations against sample depth show little systematic variation. As a proportion of the total concentration of the element present, the variation for each element increases through the REE series. For La the variation is barely discernible, whilst for Gd and the heavier REE the range of concentration is of the order of 20% of the maximum observed (fig. 4.1). Note that the variation is principally evident in the leachable fraction of the REE. Calculation of the leachable REE as a proportion of the total in the sample shows the elements Gd, Dy & Ho to have the greatest (30–40%) leachable proportions. This is in contrast with the data for Buzzards Bay sediments reported in Elderfield & Sholkovitz (1987), where there appears to be no systematic variation of the labile proportions of the REE with atomic number, with all the REE yielding leach/total ratios in the range 0.32–0.43. A plot of the leach/total ratios against depth for La, Nd & Gd is shown in fig. 4.2. Gd displays greater variability in the leach/total ratio as well as a higher absolute value.

Shale normalised REE patterns for these sediments are broadly similar for all samples. The total analyses give patterns (fig. 4.3) which are light REE enriched, with a gradual decline in the sample/shale ratios from 0.85 to 0.55 between La and Yb. In contrast, the leachable REE (fig. 4.3) have a relative enrichment of the middle REE, peaking around the elements Sm-Gd, with no obvious difference in sample/shale ratio between La and Yb. This contrasts with the Buzzards Bay data which show no distinct differences between the shale normalised patterns of the leachable and total REE. Since the Buzzards Bay sediments were leached

with the same procedures as used in this work, and show very similar shale normalised REE patterns from the total analyses, this must be due to the presence of material containing REE with distinctly different relative abundances in the leachable fraction of the Tamar sediments. Note that the logarithmic scale used on the shale normalised diagrams results in compression of differences between samples at higher sample/shale ratios such that a 5 ppm difference between Nd concentrations in two total analyses (where sample/shale \approx 0.8) will appear as a smaller displacement on the graph than a difference of 5 ppm between the Nd concentrations in two leach analyses where sample/shale \approx 0.2.

Comparison of samples from intervals showing high (8–9 cm) and low (4–5 cm) Gd concentrations (fig. 4.4) reveals that the REE patterns have similar profiles and are merely displaced vertically relative to each other. This indicates that the differences in levels of leachable REE are common across the series. Given the trace metal behaviour in these sediments (section 3.1.2), it would seem likely that these differences are also due simply to dilution of the REE bearing aluminosilicates with a REE-poor phase such as quartz. However, the leach/total ratios of the bulk sediment would be preserved in such a case, and the data (fig. 4.2) show that the leach/total ratios are higher in the 8–9 cm sample. This suggests that the assemblage of mineral phases containing the REE is not uniform throughout the core, and contrasts with the findings in section 3.1.2.

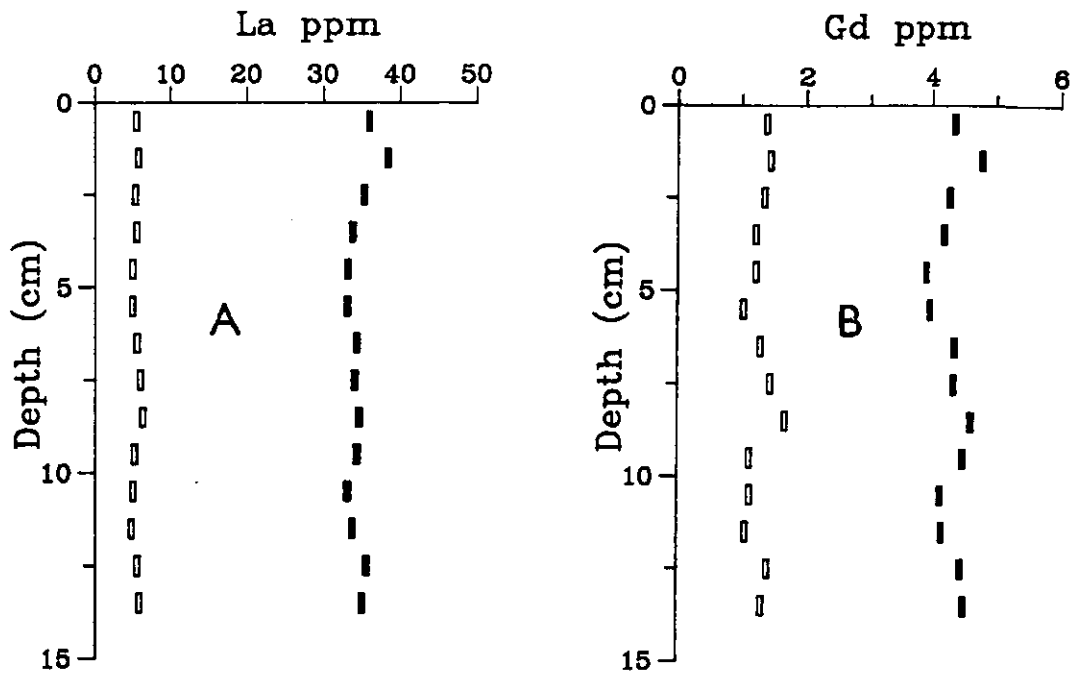


Figure 4.1: Core 1: A - La vs. depth, B - Gd vs. depth. Filled symbols - total, open symbols - leachable.

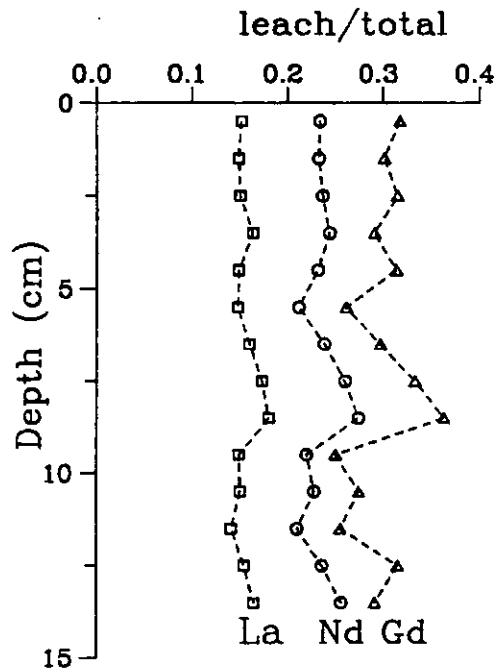


Figure 4.2: Sediment core 1: REE leach/total ratios vs. depth

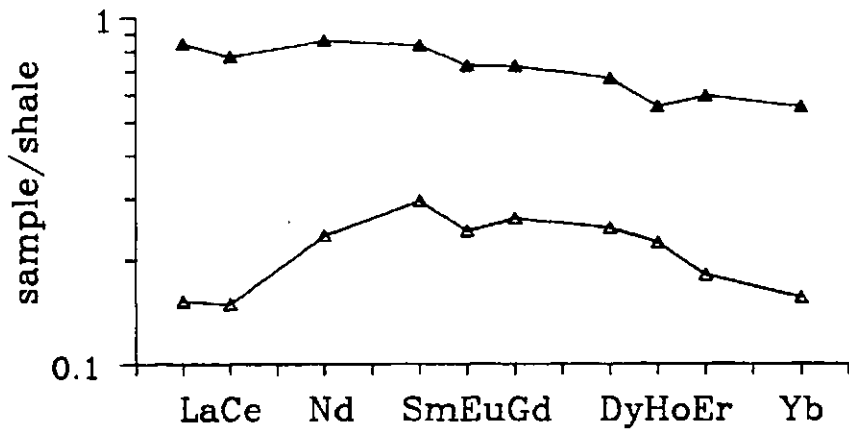


Figure 4.3: Sediment core 1: shale normalised REE patterns for the 8-9 cm interval. Filled symbols - total, open symbols - leachable.

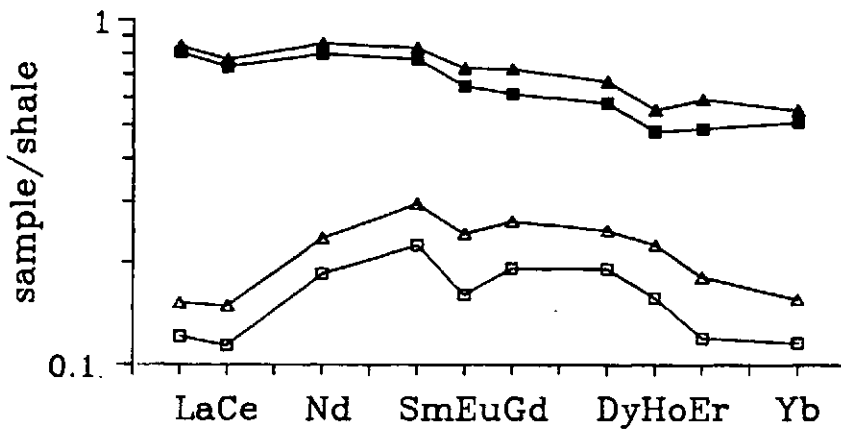


Figure 4.4: Core 1: shale normalised REE patterns for the 4-5 cm (squares) and 8-9 cm (triangles) intervals. Filled symbols - total, open symbols - leachable.

4.2 Pore Waters

As mentioned in section 2.4.2, the REE data from the pore waters are of rather poorer quality than would be desirable. The data from core 1 are particularly sparse, but consistent data were obtained from cores 2 & 3 and the concentration vs. depth profiles are presented here.

REE concentrations in the pore waters are enriched relative to the estuarine waters found over or near the coring site in the axial surveys (Elderfield *et al.*, 1990). The REE concentrations in the overlying waters vary tidally, but show that the enrichment for Nd lies in the range 2–20 times the concentrations found in the overlying water.

Figure 4.5 shows the profiles for Nd in cores 2 & 3. In core 2 there appears to be a subsurface maximum in the 1–2 *cm* interval, followed by a gradual increase in the Nd concentration from approximately 350 pmol kg^{-1} to 600 pmol kg^{-1} . In contrast, core 3 shows a rise in Nd concentration down to the 6–7 *cm* interval, with no distinct subsequent change. However the profiles lack continuity and display considerable scatter, which limits the observations to the facts that Nd concentrations are elevated over the overlying waters and do increase with depth. The profiles for Ce shown in fig. 4.6 show similar scatter, and do not reveal any depth related increases. The only common feature is maximum in concentration at or near the sediment water interface in both cores.

The Sm data are clearer (fig. 4.7). Core 2 shows a gradual increase in Sm levels with depth, whilst in core 3 the Sm concentrations do not increase below 10 *cm*. Given the identity of the nutrient profiles in cores 2 & 3, (section 3.2) there is no reason to expect the REE to display different profiles in the two cores, and as the Sm data from core 3 show considerable scatter, the profile could equally be interpreted as a continuous increase in pore water Sm concentrations with depth. The lack of any apparent subsurface maximum of pore water Sm in core 2 may simply be due to the absence of data for the 1–2 *cm* interval.

The Dy profile for core 2 (fig. 4.8) is rather scattered, but still shows increasing concentrations with depth. Core 3 shows a much clearer plateau of pore water Dy concentrations, and this behaviour is also shown by Er and Eu (fig. 4.9).

The only profile for core 1 shown here is for Nd (fig. 4.10). The Nd concentration appears steady down to 10 cm and then to increase rapidly. Comparison of these REE data with the nutrient and other data (section 3.2) for core 1 shows similarities. Bioturbation influences NH_4^+ and HCO_3^- for example, which show little change down to 10 cm, and an increase with depth thereafter, indicating the establishment of undisturbed reducing conditions. Given the REE profiles in the porewaters from cores 2 & 3 one might expect the REE in core 1 to show sensitivity to any irrigation of the sediment. The Nd profile in figure 4.10 suggests that this is so, but is not conclusive. The other REE data from core 1 do not have sufficient data points to allow discussion of profiles.

These pore water data are not of sufficient quality to show the subsurface maxima and continuous increases with depth which are seen for all REE in the Buzzards Bay porewaters (Elderfield & Sholkovitz, 1987), but do confirm the diagenetic mobility of the REE. Significantly, however, the shale normalised REE patterns for these Tamar sediment pore waters do not behave in the same way as the Buzzards Bay porewaters, which show a progressive shift from a profile consistent with the overlying water near the surface, to one similar to the bulk sediment at depth. Figure 4.11 shows the patterns for selected samples in core 3. Note the similarity in shape for the 2–3 cm and 10–11 cm samples, indicating that porewater REE at these two depths are derived from a similar source. This lack of change is reflected in interelement ratios shown in table 4.1. The estuarine water and sediment data shown indicate that the pore waters, even at depth, have relative REE abundances similar to those in the estuarine waters rather than the bulk sediment. Sholkovitz *et al.* (1989) in an extension of the study of Elderfield & Sholkovitz (1987) report that at depths greater than 40 cm the porewater concentrations of the REE begin to decline and the abundances fractionate due to interaction with diagenetic phases, but this cannot be addressed here as the cores are not deep enough.

For comparison, the shale normalised REE patterns in the estuarine waters are shown in figure 4.12 (data from Elderfield *et al.*, 1990). It is clear that the porewaters have patterns similar to the dissolved riverine and estuarine REE, and lack the light REE enrichment which would indicate that they had been

Molar REE ratios		
	Nd/Er	Ce/Nd
Overlying estuarine waters	5–8.5	0.97–1.45
Pore waters:		
2–3 <i>cm</i>	7.0	1.28
6–7 <i>cm</i>	7.3	1.51
10–11 <i>cm</i>	5.1	1.35
Sediment:		
bulk sediment	18.1	2.06
leachable sediment	16.9	1.41

Table 4.1: Comparison of molar REE ratios in estuarine waters, sediments, and pore waters.

Sample	La_N/Yb_N
Riverine water	0.41
Water overlying coring site	0.3–0.67
Pore waters	0.28–0.38
Bulk sediment	1.49
Leachable sediment	1.01

Table 4.2: Comparison of light REE enrichments in estuarine samples.

derived from a sediment source (fig. 4.3) without fractionation. This light REE enrichment can be quantified as La_N/Yb_N (where La_N is the shale normalised La concentration, *etc.*). A comparison of values for estuarine samples is shown in table 4.2. Note that the leachable fraction of the sediment REE has a light REE enrichment intermediate between the pore water/estuarine water values and the bulk sediment.

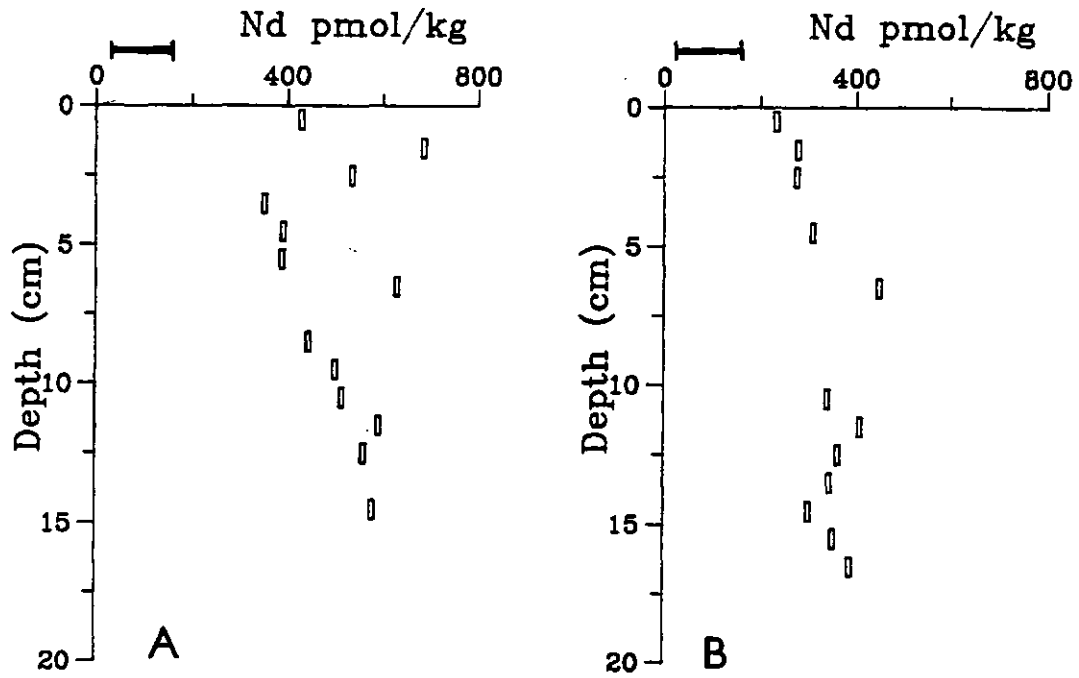


Figure 4.5: Pore water Nd vs. depth: A - core 2, B - core 3. Bar shows concentrations in overlying waters.

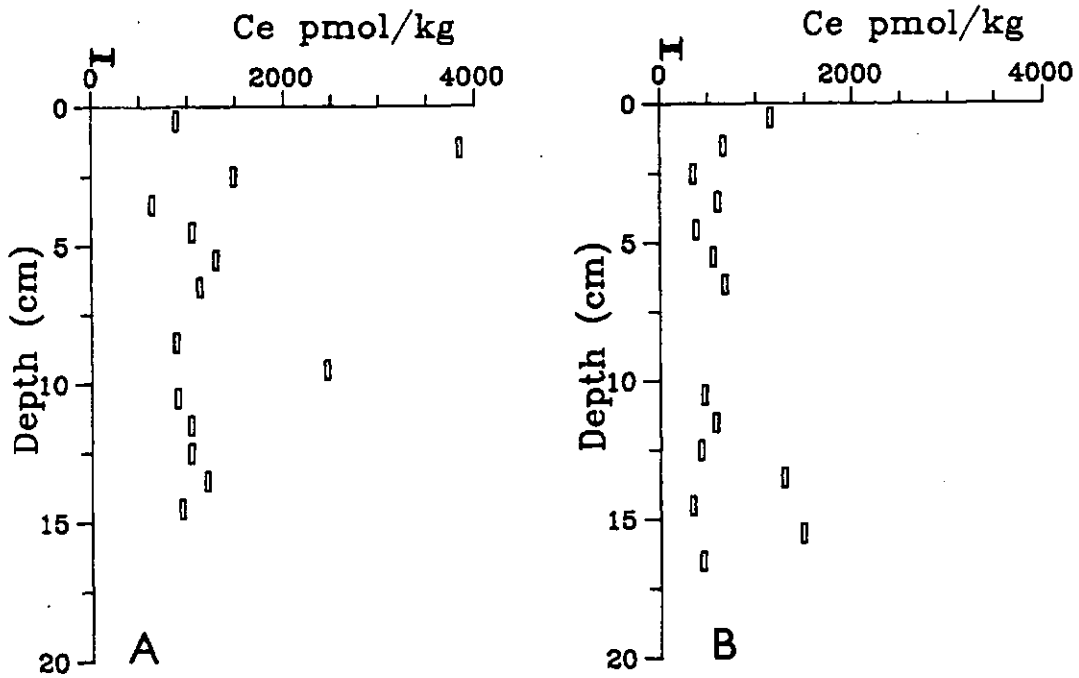


Figure 4.6: Pore water Ce vs. depth: A - core 2, B - core 3. Bar shows concentrations in overlying waters.

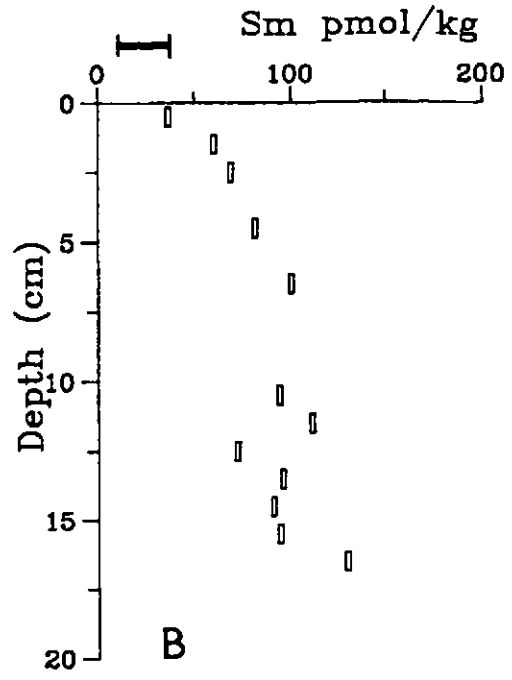
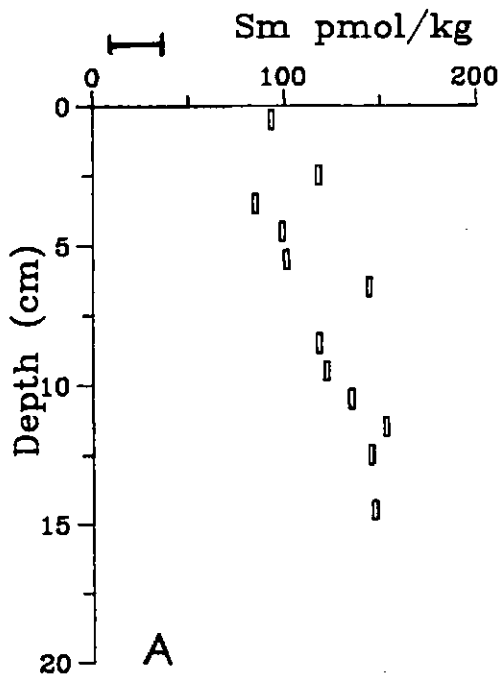


Figure 4.7: Pore water Sm vs. depth: A - core 2, B - core 3. Bar shows concentrations in overlying waters.

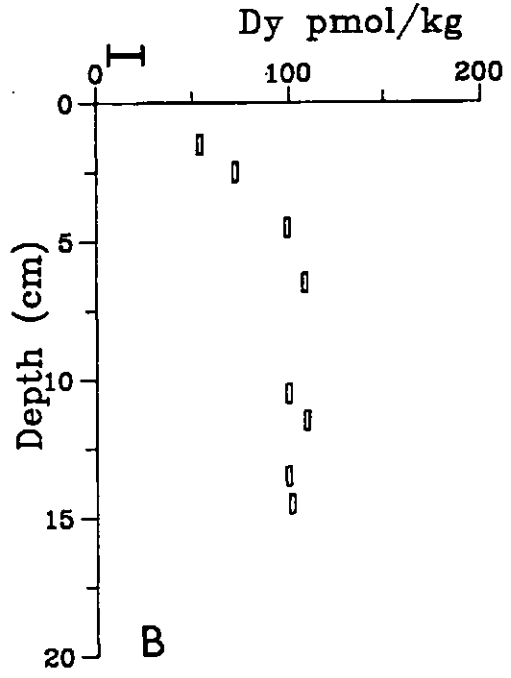
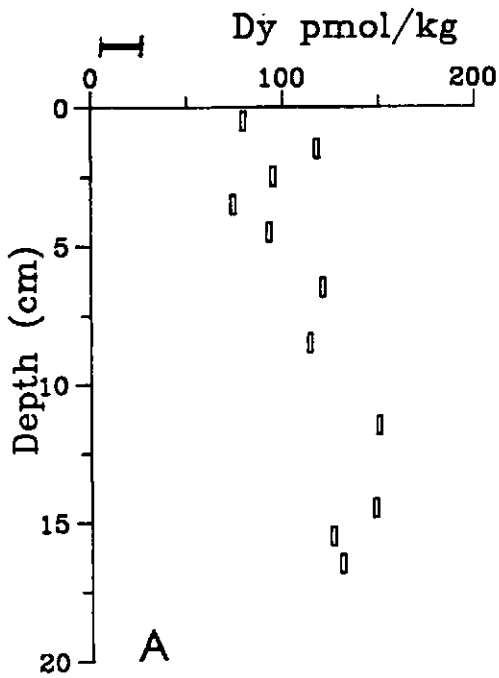


Figure 4.8: Pore water Dy vs. depth: A - core 2, B - core 3. Bar shows concentrations in overlying waters.

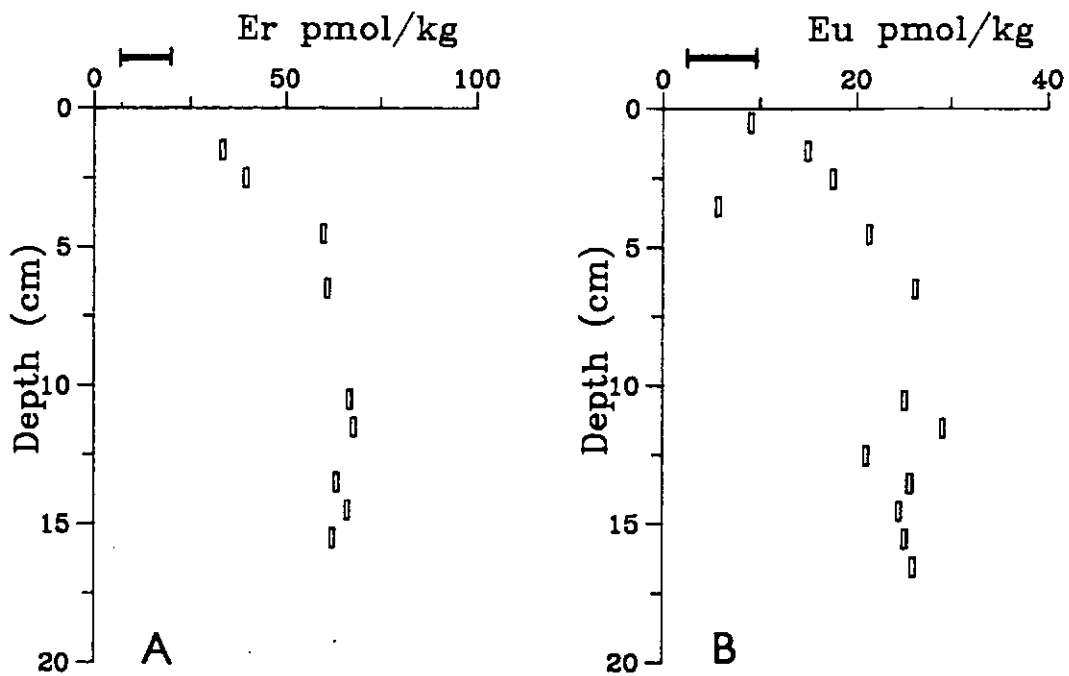


Figure 4.9: Core 3: A - pore water Er, B - pore water Eu. Bar shows concentrations in overlying waters.

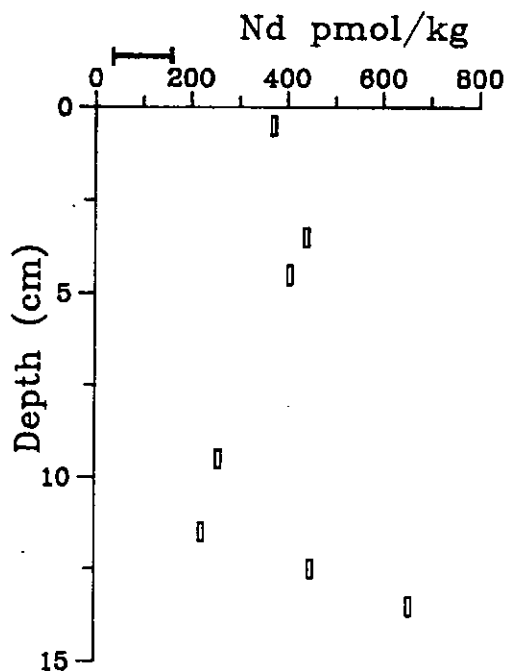


Figure 4.10: Core 1: pore water Nd vs. depth. Bar shows concentrations in overlying waters.

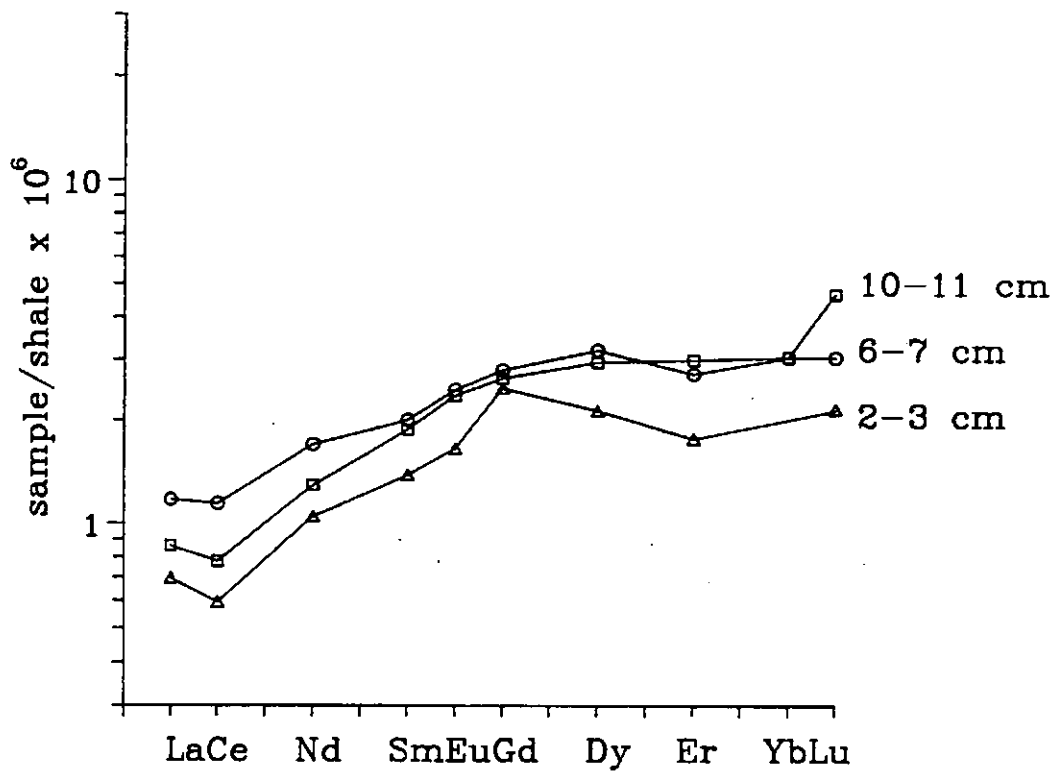


Figure 4.11: Core 3: shale normalised REE patterns for porewater REE.

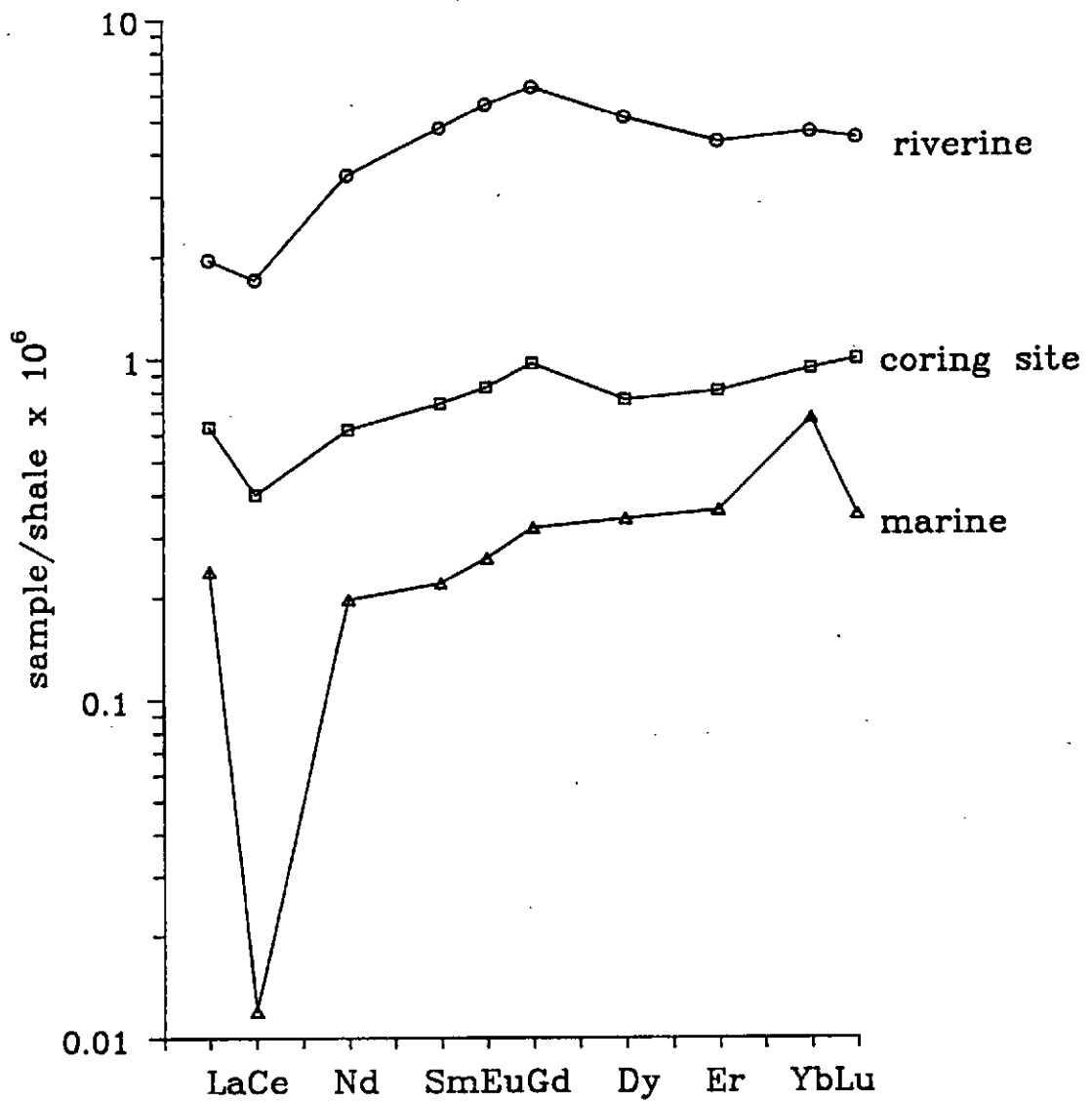


Figure 4.12: Shale normalised REE patterns from dissolved estuarine REE collected during neaps survey (data from Elderfield *et al.*, 1990).

4.3 Spring Tide Axial Survey

In contrast with elements such as Cu and Mn (section 3.3.3), levels of the total and leachable REE in the suspended particles show little variation along the estuary. Figure 4.13 shows the profiles for Nd. Most other REE analysed behave similarly, but note that the heavy REE show slightly lower concentrations in the high salinity samples (fig. 4.14 and table 4.3). The only exception to this behaviour shown by Gd (fig. 4.15), where there is a pronounced increase in the residual or detrital (*i.e.* total minus leachable) particulate Gd in the upper 15 km of the estuary, corresponding with the zone of increased turbidity (fig. 3.9).

Levels of REE are higher overall in the suspended particles than in the sediments, with typical Nd concentrations of 37 and 33 ppm respectively (S.D.= 0.8 ppm). Shale normalised REE patterns for the total REE show no significant differences between the upper and lower estuary, and appear virtually identical (fig. 4.16). Patterns show only a moderate fractionation relative to shale with light REE enrichment ($La_N/Yb_N = 1.4$). These results agree with the findings of Goldstein & Jacobsen (1988) and Sholkovitz (1988) that particulate REE input to the sea does not have a flat ($La_N/Yb_N = 1$) shale normalised pattern.

The enhanced Gd concentrations in the upper estuarine samples are reflected in the slight positive Gd anomalies visible in the shale patterns for these samples. Exactly what is responsible for this anomalous Gd behaviour is not clear. The behaviour of Ce and Eu in natural systems diverges from the rest of the REE due to their redox chemistry and this is well documented (Emmerman *et al.*, 1975; Elderfield, 1988), but anomalous behaviour for Gd is less clear cut (De Baar *et al.*, 1985). In this work, the Gd anomalies cannot easily be attributed to analytical

	ppmEr	ppmYb
3 km, 0.02 ppt	2.62	2.50
27.2 km, 28.7 ppt	2.37	2.23
Standard deviation	0.06	0.05

Table 4.3: Comparison of total heavy REE concentrations in low and high salinity SPM samples from springs survey. Standard deviations of repeat analyses included to show significance.

error as the springs survey data and the turbidity maximum data (next section), were individually normalised to different standards.

We have already seen in 3.3.3 that variations in the detrital concentrations of Cu and Ni in the SPM can be attributed to the resuspension of sediment in the upper estuary and that the distribution of the phases involved is not necessarily uniform throughout the estuarine sediments. It is likely that the behaviour of Gd is controlled in the same manner, but note that in the case of Gd, the elevated detrital concentrations are persistent throughout the entire turbidity maximum and are not restricted to the 10–15 km zone, as is the case for Cu (fig. 3.18). However, as the enhanced Gd levels are restricted to the detrital fraction and are not manifest in the leachable REE they are of less significance to the aqueous estuarine chemical processes. Note that this does imply that for Gd at least, the leachable REE abundances in some samples are independent of the REE content of the detrital silicate.

The leachable proportions of the light REE do not vary significantly (fig. 4.17), however there is variability exhibited by the mid to heavy REE in the upper estuary. Comparison of the data with those from the sediments shows that the leach/total ratios are often higher in the suspended particles. As the detrital levels of the REE are also higher, this difference must be due to elevated levels of leachable REE in the suspended particles. The lower and variable leach/total ratios in the turbid upper estuarine area could be produced simply by resuspension of bed sediment at times of tidal stress and mixing of particles with low leachable levels of REE into the water column.

The differences in the leach/total ratio between the individual REE are reflected in the different profiles obtained from shale normalised patterns for the total and leachable REE in each of the samples (fig. 4.18). The leachable REE give patterns with a very small heavy REE enrichment ($La_N/Yb_N = 0.85-0.95$), but a significant relative enrichment of the middle REE. In contrast, the total REE show a steady decline in relative abundances from La to Yb ($La_N/Yb_N = 1.33-1.47$). The patterns have the same shape as those shown by the sediments (fig. 4.3).

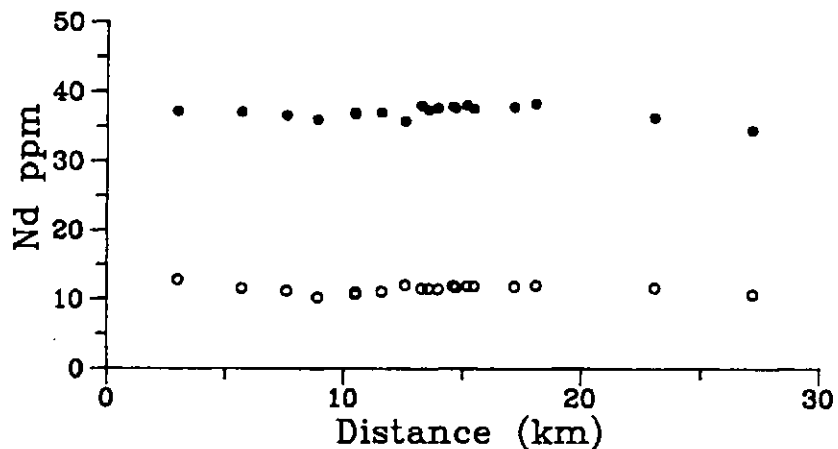


Figure 4.13: Springs survey: Nd in suspended particles vs. distance down estuary. Filled symbols - total, open - symbols leachable.

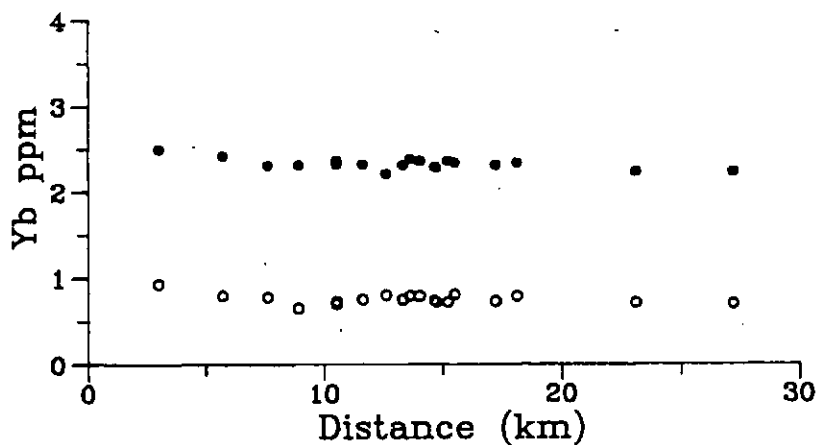


Figure 4.14: Springs survey: Yb in suspended particles vs. distance down estuary. Filled symbols - total, open symbols - leachable.

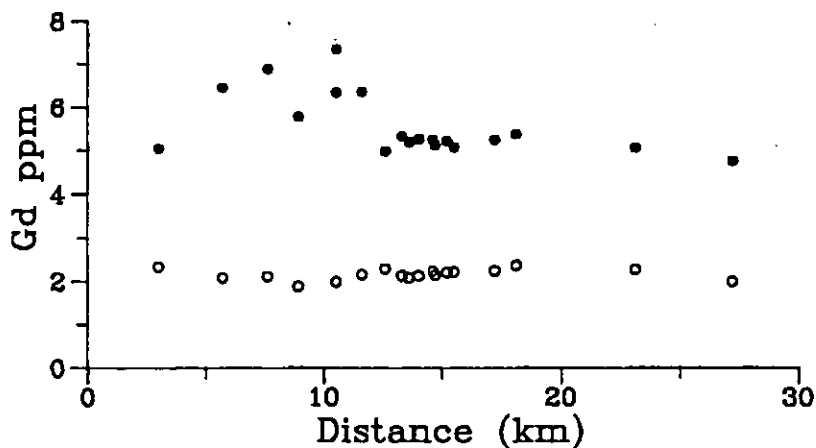


Figure 4.15: Springs survey: Gd in suspended particles vs. distance down estuary. Filled symbols - total, open symbols - leachable.

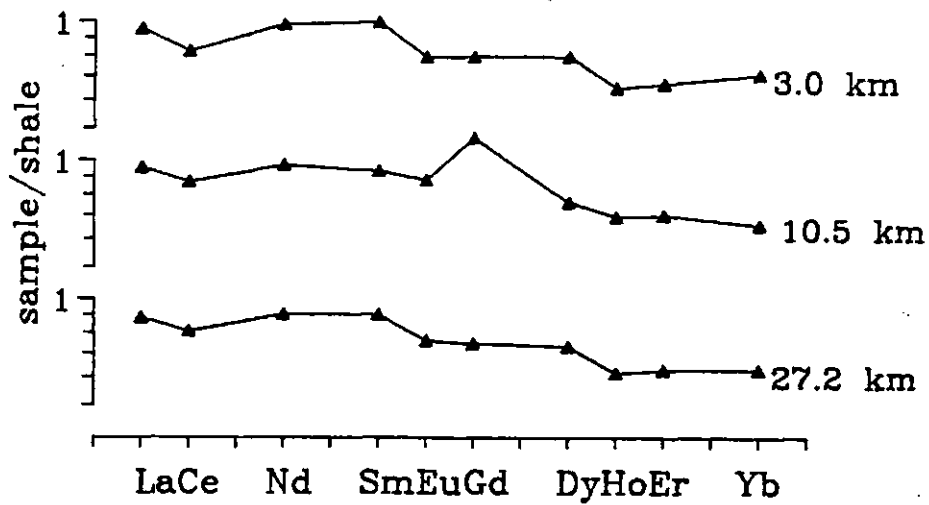


Figure 4.16: Springs Survey: examples of shale normalised patterns for total REE in the suspended particles.

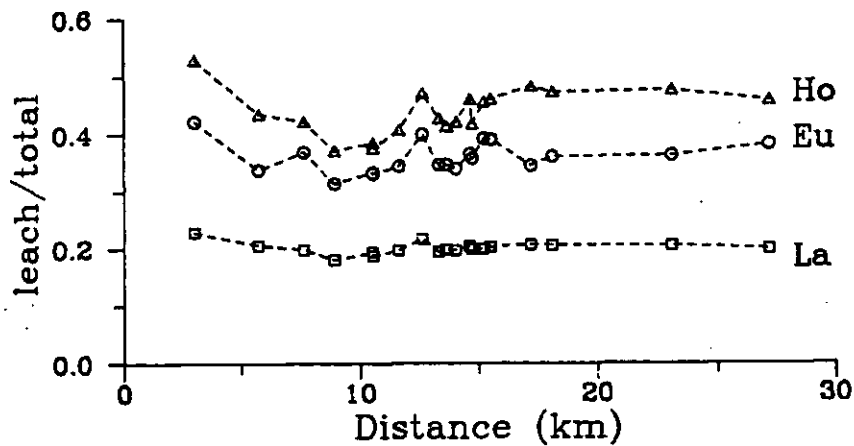


Figure 4.17: Springs Survey: REE leach/total ratios in suspended particles.

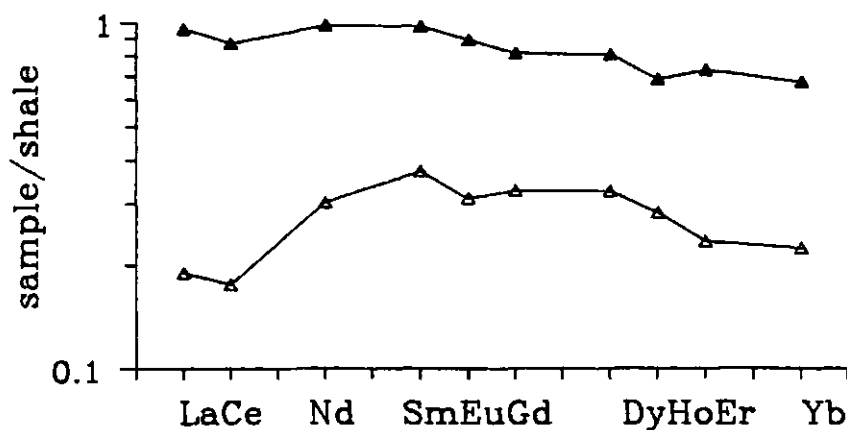


Figure 4.18: Springs Survey: comparison of shale normalised patterns for the leachable and total REE in the 13.6 km sample. Filled symbols - total, open symbols - leachable.

4.4 Turbidity Maximum, Surface Samples

These samples show very little variability in REE concentrations. The levels of leachable and total Nd and Dy for example show no significant variation in either the springs or neaps samples and appear to be independent of turbidity (figs. 4.19 & 4.20). The only anomalous behaviour is that of Gd (fig. 4.21), which shows enhanced residual levels in the more turbid spring tide samples. This increase in detrital particulate Gd is of the same magnitude as that found in the springs survey two days previously (fig. 4.15). Shale normalised REE patterns for each set of the turbidity maximum samples show correspondingly little diversity, with the sole feature being a positive Gd anomaly in the total analyses from the spring tide set (figs. 4.22 & 4.23).

Examination of the leach/total ratios for the REE reveals similar behaviour to that found in the axial survey (fig. 4.24). The ratio and its variability increase in the mid to heavy REE. Note that this scatter is restricted to samples of moderate (less than 200 mg l^{-1}) turbidity. At suspended loads greater than this, the leach/total ratios remain low. These turbidity maximum data form an extension of the spring tide axial survey data in terms of suspended load coverage. If the two data sets are combined (fig. 4.25), we see clearly the transition from high leach/total ratios at low turbidity to uniform low ratios at suspended loads in excess of 200 mg l^{-1} .

When considered along with the leach/total ratios in the sediments (fig. 4.2) this suggests that the principal control on the bulk REE composition of the suspended particles in the turbidity maximum is resuspension of bed sediment. The low turbidity samples in the axial surveys are dominated by the presence of suspended particles with relatively high levels of all the REE. The bulk composition of the high turbidity samples is conversely controlled by resuspension of the bed sediment with its lower, but not necessarily invariant, levels of REE and leach/total ratios. The moderate turbidity samples reflect a mixture of these two distinct sources of particles, with a consequent variable intermediate bulk composition.

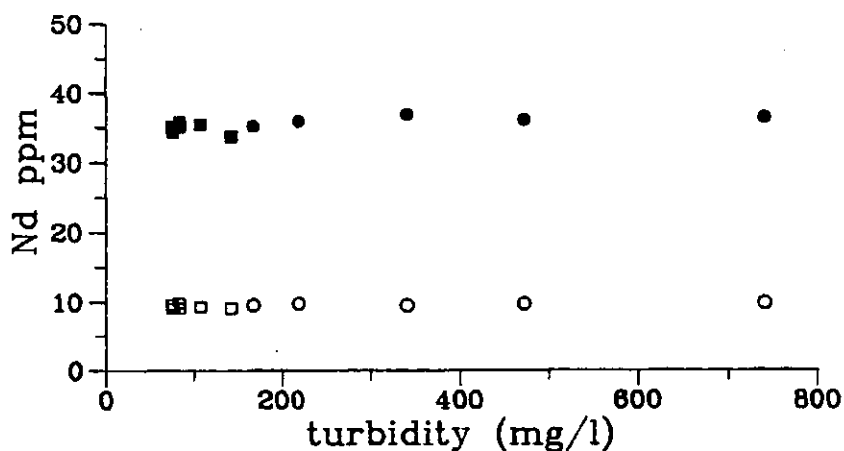


Figure 4.19: Turbidity maximum, surface samples: Nd in suspended particles vs. turbidity. Squares - neap tide, circles - spring tide. Filled symbols - total, open symbols - leachable.

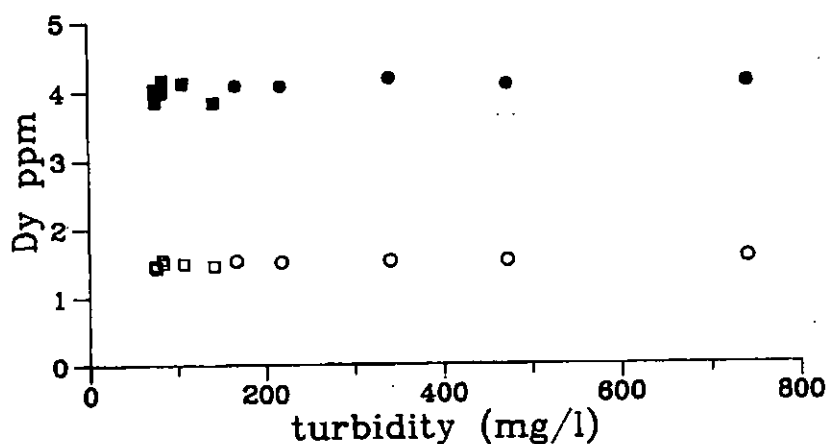


Figure 4.20: Turbidity maximum, surface samples: Dy in suspended particles vs. turbidity. Squares - neap tide, circles - spring tide. Filled symbols - total, open symbols - leachable.

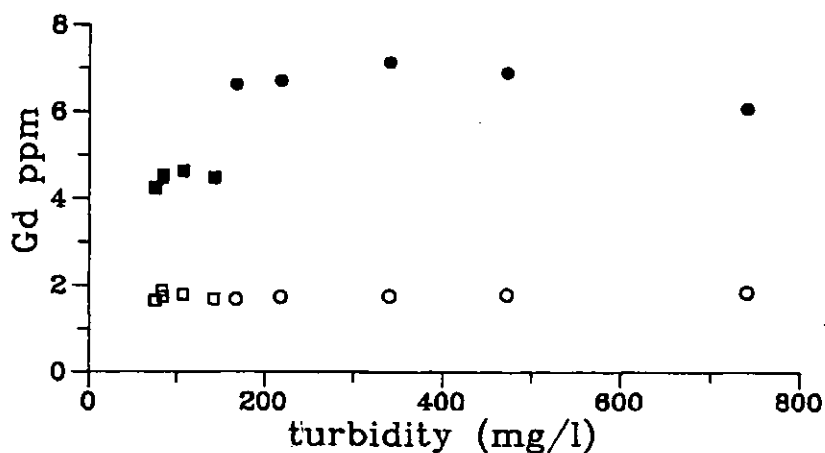


Figure 4.21: Turbidity maximum, surface samples: Gd in suspended particles vs. turbidity. Squares - neap tide, circles - spring tide. Filled symbols - total, open symbols - leachable.

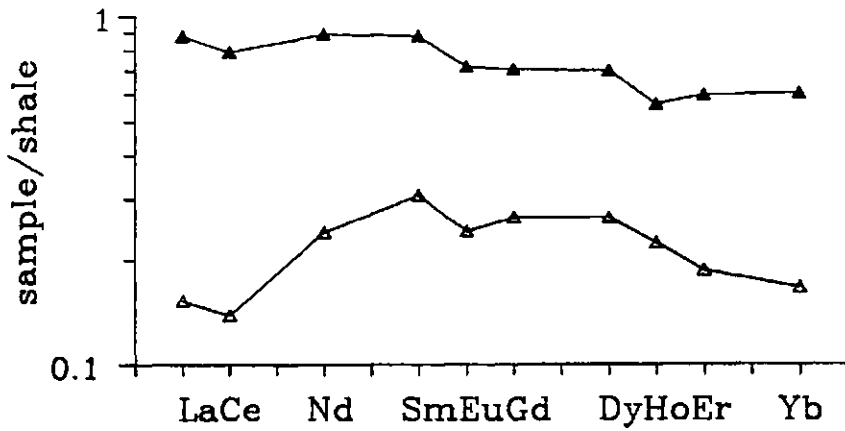


Figure 4.22: Turbidity maximum, surface samples: Shale normalised patterns for the 14:00 h neap tide sample. Filled symbols - total, open symbols - leachable.

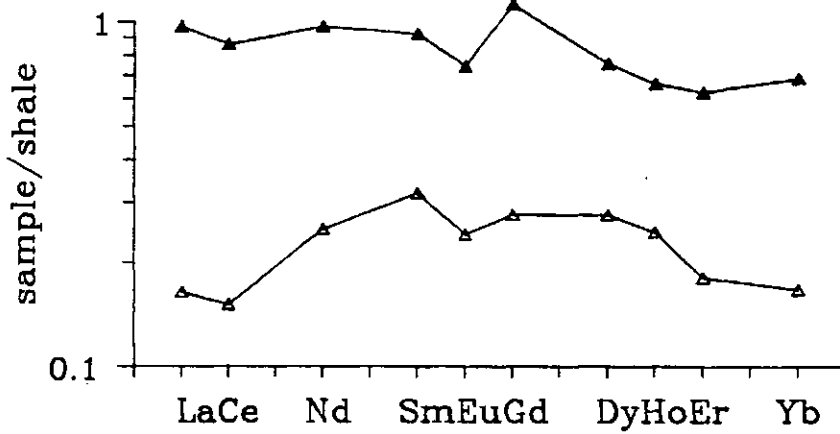


Figure 4.23: Turbidity maximum, surface samples: Shale normalised patterns for the 08:21 h spring tide sample. Filled symbols - total, open symbols - leachable.

4.5 Turbidity Maximum Profiles

Like most trace metals apart from Cu, light REE concentrations in the samples from the turbidity maximum profiles do not show systematic variations with time or depth. Figure 4.26 shows the behaviour of Nd, and is typical of the REE from La to Sm. Comparison of the data with the results from the settling procedures shows the REE levels to be comparable with those in the resuspending particles.

From Eu to Yb there are marked differences in concentrations in the samples collected after 1730 *h*. Figure 4.27 shows Gd, which is typical of all the heavy REE. The divergence of the REE from the more typical concentrations found in the 1600 *h* samples is greatest for Eu and decreases towards Yb.

Plots of concentration vs. turbidity and particle size show that this is associated with a large mean particle size and low turbidity (figs. 4.28 & 4.29). Shale normalised REE patterns from these samples show this as a distinct negative Eu anomaly, with a lesser anomaly for the heavier elements. There is a spectrum of profiles from the typical undepleted sample in fig. 4.30 to the extreme in fig. 4.31. This could represent mixing in of a population of particles of distinct composition, possibly a single mineral phase, at the prevailing physical conditions.

A likely source would be minerals from the Bodmin and Dartmoor granites, which drain into the Tamar. Eu is unique amongst the rare earths as it can exist as Eu^{2+} as well as Eu^{3+} in igneous melts. Formation of Ca-feldspars from a melt results in a relative Eu depletion in the residue as the Eu^{2+} substitutes more readily than the trivalent REE for Ca^{2+} in the crystallising feldspars (Emmerman *et al.*, 1975). Minerals formed subsequently reflect this in the form of negative Eu anomalies.

Plotting the REE from the 18:30 *h*, 2.5 *m* sample, normalised to chondrite (Nakamura, 1974) rather than standard shale (fig. 4.32) and comparing it with a chloritized mineral assemblage from the Bodmin Moor granite (data from Alderton *et al.*, 1980), shows the close similarity of the patterns. It is therefore most likely that the REE patterns displayed by the low turbidity samples are due to the dominance in the suspended particle population of mineral particles derived directly from the granites. It seems unlikely, given the uniformity of the REE in

the samples from elsewhere in the estuary, that an estuarine aqueous process is responsible for these anomalous middle REE abundances.

The spectrum of REE patterns obtained for the bulk composition of the samples could be generated by physical mixing of the 'granite' assemblage with particles of more typical estuarine composition. Note that this effect is localised. The site at which, over the same tidal cycle, large volume samples were being collected for the settling procedure, was only 300 *m* upstream of this location, yet the large negative Eu anomalies were not recorded in the 1900 *h* samples. Note that in the case of these anomalous samples, the changes in the composition of the detrital silicates, (*i.e.* the appearance of substantial negative Eu anomalies) are clearly reflected in the leachable REE extracted from the same samples (see figs. 4.30 & 4.31). This implies that the leach process is extracting REE from the detrital silicate as well as removing labile REE from the surfaces of the particles (see section 5.1).

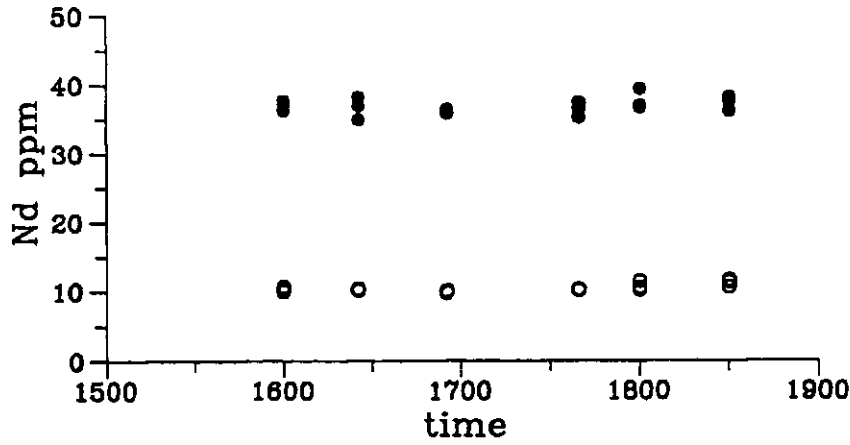


Figure 4.26: Turbidity maximum profiles: Nd in suspended particles vs. time. Filled symbols - total, open symbols - leachable.

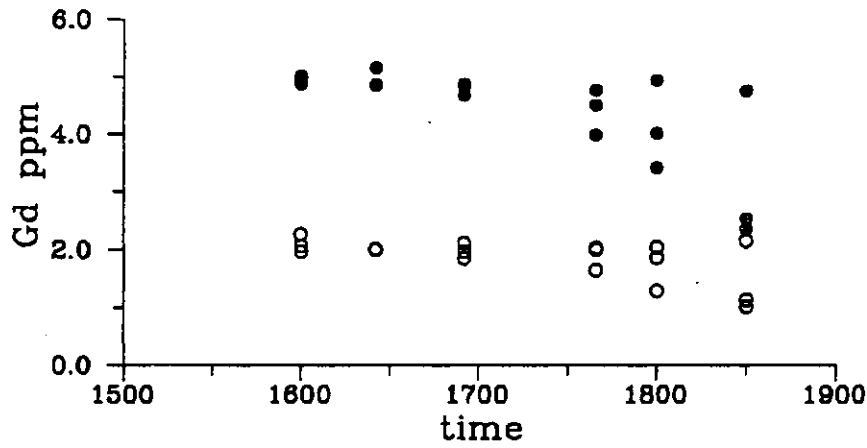


Figure 4.27: Turbidity maximum profiles: Gd in suspended particles vs. time. Filled symbols - total, open symbols - leachable.

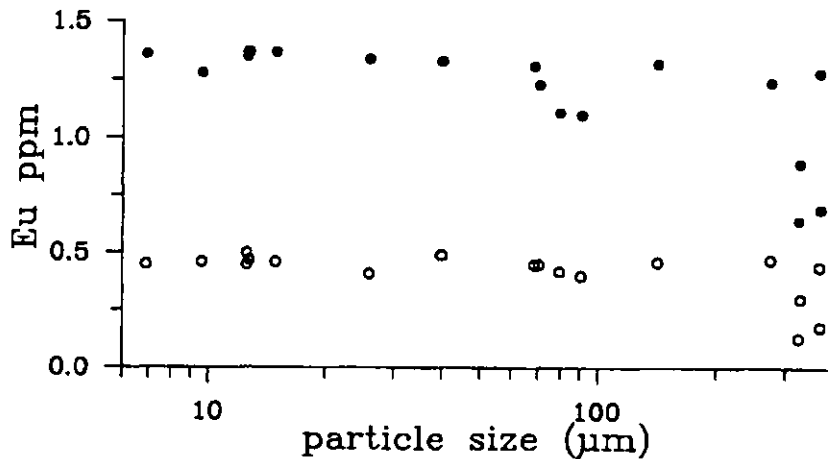


Figure 4.28: Turbidity maximum profiles: Eu in suspended particles vs. median particle size. Filled symbols - total, open symbols - leachable.

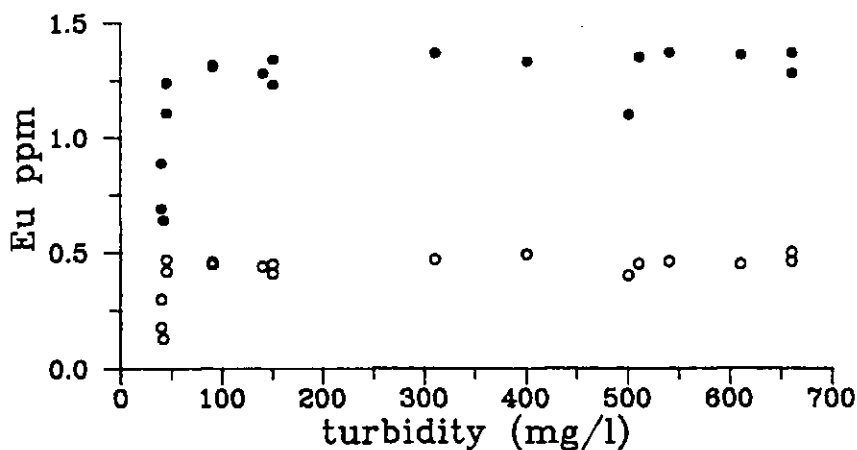


Figure 4.29: Turbidity maximum profiles: Eu in suspended particles vs. turbidity. Filled symbols - total, open symbols - leachable.

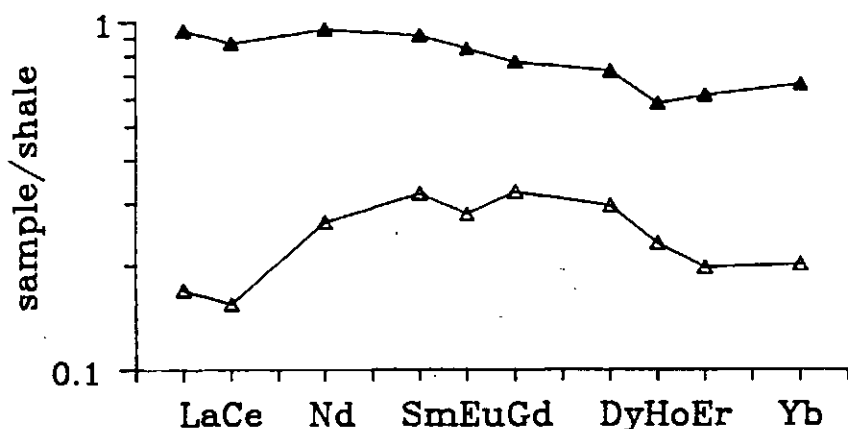


Figure 4.30: Turbidity maximum profiles: shale normalised REE in the 1600 h, 0.1 m sample. Filled symbols - total, open symbols - leachable.

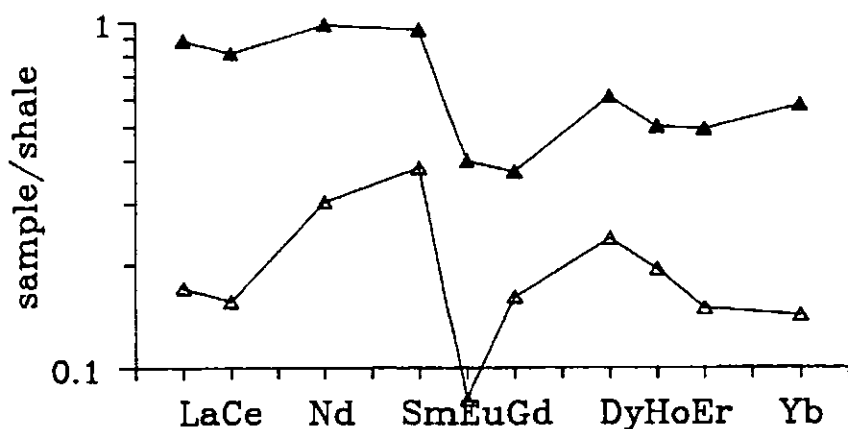


Figure 4.31: Turbidity maximum profiles: shale normalised REE in the 1830 h, 2.5 m sample. Filled symbols - total, open symbols - leachable.

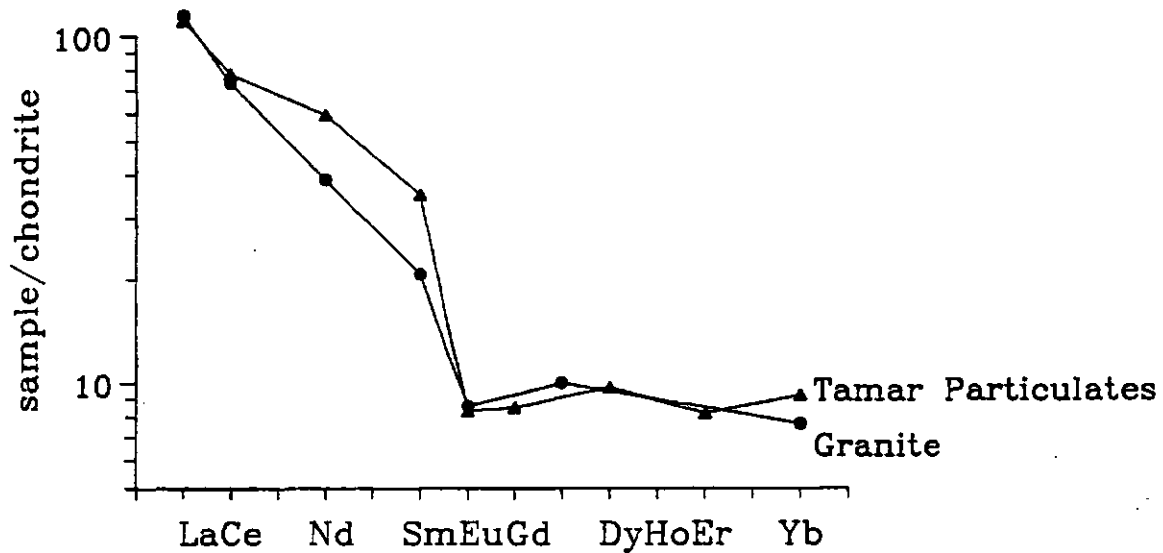


Figure 4.32: Chondrite normalised REE in the 18:30 h, 2.5 m turbidity maximum sample and granite DD7938 from Alderton *et al.*, (1980).

4.6 Settling Procedure

The data in Appendix F show that the levels of REE are generally higher in the permanently suspended particles than in those which are tidally resuspended. This agrees with the results of van der Sloot & Duinker (1982) who separated a permanently suspended fraction (with higher levels of La and Ce than the bulk) from an estuarine SPM sample by a continuous centrifugation process, and the major element data reported in section 3.6. Examples of the relationships are shown in table 4.4, and figures 4.33 & 4.34.

The differences in REE concentration between the two populations of particles (PSP & RSS) are consistent from La across to Yb, and this is reflected in the similarity of the shale normalised patterns. Figure 4.35 shows the patterns obtained from leach and total analyses of the two fractions in a single sample, and is typical of the results obtained from this study. Note that the proportional difference between the REE content of the particle populations (represented as a vertical displacement between the patterns) is greatest in the leachable fraction of the sample. Due to the logarithmic scale, a 20% difference between the REE concentrations in any pair of samples will lead to the same vertical displacement between the patterns, irrespective of their position along the Y-axis.

This means that the differences in REE composition between the two particle populations are due to variations in the amounts of leachable REE present rather than the leach merely reflecting changes in the composition of the detrital or residual silicates. This does not rule out the possibility that the variations are due to differences in the physical properties and hence chemical reactivity of the particles. The likelihood of artifacts in the leachable REE analyses is discussed in section 5.1, and the potential sources of the leachable REE in section 5.2.

The 1900 *h*, 4.5 *m* sample provides further evidence of the independence of the leachable REE from the detrital. Normally, the total REE concentrations as well as the leachable are higher in the PSP than in the RSS. But in this sample, the total REE concentrations in the PSP are lower than in the RSS, while the leachable REE in the PSP remain higher than in the RSS. This is shown in the shale normalised REE patterns in fig. 4.36. The leachable REE in the PSP appear

	Permanently Suspended		Resuspending	
	Leach	Total	Leach	Total
La	9.8	43	6.6	39
Ce	17.6	81	12.7	77
Nd	14.4	41	9.9	37
Sm	3.3	8.1	2.4	7.0
Eu	0.71	1.63	0.44	1.40
Gd	3.0	6.3	1.9	5.2
Dy	2.4	4.6	1.58	4.1
Ho	0.46	0.98	0.32	0.88
Er	1.11	2.9	0.74	2.6
Yb	0.90	2.6	0.57	2.4

Table 4.4: Comparison of REE concentrations (in ppm) in the permanently suspended and resuspending fractions of the 1030 h, 1 m sample.

	Leach/Total Ratios				
	Sediments	Springs Survey	Turb. Max.	PSP	RSS
La	0.15-0.19	0.19-0.23	0.17-0.18	0.20-0.23	0.16-0.20
Eu	0.21-0.33	0.33-0.43	0.30-0.34	0.40-0.44	0.28-0.35
Ho	0.28-0.41	0.37-0.53	0.35-0.40	0.39-0.47	0.31-0.40

Table 4.5: Comparison of REE leach/total ratios in different sample sets.

to be independent of the total REE in this case, supporting the hypothesis that their abundance, to a degree, is not dependent on the chemical composition of the detrital minerals, and that they are possibly derived (at least partially) from another source.

The leach/total ratios in the permanently suspended particles are the highest found for any of the samples in this work. A comparison of the ranges of these results with those other estuarine samples is shown in table 4.5.

Variations in the concentrations of particulate REE with tidal state are minor. Figures 4.37 and 4.38 show that the levels of leachable and total particulate Gd are relatively constant apart from in samples collected at 0840 h and 1900 h. Reference to figure 3.46 shows that this is associated with changes in the major element composition of the SPM and is hence unlikely to be the result of chemical process in the low salinity zone.

Inspection of the data in Appendix F appears to show significant differences between levels of the REE in bottom and surface water SPM. However, after exclusion of the 0840 and 1900 *h* samples to eliminate any effect of different detrital mineral composition, there is no consistent relationship between REE concentration and sample depth such as that found for Cu (fig. 3.42).

In an attempt to examine the relationships between the levels of Fe and REE in the two particle populations, correlation matrices were calculated for Fe against all the REE analysed in both particle populations and for leachable as well as total concentrations. Interpretation of the coefficients obtained (table 4.6) requires considerable care as it is difficult to distinguish between the effect of restricted sample compositions and uncorrelated variations.

The results show that the most significant correlations are between the levels of total Fe and total REE in the PSP and that the Fe-REE correlations in the RSS are barely significant. The enhanced correlations in the PSP can in part be attributed to the fact that the REE and Fe concentrations in the PSP cover a much greater range than in the RSS, hence artificially improving the correlation coefficients. To allow for this, the correlation coefficients for the PSP were recalculated without the three anomalous samples (0840*h*, 3.5 *m*; 1900 *h*, 4.5 *m*; 1900 *h*, 0.5 *m*) and are shown alongside the coefficients derived for the entire datasets. The observations noted above still hold for the reduced datasets.

Assuming that the maintenance of an estuarine turbidity maximum involves the semi-permanent suspension of particles of particular settling velocity, and hence size and density, one would expect the chemical composition of the PSP to be more restricted than the RSS, which is more likely to consist of an assemblage of phases. Additionally, if the removal of Fe and the REE from the estuarine waters is linked, and these elements are deposited onto particles in the turbidity maximum, then one might expect this to be manifest as a good correlation between Fe and the REE in the leachable portions of these samples.

Correlations in the leach results are poorer, and this may reflect uncertainties in the process of leaching heterogeneous ungraded samples (particularly in view of the substantial contribution of REE from the detrital minerals to the leachable REE abundances, as determined in section 5.3), as well as real variations in the

Fraction	Fe - REE correlation	
	La	Yb
PSP Total	0.76(0.76)	0.94(0.54)
PSP Leach	0.58(0.64)	0.69(0.43)
RSS Total	0.59	0.23
RSS Leach	0.56	0.34

Table 4.6: Comparison of correlation coefficients between Fe and REE in separated particle populations.

composition of the non-detrital phase.

These data suggest that as regards REE concentrations, the particles in the turbidity maximum comprise two distinct populations. One, the resuspending sediment (RSS), characterised by low percentages of leachable REE, with poor to insignificant interelement correlations, suggesting an assemblage of mineral phases which includes Fe-Ti oxides, zircons, tourmalines and ore minerals (sections 2.3.1 & 3.3-3.6). The other permanently suspended population (PSP) characterised by higher leachable REE contents, and relatively good interelement correlations indicating a mineralogically restricted composition dominated by the presence of aluminosilicates. Also the levels of leachable REE appear in some samples to be independent of the detrital or residual silicate, suggesting that they are derived from some other source, such as the removal of river-borne dissolved metals in the low salinity zone.

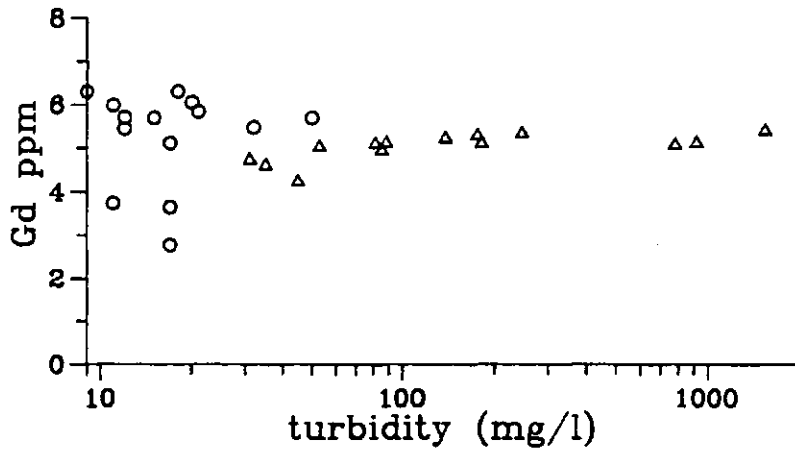


Figure 4.33: Settling procedure: total particulate Gd vs. turbidity. Circles - PSP, triangles - RSS.

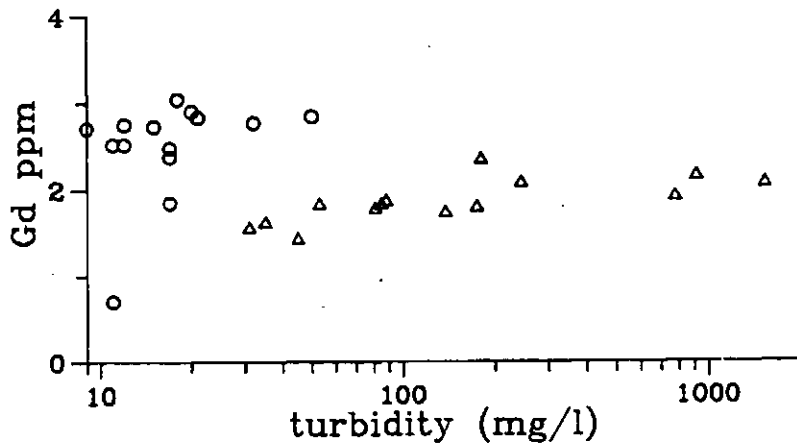


Figure 4.34: Settling procedure: leachable particulate Gd vs. turbidity. Circles - PSP, triangles - RSS.

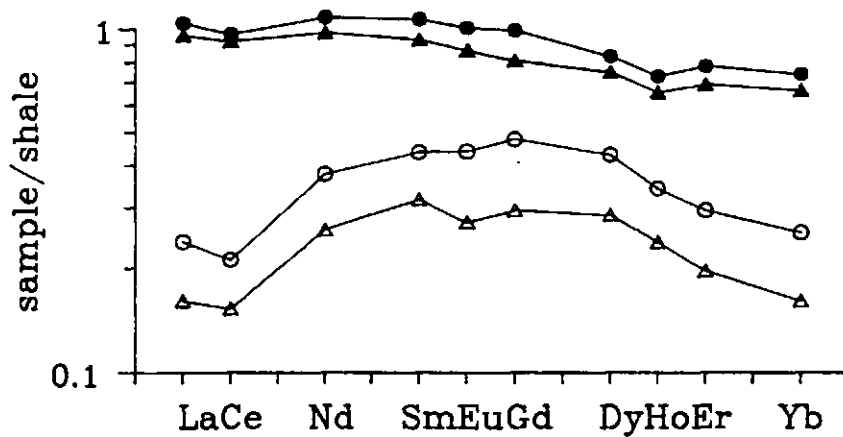


Figure 4.35: Settling procedure: Shale normalised REE patterns for the 10:30 h, 1 m sample. Circles - PSP, triangles - RSS. Filled symbols - total, open symbols - leachable.

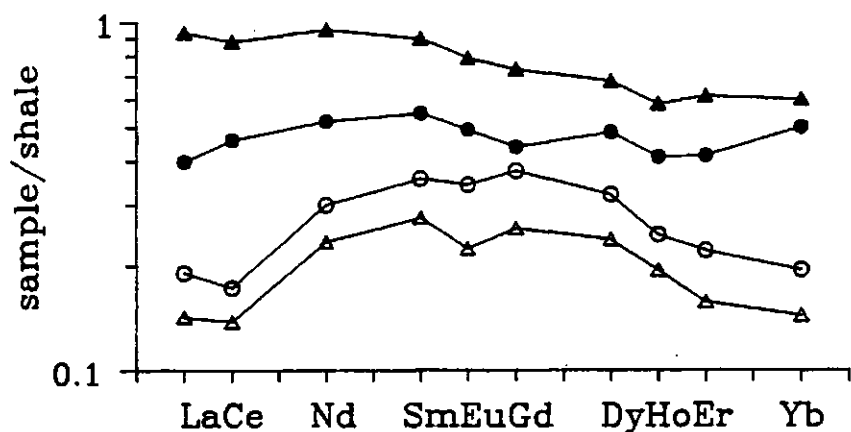


Figure 4.36: Settling procedure: Shale normalised REE patterns for the 19:00 h, 4.5 m sample. Circles - PSP, triangles - RSS. Filled symbols - total, open symbols - leachable.

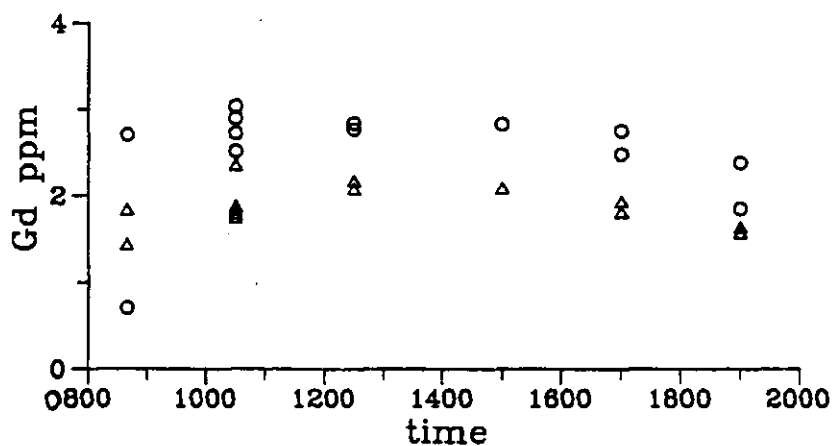


Figure 4.37: Settling procedure: Leachable Gd over tidal cycle. Circles - PSP, triangles - RSS.

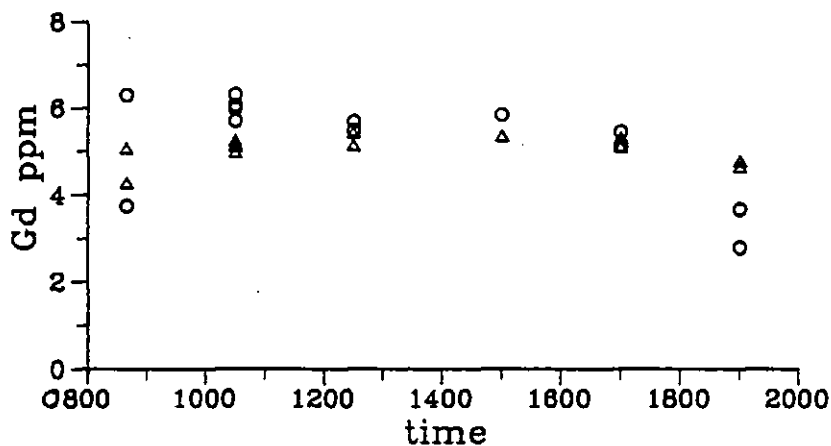


Figure 4.38: Settling procedure: Total Gd over tidal cycle. Circles - PSP, triangles - RSS.

Chapter 5

Discussion & Conclusions

5.1 Analytical Artifacts

5.1.1 Leaching

REE

Given the apparent monotony of the shale normalised patterns obtained from the leachable REE in the Tamar particle and sediment samples, the question arises as to whether these relative abundances are merely artifacts of the interaction of the 1.75M HCl used in the leach and the detrital silicates themselves, rather than representing truly labile REE attached to the surfaces of the particles. A number of recent studies (Kheboian & Bauer, 1987; Rapin *et al.*, 1986) have highlighted the fact that so-called selective leaching procedures are affected by readsorption artifacts and poor recovery of metals from the digesting phases. These can be due to pH changes during the progress of the extraction rendering the leached metals insoluble, or readsorption of leached but still soluble metals onto the surfaces of residual solid phases. Furthermore, the enhanced REE concentrations recorded in the permanently suspended particles (section 4.6) could simply be due to the larger surface area of these more buoyant particles enabling greater release of REE into the leachate than in the case of the resuspending sediment. Millward *et al.* (1990a) have shown that particle surface areas are at a maximum in the Tamar low salinity zone, and Bale *et al.* (1990) report the presence of fragile low density aggregates of clay particles at slack water conditions in the Tamar turbidity maximum. It is important, therefore, that the validity of the leaching procedure is established before attempting a detailed interpretation of the results.

The quantities of REE obtained from a solid sample by any leaching process will depend on the interaction of the leached REE with the residual materials (in this case principally clay minerals) and the leach reagent, as well as the REE abundances in the phases which completely dissolve. In natural waters, the relative abundances of the dissolved REE are significantly controlled by complexation of the REE with CO_3^{2-} ligands (Cantrell & Byrne, 1987; Turner *et al.*, 1981), with minor SO_4^{2-} and Cl^- complexation in seawater. The enhanced stability of the Lu- CO_3 complex over the La- CO_3 complex is evident in the chemical weathering products delivered by the Tamar river, namely, heavy REE enriched shale normalised patterns obtained for the river waters (section 4.2) which contrast with the light REE enriched patterns shown by the suspended particulates and estuarine sediments. Extrapolation of the smooth progression of complex stability constants (Cantrell & Byrne, 1987) from the limited data on natural systems to the leaching procedure (where pH is less than 0) is not appropriate, so the effect of the leach had to be tested by some other means.

To do this a deep-sea clay sediment was subjected to the total digestion and HCl leaching procedures described in chapter 2. These results were then compared with the Tamar data, and data from Buzzards Bay sediments (Elderfield & Sholkovitz, 1987) which were also subjected to the same analytical procedures. The data are presented as leach/total ratios in fig. 5.1. It is clear from the profiles obtained that the fractionation of the REE between the leachable and total analyses, as seen in the Tamar samples, is not the same for all sample types. The deep sea sediment does display the enrichment in the leach of the middle REE seen in the Tamar sample, but lacks the overall increase in leach/total ratio between La and Yb. This heavy REE enrichment is seen in only one of the Buzzards Bay samples (mean shale normalised REE patterns for the Buzzards Bay samples show virtually no fractionation at all between the leachable and total REE).

The conclusion from these results is that the different leach and total shale normalised REE patterns obtained from the Tamar samples are due to significant differences between the relative abundances (and hence sources) of the leachable and detrital REE.

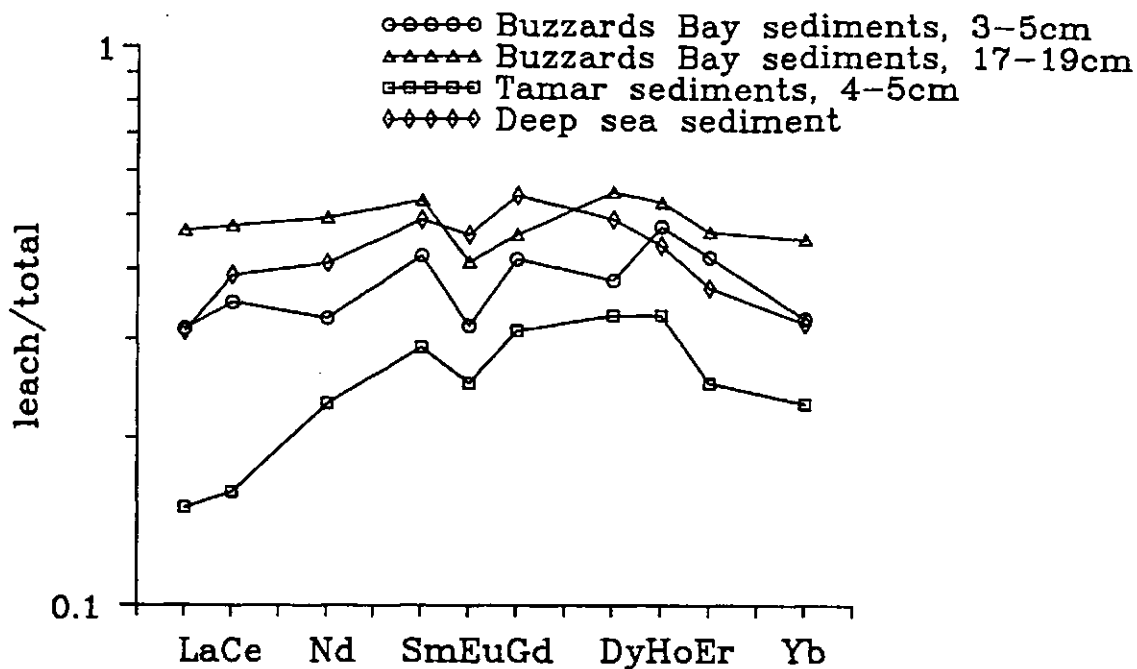


Figure 5.1: Comparison of leach/total ratios obtained from other estuarine and marine sediments with Tamar sediments.

This finding does not completely resolve the problem as there is apparently very little change in the shale normalised pattern of the leachable REE as the proportion of leachable REE increases (compare figs. 4.4 & 4.35). Assuming that there are two distinct sources for the labile and detrital REE, and that the increased proportions of leachable REE observed in the permanently suspended particles were generated by additional quantities of acid labile phases adhering to the detrital silicate substrate, one would expect this to be reflected in a change in the shale normalised patterns of the leachable REE as the proportion of labile REE increased. Close comparison of the mean shale normalised REE patterns from the PSP and sediments (fig. 5.2) shows that in fact the PSP have higher relative abundances of leachable Eu, Gd & Dy. Note that in the material removed from solution in the low salinity zone of the Tamar Estuary (data from Elderfield *et al.*, 1990) these REE have the greatest shale normalised abundances.

However, these differences are small. If the truly labile REE content is genuinely higher in the PSP, and derived from a distinct source, then it is likely to be accompanied by an increase in the contribution to the leachable REE from the residual silicate in order to maintain broadly similar relative abundances in the

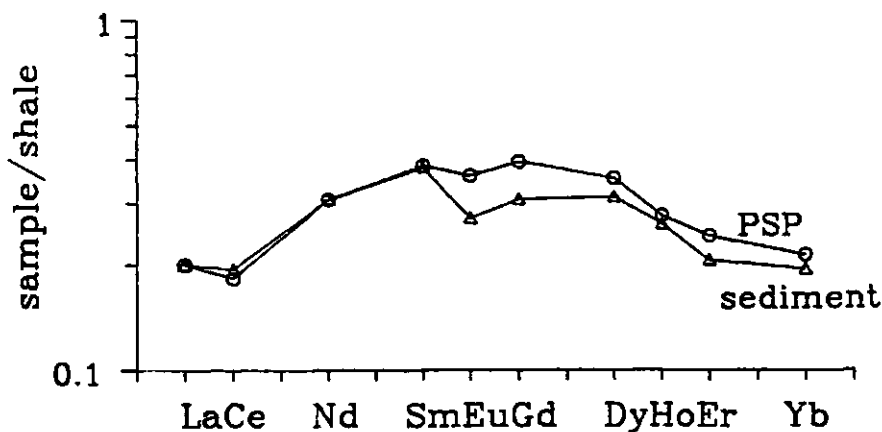


Figure 5.2: Comparison of mean leachable shale normalised REE patterns from Tamar sediments and PSP. Sediment values normalised so that $La_N(\text{sediment})=La_N(\text{PSP})$ to enable close comparison of patterns.

leachate. Enhanced extraction of the detrital REE during the leaching process could be due to larger surface area per unit mass of the permanently suspended particles. This would offset any increase in the genuinely labile REE and so maintain broadly similar relative abundances in the leachate. In this way, the similarity of the relative abundances of the REE in the permanently suspended particles and estuarine sediments would not detract from the conclusion that there are real variations in the amounts of labile particulate REE and that they are derived substantially from a source which is distinct from that of the detrital REE.

The utility of HCl leaching for determination of 'labile' REE in solid samples has more recently been investigated in detail by Sholkovitz (1989). He demonstrates that when performing leaches with HCl solutions stronger than 0.3N there is no significant reabsorption of the solubilized REE onto the detrital substrate, and so there are not likely to be reabsorption artifacts in the REE abundances obtained from such simple leaches. Martin *et al.* (1987) point out that no single leach reagent is capable of dissolving all the oxide and/or sulphide phases in a sediment without also significantly extracting metals from the detrital silicates. Such extraction is evidently occurring in the process used here, and the contribution of the detrital REE to the levels of leachable REE obtained in this work is discussed in section 5.3.

Major and Trace Elements

Evidence for the validity of the leaching procedure as regards the major and other trace elements can be found in inter-element ratios from the Tamar samples. Table 5.1 shows the mean Fe/Al and Co/Al ratios obtained from the sediments and springs survey SPM. The Fe/Al ratios are particularly useful as we can see that, despite the total analyses for the two sample types having very similar ratios, the leach analyses yield significantly different values. In the case of Co the picture is complicated by the fact that element/Al ratios for the total analyses of the two sample types do differ, but this can be resolved by comparing the numerical ratio of the leached and total Co/Al ratios obtained from each sample type. This ratio has the value 11.3 in the sediments and 15.4 in the springs survey SPM. These results could only be generated if the leaching process is digesting a phase or phases of distinct (and variable) composition rather than merely attacking the detrital silicate mineral assemblage to different degrees.

5.1.2 Settling Procedure

The differences in composition between the PSP and RSS, as obtained from the settling procedure, could also be due to an artifact. Higher total concentrations of any given element in the PSP could be due to the presence in the RSS of greater concentrations of a less buoyant and metal poor phase, such as quartz. Also, as discussed above, the enhanced leachable concentrations of Fe, Co & REE observed in the PSP could simply be due to the effect of greater surface area available for attack by the leach reagent, as mentioned in 5.1.1.

Considering the abundances of individual elements first, Fe provides useful information. Simple dilution of the clay minerals in a sample with quartz would not alter the leach/total ratios as the relative proportions of the phases yielding the Fe would remain unchanged (assuming that quartz provides an unfavourable substrate for the attachment of the labile phase(s)). However leach/total ratios for Fe are higher in the PSP (0.38–0.45) than in the RSS (0.29–0.32). The same is also true for the REE (see table 4.5). Changes in the quartz/clay ratio cannot therefore account for these compositional differences between the two particle populations.

	Fe/Al	Co $\times 10^4$ /Al
Sediments		
Total	0.58	2.4
Leach	4.2	27
Springs Survey		
Total	0.59	4.1
Leach	5.1	63

Table 5.1: Mean Fe/Al and Co/Al ratios in Tamar sediments and Springs Survey SPM.

	Fe/Al	Co $\times 10^4$ /Al	Nd $\times 10^4$ /Al
PSP			
Total	0.70	2.7	4.9
Leach	6.9	36	41
RSS			
Total	0.58	2.3	3.6
Leach	4.2	30	22

Table 5.2: Mean element-Al ratios in the permanently suspended particles (PSP) and the resuspending sediment (RSS).

Inter-element ratios provide further evidence for the significance of the chemical distinctions between the PSP and RSS. If the high leachable concentrations of Fe and other trace metals are simply due to greater surface area of the PSP allowing more extensive leaching of the silicate mineral matrices of the particles, we would expect the element/Al ratios to be similar in the PSP and RSS as changes in surface area do not necessarily imply relative changes in the leachability of the different elements in the mineral lattice. Table 5.2 shows element/Al ratios calculated from mean elemental concentrations in the PSP and RSS. The PSP clearly yield greater element/Al ratios for Fe, Co & Nd than the RSS, particularly in the leachable fraction. If we were to consider the RSS to represent the 'normal' values, then the PSP contain higher concentrations of these three elements than the clay content (as defined by Al_2O_3 concentrations) would predict (by a factor of nearly 2 in the case of Nd). Changes in the surface area of the suspended particles cannot explain such differences between the two populations of particles. The conclusion is therefore that the settling procedure is separating the bulk samples into fractions of distinct geochemical characteristics, and that these differences cannot easily be attributed to an artifact of their physical properties or variations in bulk composition.

5.2 Particle Populations

The major and trace element data from the Tamar particle samples indicate that the physical process of sediment resuspension plays a significant role in controlling the bulk chemical composition of the SPM. Variations in both major and trace element composition are observed over distances of tens of meters, and can be unique events (*e.g.* the large negative Eu anomalies present in some samples from the turbidity maximum profiles), or occur regularly on a tidal basis (*e.g.* the Cu-turbidity relationships).

A number of studies (Duinker *et al.*, 1980, 1982b & 1985; Morris *et al.*, 1982c, 1987) have suggested that the SPM in estuarine turbidity maxima comprise two different populations, one permanently suspended and the other undergoing tidal resuspension, but this has been inferred from the physical conditions prevalent at the time of sampling and the turbidity-composition relationships of the various samples. Apart from the continuous centrifugation experiments of van der Sloot & Duinker (1981) and Wellershaus (1981), no direct separation of the sub-populations from the bulk samples has been carried out. The data from the SPM and sediment samples in this work also point to such a distinction, but due to the uncertainties as to the history of any particular body of water sampled it is not possible to assert that even the lowest turbidity samples represent the PSP.

However, given the experimental validity of the settling experiment procedure, as discussed in the previous section, it is possible to state that, as well as short term variations in bulk composition due to physical processes, there are significant differences between the major and trace element compositions of the PSP and RSS in the turbidity maximum. Their distinguishing characteristics are summarised in table 5.3 along with data from the sediments and springs survey for comparison.

In summary, we see that the PSP have enhanced levels of a number of leachable trace and major components (figs. 3.49, 3.51, 3.53, 4.33 & 4.34), they have high organic carbon contents and greater abundances of associated bacteria. Also, the composition of the RSS is relatively constant, whereas the PSP have a significant range of compositions.

	PSP	RSS	Sediments	Springs
Total Al ₂ O ₃ wt.%	19.6	18.0	14.1	19.0
Total Fe ₂ O ₃ wt.%	10.4	8.1	6.2	8.6
Fe ₂ O ₃ leach/total ratio	0.43	0.31	0.27	0.36
Total Co ppm	27	23	18	27
Co leach/total ratio	0.58	0.57	0.44	0.67
Total Nd ppm	39	37	32	37
Nd leach/total ratio	0.32	0.26	0.24	0.31
Leachable Fe/Al	6.9	4.2	4.2	5.1
Leachable P/Al	0.66	0.33	0.31	0.39
Leachable Co×10 ⁴ /Al	34	32	27	63
Leachable Nd×10 ⁴ /Al	28	25	27	26
Bacterial colonisation on particles	high	low		
Organic carbon content	high	low		

Table 5.3: Summary of principal geochemical characteristics of sample sets analysed. Figures represent mean values of all properties listed for each data set. Bacterial count and organic carbon information from Plummer *et al.* (1987).

The springs survey SPM and sediment data shown support the view that the estuarine SPM generally comprise a mixture of these two sub-populations with a continuum of compositions between the two extremes. The differences between the sediment and RSS data reflect the lower tidal energy of the Neal Point site compared to the turbidity maximum. There may also be an effect due to the timing of the April sediment sampling as opposed to the July/August water column work. Note however that the seasonal variations in sediment composition reported in Ackroyd *et al.* (1987) are most significant in the upper estuary rather than 21 km down estuary at Neal Point.

Although the differences between the particle populations obtained from the settling procedure cannot be attributed to their physical properties (*i.e.* buoyancy) *per se*, it is likely that the acquisition of the geochemical characteristics recorded is dependent on those properties.

The ability of particulate material to adsorb metals from solution is highly dependent on surface area. Titley *et al.* (1987) have shown that the acquisition of Fe/Mn oxide coatings, especially when fresh rather than aged, significantly increases the surface area of estuarine SPM, and that the highest surface areas are found on particles in the low salinity zone. The PSP have significantly higher proportions of leachable (*i.e.* non-detrital) Fe than the RSS, which would enhance their ability their ability to adsorb trace metals from solution as well as more Fe/Mn oxide material. The effect of organic coatings on particles is more difficult to assess. This material is not amenable to measurements of surface area as determined by the B.E.T. method of Titley *et al.* (1987), but may have significant metal complexing capacity, so that the reduction in B.E.T. surface area caused by the presence of organic coatings on particles may not affect their metal scavenging ability. Whether the coincidence between the high leachable metal contents and bacterial counts is a causal or coincidental one is not clear, but there is evidence to suggest that metal ions will readily bind to bacterial surfaces (Simões-Gonçalves *et al.*, 1987).

The chemical composition of the PSP is by definition independent of the physical process of resuspension, and the Fe-Al and P-Al relationships (figs. 5.3 & 5.4) indicate that the composition of the leachable material is also largely

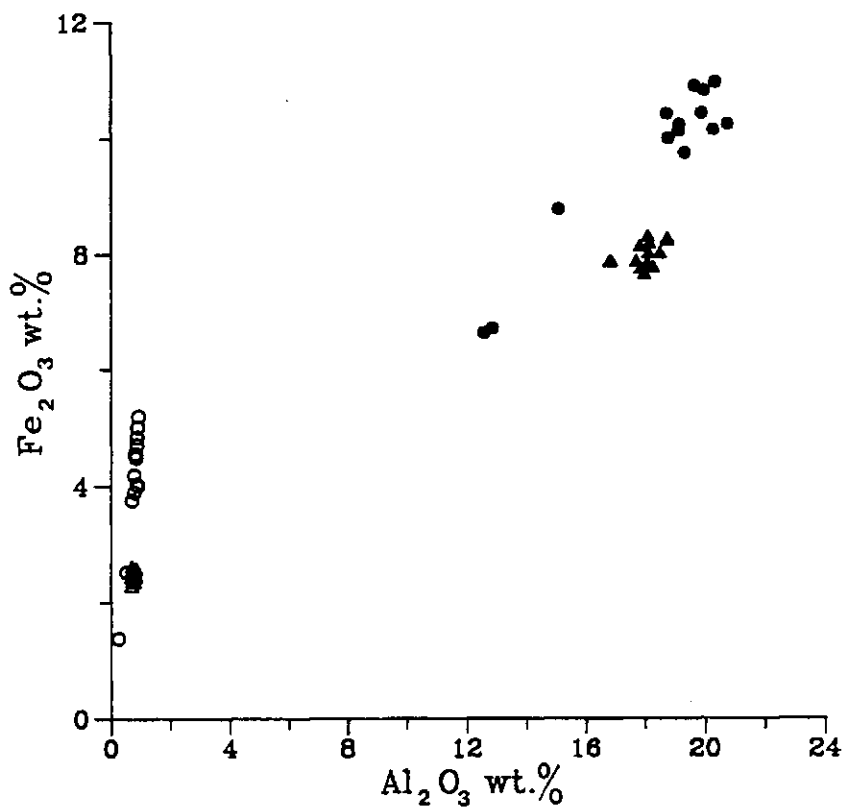


Figure 5.3: Settling procedure: Particulate Fe₂O₃ vs. Al₂O₃. Triangles - RSS, circles - PSP. Open symbols - leachable, filled symbols - total.

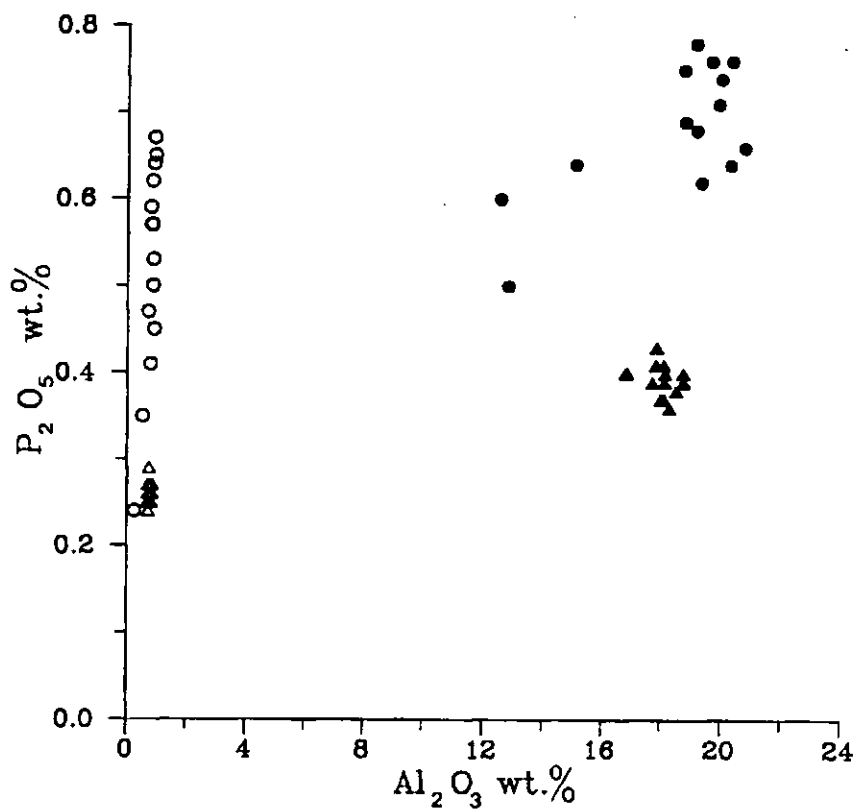


Figure 5.4: Settling procedure: Particulate P₂O₅ vs. Al₂O₃. Triangles - RSS, circles - PSP. Open symbols - leachable, filled symbols - total.

independent of the bulk composition (*i.e.* clay content) of the silicate substrates. It is important therefore to determine the origins of this 'labile' material, and, if possible, to investigate what process ultimately controls the composition of the SPM.

The significant chemical process occurring in the turbidity maximum is of course the non-conservative removal from solution of a number of metals, including Fe, Mn and the REE. Chemical scavenging by suspended particles has been implicated as a significant mechanism in this, but previous studies of the composition of the SPM in the Tamar turbidity maximum (Morris *et al.*, 1987) have been unable to identify the destination of the removed Fe, Mn, Zn or Cu as the advection of bottom sediment produces an SPM bulk composition which is depleted in these elements relative to other estuarine SPM.

Calculations on the relative magnitudes of the fluxes of removed Fe and particulate Fe through the turbidity maximum (Morris *et al.*, 1986a) indicate that the amount of Fe removed from solution would not be enough to significantly modify the composition of the resuspending sediment. However, such models assume that all the material which is being cycled through the turbidity maximum will have the same scavenging capacity. The results of the settling experiment demonstrate that this is unlikely, and, as we will see below, the RSS is likely to have less scavenging ability than the PSP. We have also seen from the data on the Tamar suspended particles (section 3.3) that significant fractionation of the SPM can take place during the process of resuspension, and the work of Schubel (1971) shows that there are considerable variations in the settling velocities of estuarine particles. In addition, some particles can remain permanently trapped in the turbidity maximum (Festa & Hansen, 1978). As surface area and settling velocity are essentially inversely related it is likely that concentrations of adsorbed species on an actively scavenging particle will be further enhanced by the additional time it can spend in the water column compared to its more dense brethren.

Consider the case of a relatively coarse-grained, dense and quartz rich sample versus finer and clay-rich particles, for example. The buoyant clay rich particles (PSP) will initially have a greater scavenging ability. For any given unit of time

spent suspended, the PSP will be able to adsorb more trace metals and Fe than the less buoyant population (RSS). Note that we cannot tell whether this difference is due to the adsorption being limited by the number of sites available, and reaching saturation for both cases, or if the rate of uptake is actually different due to greater adsorption site density in the case of the PSP. Here we can only measure the resultant composition, the question of capacity *vs.* rate control would have to be addressed by laboratory experiments. There is some evidence (Gadde & Laitinen, 1974), however, that uptake of metals onto hydrous Fe/Mn oxides is capacity limited and is independent of the metal concentration in the surrounding solution.

As time goes on, the compositions of the two populations will diverge. The differences will grow as the acquired Fe/Mn coatings increase the effective surface area of the PSP. Additionally, the PSP spend more time aloft, and are able to 'filter' far larger volumes of water than the RSS which lie intermittently on the river bed. Thus two populations of particles which might have initially had similar compositions in terms of leach/total ratios and Fe, Co *etc.*/Al ratios can rapidly become quite distinct. The only significant original difference between the two populations was their settling velocity. Thus we see that water column residence time, which is influenced by settling velocity, exerts a significant control on the final composition of estuarine SPM.

The relatively invariant composition of the RSS supports this conclusion, as the bulk of the suspended material had visibly settled out within 30 minutes of commencing the settling procedure, *i.e.* there was little significant (in terms of mass proportions) variation observed the RSS settling velocities. In contrast, the PSP compositions vary quite substantially, (figs. 5.3 & 5.4) which reflects the varying histories (and hence PSP residence times) of the water masses sampled as the turbidity maximum moved past the sampling site.

Further discussion of the origins of the differences between the PSP and the RSS must therefore examine the possible origins of the 'labile' material, and whether or not the fluxes of material through the Tamar estuary could support the abundances recorded.

5.3 Sources of Metals in Suspended Particles

Due to the absence of a natural tracer the major and trace element data for the samples obtained from the Tamar Estuary cannot provide us with information as to the sources of the elements analysed, although the data do allow us to establish the importance and effect of the physical processes operating in the estuary. Normalisation of the REE abundances does however provide us with a tracer, and we have already seen the utility of this in the discussion of the turbidity maximum profile data in section 4.5. Looking at the shale normalised REE patterns from the leach analyses of solid samples, the sediment porewaters and the estuarine waters we can see similarities. In particular, the estuarine waters and porewaters have a very close resemblance. The leach analyses of particles and sediments show similar patterns with an enrichment of the middle REE, but the La_N/Yb_N is only slightly less than 1 rather than very much less. This would suggest that the REE in the porewaters are perhaps wholly derived from the riverine REE, and that a proportion of the labile particulate REE also come from this source. To determine whether or not this is likely, we must examine more closely the relationships between the various dissolved and solid phase REE patterns.

The dissolved REE data for the Tamar show distinct non-conservative behaviour during estuarine mixing with substantial removal of the REE from solution in the low salinity - high turbidity zone of the estuary (Elderfield *et al.*, 1990) between 0 and 5 ppt. The shale normalised pattern of the REE which are removed from solution is shown in fig. 5.5. This was derived by calculating, for each element, the difference between the actual value of the dissolved REE concentration in the 5.63 ppt sample, and the value predicted for it by a simple conservative mixing model for the neaps survey. Although this shows a more pronounced enrichment of the middle REE the overall shape and slope of the profile is similar to that displayed by the porewaters.

Comparison of this removed REE profile with the patterns in the leachable particulate REE reveals similarities, but it is clear that $La_N/Yb_N \ll 1$ in the removed REE but ≈ 1 in the leachable REE. Note that these leachable REE

data were derived by leaching the solid samples with 1.75M HCl. It is likely that as well as removing the labile REE (potentially derived from the removal flux) the leaching process extracted some REE from the residual detrital silicate. Duinker *et al.* (1974) report 12% breakdown of clay minerals in a sample of estuarine suspended matter after a 24 h with 2M HCl. Mixing of REE from this source (having $La_N/Yb_N > 1$) with REE having a 'removed' pattern could perhaps produce a pattern similar to that found in the leachable REE.

To test the effect of such a combination a theoretical mixing experiment between these two end members was devised to determine the possible shapes of the patterns. The REE pattern for the detrital (as opposed to total) REE in the sediments was calculated from the mean of the residuals (total - leach) of all the sediment samples.

Unfortunately, answering the question 'What pattern would be generated if 50% of the REE were detritally derived and 50% derived from the removal flux?' is not possible due to the different fractionation of the two sources. If we were attempting to calculate the relative abundances generated by the mixing of two patterns, distinguished only by the presence or absence, say, of a cerium anomaly, the task could be achieved by normalising the sample/shale values for one sample so that La_N , Nd_N *etc.* were the same for both samples, and then interpolating until the matching magnitude of Ce anomaly was generated. Such a procedure is prevented in this case by the quite different fractionation of the two patterns involved. It is therefore necessary to base the calculations on the question 'What pattern would be generated if 50% of, say, Nd were derived from a detrital source and 50% from a removal source, the abundances of the other REE being determined from their relative abundances in the two sources?'

A further complication is introduced by the fact that the shale normalised concentrations used reflect the absolute concentrations of the individual REE in their respective samples as well as any fractionation in their relative abundances. In order to eliminate any bias that this might introduce, the sample/shale values for one sample must be normalised so that the two patterns overlap as much as possible. In this case this was achieved by normalising the detrital data so that $Nd_N(\text{detrital}) = Nd_N(\text{removal}) \times 10^6$. Calculation of the change in slope of the mix-

ing product of two arbitrary straight-line patterns of complementary La_N/Yb_N showed that the best overlap (*i.e.* where Gd_N for the two samples are identical) results in a linear relationship between the logarithm of the slope and the percentage of mixing. There is such a linear relationship for the patterns generated by the use of Nd as the normalisation element.

The results are shown in fig. 5.5. The patterns derived clearly show that it is possible to generate shale normalised REE patterns similar to those found in the leachable fractions of the estuarine particles by mixing of REE from a detrital sediment source with REE from a riverine removal source. Close comparison reveals that 40% detrital REE mixed with 60% removed REE generates a pattern which is a good match for the leachable REE shown in figure 5.2. Figure 5.6 shows the best fit pattern isolated and compared with the pattern for the mean springs survey SPM (normalised so that $La_N(\text{theoretical})=La_N(\text{actual})$). The lack of precise correspondence is unsurprising considering the single survey data used to calculate the removal flux and the limited number of SPM samples.

Note that use of a different element for the normalisation point does not generate different patterns, but simply changes the mixing ratio at which the generated pattern corresponds with the real pattern in the leachable particulate REE.

The implication is therefore that the labile REE attached to the particulate samples, whether in Fe/Mn oxide coatings or organically associated, are in fact derived from the REE removed from solution during estuarine mixing. By implication, this may also be true for other elements such as Fe, Co, Zn *etc.* for which estuarine removal has been documented.

In addition to the Nd based mixing, calculations of pattern slopes generated by normalising to $REE_N(\text{detrital})=REE_N(\text{removed})$ for all other elements. The results showed that limits were set by equal La_N and Gd_N , for which patterns closest to those of the leachable SPM REE would be generated by 40% and 80% removal content respectively.

The porewater REE patterns cannot be analysed so definitively as the data are poorer. There is evidence in the fragmentary patterns obtained to suggest that these REE are derived from reductive solubilisation of the non-detrital REE. The

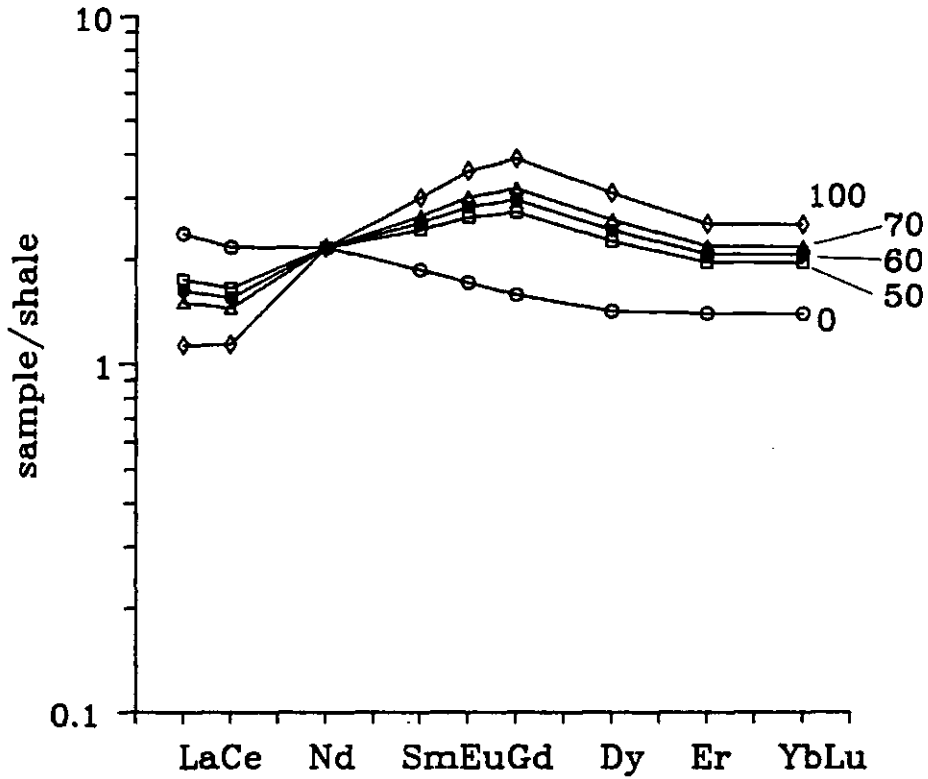


Figure 5.5: Shale normalised REE patterns generated by mixing of removed riverine REE with residual sediment REE. Top-bottom: 100% riverine, 70%, 60%, 50%, 0% (i.e. 100% residual sediment).

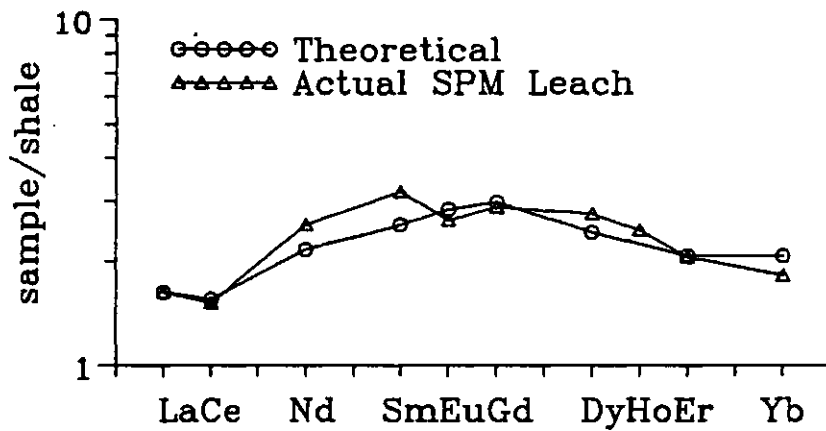


Figure 5.6: Comparison of theoretical(60% riverine/40% detrital) and actual leachable REE patterns. SPM pattern represents mean of Springs Survey samples.

closer similarity of these porewater patterns to the removal pattern shown above reflects the lack of influence of the detrital phase on these REE abundances, and suggests that organic diagenesis is solubilising only loosely bound exchangeable metals, organically associated metals and oxide phases, and not attacking the detrital phases. In contrast the Buzzards Bay porewater data reported by Elderfield & Sholkovitz (1987) show a progressive shift with depth towards a detrital type pattern. The environment of these organic-poor sediments is relatively calm non-estuarine coastal water, in contrast to the extremely dynamic situation of the organic-rich sediments in the Tamar. One could speculate that given time, the Tamar sediment porewaters would develop patterns reflecting the incorporation of detrital REE, but this cannot be resolved without deeper cores or perhaps long-term sediment incubation experiments.

There is no evidence that the diagenetic process affects the levels of labile REE left on the sediments, and in any case this is unlikely as the masses of labile sediment REE and porewater REE differ by 5–6 orders of magnitude. The production of 0.5 *pmol* (≈ 70 *pg*) of Nd in 1 *ml* of porewater would not be detectable on 1 *g* of sediment containing 10 μ *g* of Nd. It is more likely that the low levels of labile REE (and by implication other trace metals) on the sediments, are due to the surface properties of the sediment, its location and behaviour during tidal resuspension, rather than being a result of diagenetic processes.

5.4 Fluxes of Metals in the Tamar

5.4.1 REE

A major consideration in this study of estuarine cycling of the REE is whether or not the REE removed from solution in the low salinity zone can make a measurable contribution to the total amounts of REE present in the particulate material. We have already examined the possible origins of the leachable REE in terms of mixing of detrital and removal sources, and observed that chemical scavenging in the low salinity zone could significantly modify particle compositions. We must now attempt to determine whether their estuarine fluxes support these conclusions. Crudely, the proportion of REE in the sediments which is derived from the removal processes in the low salinity zone will depend on the balance between the quantity of REE removed from solution, and the mass of sediment onto which this removed material is deposited. Unfortunately, the extremely dynamic nature of the estuary means this sediment mass cannot be determined easily, so two possible approaches have been considered, and are discussed in turn.

Turbidity Maximum Resuspension

Morris *et al.* (1986a) calculated, for stable summer conditions, the effect that non-conservative removal of Fe onto particles would have on the levels of particulate Fe in the resuspending material in the turbidity maximum. Their results show that, on a daily basis, the additional Fe on the particles would not be measurable with the analytical method employed. Using their equation $E = 0.0213CR$ (where E = enhancement of metal concentration on the particles in ppm, C = riverine metal concentration in $\mu g l^{-1}$ and R = percentage of riverine metal removed from solution in the turbidity maximum) and substituting the range of values for Nd removal in Elderfield *et al.* (1990) of 200–900 $pmol kg^{-1}$ we obtain a value of 0.06–0.28 ppm augmentation of the original detrital Nd concentration. Given that the leachable sediment Nd comprises 7.7 ppm with a precision of 2.5% this is on the margins of detectability. However, the caveats mentioned in section 5.2 must be borne in mind. It is not likely that all the particles passing through the turbidity maximum collect the same quantity of non-detrital REE as some minerals will be

relatively inert, *e.g.* large quartz grains. It also worth noting that the variations in the amounts of leachable REE between the various populations are of an order of magnitude greater than this figure, and hence reliably measurable.

Riverine Detrital Input

As we cannot determine the time that any given particle population might spend actively scavenging in the turbidity maximum, or their relative contributions to the bulk of the suspended material, it is not possible to modify the above calculation, and we must approach the problem from a different perspective. Bale *et al.* (1985) provide data on the net annual fluxes of sediment through the turbidity maximum. If we consider the dissolved REE to be scavenged by the unmodified (by estuarine processes) riverine detrital material we can easily perform a calculation on the effect of the removal on the SPM Nd concentrations. Using an annual mean river flow of $18 \text{ m}^3 \text{ s}^{-1}$ (Uncles *et al.*, 1983), annual riverine sediment supply of $3.2 \times 10^7 \text{ kg}$ (Bale *et al.*, 1985) and the Nd removal rates mentioned above, we obtain an enhancement of 0.52–2.3 ppm Nd. Variations of such a magnitude would certainly be measurable by the ICP method used. Also, referring to section 5.3 where the conclusion was reached that 40% of the leachable REE are detritally derived, we are seeking to supply only 4.6–7.6 ppm Nd from a non-detrital source. Considering the crude nature of the calculation and the limited nature of the data, particularly the removal fluxes, this correspondence is quite good. In addition, it is possible that the values used for the removal fluxes are lower than the annual average as the surveys were carried out at a time of unseasonally high rainfall, with a consequent dilution of the solutes produced by chemical weathering. The agreement between the two results is therefore likely to be better. Also, as significant proportion of the sediment delivered by the river arrives during winter spates and flushes through the estuary rapidly the mass of sediment participating in the removal processes may be less than the total.

These are of course mean values for labile REE acquisition. As mentioned in section 5.2 it is likely that not all the sediment is present in the water column for the same duration, and consequently differences in the quantities of labile REE adsorbed will develop. This begs the question as to why, if some particles

are gathering more dissolved REE than others, are the shale normalised patterns not different? This has already been answered in section 5.1.1. Particles which scavenge more successfully are likely to have larger surface areas, enabling greater release of detrital REE on leaching. The net result being similar patterns of shale normalised values for the different sample sets. The reader is referred to figure 5.2 for an example which shows that the compensation effect is not perfect and that there remain subtle differences between the shale normalised REE patterns for the various particle populations.

The conclusion is therefore that, on the basis of likely fluxes, the removed REE exert a significant effect on the abundances of REE in the estuarine SPM and sediments.

5.4.2 Other Metals

This conclusion might also apply to other metals with non-conservative behaviour. Performing the above calculation with the range of Fe removal values quoted in Morris *et al.* (1986a) we find that the Fe removal flux could support up to 0.38 wt.% Fe₂O₃ on the sediments (*i.e.* 21% of the leachable Fe). As was the case for the REE, not all the leachable Fe is likely to be of non-detrital origin. We do not have the benefit of a tracer for Fe to allow us to calculate what proportion is non-detrital, but given the leach/total ratios for Fe of 0.27–0.43, compared with 0.24–0.32 for Nd, and the above result it seems likely that the figure is similar to that for Nd of 60% of the leachable material being non-detrital in origin.

Data for removal of Cu, Ni and Zn in the low salinity zone of the Tamar are reported in Elderfield *et al.* (1986). These are presented in table 5.4 along with sediment enhancement values calculated using the riverine detrital input model as above .

One can see that there is a good correspondence between the effect that the removal flux would have on the riverine detrital material and the levels of leachable metals actually observed in the Tamar samples. There appears to be a better correspondence for Ni than Cu & Zn, but note that the leach/total ratios in the Neal Point sediments for the latter two elements are very high (≈ 0.7 – 0.8) as opposed to ≈ 0.3 for Ni. That is to say, there is a much larger contribution from

Element	Removal ($\mu\text{g l}^{-1}$)	Sediment Enhancement (ppm)	Particulate Leachable (ppm)
Cu	5	90	160-204
Ni	1	18	17-36
Zn	5	90	260-365

Table 5.4: Trace element removal data (from Elderfield *et al.*, 1986), with calculated enhancement of particulate concentrations and ranges of leachable concentrations in Tamar sediments and SPM.

the detrital material to the leachable concentrations of Cu and Zn than is the case for Ni. It is therefore not necessary to invoke such a high contribution from the non-detrital source for Cu & Zn to account for the leachable concentrations as is the case for Ni.

The close correspondences between the observed riverine removal fluxes and the quantities of leachable trace elements serve to confirm that this model of the riverine sediment supply as the effective sink for the removed elements is a useful means of assessing the net effect of the trace metal removal processes operating in the turbidity maximum. The discrepancies noted indicate that either the removal fluxes are poorly constrained (as mentioned above for the REE) or that the estimate of the quantity of sediment actively involved needs revision. There is no reason to assume that all the detrital material delivered to the estuary is involved in the resuspension. This work has sampled either suspended particles or sediment from intertidal mudflats, by definition the more mobile and hence active material. We cannot assume that any of the samples analysed represent material with the estuarine minimum of non-detrital content.

5.5 Conclusions

The results of this study provide both confirmatory and novel conclusions about the estuarine cycling of trace metals, and the processes that control the chemical composition of estuarine suspended particles.

The major and (apart from the REE) trace element data collected confirm previous findings that the significant local control on the bulk chemical composition of the estuarine suspended particles, especially in the turbidity maximum, is provided by the physical process of resuspension of bed sediment. The trace metal data in particular serve to illustrate the lateral heterogeneity of the estuarine sediments, and the possibility of physical fractionation of the sediment due to the selective resuspension or redeposition of individual mineral phases on the basis of their density and settling characteristics.

The rare earth element data for the estuarine sediments and suspended particles in themselves constitute the first comprehensive study of particulate REE abundances in a relatively pristine (as regards anthropogenic REE input) U.K coastal environment. These data served as a baseline for identification of the anomalous REE abundances reported in Vivian (1986). The use of normalised REE abundances confirms the conclusion from the other trace metal data that the effects of sediment resuspension on bulk particle composition can be extremely localised down to a scale of a few tens of meters.

The most important information as regards particle composition was provided by the settling procedure. This has clearly demonstrated, as had been suspected from a number of previous studies, that in the Tamar turbidity maximum there are significant compositional differences between the particles which remain permanently in suspension and those which are tidally resuspended. Significantly, the compositional differences between the two populations of particles are controlled by their behaviour during resuspension, and the resultant time spent suspended in the water column, rather than being pre-determined by the inherent chemical composition of the particles.

The actual, as opposed to inferred, fate of the dissolved metals removed from solution during estuarine mixing has long been unresolved due to the lack of a

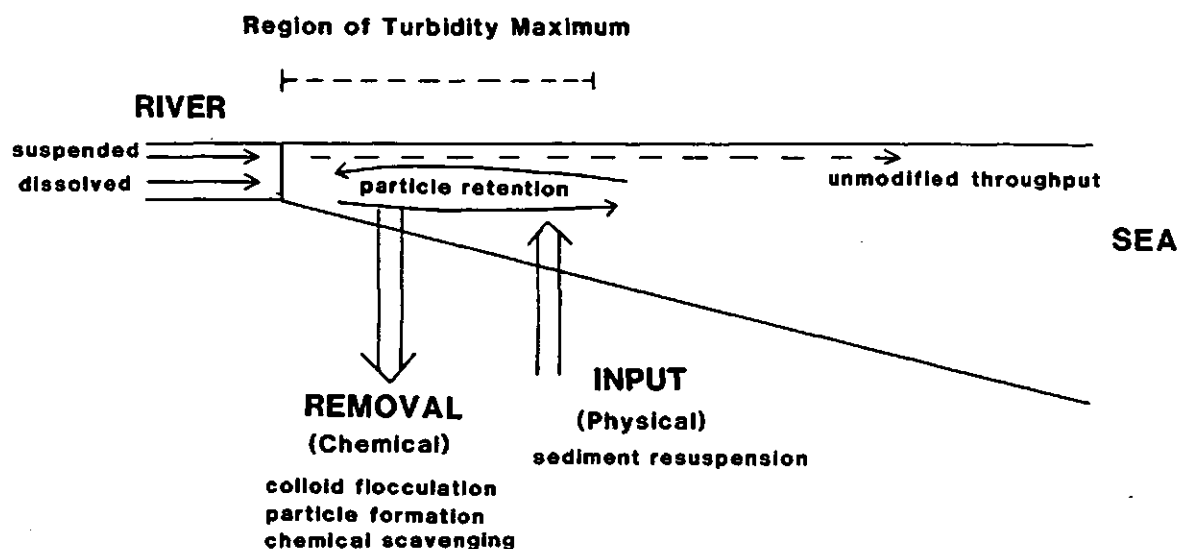


Figure 5.7: Schematic diagram of processes and fluxes controlling estuarine particle compositions.

tracer and the metal depleted particle compositions found in estuarine turbidity maxima caused by advection of bottom sediment. Comparison of shale normalised REE data from the leaches of estuarine particles with dissolved REE data from the Tamar has enabled us to show that the removed REE do actually become incorporated into the estuarine SPM, and, if we assume that riverine detrital input provides the sediment involved, this material makes a significant contribution to the total REE abundances in the particles. The patterns also confirm that the permanently suspended particles identified by the settling procedure have accumulated more of the removed REE than the resuspending sediment. Figure 5.7 shows schematically the processes and fluxes which act to control the overall composition of suspended particles in the Tamar.

The presence of this non-detrital material on the estuarine particles is also reflected in the shale-normalised patterns found for the REE in the sediment porewaters. These correspond with the patterns of the material removed in the low salinity zone, rather than indicating that the porewater REE are derived from the detrital sediments or the waters overlying the coring site.

Extension of the model of riverine detrital input as the sink for the removed material to the behaviour of different trace metals studied by other workers in the Tamar, suggests that significant modification of particle compositions by the estuarine removal processes is not restricted to the REE. However, in the absence of a natural tracer this cannot be tested. This contradicts earlier findings, and indicates that assessment of the effects of estuarine removal processes needs to be done on the basis of net annual fluxes rather than for specific sets of conditions. Furthermore, we must not assume that all of the sediment mass invoked in the model plays an active part in the chemical interactions.

These conclusions need not be restricted to the Tamar. The extensive studies of Duinker and co-workers on the estuaries of the German Bight indicate that the compositional distinction between particle populations in estuaries may be common. Millward *et al.* (1990b), have shown that maxima in particle surface area can be identified in other estuaries which have turbidity maximum zones. It is likely therefore that preferential uptake of dissolved metals onto buoyant particles rather than intermittently resuspending bed sediment is occurring in other estuaries. The significance of this uptake will of course depend on the mass balance between the removal and detrital fluxes in the individual estuaries, and the control that the discharge and tidal forces have on the internal cycling of sediment.

Inevitably, there remain unresolved problems. From a theoretical perspective the observed compositional distinctions between particle populations in the turbidity maximum do not allow us to examine the mechanisms which control their development. It would require experiments to determine whether the implicated surface area differences between the PSP and RSS result in different rates of uptake of metals from solution, or if the effect is due to different adsorption site availability. It would also be desirable to know the likely residence times of a spectrum of particle size fractions in the estuary in order to determine to what extent each could participate in the chemical removal processes. At the time of writing experiments were being conducted by Dr. A.J.Bale of the Plymouth Marine Laboratory into the use of fluorescent plastic grains as tracers for natural particles, the successful use of which would be of considerable importance to

studies such as this.

The diagenetic behaviour of the REE also warrants further study. In particular it would be instructive to determine whether at greater depths in the sediment, or after extended diagenesis, the porewater REE abundances are affected by the presence of detrital REE rather than only REE from the diagenetically reduced hydrous oxide phases. This would be of particular importance to studies of the behaviour of potentially toxic metals which undergo the typical estuarine removal processes and subsequent organic diagenesis.

However, the most important implication for the future study of estuarine cycling of trace metals is that, contrary to previous findings, we must base our investigations on the premise that the removal processes operating in the low salinity zone can significantly affect the chemical composition of the estuarine suspended particles, and that the uptake of dissolved metals onto particles is not uniform.

References

- Abbey, S., 1979: Canadian Center for Mineral and Energy Technology, report 79-35; *Reference materials - rock samples SY-2, SY-3, MRG-1*. 66 pp.
- Ackroyd, D.R., Bale, A.J., Howland, R.J.M., Knox, S., Millward, G.E. & Morris, A.W., 1986: Distributions and behaviour of dissolved Cu, Zn and Mn in the Tamar Estuary. *Estuar. Coast. Shelf Sci.*, **23**, 621-640.
- Ackroyd, D.R., Millward, G.E. & Morris, A.W., 1987: Periodicity in the trace metal content of estuarine sediments. *Oceanol. Acta*, **10**, 161-168.
- Agemian, H. & Chau, A.S.Y., 1976: Evaluation of extraction techniques for the determination of metals in aquatic sediments. *Analyst, Lond.*, **101**, 761-767.
- Agemian, H. & Chau, A.S.Y., 1977: A study of different analytical extraction methods for non-detrital heavy metals in aquatic sediments. *Arch. Environ. Contam. Toxicol.*, **6**, 69-82.
- Alderton, D.H.M., Pearce, J.A., & Potts, P.J., 1980: Rare earth element mobility during granite alteration: evidence from southwest England. *Earth Planet. Sci. Lett.*, **49**, 149-165.
- Alexander, W.R., 1985: Inorganic diagenesis in anoxic sediments of the Tamar Estuary. *Ph.D. thesis*, University of Leeds. 268 pp.
- Aller, R.C., 1978: Experimental studies of changes produced by deposit feeders on pore water, sediment, and overlying water chemistry. *Am. J. Sci.*, **278**, 1185-1234.
- Aller, R.C. & Yingst, J.Y., 1978: Biogeochemistry of tube dwellings: a study of the sedentary polychaete *Amphitrite ornata* (Leidy). *J. Mar. Res.*, **36**, 201-254.
- Aplin, A.C. & Cronan, D.S., 1985: Ferromanganese deposits from the central Pacific Ocean, II. Nodules and associated sediments. *Geochim. Cosmochim. Acta*, **49**, 437-451.
- Aston, S.R. and Chester, R., 1973: The influence of suspended particles on the precipitation of iron in natural waters. *Estuar. Coast. Mar. Sci.*, **1**, 225-231.

- de Baar, H.J.W., Brewer, P.G. & Bacon, M.P., 1985: Anomalies in rare earth element distributions in seawater: Gd and Tb. *Geochim. Cosmochim. Acta*, **49**, 1961–1969.
- Bale, A.J., Barrett, C.D., West, J.R. & Oduyemi, K.O.K., 1990: Use of in-situ laser diffraction particle sizing for particle transport studies. In: J. McManus & M. Elliott, (Eds.), *Developments in Estuarine Study Techniques*, Olsen & Olsen. pp133–138
- Bale, A.J. & Morris, A.W., 1981: Laboratory simulation of chemical processes induced by estuarine mixing: the behaviour of iron and phosphate in estuaries. *Estuar. Coast. Mar. Sci.*, **13**, 1–10
- Bale, A.J., Morris, A.W. & Howland, R.J.M., 1985: Seasonal sediment movement in the Tamar estuary. *Oceanol. Acta*, **8**, 1–6.
- Balzer, W., 1982: On the distribution of iron and manganese at the sediment-water interface: thermodynamic versus kinetic control. *Geochim. Cosmochim. Acta*, **46**, 1153–1161.
- Booker, F., 1971: *The Industrial Archaeology of the Tamar Valley*. David & Charles, Newton Abbot, 308pp.
- Boust, D. & Saas, A., 1982: Méthode d'étude par extractions successives de quelques éléments majeurs, ou en traces, dans l'estuaire de la Seine. *Mem. Soc. Géol. Fr.*, **144**, 93–99.
- Boyle, E.A., Collier, R., Dengler, A.T., Edmond, J.M., Ng, A.C. & Stallard, R.F., 1974: On the chemical mass balance in estuaries. *Geochim. Cosmochim. Acta*, **38**, 1719–1728.
- Boyle, E.A., Edmond, J.M. & Sholkovitz, E.R., 1977: The mechanism of iron removal in estuaries. *Geochim. Cosmochim. Acta*, **41**, 1313–1324.
- Brenner, I.B., Jones, E.A., Watson, A.E. & Steele, T.W., 1984: The application of a N₂-Ar medium power ICP and cation-exchange chromatography for the spectrometric determination of the rare earth elements in geological materials. *Chem. Geol.*, **45**, 135–148.

- Cantrell, K.J. & Byrne, R.H., 1987: Rare earth complexation by carbonate and oxalate ions. *Geochim. Cosmochim. Acta*, **51**, 597-605.
- Chester, R. & Hughes, M.J., 1967: A chemical technique for the separation of ferromanganese minerals, carbonate minerals, and adsorbed trace metals from pelagic sediments. *Chem. Geol.*, **2**, 249-262.
- Clifton, R.J. & Hamilton, E.I., 1979: Lead-210 chronology in relation to levels of elements in dated sediment core profiles. *Estuar. Coast. Mar. Sci.*, **8**, 259-269.
- Cotton, F.A. & Wilkinson, G., 1980: *Advanced Inorganic Chemistry* (4th Edn.). John Wiley, New York, 1396pp.
- Crock, J.G. & Lichte, F.E., 1982: Determination of rare earth elements in geological materials by inductively coupled argon plasma/atomic emission spectrometry. *Analyt. Chem.*, **54**, 1329-1332.
- Crocke, J.G., Lichte, F.E. & Wildemann, T.R., 1984: The group separation of the rare earth elements and yttrium from geologic materials by cation-exchange chromatography. *Chem. Geol.*, **45**, 149-163.
- Duinker, J.C., Van Eck, G.T.M. & Nolting, R.F., 1974: On the behaviour of copper, zinc, iron and manganese, and evidence for mobilisation processes in the Dutch Wadden Sea. *Neth. J. Sea Res.*, **8**, 214-239.
- Duinker, J.C., Hillebrand, M.T.J., Nolting, R., F.; Wellershaus, S. & Kingo Jacobsen, N., 1980: The River Varde Å: Processes affecting the behaviour of metals and organochlorines during estuarine mixing. *Neth. J. Sea Res.*, **14**, 237-267.
- Duinker, J.C., Hillebrand, M.T.J., Nolting, R., F. & Wellershaus, S., 1982a: The River Elbe: Processes affecting the behaviour of metals and organochlorines during estuarine mixing. *Neth. J. Sea Res.*, **15**, 141-169.
- Duinker, J.C., Hillebrand, M.T.J., Nolting, R., F. & Wellershaus, S., 1982b: The River Weser: Processes affecting the behaviour of metals and organochlorines during estuarine mixing. *Neth. J. Sea Res.*, **15**, 170-195.

- Duinker, J.C., Hillebrand, M.T.J., Nolting, R.,F. & Wellershaus, S., 1985: The River Ems: Processes affecting the behaviour of metals and organochlorines during estuarine mixing. *Neth. J. Sea Res.*, **19**, 19-29.
- Duinker, J.C. & Nolting, R.F., 1978: Mixing, removal and mobilization of trace metals in the Rhine Estuary. *Neth. J. Sea Res.*, **12**, 205-223.
- Duinker, J.C., Wollast, R. & Billen, G., 1979: Behaviour of manganese in the Rhine and Scheldt Estuaries II. Geochemical cycling. *Estuar. Coast. Mar. Sci.*, **9**, 727-738.
- Eaton, A., 1979: The impact of anoxia on Mn fluxes in the Chesapeake Bay. *Geochim. Cosmochim. Acta*, **43**, 429-432.
- Ebdon, L. & Cave, M.R., 1982: A study of pneumatic nebulisation systems for inductively coupled plasma emission spectrometry. *Analyst*, **107**, 172-178.
- Eckert, J.M. & Sholkovitz, E.R., 1976: The flocculation of dissolved iron, aluminium and humates from river water by electrolytes. *Geochim. Cosmochim. Acta.*, **40**, 847-848.
- Eisma, D., Kalf, J. & Veenhuis, M., 1980: The formation of small particles and aggregates in the Rhine Estuary. *Neth. J. Sea Res.*, **14**, 172-191.
- Elderfield, H., 1988: The oceanic chemistry of the rare-earth elements. *Phil. Trans. Roy. Soc. Lond.*, **A 325**. 105-126.
- Elderfield, H. & Greaves, M.J., 1983: Determination of the Rare Earth Elements in Sea Water. In: C.S. Wong, K.W. Bruland, J.D. Burton & E.D. Goldberg (Eds.), *Trace Metals in Sea Water.*; Plenum, New York. pp427-445.
- Elderfield, H., Mc Caffrey, R.J., Luedtke, N., Bender, M. & Truesdale, V.W., 1981: Chemical diagenesis in Narragansett Bay sediments. *Am. J. Sci.*, **281**, 1021-1055.
- Elderfield, H., Morris, A.W., Whitfield, M., Upstill-Goddard, R.C. & Findlay, J.S., 1986: Variations in chemical composition of suspended particles in estuaries: the role of benthic fluxes and processes at the turbidity maximum in chemical scavenging. *N.E.R.C. Progress Report on Special Topic Grant GST/02/63*.

- Elderfield, H. & Sholkovitz, E.R., 1987: Rare earth elements in the porewaters of reducing nearshore sediments. *Earth Planet. Sci. Lett.*, **82**, 280-288.
- Elderfield, H., Upstill-Goddard, R. & Sholkovitz, E.R., 1990: The rare earth elements in rivers, estuaries and coastal seas and their significance for the composition of ocean waters. *Geochim. Cosmochim. Acta*, **54**, 971-991.
- Emmerman, R., Daeiva, L., & Schneider, J., 1975: The petrologic significance of rare earth distribution in granites. *Contrib. Mineral. Petrol.*, **52**, 267-183.
- Faure, G., 1986, *Principles of Isotope Geology*, 2nd Edition. John Wiley, London. 464 pp.
- Festa, J.F. & Hansen, D.V., 1978: Turbidity maxima in partially mixed estuaries: a two dimensional numerical model. *Estuar. Coast. Mar. Sci.*, **7**, 347-359.
- Flanagan, F.J., 1973: 1972 values for international geochemical reference samples. *Geochim. Cosmochim. Acta*, **37**, 1189-1200.
- Fleet, A.J., 1984: Aqueous and sedimentary geochemistry of the rare earth elements. In: P.Henderson (Ed.), *Developments in Geochemistry 2: Rare Earth Element Geochemistry*, Elsevier, Amsterdam. pp. 343-373.
- Gadde, R.R. & Laitenen, H.A., 1974: Studies of heavy metal adsorption by hydrous iron and manganese oxides. *Analyt. Chem.*, **46**, 2022-2026.
- Gendron, A., Silverberg, N., Sundby, B. & Lebel, J., 1986: Early diagenesis of cadmium and cobalt in sediments of the Laurentian Trough. *Geochim. Cosmochim. Acta*, **50**, 741-747.
- Goldberg, E.D., 1954: Marine Geochemistry I. Chemical scavengers of the sea. *J. Geol.*, **62**, 249-265.
- Goldhaber, M.B., Aller, R.C., Cochran, J.K., Rosenfeld, J.K., Martens, C.S. & Berner, R.A., 1977: Sulfate reduction, diffusion and bioturbation in Long Island Sound sediments: report of the F.O.A.M. group. *Am. J. Sci.*, **277**, 193-237.
- Goldstein, S.J. & Jacobsen, S.B., 1987: Rare earth elements in river waters. *Earth Planet. Sci. Lett.*, **89**, 35-47.

- Greaves, M.J., Elderfield, H. & Klinkhammer, G.P., 1989: The determination of the rare earth elements in natural waters by isotope dilution mass spectrometry. *Analytica Chim. Acta*, **218**, 265–280.
- Hamilton-Jenkin, A.K., 1974: *Mines of Devon (Vol. 1): The Southern Region*. David & Charles, London, 154pp.
- Henderson, P., 1984: General geochemical properties and abundances of the rare earth elements. In: P.Henderson (Ed.), *Developments in Geochemistry 2: Rare Earth Element Geochemistry*, Elsevier, Amsterdam. pp. 1–32.
- Henderson, P. & Pankhurst, R.J., 1984: Analytical Chemistry (of the rare earth elements). In: P.Henderson (Ed.), *Developments in Geochemistry 2: Rare Earth Element Geochemistry*, Elsevier, Amsterdam. pp. 467–499.
- Hoyle, J., Elderfield, H., Gledhill, A. & Greaves, M.J., 1984: The behaviour of the rare earth elements during mixing of river and sea waters. *Geochim. Cosmochim. Acta*, **48**, 143–149.
- Kennedy, H.A. & Elderfield, H., 1985: Determination of the rare earth elements in marine porewaters and associated sediments. D.O.E. Report no: DOE/RW/85/002, 19pp.
- Kersten, M. & Förstner, U., 1987: Effects of sample pretreatment on the reliability of solid speciation data of heavy metals – implications for the study of early diagenetic processes. *Mar. Chem.*, **22**, 299–312.
- Kheboian, C. & Bauer, C.F., 1987: Accuracy of selective extraction procedures for metal speciation in model aquatic systems. *Analyt. Chem.*, **59**, 1417–1423.
- Knox, S., Turner, D.R., Dickson, A.G., Liddicoat, M.I., Whitfield, M. & Butler, E.I., 1981: Statistical Analysis of estuarine profiles: Application to manganese and ammonium in the Tamar Estuary. *Est. Coast. Shelf Sci.*, **13**, 357–372.
- Kuehner, E.C., Alvarez, R., Paulsen, P.J. & Murphy, T.J., 1972: Production and analysis of special high-purity acids by sub-boiling distillation. *Analyt. Chem.*, **44**, 2050–2056.

- Lee, F.Y. & Kittrick, J.A., 1984a: Electron microprobe analysis of elements associated with zinc and copper in an oxidizing and anaerobic soil environment. *Soil Sci. Soc. Am.*, **48**, 548-554.
- Lee, F.Y. & Kittrick, J.A., 1984b: Elements associated with the cadmium phase in a harbor sediment as determined with the electron beam microprobe. *J. Environ. Qual.*, **13**, 337-340.
- Lerman, A., 1980: Controls on river water composition and the mass balance of river systems. In: *River Inputs to Ocean Systems*, Eds:- Martin, J.-M., Burton, J.D. & Eisma, D.. UNEP/UNESCO, Switzerland. pp. 1-4.
- Li, Y.-H., Burkhardt, L. & Teraoka, H., 1984: Desorption and coagulation of trace metals during estuarine mixing. *Geochim. Cosmochim. Acta*, **48**, 1879-1884.
- Lion, W.L., Altmann, R.S. & Leckie, J.O., 1982: Trace metal adsorption characteristics of estuarine particulate matter: evaluation of contributions of Fe/Mn oxide and organic surface coatings. *Environ. Sci. Technol.*, **16**, 660-666.
- Liss, P.S., 1976: Conservative and non-conservative behaviour of dissolved constituents during estuarine mixing. In: *Estuarine Chemistry*, Eds:- Burton, J.D. & Liss, P.S.. Academic Press. London. pp. 93-130.
- Loring, D.H., 1978: Geochemistry of zinc, copper and lead in the sediments of the estuary and Gulf of St. Lawrence. *Can. J. Earth Sci.*, **15**, 757-772.
- Loring, D.H., 1979: Geochemistry of cobalt, nickel, chromium and vanadium in the sediments of the estuary and open Gulf of St. Lawrence. *Can. J. Earth Sci.*, **16**, 1196-1209.
- Loring, D.H., Rantala, R.T.T., Morris, A.W., Bale, A.J. & Howland, R.J.M., 1983: Chemical composition of suspended particles in an estuarine turbidity maximum Zone. *Can. J. Fish. Aquat. Sci.*, **40**(suppl. 1), 201-206.
- Malo, B.A., 1977: Partial extraction of metals from aquatic sediments. *Environ. Sci. Technol.*, **11**, 277-282.
- Marchant, J.W. & Klopper, B.C., 1978: Microgram metal contamination of water/nitric acid after four years in linear polyethylene containers. *J. Geochem. Explor.*, **9**, 103-107.

- Martin, J.M., Nirel, P. & Thomas, A.J., 1987: Sequential extraction techniques, promises and problems. *Mar. Chem.*, **22**, 313-341.
- Mayer, L.M., 1982: Aggregation of colloidal iron during estuarine mixing: kinetics, mechanism, and seasonality. *Geochim. Cosmochim. Acta*, **46**, 2527-2535.
- Michard, A., Albarede, F., Michard, G., Minster, G.F. & Charlou, J.L., 1983: Rare-earth elements and uranium in high temperature solutions from East Pacific Rise hydrothermal vent field (13° N). *Nature*, **303**, 795-797.
- Millward, G.E. & Moore, R.M., 1982: The adsorption of Cu, Mn and Zn by iron oxyhydroxide in model estuarine solutions. *Wat. Res.*, **16**, 985-991.
- Millward, G.E., Glasson, D.R., Glegg, G.A., Titley, J.G. & Morris, A.W., 1990a: Molecular probe analyses of estuarine particles. In: J. McManus & M. Elliott (Eds.), *Developments in Estuarine Study Techniques*, Olsen & Olsen. pp 115-120.
- Millward, G.E., Turner, A., Glasson, D.R. & Glegg, G.A., 1990b: Intra- and inter-estuarine variability of particle microstructure. *Sci. Total Environ.*, In Press.
- Moody, J.R. & Lindstrom, R.M., 1977: The selection and cleaning of plastic containers for the storage of trace metal samples. *Analyt. Chem.*, **49**, 2264-2267.
- Morris, A.W., 1986: Removal of trace metals in the very low salinity regions of the Tamar Estuary, England. *Sci. Total Environ.*, **49**, 297-304.
- Morris, A.W. & Bale, A.J., 1979: Effect of rapid precipitation of dissolved Mn in river water on estuarine Mn distributions. *Nature*, **279**, 318-319.
- Morris, A.W., Bale, A.J. & Howland, R.J.M., 1981: Nutrient distributions in an estuary: evidence of chemical precipitation of dissolved silicate and phosphate. *Estuar. Coast. Shelf Sci.*, **13**, 205-216.
- Morris, A.W., Bale, A.J. & Howland, R.J.M., 1982a: Chemical variability in the Tamar Estuary, South-West England. *Estuar. Coast. Shelf Sci.*, **14**, 649-661.

- Morris, A.W., Bale, A.J. & Howland, R.J.M., 1982b: The dynamics of estuarine manganese cycling. *Estuar. Coast. Shelf Sci.*, **14**, 175-192.
- Morris, A.W., Bale, A.J., Howland, R.J.M., Loring, D.H. & Rantala, R.T.T., 1987: Controls on the chemical composition of particle populations in a macrotidal estuary. *Cont. Shelf Res.*, **7**, 1351-1355.
- Morris, A.W., Bale, A.J., Howland R.J.M., Millward, G.E., Ackroyd, D.R., Loring, D.H. & Rantala, R.T.T., 1986a: Sediment mobility and its contribution to trace metal cycling in a macrotidal estuary. *Wat. Sci. Technol.*, **18**, 111-119.
- Morris, A.W., Howland, R.J.M. & Bale, A.J., 1986b: Dissolved aluminium in the Tamar Estuary, southwest England. *Geochim. Cosmochim. Acta*, **50**, 189-197.
- Morris, A.W., Loring, D.H., Bale, A.J., Howland, R.J.M., Mantoura, R.F.C. & Woodward, E.M.S., 1982c: Particle dynamics, particulate carbon, and the oxygen minimum in an estuary. *Oceanol. Acta*, **5**, 349-353.
- Morris, A.W., Mantoura, R.F.C., Bale, A.J. & Howland, R.J.M., 1978: Very low salinity regions of estuaries, important sites for chemical and biological reactions. *Nature*, **274**, 678-680.
- Nakamura, N., 1974: Determination of REE, Ba, Fe, Mg, Na and K in carbonaceous and ordinary chondrites. *Geochim. Cosmochim. Acta*, **38**, 757-775.
- Norrish, K. & Chappell, B.W., 1977: X-ray fluorescence spectrometry. In: J. Zussman (Ed.), *Physical Methods in Determinative Mineralogy*. Academic Press, New York, N.Y.. 2nd Edition, pp 201-272.
- Officer, C.B., 1976: *Physical Oceanography of Estuaries (and associated coastal waters)*. John Wiley, Chichester. 465pp.
- Perkins, J.W., 1972: *Geology Explained: Dartmoor and the Tamar Valley*. David & Charles, Newton Abbot, 196pp.
- Piper, D.Z., 1974: Rare earth elements in the sedimentary cycle: a summary. *Chem. Geol.*, **14**, 285-304.

- Plummer, D.H., Owens, N.J.P. & Herbert, R.A., 1987: Bacteria-particle interactions in turbid estuarine environments. *Cont. Shelf Res.*, **7**, 1429–1433.
- Price, W.J., 1979: *Spectrochemical Analysis by Atomic Absorption*. Heyden, London. 392pp.
- Rapin, F., Tessier, A., Campbell, P.G.C. & Carignan, R., 1986: Potential artifacts in the determination of metal partitioning in sediments by a sequential extraction procedure. *Environ. Sci. Technol.*, **20**, 836–840.
- Robertson, D.E., 1968a: Role of contamination in trace element analysis of sea water. *Analyt. Chem.*, **7**, 1067–1072
- Robertson, D.E., 1968b: The adsorption of trace elements in sea water on various container walls. *Analytica Chim. Acta*, **42**, 533–536.
- Robinson, G.D., 1984: Sequential chemical extractions and metal partitioning in hydrous Mn-Fe oxide coatings: reagent choice and substrate composition affect results. *Chem. Geol.* **47**, 97–112.
- Rosenbauer, R.J., Bischoff, J.L. & Seyfried W.E., 1979: Determination of sulfate in seawater and natural brines by ^{133}Ba and membrane dialysis. *Limnol. Oceanogr.*, **24**, 393–396.
- Schubel, J.R., 1971: Tidal variations in the size distribution of suspended sediment at a station in the Chesapeake Bay. *Neth. J. Sea Res.*, **5**, 252–266.
- Sholkovitz, E.R., 1976: Flocculation of dissolved organic and inorganic material during the mixing of river water and sea water. *Geochim. Cosmochim. Acta*, **40**, 831–845.
- Sholkovitz, E.R., 1978: The flocculation of dissolved Fe, Mn, Al, Cu, Ni, Co and Cd during estuarine mixing. *Earth Planet. Sci. Lett.* **41**, 77–86.
- Sholkovitz, E.R., 1988: Rare earth elements in the sediments of the North Atlantic Ocean, Amazon Delta, and East China Sea: Reinterpretation of terrigenous input patterns to the oceans. *Am. J. Sci.*, **288**, 236–281.
- Sholkovitz, E.R., 1989: Artifacts associated with the chemical leaching of sediments for rare earth elements. *Chem. Geol.*, **77**, 47–51.

- Sholkovitz, E.R., Boyle, E.A. & Price, N.B., 1978: The removal of dissolved humic acids and iron during estuarine mixing. *Earth Planet. Sci. Lett.*, **40**, 130–136.
- Sholkovitz, E.R., Piepgras, D.J. & Jacobsen, S.B., 1989: The pore water chemistry of rare earth elements in Buzzards Bay sediments. *Geochim. Cosmochim. Acta*, **53**, 2847–2856.
- Simões-Gonçalves, M de L., Sigg, L., Reutlinger, M. & Stumm, W., 1987: Metal ion binding by biological surfaces: voltammetric assessment in the presence of bacteria. *Sci. Total Environ.*, **60**, 105–119.
- van der Sloot, H.A. & Duinker, J.C., 1982: Isolation of different suspended matter fractions and their trace metal contents. *Environ. Technol. Lett.*, **2**, 511–520.
- Strelow, F.W.E., 1960: An ion exchange selectivity scale of cations based on equilibrium distribution coefficients. *Analyt. Chem.*, **32**, 1185–1188.
- Strelow, F.W.E., 1966: Separation of trivalent rare earths plus Sc(III) from Al, Ga, In, Tl, Fe, Ti, U and other elements by cation-exchange chromatography. *Analytica Chim. Acta*, **34**, 387–393.
- Strelow, F.W.E., 1980: Quantitative separation of lanthanides and scandium from barium, strontium and other elements by cation-exchange chromatography in nitric acid. *Analytica Chim. Acta*, **120**, 249–254.
- Strelow, F.W.E., Rethemeyer, R. & Bothma, C.J.C., 1965: Ion exchange selectivity scales in nitric acid and sulphuric acid media with a sulfonated polystyrene resin. *Analyt. Chem.*, **37**, 106–110.
- Tessier, A., Campbell, P.G.C. & Bisson, M., 1979: Sequential extraction procedure for the speciation of particulate trace metals. *Analyt. Chem.*, **51**, 844–851.
- Thirlwall, M.F., 1982: A triple filament method for the rapid and precise determination of the rare earth elements by isotope dilution. *Chem. Geol.*, **35**, 155–166.
- Thompson, M. & Walsh, J.N., 1983: *A Handbook of ICP Spectrometry*. Blackie, Glasgow. 273 pp

- Tipping, E., Hetherington, N.B., Hilton, J., Thompson, D.W., Bowles, E. & Hamilton-Taylor, J., 1985: Artifacts in the use of selective chemical extraction to determine the distributions of metals between the oxides of manganese and iron. *Analyt. Chem.*, **57**, 1944–1946.
- Titley, J.G., Glegg, G.A., Glasson, D.R. & Millward G.E., 1987: Surface areas and porosities of particulate matter in turbid estuaries. *Cont. Shelf Res.*, **7**, 1363–1366.
- Turner, D.R., Whitfield, M. & Dickson, A.G., 1981: The equilibrium speciation of dissolved components in freshwater and seawater at 25°C and 1 atm. pressure. *Geochim. Cosmochim. Acta*, **45**, 855–881.
- Uncles, R.J., Bale, A.J., Howland, R.J.M., Morris, A.W., Elliot, R.C.A., 1983: Salinity of surface water in a partially mixed estuary and its dispersion at low run-off. *Oceanol. Acta*, **6**, 289–296.
- Upstill-Goddard, R.C., 1985: The Geochemistry of the Halogens in the Tamar Estuary. *Ph.D. thesis*, Univ. of Leeds. 341pp
- Upstill-Goddard, R.C., Alexander, W.R., Elderfield, H. & Whitfield, M., 1989: Chemical Diagenesis in the Tamar Estuary, *Contributions to Sedimentology*, No. 16., Eds. H. Füchtbauer, A.P. Lisitzyn, J.D. Milliman & E. Seibold. E. Schweizerbart'sche Verlagsbuchhandlung (Nägele u. Obermiller), Stuttgart. 49 pp.
- Vivian, C.M.G, 1986: Rare earth element content of sewage sludges dumped at sea in Liverpool Bay, U.K.. *Environ. Technol. Lett.*, **7**, 593–596.
- Walsh, J.N., 1980: The simultaneous determination of major, minor and trace constituents of silicate rocks using inductively coupled plasma spectrometry. *Spectrochim. Acta*, **35B**, 107–111.
- Walsh, J.N., Buckley, F. & Barker, J., 1981: The simultaneous determination of the rare earth elements in rocks using inductively coupled plasma source spectrometry. *Chem. Geol.*, **33**, 141–153.

- Walsh, J.N. & Howie, R.A., 1980: An evaluation of the performance of an inductively coupled plasma source spectrometer for the determination of the major and trace constituents of silicate rocks and minerals. *Mineralog. Mag.*, **43**, 967–974.
- Watson, P.G., Frickers, P.E. & Goodchild, C.M., 1985: Spatial and seasonal variations in the chemistry of sediment interstitial waters in the Tamar Estuary. *Estuar. Coast. Shelf Sci.*, **21**, 105–119.
- Van der Weijden, C.H., Arnoldus, M.J.H.L. & Meurs, C.J., 1977: Desorption of metals from suspended matter in the Rhine Estuary. *Neth. J. Sea Res.*, **11**, 130–145.
- Wellershaus, S., 1981: Dredged coastal plain estuaries: organic carbon in the turbidity maximum. *Environ. Technol. Lett.*, **2**, 153–160.
- Wilson, T.R.S., 1983: A microcomputer controlled alkalinity titration: methods and results. *Analyt. Proc.*, **20**, 460–462.

Appendix A

Neal Point, Core 1: Sediments									
Sample depth (cm.)	Major elements, wt.% - total analysis.								
	Al ₂ O ₃	Fe ₂ O ₃	MgO	CaO	Na ₂ O	K ₂ O	TiO ₂	P ₂ O ₅	MnO
0-1	14.1	6.45	1.41	1.14	1.59	2.31	0.65	0.33	0.11
1-2	14.8	6.21	1.49	1.09	1.75	2.37	0.70	0.27	0.07
2-3	14.1	6.27	1.43	1.14	1.65	2.32	0.66	0.26	0.07
3-4	13.8	6.21	1.44	1.46	1.71	2.27	0.65	0.26	0.07
4-5	13.3	5.97	1.39	1.48	1.69	2.22	0.63	0.25	0.07
5-6	13.9	5.90	1.43	1.45	1.77	2.47	0.70	0.24	0.07
6-7	14.2	5.92	1.48	1.26	1.89	2.57	0.65	0.22	0.07
7-8	14.6	6.48	1.52	1.35	1.94	2.57	0.67	0.24	0.07
8-9	15.8	7.11	1.61	1.50	2.19	2.70	0.66	0.27	0.07
9-10	13.1	5.76	1.40	1.55	1.69	2.28	0.61	0.21	0.07
10-11	13.3	5.65	1.39	1.49	1.72	2.48	0.67	0.20	0.07
11-12	13.1	5.87	1.35	1.50	1.66	2.39	0.66	0.20	0.07
12-13	14.8	6.55	1.50	1.05	2.06	2.56	0.72	0.25	0.08
13-14	14.2	6.32	1.43	0.91	1.89	2.35	0.65	0.24	0.08
Sample depth (cm.)	Major elements, wt.% - leach analysis.								
	Al ₂ O ₃	Fe ₂ O ₃	MgO	CaO	Na ₂ O	K ₂ O	P ₂ O ₅	MnO	
0-1	0.51	1.81	0.42	0.85	0.90	0.10	0.23	0.07	
1-2	0.55	1.44	0.44	0.80	1.07	0.12	0.19	0.03	
2-3	0.52	1.60	0.41	0.84	0.99	0.12	0.18	0.03	
3-4	0.51	1.81	0.44	1.19	1.03	0.11	0.19	0.04	
4-5	0.45	1.55	0.39	1.06	0.96	0.10	0.16	0.03	
5-6	0.43	1.44	0.38	1.07	0.92	0.10	0.16	0.03	
6-7	0.60	1.64	0.44	0.94	1.03	0.12	0.14	0.03	
7-8	0.65	1.94	0.48	1.05	1.13	0.14	0.16	0.03	
8-9	0.63	2.27	0.53	1.20	1.41	0.16	0.17	0.03	
9-10	0.51	1.61	0.42	1.24	0.94	0.11	0.15	0.03	
10-11	0.51	1.45	0.38	1.12	0.83	0.10	0.13	0.03	
11-12	0.55	1.55	0.38	1.06	0.81	0.10	0.13	0.03	
12-13	0.56	1.95	0.47	0.79	1.25	0.13	0.16	0.04	
13-14	0.57	1.90	0.46	0.67	1.26	0.13	0.17	0.04	

Neal Point, Core 1: Sediments									
Sample depth (cm.)	Trace elements, ppm - total analysis.								
	Ba	Co	Cu	Li	Ni	Sr	V	Zn	Y
0-1	333	20	210	108	52	125	103	322	18.7
1-2	321	19	221	115	56	119	109	318	20.3
2-3	313	19	204	110	55	111	108	318	18.8
3-4	270	19	205	107	52	121	103	310	18.0
4-5	293	18	193	104	50	121	98	300	16.7
5-6	337	16	205	116	49	130	99	292	17.1
6-7	351	18	220	117	50	126	102	310	17.8
7-8	348	18	253	118	51	129	110	348	18.2
8-9	338	19	305	125	53	146	121	401	19.3
9-10	326	16	191	103	47	126	93	294	17.9
10-11	350	15	207	110	45	131	93	298	17.0
11-12	340	16	200	108	46	123	95	320	17.4
12-13	366	19	260	116	53	129	112	363	19.0
13-14	327	18	251	108	51	114	107	344	19.0
Sample depth (cm.)	Trace elements, ppm - leach analysis.								
	Ba	Co	Cu	Ni	Sr	V	Zn	Y	
0-1	22	9	153	20	50	15	258	6.0	
1-2	20	9	166	21	44	18	276	6.3	
2-3	18	8	152	19	40	19	266	6.0	
3-4	21	8	151	18	50	19	264	5.8	
4-5	17	7	139	15	47	17	233	5.4	
5-6	20	7	138	17	48	15	210	5.0	
6-7	27	8	150	15	43	19	244	5.7	
7-8	27	8	177	15	48	22	280	6.2	
8-9	24	8	227	17	61	26	324	6.8	
9-10	25	7	143	14	52	17	235	5.1	
10-11	23	6	126	13	47	16	231	5.0	
11-12	24	7	120	15	41	16	232	4.9	
12-13	25	9	196	18	44	20	296	5.8	
13-14	25	8	201	19	40	20	292	6.0	

Neal Point, Core 1: Sediments										
Sample depth (cm.)	Rare earth elements, ppm - total analysis.									
	La	Ce	Nd	Sm	Eu	Gd	Dy	Ho	Er	Yb
0-1	35.9	66	33.2	6.4	1.17	4.4	3.52	0.70	2.13	1.95
1-2	38.4	71	35.3	6.8	1.23	4.8	3.79	0.77	2.28	2.17
2-3	35.2	65	32.5	6.3	1.14	4.3	3.56	0.70	2.10	1.98
3-4	33.7	62	31.1	6.1	1.10	4.2	3.37	0.68	2.00	1.85
4-5	33.1	61	30.4	5.8	1.04	3.9	3.18	0.64	1.83	1.80
5-6	33.0	63	31.9	5.9	1.06	4.0	3.26	0.65	1.94	1.83
6-7	34.2	64	32.2	6.1	1.14	4.3	3.42	0.69	2.11	1.95
7-8	33.9	64	32.4	6.1	1.12	4.3	3.50	0.70	2.07	1.95
8-9	34.5	64	32.6	6.2	1.17	4.6	3.67	0.74	2.22	1.95
9-10	34.2	65	32.6	6.0	1.06	4.5	3.49	0.70	2.06	1.92
10-11	33.0	63	31.0	5.8	1.06	4.1	3.28	0.67	1.97	1.80
11-12	33.6	64	31.7	5.9	1.03	4.2	3.33	0.67	1.95	1.83
12-13	35.4	66	33.2	6.3	1.15	4.5	3.64	0.75	2.19	2.07
13-14	34.8	66	33.3	6.3	1.16	4.5	3.63	0.74	2.17	2.03
Sample depth (cm.)	Rare earth elements, ppm - leach analysis.									
	La	Ce	Nd	Sm	Eu	Gd	Dy	Ho	Er	Yb
0-1	5.5	10.3	7.8	1.90	0.30	1.38	1.19	0.23	0.52	0.51
1-2	5.7	10.9	8.2	2.02	0.33	1.44	1.25	0.26	0.55	0.50
2-3	5.3	10.3	7.7	1.89	0.32	1.35	1.19	0.24	0.53	0.43
3-4	5.5	10.4	7.6	1.90	0.28	1.22	1.14	0.24	0.51	0.46
4-5	5.0	9.5	7.0	1.68	0.26	1.22	1.05	0.21	0.45	0.41
5-6	4.9	9.4	6.8	1.66	0.22	1.03	0.97	0.18	0.38	0.40
6-7	5.5	11.1	7.7	1.92	0.28	1.29	1.11	0.23	0.51	0.45
7-8	5.9	11.7	8.4	2.09	0.33	1.44	1.25	0.27	0.58	0.50
8-9	6.2	12.4	8.9	2.21	0.39	1.67	1.36	0.30	0.68	0.55
9-10	5.1	10.5	7.2	1.72	0.26	1.12	1.03	0.21	0.44	0.37
10-11	5.0	10.2	7.1	1.68	0.26	1.13	1.01	0.21	0.44	0.36
11-12	4.8	9.3	6.7	1.61	0.22	1.06	0.94	0.19	0.41	0.39
12-13	5.5	11.1	7.8	2.01	0.30	1.40	1.14	0.23	0.55	0.45
13-14	5.8	11.0	8.5	1.97	0.30	1.31	1.24	0.24	0.52	0.53

Appendix B

Neal Point, Core 1: Pore Waters							
Sample depth (cm.)	NH ₄ ⁺ μM	PO ₄ ³⁻ μM	SO ₄ ²⁻ mM	HCO ₃ ⁻ mM	Si μM	Fe μM	Mn μM
0-1	115	5	16.9	3.39	110	38.0	93
1-2	150	36	19.8	3.15	165	330	74
2-3	155	81	20.4	2.61	195	414	50
3-4	160	68	21.6	2.65	205	309	54
4-5	160	94	21.2	3.30	215	238	52
5-6	160	81	21.1	3.31	230	225	55
6-7	165	98	20.8		215	159	51
7-8	185	115	20.8	3.12	215		46
8-9	185	102	20.7	3.01	205	76	76
9-10	175	93	21.0	2.95	220	66	42
10-11	200	90	20.3	3.19	220	59	42
11-12	210	92	20.1		230	22	61
12-13	265	135	20.0	3.86	270	46	53
13-14	305	161	20.1	4.28	290	45	57

Neal Point, Core 1: Pore Waters										
Sample depth (cm.)	Rare earth elements, pmol kg ⁻¹ .									
	La	Ce	Nd	Sm	Eu	Gd	Dy	Er	Yb	Lu
0-1	360	620	370	83	15.6	94	70	40	35	5.6
1-2		600								
2-3										
3-4		2310	440	87	17.1		72	43	243	11.2
4-5		830	410	92	21.3					37
5-6										
6-7										
7-8										
8-9					24.1			29		
9-10	255	570	260	57	13.0		132	21	116	
10-11										
11-12		460	220	51	12.2		43	24		
12-13		1830	450	104	24.9		97	49		
13-14	750	1690	660	140	34.0	156	111	62	54	8.5

Neal Point, Core 2: Pore Waters							
Sample depth (cm.)	NH ₄ ⁺ μM	PO ₄ ³⁻ μM	SO ₄ ²⁻ mM	HCO ₃ ⁻ mM	Si μM	Fe μM	Mn μM
0-1	165	8	14.8	4.25	136	10	2.63
1-2	220	29	19.1	4.34	180	448	4.19
2-3	290	66	17.0	4.65	215	602	2.27
3-4	350	82		4.95	255	555	2.98
4-5	405	127	17.6	6.79	315	450	3.50
5-6	465	150	16.5	8.09	335	323	3.48
6-7	535	184	16.5		390		0.00
7-8	575	203	16.2	10.5	390	67	3.34
8-9	625	231	14.7	11.9	410	92	
9-10	690	239	13.6	12.7	400		
10-11	740	250	13.4	13.5	415	59	2.86
11-12	765	255	13.4	14.1	385	49	3.01
12-13	795	263	13.2	14.5	400	41	2.74
13-14	835	265	12.5	14.8	370	13	3.39
14-15	895	275	12.2	15.8	410	40	2.75
15-16	900	281	10.8	16.1	410		
16-17	930	274	10.7	16.4	440	24	2.86

Neal Point, Core 2: Pore Waters										
Sample depth (cm.)	Rare earth elements, pmol kg ⁻¹ .									
	La	Ce	Nd	Sm	Eu	Gd	Dy	Er	Yb	Lu
0-1	390	890	430	93	20.7		80	45	283	
1-2		3860	690		35		118	62		11.1
2-3	320	1490	540	118	26.2		95(±20)	41		
3-4		640	350	85	21.3		74	44	246	8.7
4-5		1050	390	99	24.5		93	46		
5-6	300(±50)	1300	390	101	25.6			41	96	
6-7	760	1130	630	144	35		121	70		
7-8										
8-9		890	450	118	29.7		114	63		
9-10	380(±90)	2460	500	122	25.9					
10-11	540	900	520	135	33.6					
11-12	450	1040	590	153	22.6		150	91	220	
12-13		1040	560	145	36				165	
13-14		1200								
14-15		940	580	147	36.7		148	92	249	
15-16					31.8		126	85	308	
16-17							131	71	237	

Neal Point, Core 3: Pore Waters				
Sample depth (cm.)	NH ₄ ⁺ μM	PO ₄ ³⁻ μM	SO ₄ ²⁻ mM	Si μM
0-1	175	7	15.6	135
1-2	190	23	18.5	195
2-3	230	69	18.6	285
3-4	270	100	18.7	320
4-5	340	118	18.7	350
5-6	410	147	17.8	410
6-7	475	171	17.5	450
7-8	560	202	17.5	455
8-9	585	226	16.5	445
9-10	640	219	15.8	465
10-11	675	232	16.3	445
11-12	730	240	14.3	440
12-13	770	255	14.9	455
13-14	810	260	15.2	440
14-15	855	265	14.5	440
15-16	875	266	13.1	440
16-17	925	265	13.3	420
17-18	1050	287	12.5	445

Neal Point, Core 3: Pore Waters										
Sample depth (cm.)	Rare earth elements, pmol kg ⁻¹ .									
	La	Ce	Nd	Sm	Eu	Gd	Dy	Er	Yb	Lu
0-1		1160	230	37	9.1				295	
1-2		660	280	60	14.9	105	54	34		9
2-3	205	350	280	69	17.5	100	72	40		7.5
3-4	390	610			5.7					
4-5	230	380	310	81	21.3	106	99	60	79	9.1
5-6	460	560								
6-7	350	680	450	100	26	113	108	61	62	10.6
7-8										
8-9										
9-10										
10-11	250(±70)	460	340	94	25	107	100	67	62	16.2
11-12	260	580	410	111	29.1		109	68	82	10.9
12-13	200	420	360	72	21				289	
13-14	230	1290	340	96	25.5		100	64		14.4
14-15	370(±80)	340	300	90	24.4	123	101	66	70	
15-16		1470	350	94	25			62	231	
16-17		450	390	129	25.8				325	
17-18										

Appendix C

Axial Surveys: Back-up Data					
Neaps Survey - 12/8/85					
Distance down estuary (km)	Salinity ppt	Turbidity mg l ⁻¹	Si μM	Fe μmol kg ⁻¹	Mn μmol kg ⁻¹
3.0	0.04	30.9	97.5	2.36	1.77
4.9	0.04	46.4	97.3	2.47	1.62
7.6	0.04	46.2	94.5	2.32	1.92
9.9	0.05	78.8	92.4	2.36	2.19
11.6	0.06	75.8	92.4	3.91	3.30
12.0	0.36	80.4	91.6	2.62	2.16
12.2	0.60	84.2	91.0	2.10	2.31
12.5	0.78	80.9	90.3	1.99	2.21
12.8	1.80	65.4	83.0	2.64	2.03
13.2	3.02	67.8	81.9	2.40	2.93
17.7	5.63	33.0	67.4	0.70	1.68
20.5	8.92	21.9	62.0	1.34	1.20
20.6	11.20	17.9	56.7	1.59	1.33
21.0	14.48	17.5	40.9	1.33	2.53
26.0	18.71	8.7	29.0	0.55	0.61
27.0	21.62	6.9	25.5	0.37	0.39

Springs Survey - 19/8/85					
Distance down estuary (km)	Salinity ppt	Turbidity mg l ⁻¹	Si μM	Fe μmol kg ⁻¹	Mn μmol kg ⁻¹
3.0	0.02	13.6	101.5	1.70	0.85
5.7	0.02	109.5	101.5	2.08	0.92
7.6	0.02	148.7	102.9	2.05	0.96
8.9	0.04	157.7	102.5	2.10	1.07
10.5	0.24	165.7	101.5	2.01	1.09
10.5	0.42	127.3	98.7	1.33	1.27
11.6	2.73	78.8	92.4	1.50	
12.6	3.20	51.0	90.3	1.12	1.88
13.3	3.89	42.1	89.9		
13.6	4.20	37.6	86.1	0.40	1.92
14.0	6.95	33.7	78.8	0.43	1.97
14.6	9.25	25.5	69.3	0.37	1.51
14.7	12.60	23.1	58.8	0.26	0.91
15.2	14.59	19.2	52.1	0.46	0.72
15.5	16.50	16.6	46.2	0.39	0.50
17.2	19.56	17.0	38.2	0.38	0.46
18.1	22.79	14.7	24.8	0.26	0.41
23.1	25.27	8.3	19.2	0.30	0.45
27.2	28.68	6.2	11.6	0.67	0.74

Neaps Survey: Suspended Particles									
Distance down estuary (km)	Major elements, wt.% - total analysis.								
	Al ₂ O ₃	Fe ₂ O ₃	MgO	CaO	Na ₂ O	K ₂ O	TiO ₂	P ₂ O ₅	MnO
3.0	18.5	9.27	0.96	0.83	0.53	2.85	0.67	0.53	0.49
4.9	17.7	8.82	0.93	0.78	0.51	2.70	0.63	0.48	0.43
7.6	19.5	9.10	1.02	0.77	0.52	2.91	0.66	0.47	0.35
9.9	19.3	8.74	0.99	0.69	0.53	3.07	0.66	0.42	0.40
11.6	19.4	8.86	0.97	0.73	0.52	3.00	0.64	0.43	0.40
12.0	17.8	8.14	0.99	0.56	0.51	2.76	0.63	0.42	0.33
12.2	19.5	8.88	1.07	0.53	0.57	3.04	0.67	0.45	0.38
12.5	20.3	9.25	1.11	0.52	0.61	3.21	0.72	0.48	0.38
12.8	19.1	8.80	1.07	0.45	0.61	3.07	0.68	0.45	0.33
13.2	19.8	9.23	1.10	0.45	0.66	3.13	0.70	0.51	0.31
17.7	18.2	9.51	1.50	0.57	0.85	2.80	0.66	0.60	0.59
20.5	17.7	9.80	1.56	0.58	1.17	2.83	0.53	0.63	0.84
20.6	18.6	10.0	1.62	0.63	0.67	2.80	0.69	0.64	0.77
21.0	19.2	9.72	1.44	0.44	0.72	2.99	0.68	0.57	0.17
26.0	17.8	7.49	1.69	0.71	3.90	2.82	0.58	0.46	0.62
27.0	17.4	8.28	1.75	0.91	4.31	2.78	0.52	0.58	0.90
Distance down estuary (km)	Major elements, wt.% - leach analysis.								
	Al ₂ O ₃	Fe ₂ O ₃	MgO	CaO	Na ₂ O	K ₂ O		P ₂ O ₅	MnO
3.0	0.96	3.63	0.15	0.70	0.03	0.08		0.29	0.52
4.9	1.00	3.67	0.16	0.68	0.04	0.08		0.30	0.48
7.6	0.92	3.56	0.17	0.64	0.02	0.08		0.27	0.37
9.9	0.76	2.97	0.15	0.58	0.04	0.07		0.23	0.43
11.6	0.77	2.99	0.17	0.59	0.04	0.08		0.23	0.43
12.0	0.74	2.99	0.27	0.44	0.07	0.07		0.25	0.38
12.2	0.74	3.01	0.28	0.38	0.09	0.07		0.25	0.42
12.5	0.72	2.96	0.27	0.33	0.10	0.08		0.25	0.39
12.8	0.84	3.35	0.33	0.32	0.13	0.09		0.26	0.38
13.2	0.73	3.16	0.31	0.28	0.16	0.10		0.29	0.32
17.7	1.10	4.57	0.56	0.42	0.49	0.13		0.42	0.65
20.5	1.05	4.55	0.60	0.42	0.78	0.16		0.45	0.84
20.6	1.29	5.21	0.63	0.49	0.30	0.15		0.49	0.86
21.0	0.91	4.16	0.26	0.22	0.27	0.10		0.40	0.14
26.0	1.00	2.33	0.68	0.53	3.55	0.23		0.26	0.60
27.0	0.93	3.25	0.77	0.75	3.92	0.22		0.40	0.88

Springs Survey: Suspended Particles									
Distance down estuary (km)	Major elements, wt.% - total analysis.								
	Al ₂ O ₃	Fe ₂ O ₃	MgO	CaO	Na ₂ O	K ₂ O	TiO ₂	P ₂ O ₅	MnO
3.0	15.4	9.7	1.10	0.82	0.62	2.31	0.69	0.78	0.78
5.7	16.7	8.1	1.26	0.87	0.67	2.61	0.68	0.44	0.21
7.6	17.5	8.1	1.31	0.77	0.63	2.75	0.59	0.39	0.29
8.9	18.8	8.1	1.45	0.71	0.58	2.99	0.70	0.39	0.30
10.5	19.2	8.2	1.55	0.59	0.58	3.07	0.66	0.40	0.19
10.5	20.8	8.8	1.68	0.56	0.60	3.18	0.57	0.40	0.20
11.6	20.5	8.9	1.70	0.52	0.63	3.13	0.66	0.46	0.27
12.6	20.8	9.1	1.64	0.47	0.62	3.19	0.72	0.49	0.28
13.3	21.0	9.2	1.67	0.47	0.68	3.20	0.75	0.49	0.28
13.6	20.0	8.8	1.64	0.48	0.64	3.06	0.72	0.48	0.29
14.0	20.6	9.0	1.70	0.50	0.78	3.12	0.72	0.48	0.35
14.6	20.3	9.0	1.75	0.54	0.64	3.07	0.72	0.51	0.49
14.7	20.9	9.4	1.81	0.56	0.86	3.06	0.74	0.51	0.65
15.2	18.5	8.9	1.76	0.62	0.54	2.75	0.65	0.52	0.79
15.5	18.3	9.0	1.74	0.64	0.97	2.66	0.70	0.53	0.85
17.2	18.8	8.5	1.73	0.63	0.92	2.81	0.67	0.54	0.69
18.1	18.2	8.2	1.68	0.87	0.88	2.71	0.66	0.45	0.60
23.1	17.5	7.8	1.77	1.10	1.89	2.63	0.65	0.49	0.64
27.2	16.9	7.7	1.73	2.19	1.66	2.52	0.62	0.52	0.63
Distance down estuary (km)	Major elements, wt.% - leach analysis.								
	Al ₂ O ₃	Fe ₂ O ₃	MgO	CaO	Na ₂ O	K ₂ O		P ₂ O ₅	MnO
3.0	0.91	3.90	0.13	0.57	0.05	0.07		0.51	0.68
5.7	0.84	2.94	0.23	0.73	0.03	0.07		0.32	0.20
7.6	0.85	2.97	0.22	0.66	0.02	0.06		0.29	0.28
8.9	0.83	2.86	0.26	0.59	0.04	0.07		0.28	0.30
10.5	0.83	2.89	0.33	0.44	0.08	0.08		0.28	0.15
10.5	0.84	2.93	0.35	0.42	0.11	0.09		0.28	0.17
11.6	0.85	3.20	0.43	0.37	0.16	0.10		0.31	0.25
12.6	0.87	3.40	0.40	0.35	0.17	0.10		0.33	0.26
13.3	0.86	3.41	0.42	0.34	0.22	0.11		0.32	0.26
13.6	0.85	3.44	0.46	0.36	0.21	0.10		0.32	0.28
14.0	0.85	3.40	0.47	0.36	0.34	0.12		0.33	0.33
14.6	0.85	3.41	0.52	0.39	0.19	0.08		0.32	0.49
14.7	0.82	3.29	0.52	0.39	0.38	0.10		0.31	0.61
15.2	0.79	3.21	0.57	0.42	0.10	0.08		0.30	0.69
15.5	0.80	3.19	0.56	0.43	0.51	0.11		0.31	0.74
17.2	0.81	3.22	0.59	0.50	0.54	0.15		0.35	0.73
18.1	0.79	3.09	0.57	0.75	0.61	0.14		0.30	0.64
23.1	0.74	3.02	0.69	0.98	1.66	0.17		0.33	0.67
27.2	0.65	2.41	0.59	1.78	1.16	0.13		0.31	0.55

Neaps Survey: Suspended Particles								
Distance down estuary (km)	Trace elements, ppm - total analysis.							
	Ba	Co	Cu	Li	Ni	Sr	V	Zn
3.0	548	43	120	121	112	115	141	404
4.9	516	38	119	114	100	109	137	386
7.6	510	29	113	127	77	117	150	318
9.9	505	29	110	127	74	111	151	309
11.6	506	28	94	124	75	115	154	294
12.0	452	25	89	115	66	112	144	275
12.2	497	29	92	125	75	123	158	297
12.5	513	29	96	132	72	126	165	255
12.8	474	28	84	126	66	127	156	265
13.2	486	29	88	127	72	131	165	280
17.7	426	34	142	120	73	144	165	364
20.5	409	41	163	121	72	149	167	362
20.6	422	40	185	129	76	151	174	398
21.0	451	19	195	130	77	114	166	338
26.0	396	46	191	121	80	134	161	510
27.0	393	52	175	120	72	167	160	463

Distance down estuary (km)	Trace elements, ppm - leach analysis.							
	Ba	Co	Cu	Ni	Sr	V	Zn	
3.0	104	37	93	76	27	18	273	
4.9	102	35	98	72	26	18	278	
7.6	67	22	87	44	26	25	181	
9.9	56	23	81	45	23	21	166	
11.6	59	23	73	40	28	20	157	
12.0	45	21	72	42	32	21	147	
12.2	46	22	66	44	33	21	153	
12.5	37	21	61	34	30	21	127	
12.8	32	24	60	34	40	24	146	
13.2	25	22	59	31	39	24	153	
17.7	25	29	120	37	68	44	253	
20.5	24	32	131	32	73	50	261	
20.6	24	35	164	42	79	57	336	
21.0	24	9	153	27	28	37	235	
26.0	14	35	154	36	55	44	408	
27.0	20	41	138	33	88	48	368	

Springs Survey: Suspended Particles									
Distance down estuary (km)	Trace elements, ppm - total analysis.								
	Ba	Co	Cu	Li	Ni	Sr	V	Zn	Y
3.0	456	67	398	99	144	102	120	714	25.0
5.7	398	31	362	117	85	109	123	448	24.0
7.6	391	31	308	124	80	110	130	386	22.3
8.9	432	29	261	134	80	115	141	353	22.7
10.5	447	26	244	134	70	119	145	353	22.6
10.5	490	28	254	152	75	129	156	387	22.3
11.6	444	32	246	147	75	138	160	391	22.6
12.6	489	35	212	147	72	137	165	380	21.9
13.3	495	39	177	145	71	139	168	361	23.0
13.6	469	38	164	139	66	138	163	362	23.4
14.0	475	45	159	142	69	143	167	368	23.0
14.6	471	49	161	142	70	151	167	379	22.6
14.7	488	56	161	143	74	157	174	376	23.1
15.2	424	61	161	131	70	153	160	374	22.8
15.5	417	65	161	127	74	152	164	394	22.6
17.2	421	50	169	130	75	144	162	369	22.4
18.1	402	40	180	129	64	149	155	347	22.9
23.1	382	33	169	124	63	157	154	352	22.0
27.2	371	23	184	123	61	188	148	348	21.3

Distance down estuary (km)	Trace elements, ppm - leach analysis.								
	Ba	Co	Cu	Ni	Sr	V	Zn	Y	
3.0	86	45	372	95	24	14	677	11.5	
5.7	54	22	332	52	28	16	468	9.5	
7.6	44	20	280	45	28	21	385	9.3	
8.9	41	19	231	43	32	23	337	8.2	
10.5	33	15	202	31	35	23	327	8.8	
10.5	32	15	191	31	36	25	325	8.4	
11.6	29	19	182	30	46	28	325	9.0	
12.6	29	23	157	28	44	31	327	9.6	
13.3	29	25	128	25	45	32	307	9.1	
13.6	29	26	120	25	51	33	313	9.0	
14.0	31	31	115	25	53	34	309	9.0	
14.6	29	36	116	25	61	36	310	9.3	
14.7	29	40	122	25	60	37	292	9.0	
15.2	24	40	129	27	67	38	300	9.3	
15.5	26	44	133	29	68	40	321	9.4	
17.2	29	37	142	34	64	41	333	9.2	
18.1	31	28	156	24	71	42	306	9.5	
23.1	32	23	146	25	82	47	320	9.2	
27.2	31	12	152	19	104	42	282	8.4	

Springs Survey: Suspended Particles										
Distance down estuary (km)	Rare earth elements, ppm - total analysis.									
	La	Ce	Nd	Sm	Eu	Gd	Dy	Ho	Er	Yb
3.0	39.1	68	37.2	7.5	1.28	5.1	4.38	0.87	2.50	2.50
5.7	39.5	71	37.1	7.2	1.45	6.5	4.38	0.92	2.62	2.42
7.6	38.8	71	36.6	7.2	1.41	6.9	4.09	0.90	2.51	2.31
8.9	39.1	71	36.0	7.2	1.40	5.8	4.17	0.89	2.53	2.31
10.5	39.0	72	37.0	7.0	1.41	6.4	4.25	0.91	2.63	2.36
10.5	39.1	72	36.8	7.0	1.42	7.4	4.19	0.93	2.63	2.32
11.6	39.0	72	37.0	7.2	1.42	6.4	4.27	0.91	2.60	2.32
12.6	37.2	69	35.8	7.0	1.35	5.0	4.20	0.87	2.51	2.21
13.3	40.2	74	38.0	7.4	1.44	5.3	4.35	0.89	2.67	2.31
13.6	39.3	72	37.4	7.3	1.44	5.2	4.46	0.92	2.74	2.38
14.0	40.0	73	37.7	7.5	1.44	5.3	4.36	0.90	2.67	2.36
14.6	39.6	73	37.9	7.4	1.45	5.3	4.27	0.87	2.59	2.29
14.7	39.8	72	37.7	7.3	1.37	5.1	4.37	0.91	2.63	2.28
15.2	40.2	73	38.1	7.4	1.40	5.2	4.35	0.90	2.59	2.36
15.5	39.7	73	37.6	7.4	1.33	5.1	4.26	0.89	2.53	2.34
17.2	39.7	73	37.8	7.4	1.42	5.2	4.20	0.85	2.57	2.31
18.1	40.1	73	38.3	7.4	1.44	5.4	4.35	0.89	2.58	2.34
23.1	38.3	71	36.3	7.1	1.35	5.1	4.19	0.84	2.51	2.23
27.2	36.2	67	34.4	6.8	1.23	4.8	4.05	0.83	2.37	2.23

Distance down estuary (km)	Rare earth elements, ppm - leach analysis.									
	La	Ce	Nd	Sm	Eu	Gd	Dy	Ho	Er	Yb
3.0	8.9	14.1	12.9	3.16	0.54	2.34	2.04	0.46	1.04	0.93
5.7	8.1	14.4	11.6	2.83	0.49	2.09	1.81	0.40	0.87	0.80
7.6	7.7	14.2	11.3	2.75	0.52	2.12	1.77	0.38	0.90	0.78
8.9	7.0	13.0	10.3	2.53	0.44	1.89	1.61	0.33	0.79	0.65
10.5	7.5	14.0	11.0	2.70	0.47	1.99	1.69	0.35	0.83	0.73
10.5	7.3	13.8	10.7	2.64	0.47	1.99	1.65	0.35	0.83	0.70
11.6	7.7	14.5	11.1	2.85	0.49	2.16	1.77	0.37	0.90	0.75
12.6	8.1	15.4	12.1	3.00	0.54	2.29	1.87	0.41	0.95	0.80
13.3	7.8	14.8	11.6	2.82	0.50	2.13	1.78	0.38	0.86	0.75
13.6	7.8	14.6	11.5	2.80	0.50	2.08	1.80	0.38	0.88	0.79
14.0	7.9	14.9	11.5	2.84	0.49	2.13	1.78	0.38	0.92	0.79
14.6	8.1	15.3	12.0	2.89	0.53	2.24	1.85	0.40	0.93	0.74
14.7	7.9	15.1	11.7	2.85	0.49	2.14	1.78	0.38	0.91	0.72
15.2	8.0	15.5	12.0	2.91	0.55	2.21	1.85	0.41	0.99	0.72
15.5	8.1	15.9	11.9	2.94	0.52	2.22	1.85	0.41	0.98	0.81
17.2	8.2	15.9	11.9	2.85	0.49	2.25	1.82	0.41	0.92	0.73
18.1	8.2	16.4	12.0	2.98	0.52	2.37	1.86	0.42	0.95	0.79
23.1	7.9	16.0	11.7	2.77	0.49	2.28	1.81	0.40	0.92	0.71
27.2	7.2	15.1	10.7	2.62	0.47	2.00	1.69	0.38	0.87	0.70

Appendix D

Turbidity Maximum, Surface Samples: Back-up Data				
Neaps - 14/8/85				
Time of sampling	Distance down estuary (km)	Turbidity $mg\ l^{-1}$	Salinity ppt	Fe $\mu g\ ml^{-1}$
12:41	17.0	83.8	0.35	0.117
13:20	15.3	107	0.45	0.118
14:00	13.7	142	0.45	0.141
14:44	12.6	83.0	0.35	0.139
15:18	11.8	74.7	0.35	0.122
16:00	11.7	75.9	0.35	0.143
Springs - 21/8/85				
Time of sampling	Distance down estuary (km)	Turbidity $mg\ l^{-1}$	Salinity ppt	Fe $\mu g\ ml^{-1}$
07:08	10.1	740	0.125	0.203
07:54	8.9	472	0.15	0.190
08:21	8.1	340	0.15	0.173
09:29	8.5	218	0.23	0.169
10:03	8.5	167	0.27	0.176

Turbidity Maximum, Surface Samples: Suspended Particles									
Time of sampling	Major elements, <i>wt.%</i> - total analysis.								
	Al ₂ O ₃	Fe ₂ O ₃	MgO	CaO	Na ₂ O	K ₂ O	TiO ₂	P ₂ O ₅	MnO
Neaps									
12:41	18.7	9.0	1.35	0.56	0.61	2.77	0.76	0.54	0.42
13:20	18.2	8.6	1.44	0.61	1.04	2.79	0.79	0.48	0.44
14:00	17.1	8.3	1.35	0.67	0.66	2.66	0.67	0.45	0.36
14:44	19.2	9.2	1.38	0.56	0.66	2.88	0.75	0.52	0.42
15:18	19.3	9.3	1.37	0.53	0.62	2.87	0.83	0.49	0.40
16:00	19.1	9.4	1.39	0.62	0.63	2.81	0.76	0.54	0.47
Springs									
07:08	19.3	9.0	1.49	0.70	0.60	2.78	0.63	0.40	0.15
07:54	19.6	9.0	1.55	0.71	0.58	2.84	0.62	0.38	0.15
08:21	21.1	9.7	1.67	0.71	0.54	2.98	0.61	0.38	0.16
09:29	20.7	9.3	1.66	0.68	0.54	3.01	0.62	0.43	0.13
10:03	20.3	9.6	2.04	0.85	0.53	2.91	0.48	0.44	0.13
Time of sampling	Major elements, <i>wt.%</i> - leach analysis.								
	Al ₂ O ₃	Fe ₂ O ₃	MgO	CaO	Na ₂ O	K ₂ O		P ₂ O ₅	MnO
Neaps									
12:41	0.70	2.79	0.19	0.34	0.11	0.08		0.31	0.35
13:20	0.66	2.50	0.27	0.36	0.47	0.10		0.28	0.36
14:00	0.65	2.42	0.24	0.41	0.12	0.09		0.27	0.29
14:44	0.70	2.78	0.19	0.34	0.11	0.08		0.30	0.35
15:18	0.69	2.84	0.16	0.30	0.09	0.07		0.28	0.32
16:00	0.72	2.90	0.20	0.38	0.13	0.09		0.31	0.39
Springs									
07:08	0.67	2.51	0.24	0.47	0.04	0.06		0.26	0.10
07:54	0.68	2.50	0.25	0.48	0.04	0.05		0.26	0.10
08:21	0.71	2.62	0.26	0.48	0.04	0.06		0.26	0.09
09:29	0.73	2.70	0.31	0.46	0.07	0.08		0.26	0.08
10:03	0.72	2.74	0.74	0.63	0.09	0.13		0.26	0.08

Turbidity Maximum, Surface Samples: Suspended Particles									
Time of sampling	Trace elements, <i>ppm</i> - total analysis.								
	Ba	Co	Cu	Li	Ni	Sr	V	Zn	Y
Neaps									
12:41	456	32	208	123	81	111	149	355	22.3
13:20	452	35	216	128	80	118	143	360	22.5
14:00	406	32	244	123	77	111	135	383	20.8
14:44	478	36	222	130	85	115	153	376	21.7
15:18	487	34	213	129	81	112	155	373	22.2
16:00	473	36	208	124	87	116	154	381	21.0
Springs									
07:08	436	27	273	135	78	122	146	418	22.5
07:54	448	29	259	137	77	122	151	385	22.4
08:21	474	31	243	143	80	126	163	413	22.8
09:29	467	27	218	139	76	126	162	384	22.2
10:03	461	29	206	131	83	138	157	424	22.2
Time of sampling	Trace elements, <i>ppm</i> - leach analysis.								
	Ba	Co	Cu		Ni	Sr	V	Zn	Y
Neaps									
12:41	35	17	177		33	24	21	271	7.6
13:20	35	19	180		32	31	19	264	7.7
14:00	34	17	213		31	29	18	311	7.5
14:44	38	19	188		34	25	21	281	8.2
15:18	40	18	179		31	20	21	271	7.7
16:00	42	20	178		37	27	22	300	7.5
Springs									
07:08	30	15	236		28	30	19	317	8.0
07:54	31	13	224		28	31	20	313	7.9
08:21	30	14	208		25	32	21	296	7.8
09:29	29	11	185		27	35	23	304	7.8
10:03	32	13	177		31	47	20	314	7.9

Turbidity Maximum, Surface Samples: Suspended Particles										
Time of sampling	Rare earth elements, ppm - total analysis.									
	La	Ce	Nd	Sm	Eu	Gd	Dy	Ho	Er	Yb
Neaps										
12:41	38.1	69	35.2	6.8	1.18	4.5	4.16	0.81	2.34	2.31
13:20	38.1	69	35.5	6.9	1.16	4.6	4.12	0.80	2.32	2.31
14:00	36.1	66	33.8	6.6	1.16	4.5	3.84	0.75	2.23	2.13
14:44	38.5	69	35.8	6.9	1.14	4.5	3.99	0.76	2.23	2.25
15:18	38.2	69	35.1	6.9	1.05	4.2	4.03	0.78	2.16	2.39
16:00	37.6	68	34.4	6.8	1.06	4.2	3.85	0.76	2.10	2.25
Springs										
07:08	39.6	71	36.4	7.1	1.22	6.1	4.10	0.84	2.37	2.24
07:54	39.2	71	36.1	6.8	1.18	6.9	4.09	0.85	2.33	2.51
08:21	39.7	72	36.9	6.9	1.20	7.2	4.18	0.89	2.35	2.43
09:29	38.5	70	35.9	6.7	1.19	6.7	4.07	0.86	2.31	2.37
10:03	38.4	69	35.2	6.8	1.15	6.6	4.08	0.87	2.31	2.35
Time of sampling	Rare earth elements, ppm - leach analysis.									
	La	Ce	Nd	Sm	Eu	Gd	Dy	Ho	Er	Yb
Neaps										
12:41	6.4	11.3	9.2	2.25	0.37	1.74	1.50	0.28	0.64	0.58
13:20	6.5	12.0	9.4	2.40	0.37	1.79	1.49	0.30	0.67	0.65
14:00	6.3	11.5	9.1	2.31	0.39	1.69	1.46	0.30	0.70	0.59
14:44	6.9	12.4	9.9	2.46	0.37	1.88	1.55	0.33	0.68	0.64
15:18	6.6	11.9	9.6	2.45	0.32	1.64	1.46	0.31	0.58	0.62
16:00	6.4	11.5	9.1	2.32	0.32	1.65	1.43	0.30	0.60	0.68
Springs										
07:08	6.7	13.0	9.9	2.44	0.42	1.85	1.56	0.31	0.75	0.63
07:54	6.7	12.4	9.7	2.38	0.39	1.79	1.52	0.31	0.70	0.63
08:21	6.7	12.5	9.5	2.40	0.39	1.76	1.52	0.33	0.68	0.59
09:29	6.6	12.3	9.8	2.43	0.39	1.74	1.51	0.32	0.72	0.65
10:03	6.7	12.4	9.6	2.43	0.39	1.69	1.53	0.32	0.68	0.66

Appendix E

Turbidity Maximum Profiles: Back-up Data				
Sampling time & depth (<i>m</i>)		Turbidity <i>mg l⁻¹</i>	Salinity <i>ppt</i>	Particle size μm
16:00	0.1	510	0.3	12.5
16:00	1.0	660	0.3	12.5
16:00	1.9	610	0.3	6.9
16:25	0.1	540	0.5	14.9
16:25	1.2	310	0.6	12.7
16:25	2.5	660	0.7	9.6
16:55	0.1	140	3.0	366
16:55	1.7	150	4.4	25.9
16:55	3.4	400	4.8	39.8
17:40	0.1	500	4.8	90.4
17:40	2.1	150	5.3	70.5
17:40	4.3	90	4.7	68.5
18:00	0.1	40	9.1	327
18:00	2.5	45	10.7	79.5
18:00	4.7	90	11.0	141.9
18:30	0.1	40	9.8	367.6
18:30	2.5	42	11.5	324.2
18:30	4.7	45	11.9	274.3

Turbidity Maximum Profiles: Suspended Particles										
Sampling time & depth (m)		Major elements, wt.% - total analysis.								
		Al ₂ O ₃	Fe ₂ O ₃	MgO	CaO	Na ₂ O	K ₂ O	TiO ₂	P ₂ O ₅	MnO
16:00	0.1	18.7	8.5	1.49	0.72	0.59	2.91	0.69	0.41	0.13
16:00	1.0	18.1	8.5	1.46	0.79	0.63	2.80	0.76	0.41	0.13
16:00	1.9	17.5	8.2	1.39	0.83	0.69	2.65	0.74	0.42	0.14
16:25	0.1	18.5	8.3	1.49	0.67	0.59	2.85	0.73	0.41	0.13
16:25	1.2	18.1	8.1	1.48	0.66	0.61	2.82	0.74	0.40	0.13
16:25	2.5	16.5	7.8	1.35	0.73	0.66	2.50	0.73	0.40	0.13
16:55	0.1	18.6	8.3	1.59	0.62	0.80	2.89	0.72	0.41	0.14
16:55	1.7	17.9	8.1	1.53	0.62	0.85	2.79	0.75	0.42	0.14
16:55	3.4	16.8	7.9	1.42	0.64	0.89	2.59	0.69	0.40	0.14
17:40	0.1	18.6	8.6	1.72	0.69	1.79	2.86	0.76	0.43	0.23
17:40	2.1	17.6	8.3	1.63	0.63	1.61	2.82	0.70	0.43	0.25
17:40	4.3	16.4	7.7	1.46	0.61	1.29	2.52	0.62	0.38	0.15
18:00	0.1	18.1	8.6	1.81	0.66	2.61	2.88	0.63	0.46	0.25
18:00	2.5	18.1	8.4	1.74	0.67	2.32	2.79	0.68	0.43	0.28
18:00	4.7	17.3	8.0	1.58	0.64	1.61	2.68	0.72	0.41	0.20
18:30	0.1	17.9	8.5	1.86	0.71	3.06	2.73	0.66	0.45	0.25
18:30	2.5	17.2	8.1	2.00	0.73	4.05	2.65	0.61	0.42	0.34
18:30	4.7	17.1	8.2	1.65	0.63	2.04	2.69	0.68	0.42	0.26
Sampling time & depth(m)		Major elements, wt.% - leach analysis.								
		Al ₂ O ₃	Fe ₂ O ₃	MgO	CaO	Na ₂ O	K ₂ O		P ₂ O ₅	MnO
16:00	0.1	0.98	2.71	0.33	0.55	0.09	0.12		0.27	0.10
16:00	1.0	1.06	2.91	0.36	0.58	0.08	0.12		0.29	0.10
16:00	1.9	0.79	2.60	0.32	0.62	0.08	0.09		0.29	0.11
16:25	0.1	0.75	2.72	0.35	0.51	0.10	0.09		0.27	0.10
16:25	1.2	0.74	2.50	0.33	0.47	0.10	0.09		0.25	0.09
16:25	2.5	0.77	2.53	0.36	0.55	0.07	0.09		0.27	0.09
16:55	0.1	0.72	2.66	0.43	0.41	0.32	0.10		0.26	0.10
16:55	1.7	0.77	2.57	0.43	0.41	0.36	0.12		0.26	0.11
16:55	3.4	0.81	2.49	0.42	0.42	0.28	0.11		0.26	0.10
17:40	0.1	0.82	2.96	0.59	0.42	1.31	0.16		0.28	0.19
17:40	2.1	0.81	2.85	0.55	0.40	1.10	0.15		0.28	0.21
17:40	4.3	0.66	2.46	0.48	0.42	0.80	0.12		0.27	0.11
18:00	0.1	0.76	3.03	0.72	0.45	2.18	0.20		0.30	0.21
18:00	2.5	0.76	2.80	0.64	0.43	1.84	0.19		0.28	0.24
18:00	4.7	0.72	2.57	0.54	0.42	1.11	0.14		0.28	0.16
18:30	0.1	0.78	3.08	0.80	0.48	2.69	0.24		0.30	0.21
18:30	2.5	0.69	2.79	0.95	0.49	3.63	0.25		0.28	0.30
18:30	4.7	0.76	2.80	0.62	0.41	1.55	0.16		0.28	0.22

Turbidity Maximum Profiles: Suspended Particles										
Sampling time & depth (m)		Trace elements, ppm - total analysis.								
		Ba	Co	Cu	Li	Ni	Sr	V	Zn	Y
16:00	0.1	463	21	241	137	65	120	140	357	21.6
16:00	1.0	450	24	269	133	70	122	137	352	22.4
16:00	1.9	427	24	298	124	71	120	131	403	22.4
16:25	0.1	460	22	222	133	67	121	140	414	23.2
16:25	1.2	457	22	222	132	64	121	138	413	22.7
16:25	2.5	403	23	290	119	66	119	126	449	21.0
16:55	0.1	468	23	212	134	66	128	142	360	20.9
16:55	1.7	448	22	218	130	63	126	136	358	22.3
16:55	3.4	411	24	290	122	64	123	127	392	21.4
17:40	0.1	502	28	194	129	84	142	145	420	21.3
17:40	2.1	467	28	222	126	71	131	130	376	21.6
17:40	4.3	390	22	285	118	62	122	124	370	21.0
18:00	0.1	491	29	175	125	71	142	145	381	19.8
18:00	2.5	470	28	205	126	73	138	143	369	19.9
18:00	4.7	409	25	270	125	68	130	133	401	21.6
18:30	0.1	490	29	164	117	77	145	144	414	18.7
18:30	2.5	461	33	173	114	78	141	139	397	18.7
18:30	4.7	430	27	228	122	67	130	122	375	22.1
Sampling time & depth (m)		Trace elements, ppm - leach analysis.								
		Ba	Co	Cu	Ni	Sr	V	Zn	Y	
16:00	0.1	44	12	208	25	36	21	345	8.4	
16:00	1.0	45	14	247	28	38	22	363	8.9	
16:00	1.9	39	14	270	29	39	20	350	8.4	
16:25	0.1	37	12	198	24	38	22	289	8.2	
16:25	1.2	36	11	191	22	38	20	285	8.2	
16:25	2.5	36	13	257	27	41	19	332	8.5	
16:55	0.1	39	11	177	23	45	21	270	8.0	
16:55	1.7	45	11	185	24	45	21	272	7.9	
16:55	3.4	35	13	247	25	43	19	344	8.4	
17:40	0.1	60	17	147	35	55	26	314	7.8	
17:40	2.1	55	18	176	26	48	25	277	8.1	
17:40	4.3	28	14	249	23	46	20	291	8.4	
18:00	0.1	57	17	134	29	57	29	262	7.5	
18:00	2.5	45	18	157	26	52	26	238	7.9	
18:00	4.7	36	16	221	25	49	22	296	8.4	
18:30	0.1	62	18	127	34	62	29	295	7.2	
18:30	2.5	53	21	130	32	60	28	259	6.8	
18:30	4.7	36	17	187	25	50	25	249	8.4	

Turbidity Maximum Profiles: Suspended Particles											
Sampling time & depth (m)		Rare earth elements, ppm - total analysis.									
		La	Ce	Nd	Sm	Eu	Gd	Dy	Ho	Er	Yb
16:00	0.1	38.8	72	36.3	6.9	1.35	4.9	3.97	0.78	2.30	2.33
16:00	1.0	39.9	73	37.1	7.0	1.37	5.0	4.09	0.79	2.42	2.47
16:00	1.9	39.7	73	37.7	7.1	1.36	5.0	4.13	0.82	2.45	2.49
16:25	0.1	40.9	76	38.2	7.3	1.37	5.1	4.29	0.86	2.49	2.46
16:25	1.2	40.0	74	36.9	6.8	1.37	4.9	4.20	0.81	2.43	2.39
16:25	2.5	36.7	70	34.9	6.9	1.28	4.8	3.94	0.81	2.32	2.25
16:55	0.1	37.5	71	36.5	6.6	1.28	4.7	4.00	0.78	2.37	2.26
16:55	1.7	38.1	72	35.9	6.9	1.34	4.9	4.14	0.85	2.47	2.35
16:55	3.4	37.1	71	35.9	6.8	1.33	4.8	4.02	0.78	2.38	2.24
17:40	0.1	38.6	72	37.4	6.9	1.10	4.0	3.93	0.84	2.24	2.30
17:40	2.1	37.5	71	36.4	6.9	1.23	4.5	4.05	0.82	2.41	2.32
17:40	4.3	37.2	71	35.1	6.9	1.31	4.8	3.96	0.80	2.42	2.30
18:00	0.1	39.7	70	39.4	7.4	0.89	3.4	3.69	0.81	1.94	2.13
18:00	2.5	38.0	70	36.9	7.3	1.11	4.0	3.78	0.84	2.20	2.21
18:00	4.7	37.8	71	36.6	6.9	1.32	4.9	4.12	0.85	2.45	2.24
18:30	0.1	37.9	69	38.1	6.8	0.69	2.5	3.37	0.70	1.81	2.09
18:30	2.5	36.4	68	37.5	7.1	0.64	2.4	3.35	0.67	1.84	2.03
18:30	4.7	37.8	71	36.1	7.0	1.24	4.8	4.24	0.90	2.47	2.39

Sampling time & depth (m)		Rare earth elements, ppm - leach analysis.									
		La	Ce	Nd	Sm	Eu	Gd	Dy	Ho	Er	Yb
16:00	0.1	7.0	12.9	10.1	2.40	0.45	2.06	1.63	0.31	0.74	0.71
16:00	1.0	7.5	14.0	10.6	2.59	0.50	2.26	1.73	0.36	0.83	0.71
16:00	1.9	6.8	12.5	10.0	2.52	0.45	1.96	1.61	0.32	0.73	0.69
16:25	0.1	6.8	13.2	10.3	2.45	0.46	2.00	1.59	0.32	0.70	0.62
16:25	1.2	6.7	12.4	10.1	2.35	0.47	2.00	1.62	0.33	0.74	0.62
16:25	2.5	7.0	13.3	10.3	2.51	0.46	2.01	1.65	0.35	0.74	0.67
16:55	0.1	6.8	13.2	9.8	2.38	0.44	1.96	1.59	0.32	0.75	0.67
16:55	1.7	6.7	13.2	9.9	2.51	0.41	1.85	1.53	0.32	0.66	0.56
16:55	3.4	7.0	13.3	10.1	2.51	0.49	2.11	1.66	0.34	0.81	0.70
17:40	0.1	7.2	13.8	10.2	2.70	0.40	1.65	1.54	0.33	0.70	0.63
17:40	2.1	7.1	13.4	10.2	2.54	0.45	2.03	1.61	0.32	0.76	0.66
17:40	4.3	6.8	13.2	10.1	2.42	0.45	2.00	1.63	0.34	0.80	0.63
18:00	0.1	7.3	13.4	11.4	2.64	0.30	1.29	1.52	0.30	0.56	0.64
18:00	2.5	7.1	13.7	10.5	2.69	0.42	1.86	1.56	0.35	0.74	0.66
18:00	4.7	7.0	13.4	10.2	2.44	0.46	2.04	1.66	0.35	0.81	0.68
18:30	0.1	7.2	13.5	11.3	2.53	0.18	1.14	1.43	0.24	0.53	0.56
18:30	2.5	7.0	13.0	11.5	2.85	0.13	1.02	1.31	0.26	0.56	0.50
18:30	4.7	7.1	14.2	10.5	2.56	0.47	2.15	1.66	0.36	0.78	0.71

Appendix F

Settling Procedure: Back-up Data						
Sampling time & depth (m)		Salinity ppt	PSP		RSS	
			Turbidity mg l ⁻¹	Mean particle size μm	Turbidity mg l ⁻¹	Mean particle size μm
08:40	3.50	12.08	11	43.63	45	43.32
08:40	0.50	5.80	9	65.01	53	54.69
10:30	2.50	6.58	11	50.99	181	67.59
10:30	2.00	4.53	20	54.69	81	33.70
10:30	1.50	3.90	12	63.03	138	69.86
10:30	1.00	2.63	18	34.95	88	27.63
10:30	0.50	2.18	15	62.28	85	19.18
12:30	0.70	0.02	50	22.67	1540	27.28
12:30	0.50	0.03	32	42.35	918	25.76
15:00	0.25	0.02	21	57.96	245	53.74
17:00	3.25	4.31	12	31.45	779	34.84
17:00	0.50	3.78	17	17.76	175	31.82
19:00	4.50	10.64	17	32.86	35	33.97
19:00	0.50	9.33	17	56.04	31	17.93

Settling Procedure: Permanently Suspended Particles										
Sampling time & depth (m)		Major elements, wt.% - total analysis.								
		Al ₂ O ₃	Fe ₂ O ₃	MgO	CaO	Na ₂ O	K ₂ O	TiO ₂	P ₂ O ₅	MnO
08:40	3.50	12.6	6.6	2.59	0.88	10.41	2.86	0.39	0.60	0.40
08:40	0.50	20.0	10.8	1.76	0.70	1.72	3.16	0.65	0.74	0.22
10:30	2.50	19.9	10.4	1.82	0.73	2.15	3.13	0.65	0.71	0.33
10:30	2.00	19.6	10.9	1.76	0.73	2.05	3.06	0.61	0.76	0.21
10:30	1.50	19.1	10.1	1.57	0.66	1.34	3.01	0.60	0.78	0.12
10:30	1.00	20.3	11.0	1.64	0.70	1.25	3.20	0.64	0.76	0.12
10:30	0.50	19.1	10.2	1.54	0.66	1.13	2.96	0.63	0.68	0.11
12:30	0.70	20.8	10.3	1.41	0.79	0.64	3.13	0.60	0.66	0.13
12:30	0.50	20.3	10.2	1.34	0.92	0.57	3.09	0.64	0.64	0.15
15:00	0.25	18.7	10.4	1.26	0.97	0.55	2.80	0.60	0.75	0.22
17:00	3.25	19.3	9.8	1.56	0.61	1.30	3.03	0.58	0.62	0.11
17:00	0.50	18.8	10.0	1.58	0.62	1.45	3.04	0.55	0.69	0.14
19:00	4.50	15.1	8.8	1.75	0.67	3.57	2.88	0.53	0.64	0.29
19:00	0.50	12.8	6.7	2.28	0.84	9.06	2.83	0.42	0.50	0.18
Sampling time & depth(m)		Major elements, wt.% - leach analysis.								
		Al ₂ O ₃	Fe ₂ O ₃	MgO	CaO	Na ₂ O	K ₂ O		P ₂ O ₅	MnO
08:40	3.50	0.26	1.38	0.96	0.37	4.66	0.40		0.24	0.19
08:40	0.50	0.89	4.84	0.71	0.55	1.30	0.18		0.64	0.21
10:30	2.50	0.84	4.49	0.77	0.55	1.73	0.21		0.62	0.31
10:30	2.00	0.90	5.01	0.79	0.58	1.65	0.21		0.67	0.18
10:30	1.50	0.78	4.19	0.60	0.51	0.96	0.19		0.59	0.09
10:30	1.00	0.93	5.20	0.64	0.55	0.80	0.16		0.65	0.09
10:30	0.50	0.85	4.55	0.57	0.51	0.74	0.16		0.57	0.09
12:30	0.70	0.90	4.01	0.42	0.65	0.23	0.12		0.45	0.09
12:30	0.50	0.86	4.04	0.30	0.80	0.14	0.14		0.50	0.12
15:00	0.25	0.81	4.55	0.30	0.84	0.15	0.11		0.57	0.18
17:00	3.25	0.78	3.90	0.61	0.47	0.93	0.16		0.41	0.08
17:00	0.50	0.88	4.71	0.71	0.56	1.18	0.20		0.53	0.12
19:00	4.50	0.71	3.76	0.93	0.56	3.16	0.35		0.47	0.28
19:00	0.50	0.52	2.52	1.53	0.71	7.33	0.70		0.35	0.15

Settling Procedure: Resuspending Sediment										
Sampling time & depth (m)		Major elements, wt.% - total analysis.								
		Al ₂ O ₃	Fe ₂ O ₃	MgO	CaO	Na ₂ O	K ₂ O	TiO ₂	P ₂ O ₅	MnO
08:40	3.50	17.9	7.8	1.63	0.66	1.49	2.94	0.72	0.43	0.15
08:40	0.50	18.7	8.2	1.60	0.55	0.89	3.00	0.76	0.40	0.10
10:30	2.50	17.8	8.1	1.59	0.60	1.08	2.90	0.77	0.41	0.14
10:30	2.00	18.1	8.2	1.55	0.59	0.87	2.84	0.72	0.40	0.14
10:30	1.50	17.7	7.9	1.54	0.61	0.83	2.77	0.80	0.39	0.13
10:30	1.00	18.1	8.0	1.54	0.59	0.73	2.90	0.80	0.39	0.13
10:30	0.50	18.7	8.3	1.58	0.58	0.68	2.94	0.79	0.39	0.12
12:30	0.70	16.8	7.9	1.38	0.80	0.67	2.62	0.78	0.40	0.14
12:30	0.50	16.9	7.9	1.32	0.87	0.63	2.60	0.77	0.40	0.15
15:00	0.25	18.1	8.3	1.42	0.86	0.57	2.83	0.82	0.41	0.15
17:00	3.25	18.5	8.0	1.61	0.63	0.83	2.99	0.82	0.38	0.13
17:00	0.50	18.1	7.8	1.58	0.62	0.81	2.92	0.81	0.37	0.12
19:00	4.50	18.0	7.7	1.60	0.57	1.32	2.93	0.70	0.37	0.13
19:00	0.50	18.3	7.8	1.62	0.56	1.23	2.99	0.74	0.36	0.12
Sampling time & depth(m)		Major elements, wt.% - leach analysis.								
		Al ₂ O ₃	Fe ₂ O ₃	MgO	CaO	Na ₂ O	K ₂ O		P ₂ O ₅	MnO
08:40	3.50	0.75	2.39	0.51	0.49	1.00	0.18		0.29	0.12
08:40	0.50	0.70	2.62	0.43	0.37	0.46	0.12		0.26	0.07
10:30	2.50	0.85	2.58	0.48	0.40	0.57	0.15		0.27	0.11
10:30	2.00	0.80	2.49	0.44	0.39	0.38	0.13		0.26	0.10
10:30	1.50	0.67	2.43	0.44	0.40	0.35	0.10		0.25	0.10
10:30	1.00	0.68	2.54	0.43	0.40	0.26	0.09		0.25	0.09
10:30	0.50	0.81	2.54	0.41	0.40	0.20	0.11		0.25	0.09
12:30	0.70	0.71	2.36	0.32	0.59	0.05	0.08		0.27	0.11
12:30	0.50	0.77	2.36	0.27	0.66	0.04	0.10		0.26	0.11
15:00	0.25	0.85	2.44	0.28	0.68	0.03	0.10		0.26	0.12
17:00	3.25	0.78	2.40	0.43	0.42	0.27	0.11		0.27	0.10
17:00	0.50	0.79	2.35	0.45	0.42	0.30	0.13		0.25	0.09
19:00	4.50	0.69	2.29	0.47	0.38	0.86	0.14		0.25	0.10
19:00	0.50	0.72	2.28	0.45	0.35	0.77	0.15		0.24	0.09

Settling Procedure: Permanently Suspended Particles										
Sampling time & depth (m)		Trace elements, ppm - total analysis.								
		Ba	Co	Cu	Li	Ni	Sr	V	Zn	Y
08:40	3.50	341	27	177	88	62	161	114	494	15.1
08:40	0.50	506	33	172	131	78	162	172	512	23.6
10:30	2.50	487	37	171	129	78	166	169	471	23.9
10:30	2.00	504	31	171	127	80	171	170	545	23.6
10:30	1.50	485	23	595	125	72	152	160	548	22.7
10:30	1.00	501	25	194	134	75	166	173	482	24.0
10:30	0.50	511	23	183	125	73	153	161	465	23.1
12:30	0.70	515	25	289	137	79	134	165	545	22.9
12:30	0.50	511	26	261	135	81	128	160	601	22.6
15:00	0.25	492	27	249	124	78	124	153	575	22.8
17:00	3.25	476	22	195	129	68	186	159	522	22.0
17:00	0.50	470	22	185	127	69	171	158	406	21.3
19:00	4.50	370	24	171	106	80	128	141	393	13.3
19:00	0.50	341	21	134	94	93	156	109	330	15.7
Sampling time & depth (m)		Trace elements, ppm - leach analysis.								
		Ba	Co	Cu	Ni	Sr	V	Zn	Y	
08:40	3.50	19	8	65	17	51	16	219	3.5	
08:40	0.50	63	22	109	35	74	42	387	10.9	
10:30	2.50	53	24	110	34	78	40	369	10.5	
10:30	2.00	65	18	118	37	87	43	411	11.2	
10:30	1.50	49	13	507	29	69	35	391	9.9	
10:30	1.00	49	14	118	33	79	41	333	11.6	
10:30	0.50	61	12	129	34	71	37	357	10.5	
12:30	0.70	62	13	221	31	49	28	362	10.8	
12:30	0.50	64	14	193	33	43	27	363	10.7	
15:00	0.25	74	16	186	35	44	29	344	11.0	
17:00	3.25	44	11	136	27	108	32	326	10.1	
17:00	0.50	54	15	134	33	98	41	373	9.8	
19:00	4.50	46	16	116	46	82	36	336	9.0	
19:00	0.50	39	12	88	60	89	25	242	7.0	

Settling Procedure: Resuspending Sediment										
Sampling time & depth (m)		Trace elements, ppm - total analysis.								
		Ba	Co	Cu	Li	Ni	Sr	V	Zn	Y
08:40	3.50	471	19	244	127	61	134	134	559	18.9
08:40	0.50	487	20	168	128	63	129	142	408	21.2
10:30	2.50	449	21	243	131	66	133	135	396	21.7
10:30	2.00	450	23	228	128	65	132	138	332	20.6
10:30	1.50	409	24	220	125	64	128	133	354	22.1
10:30	1.00	456	21	213	129	64	130	138	351	21.8
10:30	0.50	475	22	203	131	66	133	143	348	21.7
12:30	0.70	422	24	318	126	68	115	126	372	21.9
12:30	0.50	424	26	311	128	72	112	126	391	21.1
15:00	0.25	461	24	295	137	72	115	134	403	22.5
17:00	3.25	463	22	238	140	65	134	137	408	22.0
17:00	0.50	452	22	232	137	63	131	134	399	22.9
19:00	4.50	461	20	173	127	60	130	133	337	19.1
19:00	0.50	482	19	172	130	62	130	137	341	20.2
Sampling time & depth (m)		Trace elements, ppm - leach analysis.								
		Ba	Co	Cu	Ni	Sr	V	Zn	Y	
08:40	3.50	43	10	203	20	49	23	396	6.1	
08:40	0.50	37	10	139	20	43	23	296	7.7	
10:30	2.50	36	13	201	24	49	21	276	9.3	
10:30	2.00	38	13	189	22	49	20	348	7.8	
10:30	1.50	26	12	184	21	48	19	323	7.7	
10:30	1.00	27	12	177	22	48	20	306	7.7	
10:30	0.50	36	13	165	22	48	21	297	7.7	
12:30	0.70	36	15	259	29	35	17	346	8.4	
12:30	0.50	39	15	249	30	32	17	336	8.6	
15:00	0.25	47	15	244	31	32	18	319	8.4	
17:00	3.25	36	13	244	27	45	19	302	8.3	
17:00	0.50	38	11	191	24	49	19	277	7.5	
19:00	4.50	39	10	137	29	46	21	225	6.5	
19:00	0.50	45	9	134	20	43	21	227	6.8	

Settling Procedure: Permanently Suspended Particles											
Sampling time & depth (m)		Rare earth elements, ppm - total analysis.									
		La	Ce	Nd	Sm	Eu	Gd	Dy	Ho	Er	Yb
08:40	3.50	27.7	50	27.2	5.2	0.96	3.7	2.92	0.57	1.70	1.59
08:40	0.50	43.4	81	40.7	8.0	1.64	6.3	4.42	0.94	2.79	2.46
10:30	2.50	43.7	81	41.4	8.0	1.60	6.0	4.52	0.97	2.91	2.64
10:30	2.00	41.3	77	39.5	7.8	1.55	6.0	4.45	0.93	2.78	2.48
10:30	1.50	40.6	75	38.4	7.5	1.48	5.7	4.27	0.91	2.67	2.46
10:30	1.00	42.7	80	41.3	8.1	1.63	6.3	4.61	0.98	2.94	2.62
10:30	0.50	40.4	77	39.5	7.6	1.53	5.7	4.49	0.92	2.80	2.48
12:30	0.70	40.4	76	39.4	7.8	1.56	5.7	4.38	0.95	2.75	2.37
12:30	0.50	40.6	77	39.7	8.0	1.54	5.5	4.40	0.91	2.78	2.59
15:00	0.25	40.2	75	38.4	7.7	1.52	5.9	4.37	0.89	2.74	2.44
17:00	3.25	38.8	73	37.8	7.4	1.46	5.5	4.21	0.84	2.66	2.32
17:00	0.50	38.2	73	38.0	7.2	1.44	5.1	4.12	0.86	2.54	2.35
19:00	4.50	16.3	38	19.7	4.1	0.79	2.8	2.65	0.55	1.55	1.76
19:00	0.50	28.2	54	28.0	5.3	0.99	3.7	3.01	0.62	1.87	1.58
Sampling time & depth (m)		Rare earth elements, ppm - leach analysis.									
		La	Ce	Nd	Sm	Eu	Gd	Dy	Ho	Er	Yb
08:40	3.50	3.1	5.3	4.4	1.04	0.15	0.71	0.64	0.11	0.26	0.27
08:40	0.50	9.6	17.2	12.8	3.23	0.65	2.71	2.14	0.40	1.00	0.76
10:30	2.50	8.8	16.3	12.1	3.11	0.60	2.52	2.08	0.38	0.95	0.80
10:30	2.00	9.4	17.5	13.0	3.24	0.69	2.90	2.22	0.41	1.01	0.86
10:30	1.50	8.3	15.4	12.1	2.93	0.59	2.52	2.03	0.39	0.93	0.79
10:30	1.00	9.8	17.6	14.4	3.29	0.71	3.04	2.37	0.46	1.11	0.90
10:30	0.50	8.8	16.1	12.9	3.12	0.65	2.73	2.10	0.40	0.99	0.81
12:30	0.70	8.8	16.2	12.7	3.13	0.66	2.84	2.17	0.42	1.03	0.88
12:30	0.50	8.7	16.5	12.7	3.17	0.63	2.77	2.12	0.41	1.02	0.87
15:00	0.25	8.9	16.2	12.6	3.22	0.65	2.83	2.16	0.42	1.05	0.87
17:00	3.25	8.7	16.6	12.3	3.03	0.62	2.75	2.04	0.38	0.92	0.76
17:00	0.50	8.1	15.7	11.9	2.98	0.61	2.48	1.94	0.40	0.93	0.73
19:00	4.50	7.9	14.4	11.4	2.67	0.55	2.38	1.76	0.33	0.83	0.69
19:00	0.50	6.1	11.5	8.8	2.22	0.39	1.85	1.38	0.27	0.65	0.54

Settling Procedure: Resuspending Sediment											
Sampling time & depth (m)		Rare earth elements, ppm - total analysis.									
		La	Ce	Nd	Sm	Eu	Gd	Dy	Ho	Er	Yb
08:40	3.50	36.4	70	34.4	6.6	1.18	4.3	3.60	0.79	2.31	2.10
08:40	0.50	40.4	78	37.4	7.0	1.38	5.1	4.02	0.85	2.53	2.34
10:30	2.50	39.2	76	37.2	7.0	1.39	5.1	4.11	0.88	2.59	2.29
10:30	2.00	39.6	77	38.0	7.1	1.39	5.1	3.97	0.84	2.52	2.25
10:30	1.50	38.7	76	36.3	7.1	1.38	5.3	4.18	0.89	2.61	2.35
10:30	1.00	39.4	77	37.3	7.0	1.40	5.2	4.14	0.88	2.60	2.35
10:30	0.50	39.5	76	37.4	7.1	1.37	5.0	4.10	0.87	2.59	2.31
12:30	0.70	37.7	73	36.4	7.0	1.38	5.4	4.17	0.88	2.53	2.42
12:30	0.50	37.4	72	36.3	6.7	1.35	5.2	4.04	0.84	2.46	2.32
15:00	0.25	38.8	74	37.2	7.0	1.39	5.4	4.28	0.89	2.63	2.34
17:00	3.25	37.6	73	35.9	6.8	1.34	5.1	4.29	0.89	2.57	2.31
17:00	0.50	39.0	76	37.1	7.0	1.38	5.3	4.34	0.90	2.72	2.59
19:00	4.50	38.2	73	36.1	6.7	1.27	4.6	3.71	0.78	2.29	2.11
19:00	0.50	39.2	75	37.2	6.8	1.31	4.8	3.88	0.83	2.48	2.22
Sampling time & depth (m)		Rare earth elements, ppm - leach analysis.									
		La	Ce	Nd	Sm	Eu	Gd	Dy	Ho	Er	Yb
08:40	3.50	5.3	10.1	7.7	1.93	0.32	1.44	1.25	0.22	0.54	0.51
08:40	0.50	6.7	12.8	9.7	2.42	0.45	1.84	1.53	0.31	0.69	0.58
10:30	2.50	7.8	14.6	11.0	2.78	0.53	2.36	1.83	0.35	0.87	0.72
10:30	2.00	6.6	12.6	9.8	2.38	0.43	1.79	1.49	0.33	0.72	0.57
10:30	1.50	6.7	12.5	9.6	2.47	0.42	1.75	1.54	0.31	0.70	0.60
10:30	1.00	6.6	12.7	9.9	2.39	0.44	1.88	1.58	0.32	0.74	0.57
10:30	0.50	6.6	12.6	9.7	2.38	0.45	1.84	1.56	0.31	0.72	0.61
12:30	0.70	6.7	12.9	10.1	2.46	0.48	2.08	1.66	0.32	0.76	0.66
12:30	0.50	7.0	13.0	10.3	2.53	0.49	2.17	1.66	0.33	0.81	0.64
15:00	0.25	6.9	13.1	10.6	2.55	0.47	2.09	1.66	0.36	0.81	0.72
17:00	3.25	6.8	12.9	9.7	2.46	0.44	1.93	1.58	0.30	0.75	0.60
17:00	0.50	6.2	12.0	9.4	2.29	0.42	1.81	1.52	0.28	0.65	0.54
19:00	4.50	5.8	11.5	8.9	2.06	0.36	1.63	1.31	0.26	0.59	0.51
19:00	0.50	5.9	11.4	8.5	2.22	0.37	1.57	1.33	0.28	0.61	0.56